

# **The Synthesis and Application of Tetrahydrobiopterin Mimetics**

**By**

**Craig Robert McInnes**



A thesis presented to WestCHEM, Department of Pure and Applied Chemistry,  
University of Strathclyde in fulfilment of the requirements for the degree of Doctor  
of Philosophy

2012

## **Declaration of copyright**

*This thesis is the result of the author's original research. It has been composed by the author and has not been previously submitted for examination which has led to the award of a degree.*

*The copyright of this thesis belongs to the author under the terms of the United Kingdom Copyright Acts as qualified by University of Strathclyde Regulation 3.50. Due acknowledgement must always be made of the use of any material contained in, or derived from, this thesis. Images presented in this thesis are either the author's own work or used with permission from the copyright holder.*

*Signed:*

*Date:*

# Table of Contents

---

Acknowledgments	i
Abbreviations	iii
Abstract	vii
<b>Chapter 1: Introduction</b>	
1.1 General background to nitric oxide	1
1.1.1 Origins of the project	3
1.2 An overview of nitric oxide synthase and tetrahydrobiopterin	4
1.2.1 Nitric oxide synthase	4
1.2.2 Exogenous regulation and protein-protein interactions	11
1.2.3 The molecular mechanism of NO synthesis	16
1.2.4 The isoforms of NOS and their role in selected disease states	21
1.2.5 The biosynthesis of tetrahydrobiopterin	26
1.2.6 Other BH <sub>4</sub> -utilizing enzymes	28
1.3 A brief historical account of pteridines and their syntheses	32
1.3.1 The discovery of pteridines	32
1.3.2 The synthesis of pteridines from pyrimidines	34
1.3.3 The synthesis of pteridines from pyrazines	37
1.4 Analogues of tetrahydrobiopterin for study in NOS programmes	38
1.4.1 Literature compounds	38
1.4.2 The WSG compounds and their biological activities	42
1.5 A brief look at another target molecule, pyridopyrazine	43
1.5.1 The synthesis and application of pyridopyrazines	45
1.6 Synthesis with late-stage diversity	50

1.7 Aims and objectives	51
<b>Chapter 2: Results and discussion – diversity-oriented synthesis</b>	
2.1 Mesityl leaving group	56
2.2 Halide leaving groups	59
2.3 Electron-withdrawing group and chloride leaving group	60
2.4 Conclusions and further work	69
<b>Chapter 3: Results and discussion – C<sup>2</sup> expansion</b>	
3.1 Background	71
3.2 C <sup>2</sup> -Expansion	72
3.2.1 Compound evaluation	72
3.2.2 Retrosynthetic analysis	74
3.2.3 Preparation of $\alpha$ -aminoketone	76
3.2.4 Preparation of the <i>N</i> -methylpyrimidine	78
3.2.5 Nitration of 2- <i>N</i> -methyl-6-chloropyrimidin-4(3 <i>H</i> )-one	80
3.2.6 An alternative route to the <i>N</i> -methyl analogue of WSG1002	82
3.2.7 The peculiar properties of <i>N</i> -methylpyrimidines and fused pyrimidines	85
3.3 Conclusion	92
<b>Chapter 4: Results and discussion – targeted syntheses</b>	
4.1 Background	94
4.2 Synthesis of a common precursor	95
4.3 Preparation of WSG1002 ( <b>1.6</b> )	96
4.4 Preparation of WSG1007 ( <b>4.1</b> ) and WSG1060 ( <b>4.2</b> )	98

4.5 Analogues of WSG1060	99
4.6 Conclusion	105

## **Chapter 5: Results and discussion – fused pyridines**

5.1 Background	106
5.2 Preparation of 2,6-diamino-4-bromopyridine	108
5.3 Insertion of a nitrogen-based electron-withdrawing group	112
5.4 The coupling reaction	114
5.5 Other fused pyridines of interest	120
5.6 A serendipitous insight	124
5.7 Conclusions and further work	126

## **Chapter 6: Results and discussion – Biological results and compound evaluation**

6.1 Background	128
6.2 Reduction of the pteridines	129
6.3 Single-point turnover assay	131
6.4 Michaelis-Menten kinetics	135
6.4.1 Background	135
6.4.2 Michaelis-Menten kinetic results	138
6.5 Stopped-flow kinetics	140
6.6 Spartan calculations	146
6.7 GOLD analysis	150
6.8 X-Ray crystallographic studies	153
6.9 eNOS enzymatic assay	158
6.8 Conclusions and further work	160

**Chapter 7: Experimental**

7.1 General experimental 162

7.2 Experimental 165

**References** 224

Appendices Attached CD

# Acknowledgments

---

I would like to begin by thanking my supervisor, Prof. Colin J. Suckling. I feel truly indebted to you for the opportunity that you have provided me with. It's not every day that one gets to join a team with so much experience and knowledge at the helm. Your guidance has been the basis on which I am building my career and I hope to someday be as great a mentor to others, as you have been to me. Your drive to get the best out of me and encourage me when times (and chemistry) were tough has undoubtedly been a major motivator to get me through this PhD. Special thanks are due for your help throughout this last year, Colin. I would not have made it through without your support.

I would also like to extend my gratitude to my second supervisor, Dr. Colin L. Gibson. Your input over the last few years has been invaluable and this thesis, never mind the work, wouldn't have been what it is without your expertise. Thanks for creating such a friendly atmosphere; it enabled me to solve problems and to ask for a "fresh pair of eyes" when needed. Of course, thanks for the music.

Thanks are due to my internal examiner, Prof. William Kerr. Your suggestions and comments during my first and second year *viva voces* have allowed me to take a look at where I needed to improve, and have aided my growth as a chemist.

My thanks go to Dr. Simon Daff and Ben Gazur for their invaluable assistance with the biological aspect of this project. They both provided the practical support needed to get the results we have today.

My appreciation goes out to all the members of the CJS and CLG groups, both past and present for making the lab a wonderful place to work. Jonny and Gav made the lab a really welcoming and light-hearted place to work. Raghu helped me find my feet and provided much needed encouragement in the early days. Abed, your laughter is infectious and really cheers me up. Dave, we are an explosive combination. Donna, I wish I had listened to you about the doors earlier. Niaz, you're a laugh a minute and Korea was infinitely better with you there. Caro and Camille, keep on climbing. Ghjuvanni, it was a pleasure. Of course, Fraser: it's been

a laugh and frankly, thoroughly intellectual. The lab just wouldn't be what it is without you and I thank you for all the help you've given me over the years.

I wish to extend my appreciation to the staff here at the University of Strathclyde, namely Ms Pat Keating, Ms Denise Gilmour, Mr Gavin Bain and Mr Craig Irving for all going the extra mile. I would also like to thank Dr. Alan Kennedy for the X-ray crystallographic work and Dr. John Parkinson for help with the more complex NMR work.

There are a few personal friends that I wish to extend my gratitude to. Alistair Apedaile for taking the time to visit me when I was too busy to move away from my fume hood. Iain Wright for just being a great mate and really making the department funny. Of course, Martin De Cecco, for being one of my biggest inspirations.

Finally, none of this would be possible without my family. Thanks to Ashleigh and Wass for putting a roof over my head when I needed it but also for the endless encouragement. Maureen and Stuart, because family is the best support network and you both make me smile. Last but definitely not least, my dad, Cameron McInnes. You've always worked hard and always given it your best and all the time you have a smile on your face. I just quite simply wouldn't be here without you and your encouragement. Your hard work allowed me to get to university in the first place and you are the role model I needed to get through to where I am today. From the bottom of my heart, thanks Dad.



# Abbreviations

---

AAH	aromatic amino acid hydroxylase
ADMA	$N^G, N^G$ -dimethylarginine
aq.	aqueous
BH <sub>2</sub>	7,8-dihydrobiopterin
BH <sub>4</sub>	5,6,7,8-tetrahydrobiopterin
BINAP	2,2'-bis-(diphenylphosphino)-1,1'-binaphthyl
bNOS	bacterial nitric oxide synthase
Boc	<i>Tertiary</i> -butyloxycarbonyl
BOP	benzotriazol-1-yloxytris(dimethylamino)phosphonium hexafluorophosphate
<i>ca.</i>	circa
CaM	calmodulin
Cbz	carbobenzyloxy
cGMP	cyclic guanosine-5'-monophosphate
CNS	central nervous system
d	day
DBU	1,8-diazabicyclo[5.4.0]undec-7-ene
DCM	dichloromethane
DFT	density functional theory
DHFR	dihydrofolate reductase
DMF	<i>N,N</i> -dimethylformamide

DMSO	dimethylsulfoxide
dppf	1,1'-bis(diphenylphosphino)ferrocene
dppp	1,3-bis(diphenylphosphino)propane
DTT	dithiothreitol
eNOS	endothelial nitric oxide synthase
eq	equivalents
<i>et al.</i>	et alii
FAD	flavin adenine dinucleotide
FMN	flavin mono nucleotide
GTP	guanosine-5'-triphosphate
GTPCH-1	guanosine-5'-triphosphate cyclohydrolase-1
h	hour
HB-EGF	heparin-binding epidermal growth factor
HOMO	highest occupied molecular orbital
HPLC	high performance liquid chromatography
HSP90	heat shock protein-90
iNOS	inducible nitric oxide synthase
IPA	isopropyl alcohol
I.R.	infra red
$K_m$	Michaelis-Menten binding affinity
KLF2	Küppel-like factor 2
L-DOPA	L-3,4-dihydroxyphenylalanine

L-NAME	<i>N</i> <sup>0</sup> -nitro-L-arginine methyl ester
M	molar
MetHb	methaemoglobin
min	minute
M.W.	microwave
NADPH	nicotinamide adenine dinucleotide phosphate
NCS	<i>N</i> -chlorosuccinimide
NF-κB	nuclear factor κ B
NMADR	<i>N</i> -methyl-D-aspartate receptor
NMR	nuclear magnetic resonance
nNOS	neuronal nitric oxide synthase
NO	nitric oxide
NOHA	<i>N</i> <sup>G</sup> -hydroxy-L-arginine
NOS	nitric oxide synthase
NOSs	nitric oxide synthases
NOSoxy	nitric oxide synthase oxygenase domain
OxyHb	oxyhaemoglobin
P <sub>450</sub>	cytochrome P <sub>450</sub>
PKU	phenylketonuria
RNS	reactive nitrogen species
ROS	reactive oxygen species
ppm	parts per million

R.T.	room temperature
RuPhos	dicyclohexylphosphino-2',6'-di-i-propoxy-1,1'-biphenyl
s	second
SAR	structure activity relationship
sGC	soluble guanylyl cyclase
SOD	superoxide dismutase
SOMO	singularly occupied molecular orbital
TFA	trifluoroacetic acid
TFAA	trifluoroacetic anhydride
THF	tetrahydrofuran
tlc	thin layer chromatography
tPSA	total polar surface area
XPhos	2-dicyclohexylphosphino-2',4',6'-triisopropylbiphenyl
6-PTS	6-pyruvoyltetrahydropterin synthase

# Abstract

---

Nitric oxide is a small inorganic free radical which plays an essential role in mammalian biology. Nitric oxide synthases (NOSs) are responsible for producing nitric oxide within differing areas of the body and have crucial roles in various disease states, such as hypertension, septic shock and Alzheimer's disease. Modulating the activity of nitric oxide synthases may provide a viable route towards treating these and other disease states. Tetrahydrobiopterin ( $\text{BH}_4$ ) is an important coenzyme for nitric oxide synthase and, without it, nitric oxide production halts. It is with this in mind that synthetic analogues of  $\text{BH}_4$  have been prepared and tested previously. This led to the discovery of a particularly active pteridine known as WSG1002, which fell under the category of blocked dihydropteridines. One of the main aims of this PhD was to synthesise and assess various analogues of WSG1002, primarily for their NOS-activating properties. This work was carried out, not only in the hope of discovering a pteridine or related compound with a better  $\text{BH}_4$  mimetic profile but also with the aim of elucidating some of the properties that make blocked dihydropteridines such successful activators of NOS.

Chapter 1 provides an introduction to NOS and the field of pteridines and aims to put this work into its proper context.

Chapter 2 describes the work carried out towards a synthesis of a library of pteridines with variation at the 2-position. It also describes the development of challenging chemistry at the edge of what can be done with poorly activated pyrimidines.

Chapter 3 describes the targeted synthesis of an analogue of WSG1002 which has been expanded at the 2-position. This chapter presents some unusual and unpredictable chemistry observed when working with pyrimidines and the fused systems derived from them.

Chapter 4 presents the use of the Boon synthesis in an attempt to discover more active analogues of WSG1002. Variation was sought at the 5-, 6-, 7- and 8-positions

on the pteridine ring system. Resynthesis of two compounds for further study was also carried out.

Chapter 5 presents the work carried out in a bid to synthesise a deaza analogue of WSG1002. Here, pyridine chemistry was used extensively to provide a route to deazapteridines and other fused pyridines and the limitations of this chemistry are also presented.

Chapter 6 provides the biological and computational assessment of some of the compounds made and describes the in-depth evaluation of a select few. Two compounds in particular have an excellent profile when concerned with NOS activation and the data presented herein are being used to shape the development of future BH<sub>4</sub> mimetics.

Chapter 7 presents all of the experimental and analytical details.

# Chapter 1

---

## Introduction

### 1.1 General background to nitric oxide

Nitric oxide (NO) is a gaseous inorganic free radical, which plays a crucial role in many organisms as a cellular messenger and in host-immune responses.<sup>1-3</sup> The proper balance of NO within organisms is required for good health and an imbalance of NO is implicated in many disease states.<sup>1,4-8</sup> NO is produced by nitric oxide synthases (NOSs) which are multi-domain, homo-dimeric enzymes.<sup>9-12</sup> NO plays three major biological roles in mammals and is synthesised by three separate iso-enzymes:

- Immune responses, mediated by inducible-NOS (iNOS)<sup>12</sup>
- Vasorelaxation, mediated by endothelial-NOS (eNOS)<sup>9</sup>
- Neural signalling, mediated by neuronal-NOS (nNOS)<sup>11</sup>

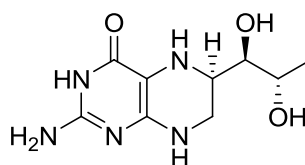
NO produced by iNOS plays an important role in a number of auto-immune responses. Inducible NO imbalance has been implicated in a number of disease states, including neurodegenerative diseases,<sup>13</sup> organ transplant rejection<sup>14,15</sup> and even vascular disease.<sup>7</sup> Most notably, NO has been implicated in septic shock and has been the focus of intense research and study over the last few decades.<sup>3,16-19</sup>

NO produced by eNOS has a central role in vasorelaxation and is the signalling molecule responsible for the relaxation of smooth muscle cells in the endothelium. Endothelial NO imbalance has been implicated in various disease states including hypertension,<sup>20</sup> atherosclerosis,<sup>21</sup> diabetic oxidative stress of the vasculature<sup>5,22,23</sup> and, as a result, heart attack and stroke.<sup>5</sup> The work carried out in this field led to the award of the 1998 Nobel Prize in Physiology or Medicine (to Robert F. Furchgott, Louis J. Ignarro and Ferid Murad) for the discovery of NO as a signalling molecule within the cardiovascular system. The award has undoubtedly furthered the expansion of research into this field.

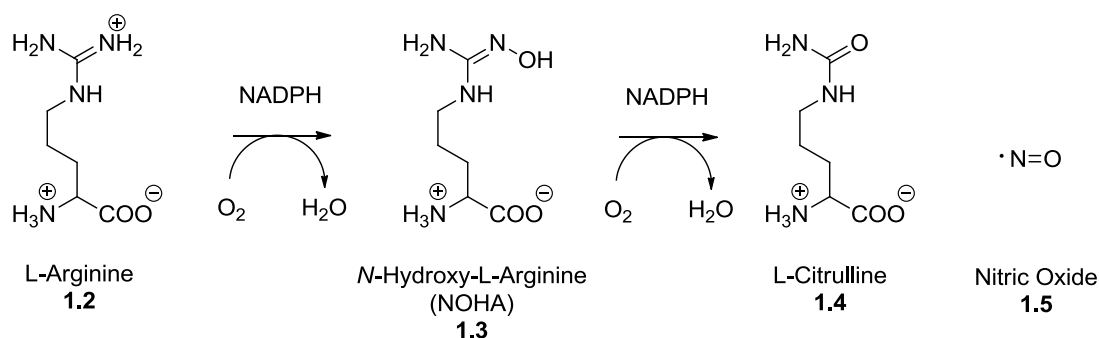
NO produced by nNOS plays a crucial role within the central nervous system (CNS) as a neural signalling molecule and is necessary for neuronal survival.<sup>24</sup> However, neuronal NO levels outside the normal range have been linked to a number of neurological diseases such as schizophrenia,<sup>6,24</sup> autism<sup>25</sup> and Alzheimer's disease.<sup>26</sup> Typically these diseases are associated with up-regulated nNOS, leading to cell death in crucial parts of the brain.<sup>27,28</sup> These pathological situations show that the ability to modulate NOS activity back to normal levels is one route of many by which a range of possible disease states could be treated; this is one of the primary concerns of this project.

Recently and far less widely studied, another form of NOS has been found within bacterial cells.<sup>29-33</sup> Bacterial NOS (bNOS) constitutes a new family of NOS isoenzymes and is an attractive new biological target for the development of new antibacterial agents.

NOS requires specific coenzymes in order to function properly, one of which is 5,6,7,8-tetrahydrobiopterin (BH<sub>4</sub>) **1.1**.<sup>34,35</sup> BH<sub>4</sub> (**1.1**) is a pteridine, which acts as an electron-shuttle in the enzymatic oxidation of L-arginine to L-citrulline and NO (**Scheme 1.1**). When the bioavailability of BH<sub>4</sub> (**1.1**) is limited, the production of NO drops significantly and NOS begins producing harmful, so-called reactive oxygen species (ROS) and reactive nitrogen species (RNS).<sup>36</sup> These molecules not only destroy what little NO there is but also contribute significantly to vascular oxidative stress.<sup>37</sup> For this reason, BH<sub>4</sub> (**1.1**) has recently received a large amount of interest as a potential drug to treat certain vascular diseases such as atherosclerosis.<sup>38,39</sup>

**1.1**



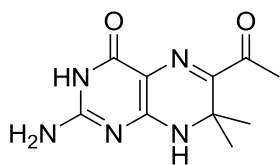


Scheme 1.1: The two mono-oxygenase reactions performed by NOS

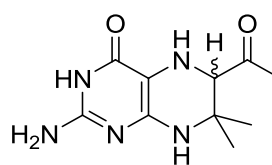
### 1.1.1 Origins of the project

Drugs that can modulate NOS activity are not well known; thus compounds that can act in this fashion should warrant further study. Similarly the molecular mechanism of NOS has not been fully characterised and compounds that can probe this could give valuable insight to the field. This line of thinking was the driving force behind the initiation of this project.

The chemistry of blocked dihydropteridines was first investigated by Wood in the late 1960s and extended greatly in collaboration with Suckling in the 1970s and 1980s.<sup>40,41,42</sup> Utilising geminal alkyl substituents at the 7-position forced the pteridine to remain at the dihydro oxidation level, hence the name, blocked dihydropteridines. In later years, some of these compounds were taken from the library and tested as potential NOS modulators. The results suggested that some compounds could act as activators or inhibitors and a programme to resynthesise and evaluate both these, and new derivatives, was initiated.<sup>43,44</sup> From these experiments one compound in particular stood out as causing a "...significant relaxation *in vitro* in rat pulmonary arteries depleted of  $\text{BH}_4$ ..."<sup>44</sup> and is known within our laboratory as WSG1002 (**1.6**). From this work it appeared that WSG1002 (**1.6**) was acting at the dihydro oxidation state and was a significantly more oxidatively stable alternative to  $\text{BH}_4$  (**1.1**). Later work suggested that WSG1002 (**1.6**) was somehow being reduced to the tetrahydro oxidation state (**1.7**) in order to act as a NOS activator.<sup>45</sup>



1.6



1.7

This project is primarily concerned with the synthesis of pteridines and their deaza analogues for use as NOS modulators, ultimately for application against the aforementioned disease states.

## 1.2 An overview of nitric oxide synthase and tetrahydrobiopterin

### 1.2.1 Nitric oxide synthase

Each NOS isoform has a distinct gene sequence from the others but the genomic structures share many similarities (**Table 1.1**) leading to the transcription of very similar proteins. The genes for each isoform occur on different chromosomes and are therefore transcribed independently of each other. There are few structural differences between the principal isoforms; however these differences affect enzymatic activity and the eventual biological outcome greatly.

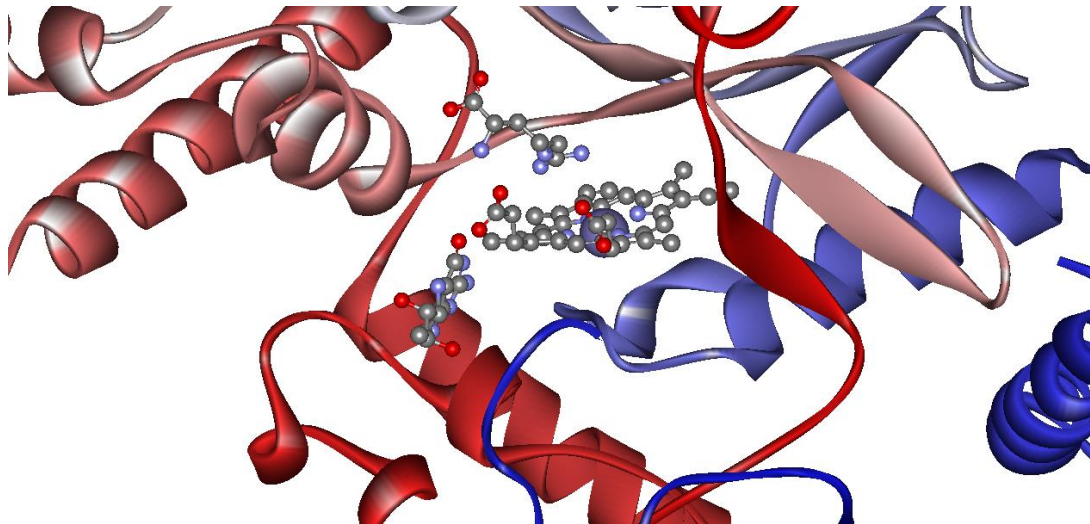
Human NOS isoform	Gene structure	Chromosomal location	Number of amino acids (aa) and protein size <sup>46</sup>
nNOS (NOS-1)	29 exons, 28 introns	Chromosome 12	1434 aa, 161 kDa
iNOS (NOS-2)	26 exons, 25 introns	Chromosome 17	1153 aa, 131 kDa
eNOS (NOS-3)	26 exons, 25 introns	Chromosome 7	1203 aa, 133 kDa

Table 1.1: Genetic information for the three principal human isoforms of NOS.

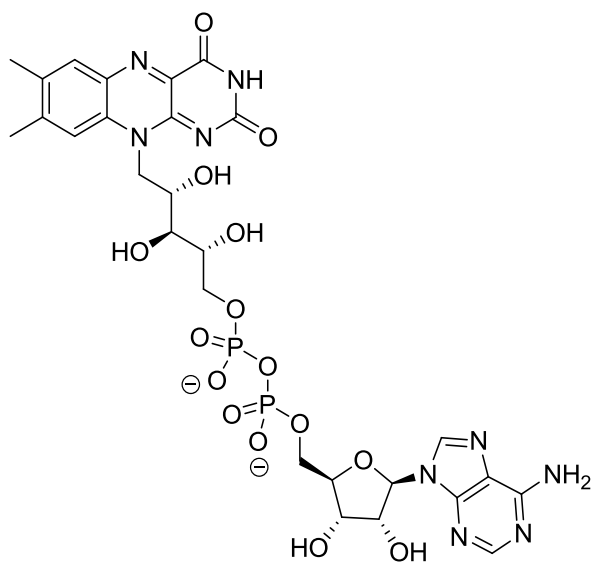
The principal splice variants of NOS (given the suffix  $\alpha$ ) catalyse the oxidation of L-arginine to L-citrulline and NO (**Scheme 1.1**). To facilitate this reaction, NOS utilises 7 different coenzymes and prosthetic groups.<sup>46-50</sup>

- A thiolate-bound iron haem, protoporphyrin IX (shown in **Figure 1.1**)
- Flavin adenine dinucleotide (FAD) **1.8**
- Fully reduced nicotinamide adenine dinucleotide phosphate (NADPH) **1.9**
- Flavin mononucleotide (FMN) **1.10**
- Zinc(II) ion (shown in **Figure 1.2**)
- Calmodulin (shown in **Figure 1.3**)
- BH<sub>4</sub> (**1.1**)

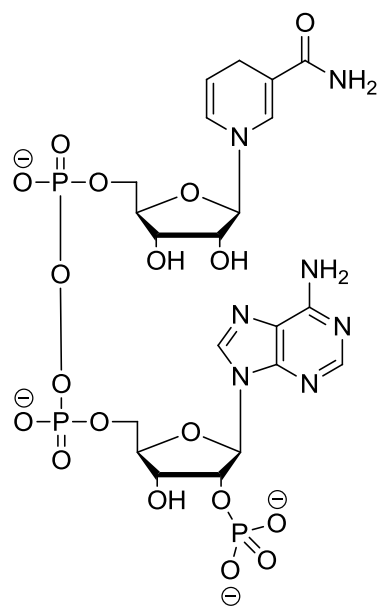
Each of these enzymes consists of an *N*-terminal oxygenase domain, which contains the haem, BH<sub>4</sub> (**1.1**) and the arginine-binding site. Each NOS also consists of a *C*-terminal reductase domain containing the FMN **1.10**, FAD **1.8**, NADPH **1.9** binding sites and a calmodulin binding site. For mammalian NOS to continue to produce NO, it must be in its coupled form. This refers to the fact that NOS is a homodimer (**Figure 1.2**) and electrons flow from the reductase domain of one monomer to the oxygenase domain of the other.<sup>51</sup> Whilst this adds an extra level of complexity to NOS catalysis, it presents an opportunity to augment the level of NO production. If, for example, the dimer can be destabilised, then NO production would fall. By the same rationale, if the dimer could be stabilised, then it is conceivable that NO production would increase.<sup>52-54</sup>



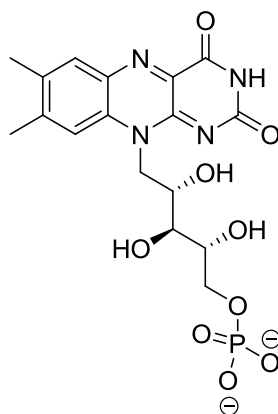
**Figure 1.1:** Tetrahydrobiopterin, L-arginine and iron haem in the active site of nNOS; arginine is seen immediately above the haem with BH<sub>4</sub> to the left close to the propionate side chains of the haem – Image constructed from the .pdb file 1OM4



1.8



1.9



1.10

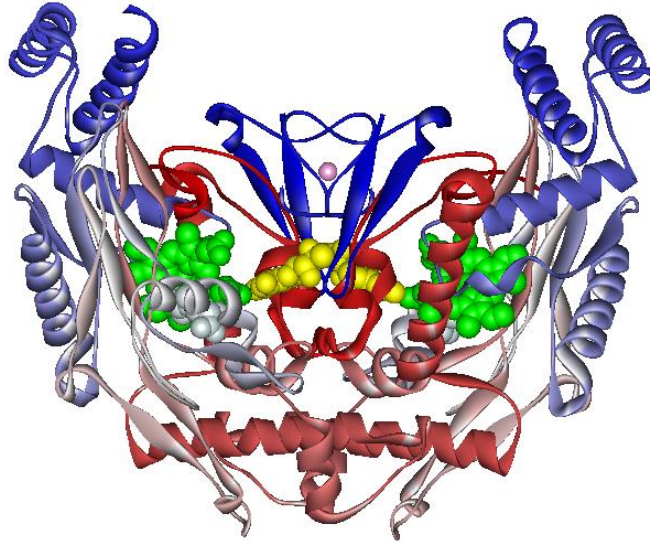


Figure 1.2: 1OM4 (pdb identifier) - nNOS coupled dimer with haem (green), BH4 (yellow), L-arginine (silver), zinc (pink)

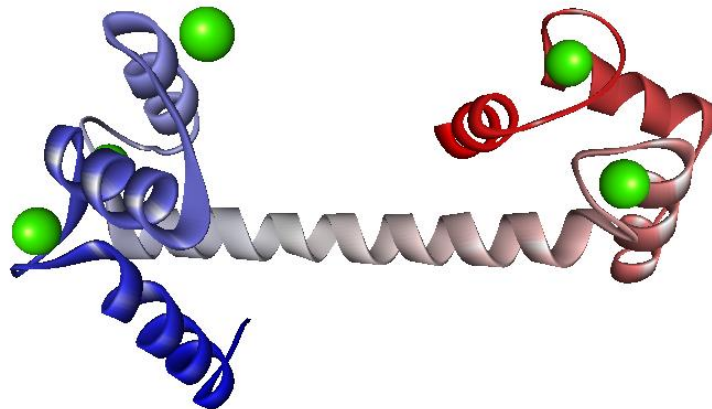


Figure 1.3: 1EXR (pdb identifier) - Calmodulin protein showing bound calcium ions (green)

The three mammalian isoforms of NOS share about a 50 – 60% sequence homology and are structurally very similar.<sup>2,51,55</sup> Much like cytochrome P<sub>450</sub>, at the catalytic centre of NOS's oxygenase domain is the haem with a cysteinyl thiolate as a proximal ligand. On the distal face of the haem is the space available for oxygen

binding and next to the haem is the available space for arginine. Arginine, which should be considered as the substrate for NOS, binds close to the haem but without direct interaction. The NOS oxygenase domain is highly conserved across isoforms and is extensively hydrogen-bonded to accommodate the appropriate cofactors. In another parallel to cytochrome P<sub>450</sub>, FAD (**1.8**) accepts two electrons at a time but will only transfer one to FMN (**1.10**), allowing mono-oxygenase chemistry.<sup>56</sup>

Associated with NOS's reductase domains, a small protein called calmodulin plays a crucial role in maintaining the quaternary structure. Calmodulin is a small, acidic protein that can bind four Ca<sup>2+</sup> ions. When calcium is bound to calmodulin in the NOS complex, a structural change is induced that initiates the electron-transfer cascade within NOS; this is the reason that NOS displays calcium dependence.<sup>12</sup> Interestingly, iNOS displays a lesser sensitivity to an external calcium concentration. As iNOS is the only isoform to lack an auto-inhibition loop, calmodulin displays a subtle increase in the affinity for calcium.<sup>57</sup> In fact, iNOS can remain active in the complete absence of an external calcium source due to its ability to retain calcium.<sup>58</sup>

Zinc(II) ions have been shown to have a subtle stabilisation role within the NOS dimer, with one zinc ion binding to four cysteine residues, one from each sub-unit, giving a zinc-tetrathiolate (ZnS<sub>4</sub>).<sup>9,48,59</sup> Interestingly, it appears that whilst the zinc has a positive effect towards stabilising the dimer, it is not necessary for catalysis. When the zinc is not present in the enzyme, the cysteines form disulfide bridges, which act in such a way as to stabilise the dimer partially.

There are differences between the structures and location of each isoform of NOS that allow each enzyme to behave in a different manner in their biological environment. nNOS and eNOS have been described as constitutive enzymes, as their genes are in a constant state of expression. iNOS has been described as an inducible enzyme, as its expression is dictated by external factors. nNOS is the most complex of the three isoforms and contains a PDZ binding domain, which is responsible for locating the protein within the nucleus of the neuron. nNOS and eNOS both contain an auto-inhibition loop (shown in **Figure 1.4**),<sup>46</sup> which can inhibit enzymatic activity by preventing electron-transfer *via* a conformational change. As iNOS lacks this feature, it is easier for this isoform to generate NO, compared with the other principal

isoforms. This is a feature that has been confirmed with splice variants of eNOS, which lack the auto-inhibition loop and have a higher turnover rate compared to the wild type.

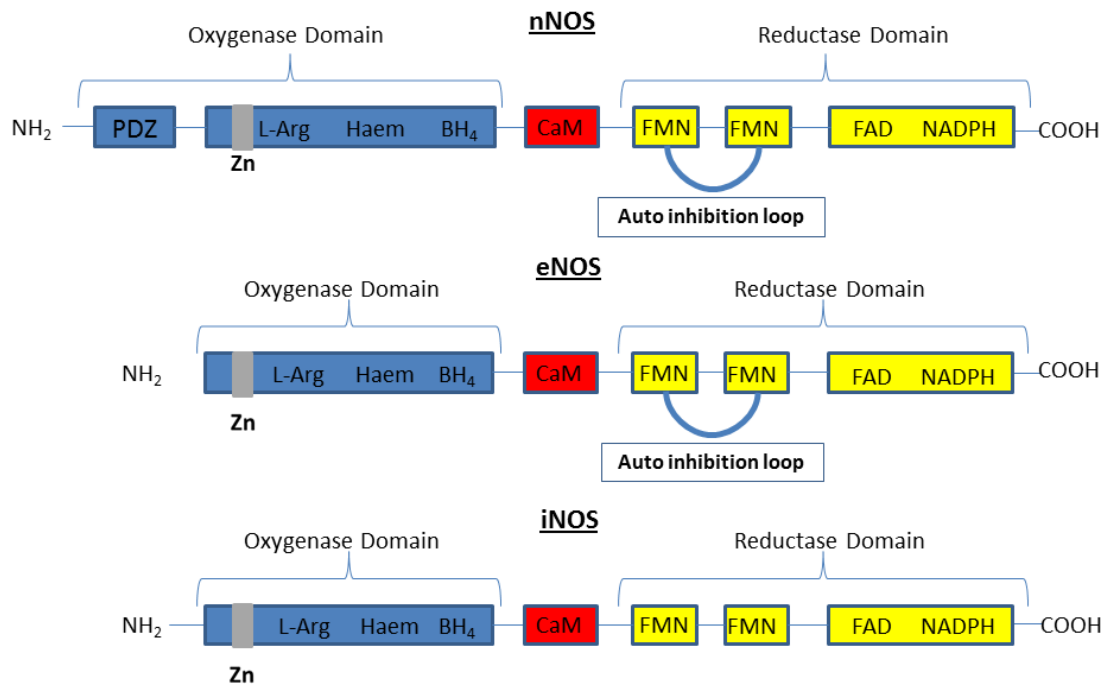


**Figure 1.4: Domain structures of the three principal isoforms of NOS divided into PDZ domain, dimer interface, calmodulin binding site and the reductase domain. Highlighted in grey is the zinc binding domain. Auto-inhibition loop shown for nNOS and eNOS.**

The final endogenous factor that affects NO production is BH<sub>4</sub> (**1.1**). BH<sub>4</sub> (**1.1**) binds within the oxygenase domain of NOS with the pyrimidine ring forming essential hydrogen bonds with the haem. BH<sub>4</sub> (**1.1**) binds near the dimer interface and its binding site includes residues from both oxygenase subunits and stacks between a tryptophan and a phenylalanine residue (**Figure 1.5**).<sup>60,61</sup>

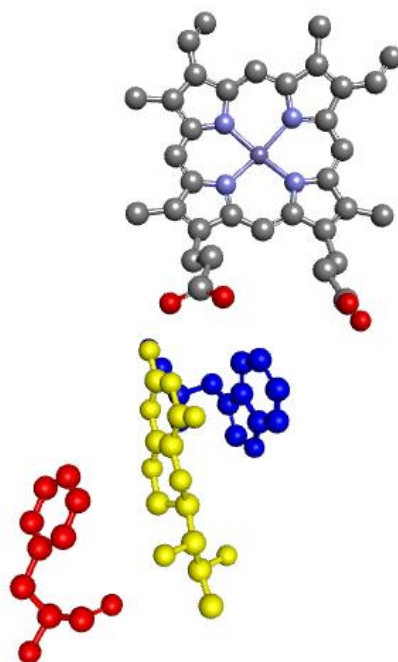


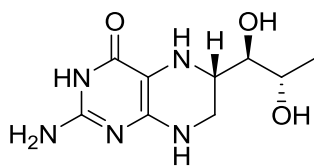
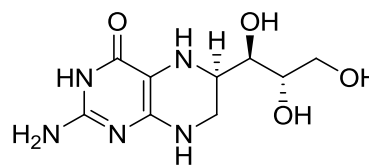
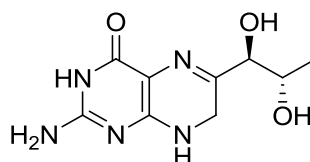
Figure 1.5:  $\text{BH}_4$  (yellow) stacked between phenyl alanine (red) and tryptophan (blue). Image constructed from X-ray data of bovine eNOS - 1NSE (protein databank file identifier).

As previously mentioned, the importance of  $\text{BH}_4$  (**1.1**) to catalysis is clearly highlighted by enzymatic activity shutting down upon removal of the coenzyme. This is further demonstrated by activity being returned again to the system upon reintroduction of  $\text{BH}_4$  (**1.1**).<sup>34,35,50</sup> Several interesting points have been noted when comparing data from studies with  $\text{BH}_4$  structural analogues:<sup>51</sup>

- NOS shows selectivity for substituents at C6. This is highlighted by NOS utilizing the natural (6*R*)- $\text{BH}_4$  (**1.1**) diastereomer and not the unnatural (6*S*)- $\text{BH}_4$  (**1.11**). This is further exemplified by (6*R*)-tetrahydroneopterin (**1.12**), which has an additional hydroxyl group in the side chain, not being employed by NOS for catalysis.<sup>62</sup>
- The tetrahydro oxidation state may not be necessary for binding but is required for catalysis. This is highlighted by the fact that  $\text{BH}_2$  (**1.13**) will bind to NOS but cannot act as a coenzyme.<sup>51</sup>
- Binding site occupation with arginine increases affinity towards  $\text{BH}_4$  (**1.1**) and *vice versa*.<sup>51</sup> Interestingly, this appears not to be the case with the  $\text{BH}_4$  analogues discussed in **Chapter 6**.



- Binding of BH<sub>4</sub> (**1.1**) to one subunit has a detrimental effect to binding in the other by an order of magnitude.<sup>51</sup>

**1.11****1.12****1.13**

BH<sub>4</sub> (**1.1**) has a number of roles in NOS activity. Firstly, it acts as a single-electron donor to the haem and is a pivotal control point for allowing the mono-oxygenase chemistry to take place. Secondly, through an extended series of  $\pi$ -stacking interactions and hydrophobic interactions (**Figure 1.5**), BH<sub>4</sub> (**1.1**) has been implicated in stabilizing the homodimer.<sup>56</sup> Finally, BH<sub>4</sub> (**1.1**) has an effect upon the spin state of the haem iron. It has been reported that BH<sub>4</sub> (**1.1**) shifts the equilibrium from the inactive low-spin state to the active high-spin state.<sup>51</sup>

### 1.2.2 Exogenous regulation and protein-protein interactions

The activity of NOS is regulated by controls on both the enzyme and its cofactors. Regulation is controlled either at the genetic, the epigenetic or the enzymatic level by specific proteins. Whilst the epigenetic processes are just beginning to be understood and therefore wider investigation into these processes would hopefully be forthcoming in the near future, the genetic and enzymatic level interactions are better characterised.

At the genetic level, two proteins have been characterised as being able to influence eNOS levels, namely NF- $\kappa$ B (nuclear factor  $\kappa$  B) and KLF2 (Küppel-like factor 2).<sup>46,63</sup> NF- $\kappa$ B is activated in high laminar shear stress environments, such as that observed in hypertensive patients. High levels of NF- $\kappa$ B activity leads to the

translocation of p50/p65 heterodimers to the nucleus of the endothelial cell. These factors bind to the eNOS gene promoter region and lead to increased gene transcription and therefore higher levels of eNOS. NF- $\kappa$ B is considered to be part of a self-terminating control-loop that assists in the regulation of normal blood-pressure. This is achieved by two main factors. Firstly as the levels of NO rise, the blood vessels dilate and the levels of translocating p50/p65 drop due to lowered shear-stress. Secondly, when NO levels are sufficiently high, nitrophosphorylation of p50 occurs and the activation of the eNOS promoter region ceases entirely.

It is thought that NF- $\kappa$ B is involved in the short-term up-regulation of eNOS, whereas KLF2 is involved in the more long-term up-regulation.<sup>63</sup> KLF2 is a major transcription factor, activated by prolonged shear stress and acting by stabilising eNOS mRNA three-fold. Whereas the effects of NF- $\kappa$ B are maximally efficacious after 15-20 minutes, KLF2 takes hours to make its effects felt. KLF2 is also involved in the self-terminating control-loop as, when levels of NO are sufficiently high, KLF2 interferes with the p65 domain and further halts the activation of the gene-promoter region.

Several genes are directly responsible for BH<sub>4</sub> levels; however, mutations in four main genes have been linked with abnormally low levels, namely, *GCHI*, *PTS*, *PCBD1* and *QDPR*. More than 200 mutations have been catalogued that could lead to lowered levels of BH<sub>4</sub> through interference with, or mutations to, these genes.<sup>63-67</sup> It is conceivable that BH<sub>4</sub> supplements or BH<sub>4</sub> mimetics could provide a useful treatment to the diseases caused by these mutations. *GCHI* is the gene responsible for the production of the protein GTPCH-1, the enzyme involved in the rate-determining step in the *de novo* synthesis of BH<sub>4</sub>. *PTS* is the gene sequence responsible for the production of the protein 6-pyruvoyltetrahydropterin synthase (6-PTS) and is another of the proteins involved in the *de novo* synthesis of BH<sub>4</sub> (discussed later in Scheme 1.5). *PCBD1* is the gene responsible for the production of 4a-hydroxytetrahydrobiopterin dehydratase, one of the proteins responsible for recycling BH<sub>4</sub> during the aromatic amino acid hydroxylase reactions (discussed in detail later in scheme 1.6). Finally *QDPR* is the gene responsible for the production

of dihydropterin reductase, another of the proteins involved in recycling  $\text{BH}_4$  during the aromatic amino acid hydroxylase reactions.

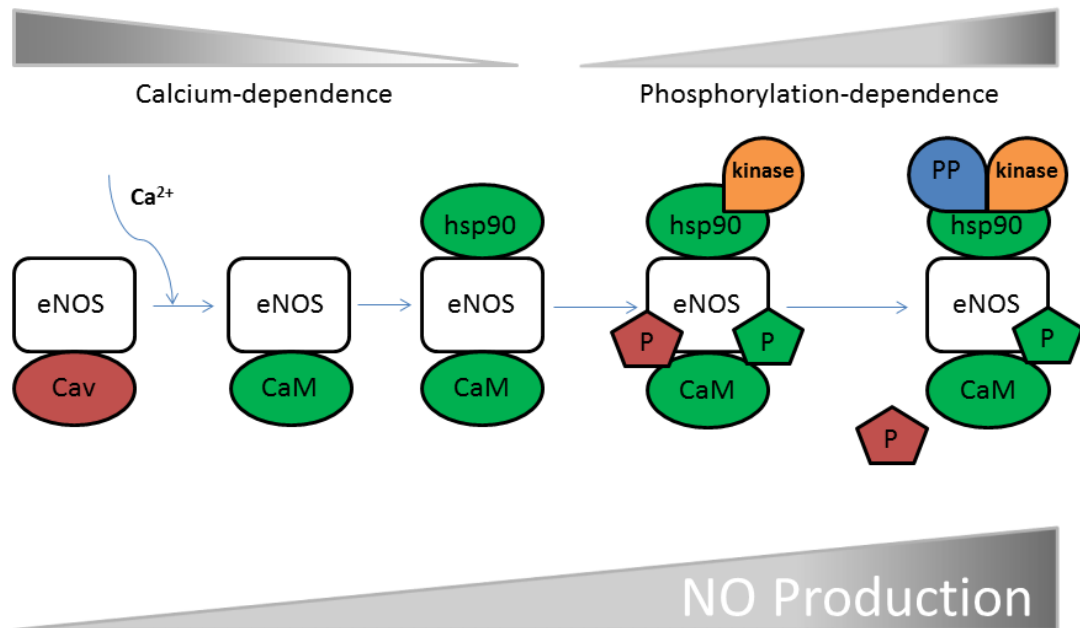


**Figure 1.6:** Showing the various protein-protein interactions that modulate eNOS activity with the left hand side of the diagram shows the protein combination that produces the least amount of NO and moving right shows the protein combinations that produce increasing amounts of NO. Cav represents the coat-protein caveolin, CaM represents calmodulin, hsp90 represents heat shock protein-90, PP represents a protein phosphatase and kinase represents any one of several bound protein kinases. P in red represents an inhibitory phosphorylation site and the P in green represents an activating phosphorylation site.

Lipidation, phosphorylation, *S*-nitrosylation and protein-protein interaction are the main post-translational modifiers that affect the function of NOS and are summarised above in **Figure 1.6**.<sup>46,68</sup> There are three sites on eNOS that undergo lipidation, the N-terminal glycine residue, cysteine-15 and cysteine-26. The N-terminal glycine undergoes an irreversible myristoylation and is a co-translational process. In contrast to this, reversible palmitoylation occurs on the cysteine residues and is a post-translational process. Lipidation on all three sites provides suitable anchors for the ‘coat-protein’ caveolin, which sequesters eNOS to micro-domains of the cell membrane and directly inhibits enzymatic-activity. Prolonged agonist stimulation of eNOS, typically high  $\text{Ca}^{2+}$ /CaM concentration, induces depalmitoylation, triggering eNOS translocation from the lipid bilayer. Depalmitoylation is catalysed by the acyl-

protein thioesterase-1 (APT-1)<sup>46</sup> and it is thought that these combined factors are a part of the dynamic regulation of eNOS activity.

Phosphorylation and, indeed, dephosphorylation networks are another of the post-translational regulators that affect eNOS activity.<sup>46,68</sup> There are several protein kinases and protein phosphatases that regulate this network and the relative order of importance is still under investigation. However, what is clear is that activity is dependent upon the site of phosphorylation and not simply whether eNOS has or has not been phosphorylated. Phosphorylation on three key serine residues (Ser-1177, Ser-635 and Ser-617) serves to inhibit calmodulin dissociation and increase the rate of internal electron-transfer, thus further increasing eNOS activity. Phosphorylation on these sites is catalysed by several different kinases and provides multiple points of enzymatic regulation and potential intervention. Phosphorylation on threonine-495 and serine-116 have an inhibitory effect on eNOS activity by attenuating the enzyme's ability to bind calmodulin. Accordingly, dephosphorylation by protein phosphatases enhances eNOS interactions with calmodulin, causing an increase in enzymatic activity.

Reversible *S*-nitrosylation is understood to be another dynamic control-point for eNOS activity, with increasing levels of *S*-nitrosylation decreasing the levels of NO production.<sup>63</sup> Opinion is divided on the mechanism of how *S*-nitrosylation affects eNOS. Some think that the disruption of the zinc-tetrathiolate cluster causes dimer-uncoupling (a mechanism that has been proposed for iNOS too) whilst others think that *S*-nitrosylation modifies substrate or coenzyme binding.<sup>63</sup> It has even been proposed that electron-transfer could be diminished at the interface between the coupled-monomers and the mechanisms are the topic of further study within the field. What is clear, though, is that effective inhibition of eNOS by *S*-nitrosylation is specific to sub-cellular location.<sup>63</sup> The environment experienced by eNOS when sequestered by caveolin – high hydrophobicity – is conducive to forming *S*-nitrothiols, whereas the reducing environment of the cytosol may be supportive of de-nitrosylation.

The interactions of HSP-90 (heat shock protein-90, **Figure 1.7**) and NOS are some of the best understood protein-protein interactions and the interactions of HSP-90 with

eNOS has been well characterised. Not only is HSP-90 responsible for the insertion of the haem and, therefore, initial formation of the active dimer, it also acts as a chaperone-protein.<sup>27</sup> HSP-90 enhances the affinity between eNOS and calmodulin as well as facilitating the binding of specific protein kinases. It has been reported that HSP-90 can bind both active and inactive Akt (a protein kinase) and is required for the interaction between eNOS and Akt (amongst other kinases). This suggests that, for maximal activation of eNOS, HSP-90 must be present. It has also been reported that HSP-90 activates eNOS at both physiological calcium concentrations as well as environments free of calcium.<sup>46,68</sup>

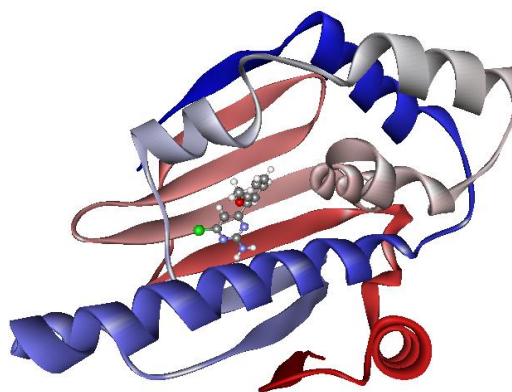
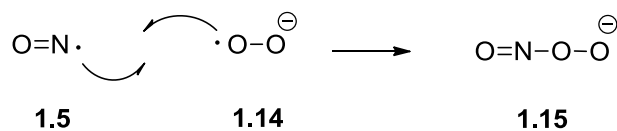


Figure 1.7: 3R4M (pdb identifier) - HSP90 with inhibitor bound<sup>69</sup>

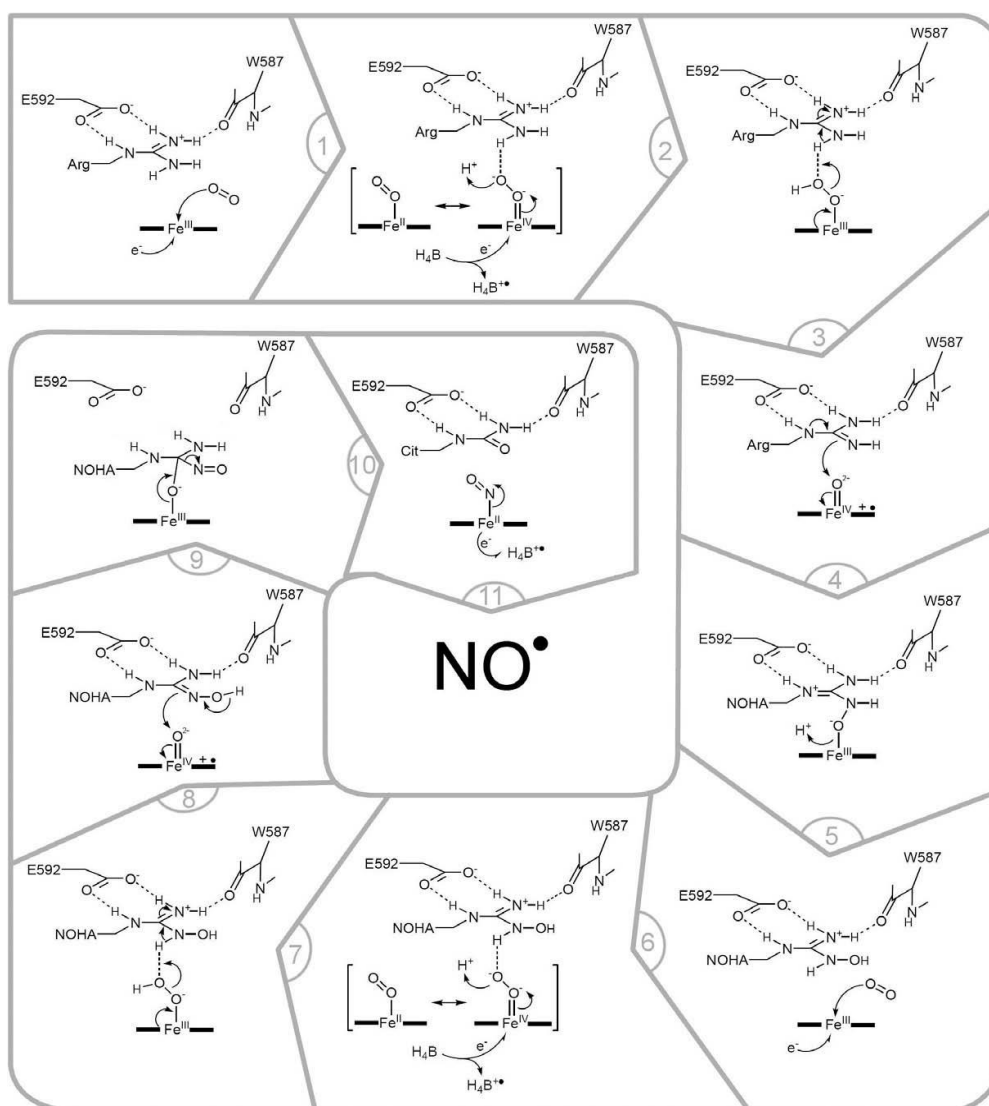
Uncoupled NOS will not bind L-arginine and will instead form the reactive oxygen species (ROS), superoxide ('O-O') **1.14** and hydrogen peroxide after oxygen binding to the haem. Not only are these ROS harmful to the body but superoxide can react with nitric oxide **1.5** (Scheme 1.2) to form the reactive nitrogen species (RNS), peroxynitrite **1.15**. The negative impact is two-fold, as it will reduce the concentration of available NO and it will also damage NOS, causing further uncoupling. The impact of these reactive species is discussed later in section **1.2.3**.



Scheme 1.2: Formation of peroxynitrite

### 1.2.3 The molecular mechanism of NO synthesis

Since the first studies into NOS concerning the mechanism of action were undertaken, it has been clear that the suggested mechanistic detail was being heavily influenced by knowledge gained from studies of cytochromes  $P_{450}$ .<sup>11,70</sup> There are both advantages and disadvantages arising from this situation. Much mechanistic detail has been understood and much can be presumed as a logical extension of  $P_{450}$  chemistry.<sup>11,70,71</sup> However, in the last few years, the assumptions about the biochemistry have fallen into question and the *precise* mechanism of the mono-oxidation reactions is still unknown. Shown below (**Scheme 1.3**) is a commonly accepted working model for the molecular mechanism of NOS.<sup>47</sup>



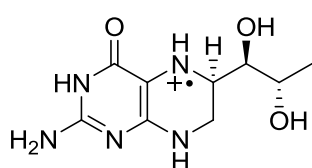
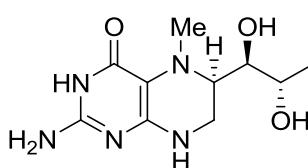
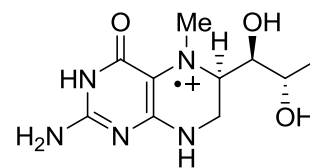
**Scheme 1.3:** A basis for the molecular mechanism of NOS<sup>47</sup>

In step one, the reduction of Fe(III) occurs, *via* a one-electron transfer process, facilitating the formation of the oxyferrous complex. The working hypothesis suggests that two electrons are transferred from NADPH (**1.9**) to FAD (**1.8**) and then FMN (**1.10**) before being transferred to the haem. It is generally thought that either FMN (**1.10**) or BH<sub>4</sub> (**1.1**) can act as a single-electron donor at this stage. Step two shows another single-electron transfer, along with protonation, to form the (presumed) hydroperoxy species.<sup>51</sup> Step three shows the abstraction of a guanidine proton from arginine to allow the liberation of one molecule of water and the formation of the oxyferryl species. Step four shows the regeneration of the Fe(III) species and the formation of the guanidinium intermediate which, when protonated in step five, produces NOHA (**1.3**). These five steps are collectively known as the first mono-oxygenation reaction of NOS (**Scheme 1.3**). This type of mono-oxygenase reaction is typical of P<sub>450</sub> biochemistry and serves to highlight the positive role that P<sub>450</sub> has played in elucidating NOS biochemistry.<sup>72</sup>

Step six shows the catalytic cycle beginning again with the regeneration of the oxyferrous complex *via* a one-electron transfer process. In step seven, the hydroperoxy species is again generated *via* a one-electron transfer process and protonation. Step eight again shows proton abstraction to liberate one molecule of water and form the oxyferryl intermediate. Step nine shows the formation of the tetrahedral intermediate and reduction of the oxyferryl species, priming the system for collapse to liberate citrulline and to form the Fe(II)-bound nitrosyl group seen in step ten. Step eleven shows the homolytic cleavage to the Fe-N bond to generate nitric oxide and regenerate the fully reduced pterin (**1.1**). It is presumed that the driving force behind the homolytic cleavage of the Fe-N bond is the regeneration of the fully reduced BH<sub>4</sub> (**1.1**). These six steps are collectively known as the second mono-oxygenase reaction of NOS (**Scheme 1.3**). This biochemistry is highly unlikely to be carried out in the usual P<sub>450</sub> manner. Typically within P<sub>450</sub>, two electrons are passed directly to the haem – a process that seems unlikely when the final homolytic step is taken into consideration.

Steps two, six and eleven all appear to require single-electron transfer between the haem and BH<sub>4</sub>. It is also probable that the electron-transfer processes in steps one

and six involve  $\text{BH}_4$ . It is the commonly held belief that an electron donated from  $\text{BH}_4$  originates from the  $N^5$  position on the pterin (**1.16**). Limited work has been performed to assess the effect of a more stable radical at this position. It has been suggested that an analogue which will more quickly transfer an electron to the haem could increase the rate of nitric oxide production. The most promising candidate for this is 5-methyl- $\text{BH}_4$  (**1.17**) which was found to donate an electron to the haem three times faster than  $\text{BH}_4$  (**1.1**), reportedly due to the increased stability of the radical (**1.18**) compared with (**1.16**).<sup>73-79</sup> However this effect is only observed at saturation levels of the pterin. 5-Methyl- $\text{BH}_4$  (**1.17**) actually functions as a poorer cofactor at comparable concentrations to  $\text{BH}_4$ .

**1.16****1.17****1.18**

Recently, and in two quite separate reviews, both Daff and Santolini suggested that there was no longer any reason to view NOS through a veil of  $\text{P}_{450}$  chemistry.<sup>47,56</sup> Furthermore, they suggested that, due to the presence of a pterin within the haem environment of NOS, now almost universally thought to have a redox role, that electron transfer within NOS is likely to be distinct from that in cytochrome  $\text{P}_{450}$ . When consulting the literature, it appears that there are three schools of thought for the mechanistic role of  $\text{BH}_4$  (**1.1**):

- The pterin solely plays a role in stabilising the dimer.
- The pterin is stabilising the dimer and playing a redox role in both mono-oxygenase reactions (**Scheme 1.1**).
- The pterin is not only stabilising the dimer but is playing a redox role solely in the first mono-oxygenase reaction (**Scheme 1.1**).

This first line of argument has all but been discredited and both literature precedent<sup>56</sup> and evidence discussed in **Chapter 6** will add weight to the contrary of this line of thought. Nevertheless, it is still held, by some, as a reasonable possibility and



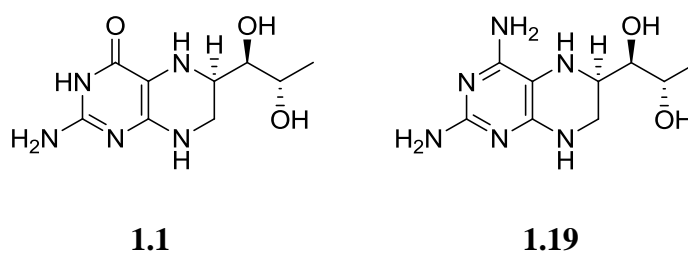
warrants a brief discussion. This argument favours a strictly structural role within NOS by stabilising the dimer. As previously stated, dimerisation is an essential process in NOS functioning as it allows the active site (oxygenase domain from one subunit) to adopt an active conformation (positioned next to the reductase domain from the other subunit), referred to as the coupled dimer. Without the pteridine stabilising this active coupled-dimer, NO production is halted. Santolini suggested that, when observing subtle differences between iNOS and the other isoforms, it is not necessary to limit BH<sub>4</sub> (**1.1**) to a purely structural role.

The next line of thought is centred on the observation made by Stuehr that BH<sub>4</sub> (**1.1**) accelerated the collapse of Fe-O<sub>2</sub> complex during the first oxidation sequence (step three).<sup>80</sup> It was also noted that NOHA could be made from the nNOSoxy (oxygenase domain) Fe(II)O<sub>2</sub> complex solely in the presence of BH<sub>4</sub> (**1.1**) in a single turnover experiment. This suggested that BH<sub>4</sub> (**1.1**) could play a redox role in the first mono-oxygenase reaction. Furthermore, the BH<sub>4</sub> radical (**1.16**) has been directly observed by EPR studies under cryogenic conditions.<sup>76</sup> The final important piece of evidence concerns the kinetic link between the stability of the pterin radical and the decomposition rate of Fe(II)O<sub>2</sub>. It appears that the more stable radical generated when using 5-methyl-BH<sub>4</sub> (**1.17**) accelerates the rate of electron transfer to three times that of BH<sub>4</sub> (see **Figure 1.14** for a fuller explanation as to radical stability).<sup>74</sup> This appears to be a fairly well established mechanism; however, the nature of whether the electron transfer is coupled to a proton transfer is still hotly debated.<sup>47,56,81</sup>

Opinion on the second mono-oxygenase reaction is still divided and due to the consumption of only one NADPH-derived electron, it appears that typical P<sub>450</sub> chemistry no longer applies. Single-electron-transfer chemistry is unknown in cytochrome P<sub>450</sub> mechanisms. Again, it appears that disappearance of the Fe(II)O<sub>2</sub> complex (step eight) is kinetically coupled to BH<sub>4</sub> (**1.1**), suggesting a mandatory role for BH<sub>4</sub> (**1.1**) in the electron-transfer process. It has been shown that NOHA (**1.3**) can form citrulline and NO with only one additional electron and it is also known that BH<sub>4</sub> (**1.1**) can readily donate a single electron. When considering this, it appears logical that BH<sub>4</sub> (**1.1**) could be the source of this single electron. To take another

view, DFT calculations suggest that electron transfer from  $\text{BH}_4$  (**1.1**) to the haem would be energetically less favourable than electron-transfer from NOHA itself.<sup>81-84</sup> As a result of these calculations, opinion remains divided on the matter. Even with the controversy surrounding the mechanistic detail, a popular example of the most widely accepted mechanism was demonstrated by Daff in his most recent review and is shown above in **Scheme 1.3**.<sup>47</sup> It should be noted, however, that by Daff's own admission, this mechanism is merely a starting point for the molecular process and needs further development.

In steps two, five and seven (**Scheme 1.3**) it can be seen that a proton source is required. The origin of these protons is a further point of debate within the field. It is also not known whether proton transfer is coupled to electron transfer – resulting in a hydride transfer similar to that seen in NADPH – or whether it is a separate process. The most commonly held view is based on  $\text{P}_{450}$  chemistry with two separate protonation steps to form a ferric-peroxide species (steps 2 and 7 in **Scheme 1.3**). Again, Santolini casts doubt on this by highlighting the not-insignificant differences in the active sites of NOS and  $\text{P}_{450}$ . As it stands, there are three possibilities for the source of the proton.  $\text{BH}_4$  **1.1**; this seems possible as the relatively acidic proton at  $N^3$  ( $\text{pK}_a = 10.6$ )<sup>51</sup> could be a likely donor. Further weight to this argument is added when the role of 4-amino- $\text{BH}_4$  **1.19** is considered. 4-Amino- $\text{BH}_4$  (**1.19**) is an inhibitor of NO synthesis and lacks the proton at  $N^3$ , suggesting a role for this particular proton in the molecular mechanism is a possibility.



L-Arginine is another possible source of a proton and the main thrust of this argument derives from crystal structures obtained by Crane.<sup>61</sup> The data show a very short distance (less than 5 Å) between the guanidinium group of arginine and the haem iron. It was suggested that arginine could bind to the haem in its protonated form and act as a proton source (seen in **Scheme 1.3**). Again, DFT calculations

suggest that this could be energetically less favourable than a mechanism which includes  $\text{BH}_4$  (**1.1**) and water.<sup>85</sup>

The role of water cannot be ruled out. This is not just because it is present in abundance in the active site (**Figure 1.8**) but also because the role of a distal water has been shown to influence the electronic properties of the  $\text{Fe(II)O}_2$  complex.<sup>86</sup>

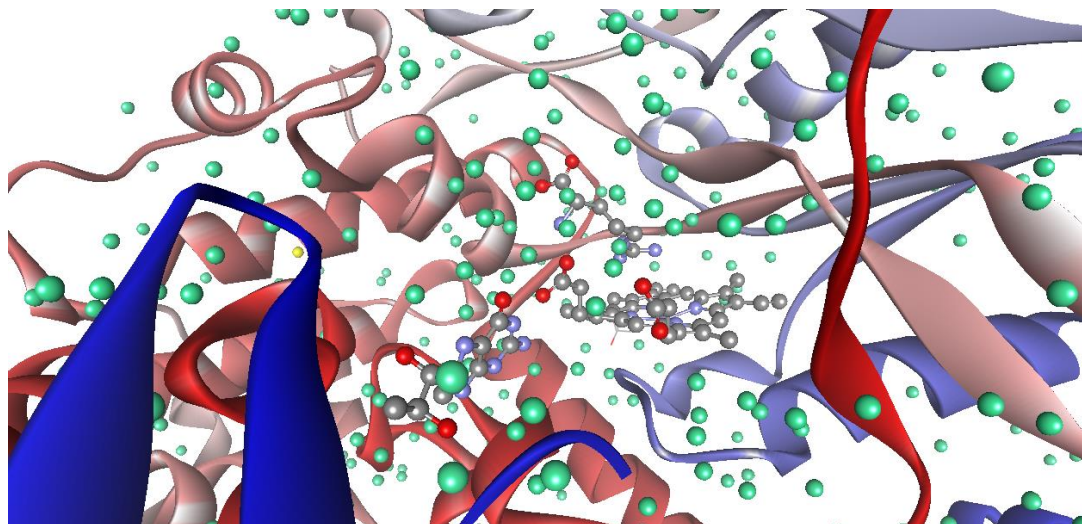


**Figure 1.8:** 10M4 (pdb identifier) - water molecules (in pale green) can access a large volume of space within NOSs and could play a role in proton-transfer within the molecular mechanism of the oxygenase reactions

If it has been shown that little is known about the role of proton transfer within the first mono-oxygenase reaction, it can be stated that even less is known about it in the second step.<sup>87</sup> It is markedly more difficult to make observations on this reaction as it is not the rate determining step in NO biosynthesis, limiting observations to single turnover reactions.<sup>73,74,88</sup>

#### **1.2.4 The isoforms of NOS and their role in selected disease states**

Depending on the concentration and the site of action, NO can have many beneficial<sup>39,89-94</sup> or harmful effects.<sup>7,25-27,91,95</sup> As a result of this widespread action, NO has been implicated in many disease states spanning all the isoforms of NOS, including bNOS. As previously mentioned, the launch point for research into this area was from the award of the Nobel Prize concerning the role of NO in the vascular system. As a result, much of the early work in this field was concerned with

activating eNOS to treat endothelial dysfunction (**Figure 1.9**) and is also the primary concern of this thesis.

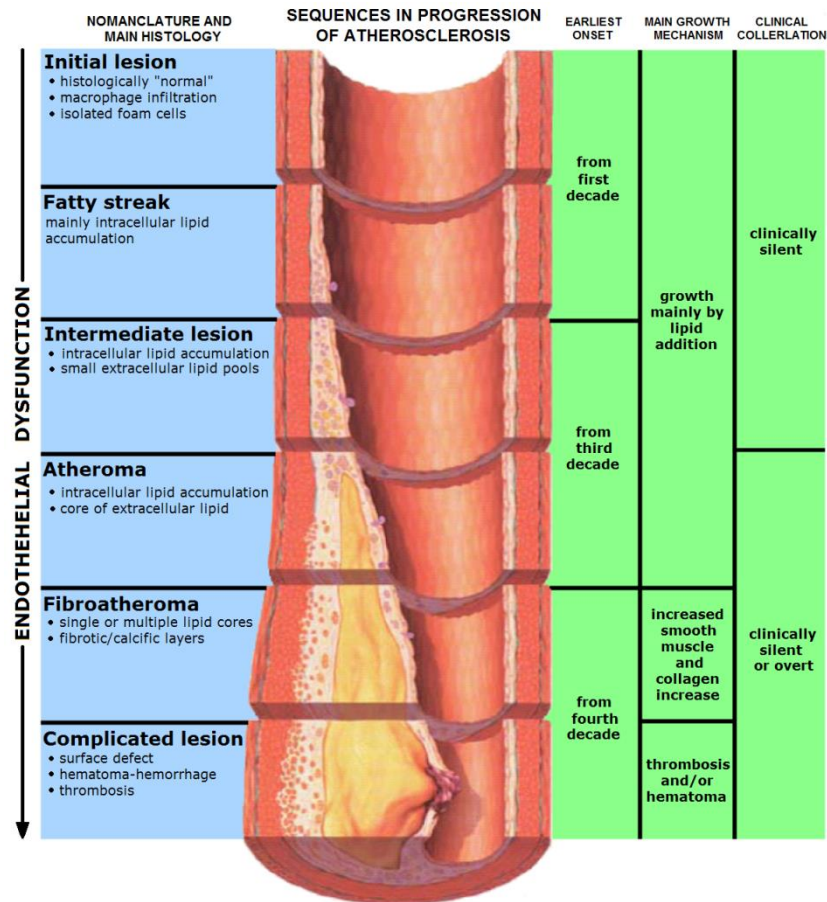
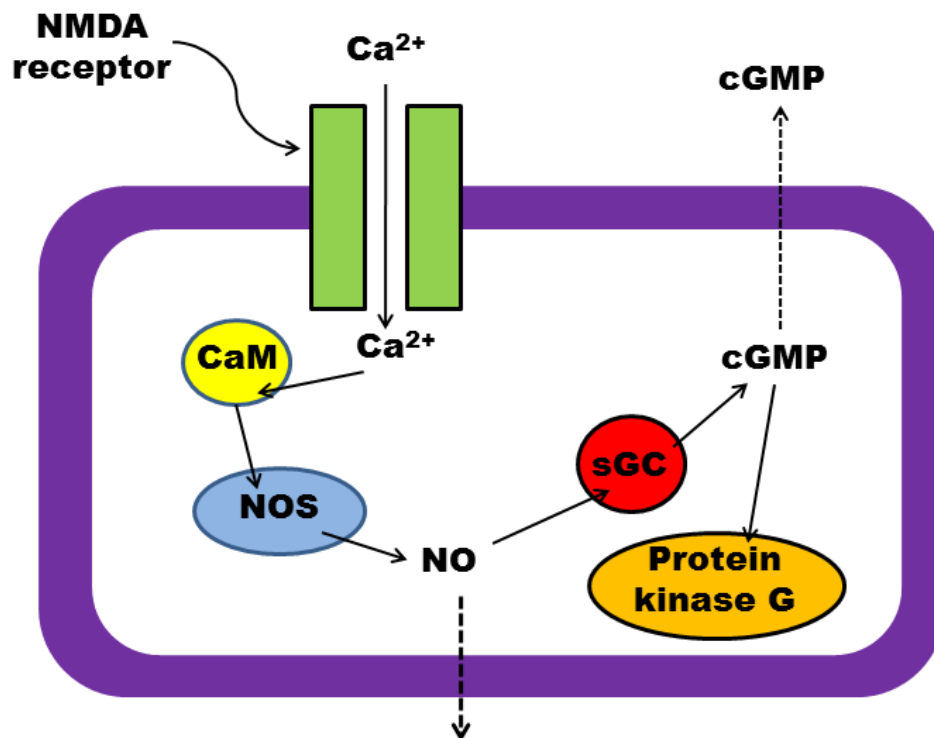


Figure 1.9: Endothelial dysfunction progression<sup>96</sup>

The disease states affected by eNOS originate from a low bioavailability of NO and a high bioavailability of ROS and RNS. Often this is caused by uncoupling of the active NOS dimer and can be further traced back to poor BH<sub>4</sub> bioavailability (as mentioned in **Section 1.2.2**). The lowering of BH<sub>4</sub> bioavailability is not solely dependent on genetics and is often caused by the products of other enzymes interacting with BH<sub>4</sub>. NADPH oxidase is largely responsible for oxidative degradation of BH<sub>4</sub> by producing large amounts of ROS, such as superoxide.<sup>97</sup> The damage caused by NADPH oxidase is not limited to oxidative degradation of BH<sub>4</sub> but is also linked to higher levels of eNOS transcription. At first glance, this may appear to be a defence against over-production of ROS and RNS; however, upregulation of eNOS is not accompanied by an upregulation of GTPCH-1. Therefore, unusually high activity of NADPH oxidase produces high levels of

*uncoupled* eNOS and only serves to increase further ROS and RNS levels. This fact further highlights the need for therapies that make use of BH<sub>4</sub> or BH<sub>4</sub>-mimetics.

Soluble guanylyl cyclase (sGC) is the principal receptor for freely diffusible nitric oxide and is the biological target which mediates the action of nitroglycerine, within certain angina medication (**Figure 1.10**).<sup>95,98</sup> As NO binds to the haem of sGC, the enzymatic cyclisation of GTP to cytosolic cyclic-GMP (cGMP) occurs. In turn cGMP targets many different classes of downstream effectors, such as ion channels and protein kinase G. In the case of eNOS, its location within endothelial cells and activation of protein kinase G ultimately causes vasodilation by the relaxation of smooth muscle cells. Eventually, these responses are terminated by phosphodiesterases, which are responsible for the hydrolysis of cGMP to 5'-GMP.<sup>98</sup>



**Figure 1.10:** Schematic showing the NO-cGMP pathway

nNOS is the most important isoform in the CNS and is highly expressed in the cerebellum.<sup>25</sup> Here, the major function of NO is to act as a retrograde signal by transferring information from postsynaptic neurons to presynaptic nerve endings (**Figure 1.11**). Nitric oxide travels by rapid passive diffusion.

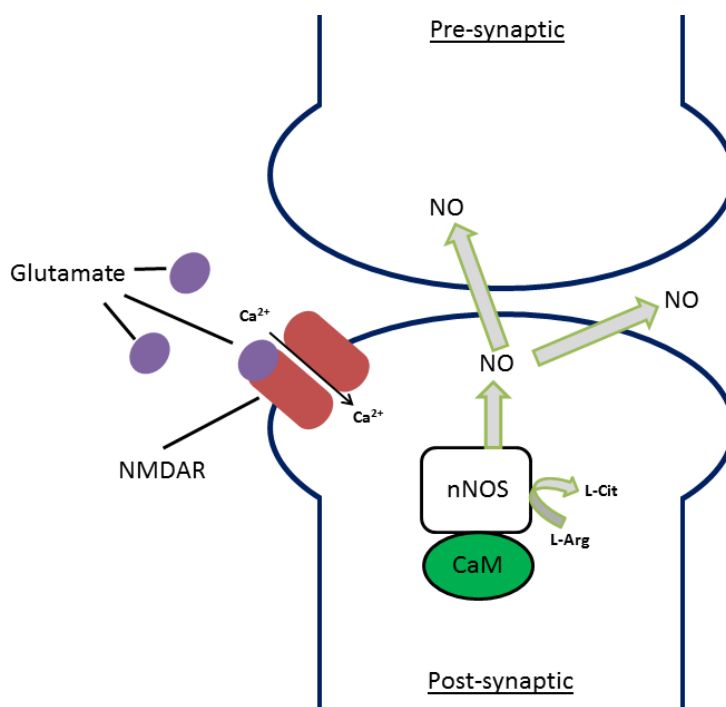


**Figure 1.11: Extracellular signalling ability of nitric oxide. NMDAR is the *N*-Methyl-D-aspartate receptor. CaM is calmodulin<sup>25</sup>**

Low levels of NO are neuroprotective; however, high levels are neurodegenerative and it is for this reason, amongst others, that several NOS inhibitors have been developed.<sup>98-102</sup> One way in which neuronal cell death occurs is the production of RNS from over-expressed NOS. This offers researchers in the field a potential therapeutic target for treating several neurodegenerative diseases, such as schizophrenia, Parkinson's disease, age-related learning difficulties and Alzheimer's disease, to name but a few.<sup>1,6,16,25,27,92,103</sup> The majority of the NOS inhibitors developed to date are L-arginine analogues, such as *N*<sub>ω</sub>-nitro-L-arginine methyl ester (L-NAME **1.20**) or *N*<sup>G</sup>,*N*<sup>G</sup>-dimethylarginine (ADMA **1.21**). Unfortunately, these analogues show no clinically useful selectivity towards the different isoforms of NOS. Recently Silverman and co-workers synthesised an enantiopure, highly potent ( $K_i = 36$  nM), nNOS-selective inhibitor **1.26** (**Scheme 1.4**).<sup>99</sup> The inhibitor acts in a similar fashion to the arginine analogues, as it is a competitive inhibitor. The use of geminal fluorines in this molecule made the compound markedly more bioavailable than its non-fluorinated analogue. This compound represents a significant step towards a clinically useful nNOS inhibitor. Pterin-based inhibitors have been



result of a highly oxidative environment, it is feasible that peroxynitrite ( $\text{ONOO}^-$ ) is responsible for cell death in a similar manner. iNOS strikes a fine balance in its expression from macrophage cells. On one hand,  $\text{ONOO}^-$  can be involved in inhibiting the growth of many pathogens, such as tumours, bacteria, fungi and parasites, whilst, on the other hand, it has been implicated in a range of auto-immune disorders such as Lupus, psoriasis, arthritis and ulcerative colitis.<sup>17,55,94,95,101,104-107</sup>

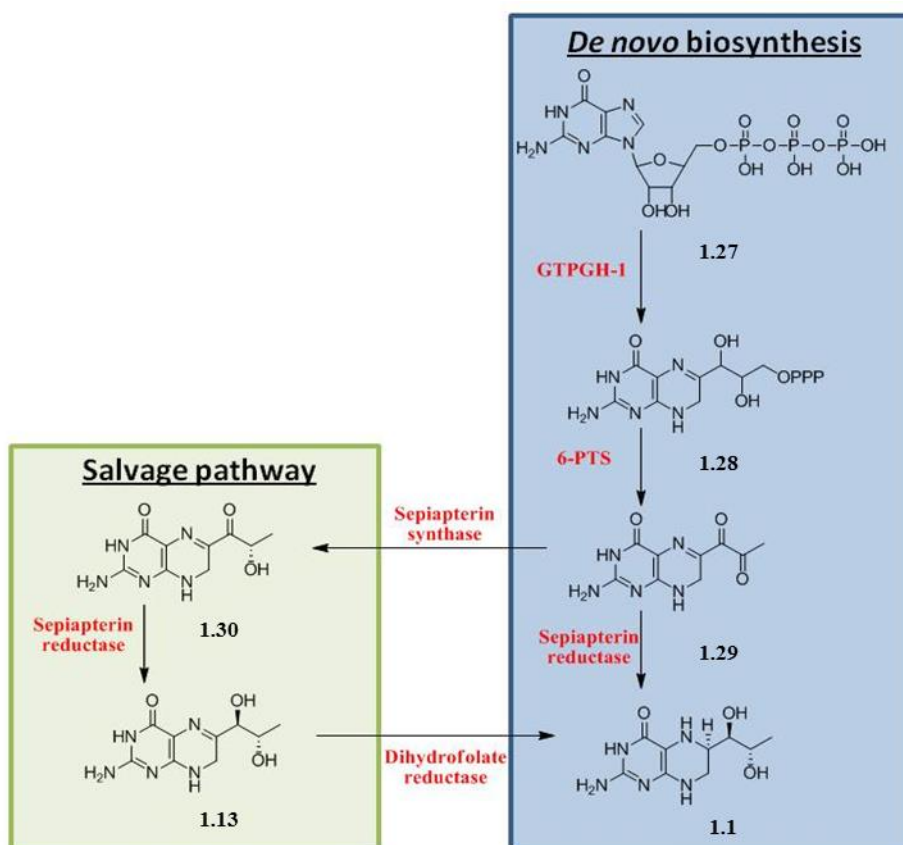
The role of bacterial NOS is not entirely clear but it has been implicated in bacterial cell signalling and pathogenesis, as well as having an evolutionary role in drug resistance.<sup>32,108</sup> bNOS appears to have a slightly different structure from mammalian NOS; however, the oxygenase domain appears to have retained key residues, allowing it to perform the same biochemistry.<sup>31,33</sup> Within subsets of bNOS, it appears that there may be some room for coenzyme promiscuity by allowing either  $\text{BH}_4$  (**1.1**) or tetrahydrofolate to function as an electron shuttle.<sup>29</sup> The obvious differences between the mammalian and bacterial enzymes make bNOS an attractive new target for anti-infective agents.

### 1.2.5 The biosynthesis of tetrahydrobiopterin

As previously stated,  $\text{BH}_4$  (**1.1**) is an essential coenzyme for NOS and a deficiency of  $\text{BH}_4$  (**1.1**) has been implicated in several disease states. It is important to know how organisms synthesise  $\text{BH}_4$  (**1.1**) to give a deeper understanding of the root causes of such disease states.  $\text{BH}_4$  (**1.1**) is biosynthesised *via* a *de novo* pathway in cells (**Scheme 1.5**).<sup>109-111</sup> The synthesis is initiated by guanosine triphosphate cyclohydrolase-1 (GTPCH-1), which is a zinc- and magnesium-dependent enzyme. The substrate for GTPCH-1 is guanosine triphosphate **1.27** (GTP) which is transformed into 7,8-dihydroneopterintriphosphate **1.28** and it is this transformation that is the rate-determining step. Dihydroneopterin triphosphate **1.28** is, in turn, converted into 6-pyruvoyl-5,6,7,8-tetrahydropterin **1.29** by 6-pyruvoyltetrahydropterin synthase (6-PTS). Finally, the tetrahydropterin **1.29** is reduced to 5,6,7,8-tetrahydrobiopterin **1.1** by sepiapterin reductase.



An alternative pathway to BH<sub>4</sub> (**1.1**) synthesis, known as the salvage pathway, has been documented in many organisms. In this enzymatic pathway 6-pyruvoyl-5,6,7,8-tetrahydropterin is converted into sepiapterin **1.30**, by a poorly defined enzyme called sepiapterin synthase.<sup>109,112,113</sup> Sepiapterin is then converted into 7,8-dihydrobiopterin **1.13** and BH<sub>4</sub> **1.1** by sepiapterin reductase and dihydrofolate reductase, respectively. An overview of the biosynthesis of BH<sub>4</sub> (**1.1**) is highlighted in **Scheme 1.5**.



**Scheme 1.5:** *De novo* biosynthesis of BH<sub>4</sub>

Typically, BH<sub>4</sub> deficiency is linked to GTPCH-1 or 6-PTS downregulation. The downregulation of these enzymes has been linked with many disease states.<sup>38,113-115</sup> As a result of this BH<sub>4</sub> deficiency, peroxynitrite (ONOO<sup>-</sup>) and other ROS levels increase, causing the oxidation of BH<sub>4</sub> (**1.1**) to dihydrobiopterin (BH<sub>2</sub> **1.13**). BH<sub>2</sub> can occupy the active site of NOS but will prevent catalysis, which can exacerbate pre-existing conditions. Moreover, a high ratio of BH<sub>2</sub>:BH<sub>4</sub> can begin the process of

uncoupling the dimer and will lead to the production of even higher levels of ROS, further perpetuating this destructive cycle.<sup>23,116</sup>

### 1.2.6 Other BH<sub>4</sub>-utilizing enzymes

BH<sub>4</sub> (**1.1**) is not exclusively involved in NOS biochemistry; it has also been known for many years to be a coenzyme to the aromatic amino-acid hydroxylase enzymes (AAH) exemplified by phenylalanine hydroxylase shown in **Figure 1.12**.<sup>117,118</sup>

- Phenylalanine hydroxylase, responsible for the oxidation of phenylalanine to tyrosine
- Tyrosine hydroxylase, responsible for the oxidation of tyrosine to L-DOPA
- Tryptophan hydroxylase, responsible for oxidation of tyrosine to 5-hydroxytryptophan and ultimately serotonin and melatonin.

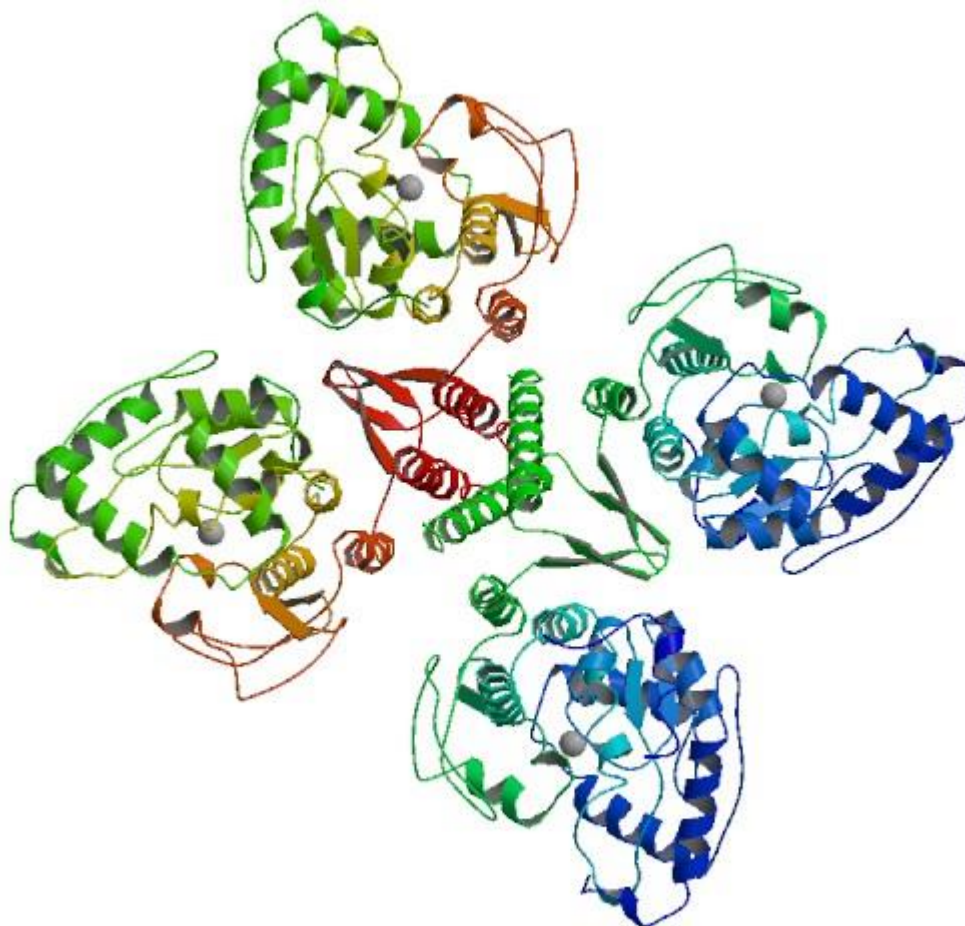


**Figure 1.12: 2PAH (pdb identifier) - The tetrameric structure of phenylalanine hydroxylase**

AAHs are tetrameric non-haem iron mono-oxygenase enzymes with a “basket-like” arrangement. Deep at the centre of this “basket” resides a catalytic iron, coordinated to two histidine residues, one glutamate residue and a variable amount of water, depending on the oxidation state of the iron. A closer picture of the basket arrangement is given in **Figure 1.13** showing the iron deep inside one of the protein’s monomers. The hydroxylation reactions that take place in the AAH enzymes are remarkably similar to the first mono-oxygenation reaction within NOS. However, the protein structure and the molecular mechanism are markedly different from NOS. The AAH proteins are tetrameric in structure, in contrast to NOS’s dimeric structure. In the AAHs,  $\text{BH}_4$  (**1.1**) plays a role in binding oxygen, acts as a two-electron donor and is released from the enzyme after each enzymatic cycle, again in contrast to NOS.<sup>51</sup> In AAH, oxygen activation appears to involve  $\text{O}_2$  binding

to the 4a-position of  $\text{BH}_4$  (**1.1**) – confirmed by  $^{18}\text{O}_2$  labelling studies – and requires the closely associated iron atom.<sup>119</sup> Iron is thought to play a fundamental role in the oxygen activation and cleavage and an overview of the mechanism is given below in **Scheme 1.6**.

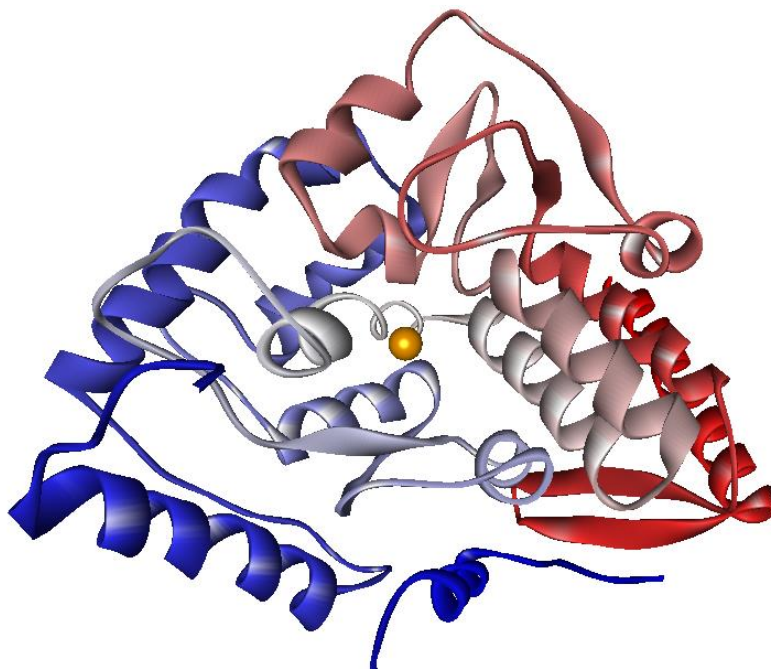
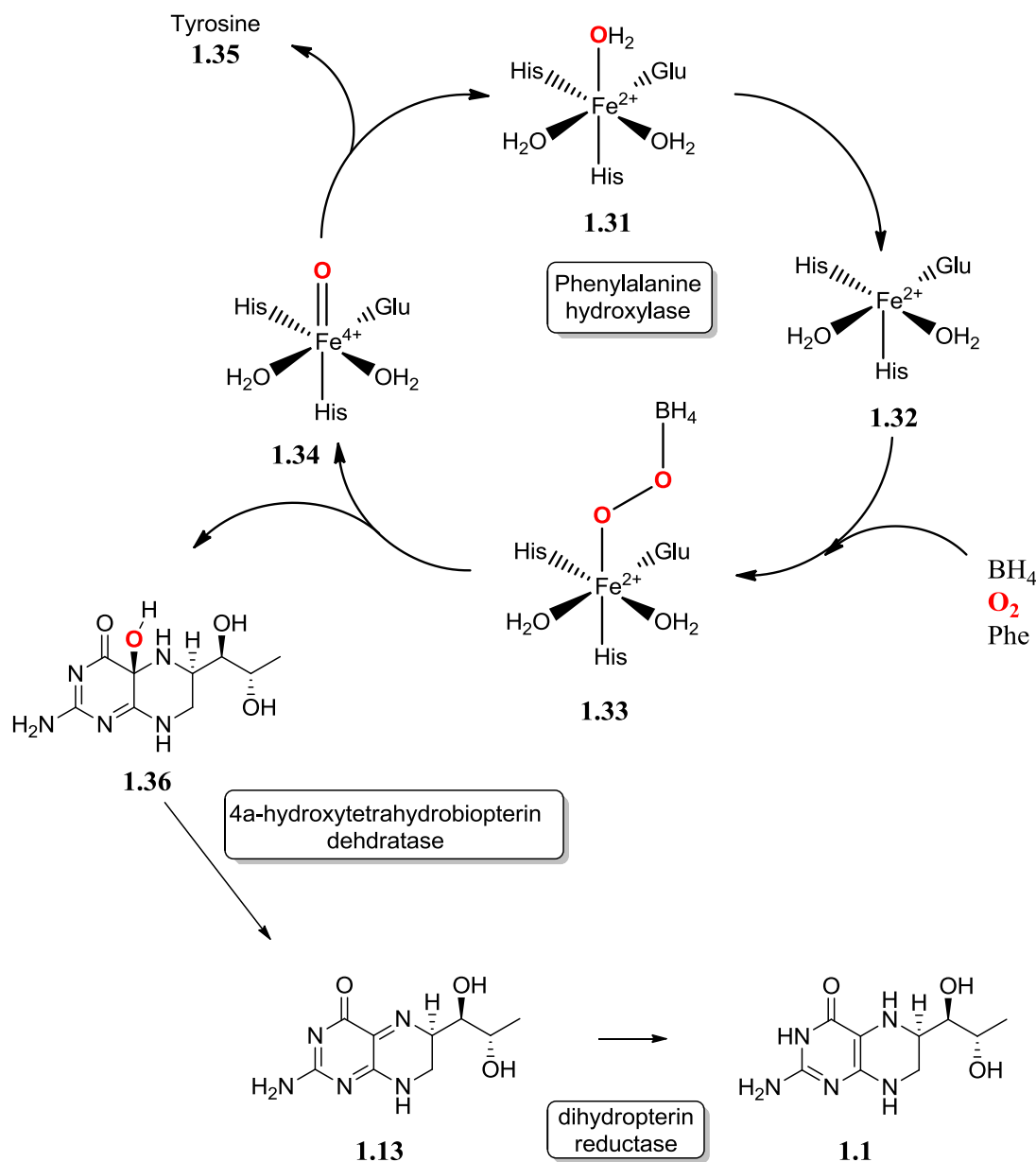


Figure 1.13: 2PAH monomer showing the basket arrangement



**Scheme 1.6: The catalytic cycle of phenylalanine hydroxylase**

As can be seen in **Scheme 1.6**, 4a-hydroxytetrahydrobiopterin (**1.36**) dissociates from the enzyme and is then enzymatically returned to BH<sub>4</sub> (**1.1**) by 4a-hydroxytetrahydrobiopterin dehydratase and dihydropterin reductase.

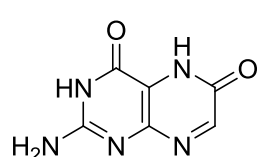
Mutations in the AAH enzymes lead to life threatening or life altering disorders such as phenylketonuria (PKU) and DOPA-responsive dystonia.<sup>120-126</sup> PKU can lead to mental retardation or brain damage and is a disorder tested for at birth. Patients with PKU must follow a strict low-phenylalanine diet and may also require BH<sub>4</sub> (**1.1**) supplementation, under the trade name Kuvan.<sup>38,39</sup> DOPA-responsive dystonia is a

genetic disorder affecting muscle tone and has Parkinson's disease-like symptoms.<sup>103</sup> Typically children with this disorder respond well to L-DOPA supplements.

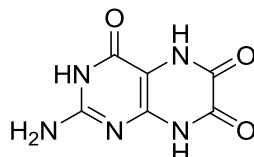
### 1.3 A brief historical account of pteridines and their syntheses

#### 1.3.1 The discovery of pteridines

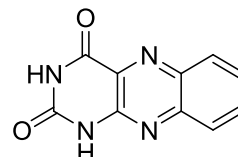
In 1857, Wöhler and Hlasiwetz both reported the first formation of a pteridine as a new yellow product from prolonged heating of uric acid in water above 100 °C in a sealed tube.<sup>127,128</sup> It was later suggested that the materials closely resembled some naturally occurring pigments from sulphur yellow butterfly wings. The structures of these pigments were later confirmed by Pfleiderer to be pteridines. It took more than 100 years for the products of these original experiments to be fully characterised and their structures elucidated as xanthopterin **1.37** and leucopterin **1.38**.<sup>129</sup>



**1.37**

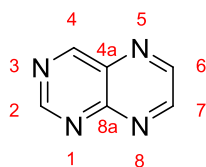


**1.38**

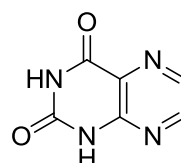


**1.39**

In 1910, Gabriel reported the first synthesis of a pteridine from a pyrazine ring by treating 2,3-pyrazinedicarboxamide with hypobromite to give the then-unrecognized alloxazine **1.39**.<sup>130</sup> Thirty years later, Kuhn and Cook prepared the related product, lumazine, by condensing 5,6-diamino-2,4(1*H*,3*H*)-pyrimidinedione with glyoxal.<sup>131</sup> In the ensuing publication, they introduced a logical numbering system (**1.40**), which is still in use to this day, along with the name, lumazine (**1.41**).



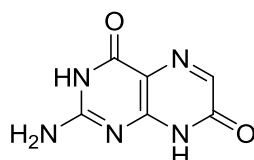
**1.40**



**1.41**

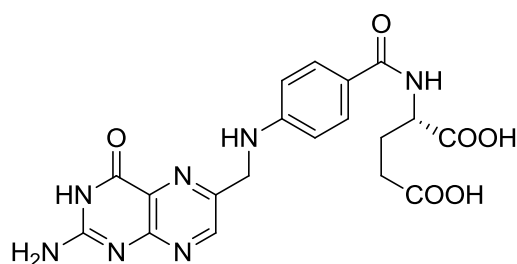
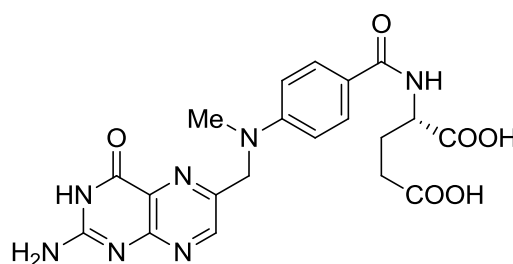
By 1924, both Schöpf and Wieland had begun an intense investigation of these pigments and, by 1933, had isolated another pigment of interest, isoxanthopterin

**1.42.**<sup>132,133</sup> Due to difficulties with elemental analyses, the structures of these compounds remained unknown until 1940. At this time, Schöpf's group finally obtained data which pointed towards a pteridine nucleus.<sup>134</sup> Upon this discovery, Purmann devised and performed the logical syntheses of all three compounds, finally confirming the structures.<sup>135-137</sup> In 1941 Schöpf suggested the name "pterin" to describe 2-aminopteridin-4(3*H*)-one and its derivatives, whilst still retaining the lumazine numbering system.<sup>138</sup>

**1.42**

With the discovery of this new heterocyclic system, the fields of both biology and chemistry surrounding pteridines underwent a dramatic expansion. The most notable advances of pteridine chemistry were:

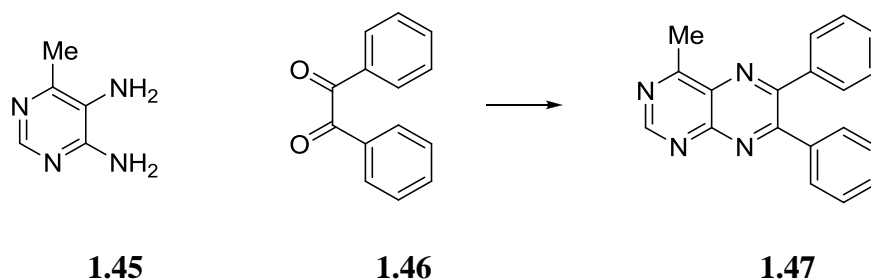
- The isolation and synthesis of folic acid **1.43**<sup>139-141</sup>
- The introduction of methotrexate **1.44** as an anti-leukaemia drug<sup>142</sup>
- The isolation and characterisation of more than 50 naturally occurring pteridines<sup>143</sup>

**1.43****1.44**

The expansion of this field has led to the application of pteridines throughout a wide range of medicinal chemistry, from oncology,<sup>144,145</sup> antiparasitics,<sup>146,147</sup> antivirals,<sup>148,149</sup> antibacterials<sup>146</sup> and coenzyme mimetics.<sup>53,78</sup>

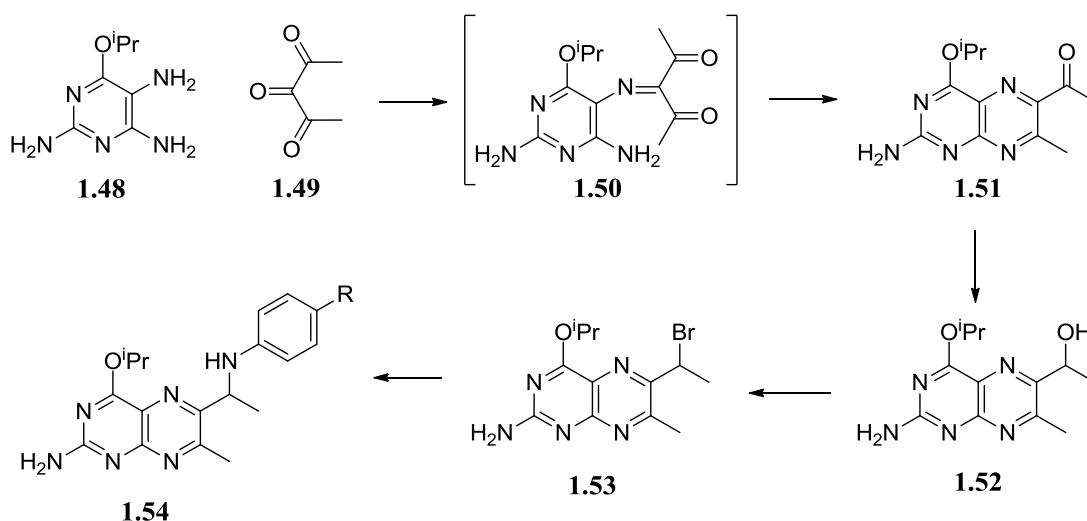
### 1.3.2 The synthesis of pteridines from pyrimidines

To date, there exist three major approaches to pteridine synthesis from pyrimidine derivatives. The first of these approaches is known as the Isay synthesis; however, Isay was, in fact, not the first person to report this type of approach. Gabriel and Colman first condensed 6-methyl-4,5-pyrimidinediamine **1.45** and benzil **1.46** to afford 4-methyl-6,7-diphenylpteridine **1.47** shown in **Scheme 1.7**.<sup>150</sup>



**Scheme 1.7:** Condensation of a pyrimidine diamine with benzil to form a pteridine

Obviously, there are certain limitations when using this style of reaction, as the use of unsymmetrical dicarbonyl compounds will give rise to differing structures, often with a mixture of substitution patterns at the 6- and 7- positions. Nevertheless, the Isay approach has still proven to be useful in modern synthetic chemistry, as **Scheme 1.8** highlights.<sup>146,151,152</sup>

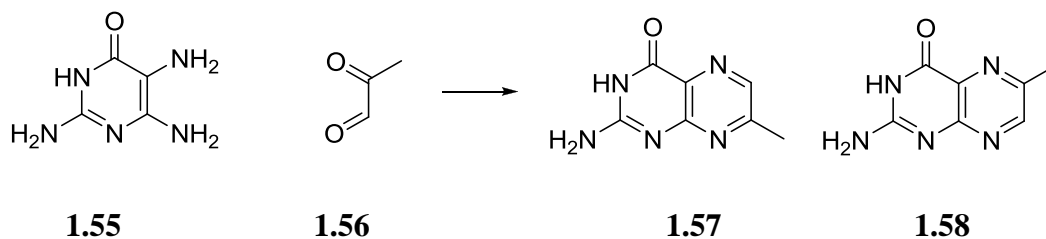


**Scheme 1.8:** A modern application of the Isay synthesis.<sup>152</sup>

The problem of regioselectivity can be addressed in a somewhat unsatisfactory manner by the use of  $\alpha$ -aldehydoketones for a limited set of pteridine targets. Here,

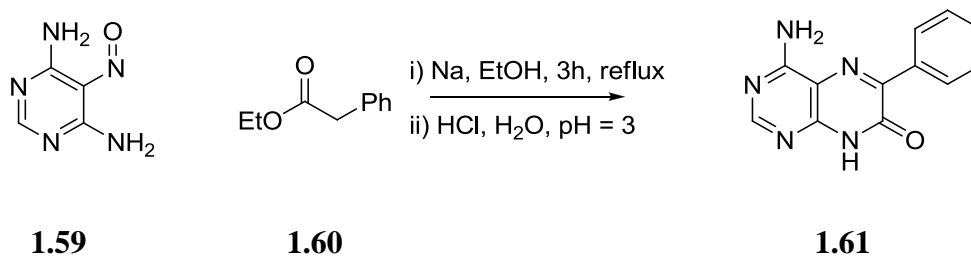
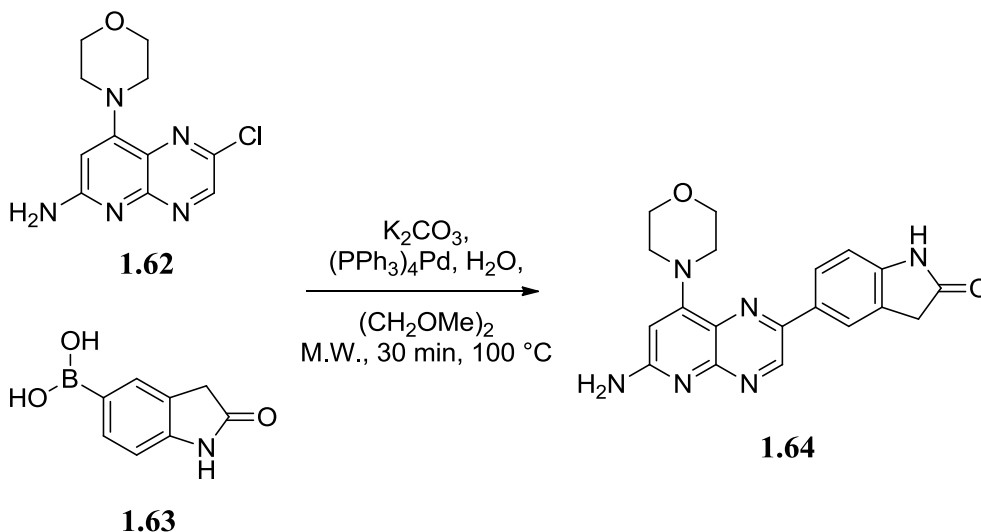


the more electrophilic carbonyl group on the aldehyde reacts significantly faster with the more nucleophilic amine at C<sup>5</sup>. This then leaves the remaining amine at C<sup>6</sup> to react with the ketone. This modified version of the Isay synthesis relies heavily on the differences of electron density on the two carbonyl groups and, as such, a mixture of major and minor products is not uncommon. This is demonstrated in **Scheme 1.9**, where **1.57** is the major product, present in a ratio of 9:1 (major to minor product).<sup>151</sup> A reversal of this regioselectivity is possible in acidic conditions.

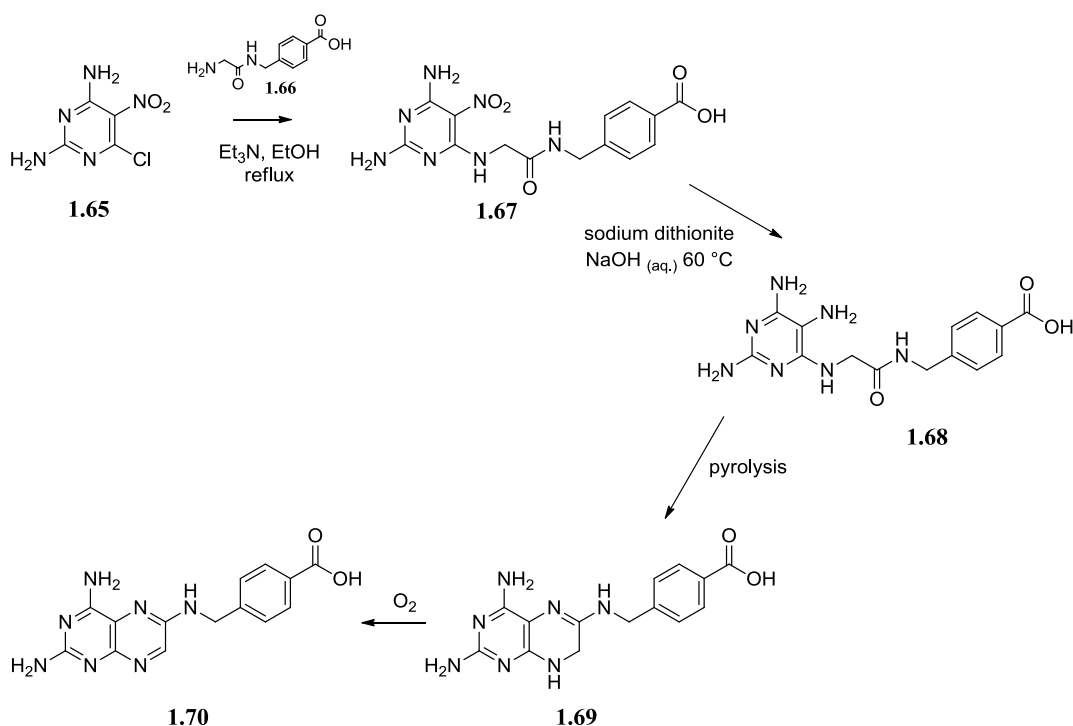


**Scheme 1.9:** Non-regioselective Isay synthesis resulting in a 9:1 mixture of **1.57**:**1.58**.<sup>151</sup>

The next approach to the synthesis of pteridines was put forward by Timmins in 1949, in which he demonstrated a method allowing differing structures to be avoided.<sup>153</sup> This synthetic route, known as the Timmins synthesis (**Scheme 1.10**), uses 5-nitroso-4-pyrimidinamines (e.g. **1.59**) and a suitably activated carbonylmethylene reagent (e.g. **1.60** **Scheme 1.10**).<sup>154</sup> Timmins' approach allowed for a regioselective synthesis giving 6-substituted pteridines, which, generally speaking, are the more biologically interesting compounds. As the methylene group has to be activated with an electron-withdrawing group, there is a limit to the pteridines that can be made *via* this methodology. Recently this synthetic methodology has been replaced by a symmetrical Isay synthesis, followed by chlorination and a palladium-catalysed cross-coupling, which allows for greater flexibility with respect to the aryl substituent.<sup>149</sup> The cross-coupling is exemplified in **Scheme 1.11**.

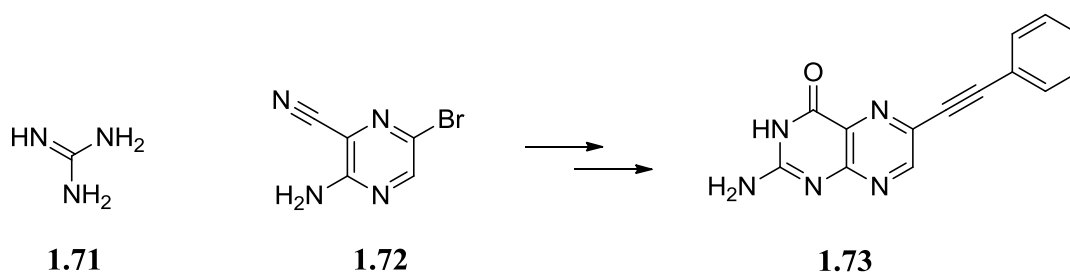
Scheme 1.10: An example of the Timmins synthesis<sup>154</sup>Scheme 1.11: A more modern method to obtain Timmins-type products<sup>149</sup>

The final approach to a pteridine from a pyrimidine ring is known as the Boon synthesis.<sup>155</sup> This approach utilizes 4-chloro-5-nitropyrimidines (or the appropriate 4-chloro-5-arylazopyrimidines), for example **1.65**, with an  $\alpha$ -aminocarbonyl-containing compound such as **1.66** (**Scheme 1.12**). The Boon synthesis can give a small range of substituents at the 6- or 7-positions which are determined by the  $\alpha$ -aminocarbonyl compound employed. The reaction proceeds *via* nucleophilic aryl substitution of the chloro group on the pyrimidine ring to give the first intermediate, which may or may not be isolated. Next, reduction of the nitro/nitroso/azo group facilitates the annulation giving the unstable tetrahydropteridine which undergoes oxidation to give the fully aromatic pteridine (**Scheme 1.12**).<sup>156</sup> Implementation of an “incomplete” Boon synthesis gives access to 7,8-blocked dihydropteridines by using an appropriate dialkylsubstituted  $\alpha$ -aminocarbonyl compound.<sup>40</sup>

Scheme 1.12: An example of the Boon synthesis<sup>156</sup>

### 1.3.3 The synthesis of pteridines from pyrazines

The synthesis of pteridines from pyrazine ring systems usually produces single products; this is therefore a rather valuable route to a desired pteridine.<sup>157-160</sup> However, this synthetic approach has not found wide use in medicinal chemistry due, in part, to the fact that it does not lend itself well to late-stage diversity (a concept discussed more fully in **Section 1.6**). This approach usually requires the synthesis of specific pyrazine rings which have limited synthetic scope. The majority of diversity is usually incorporated early into the pyrazine ring system (typically with a halogen substituent) that can be modified after ring synthesis. Variation at the 2-position of the pteridine requires specific synthesis of each guanidine. However, the Taylor synthesis has been carried out with some degree of late-stage diversity using the halide substitution strategy (**Scheme 1.13**).<sup>160</sup> After formation of the pyrimidine ring, a Sonogashira reaction was employed. It can be seen that this approach provides a higher degree of synthetic flexibility, giving access to a library of compounds.



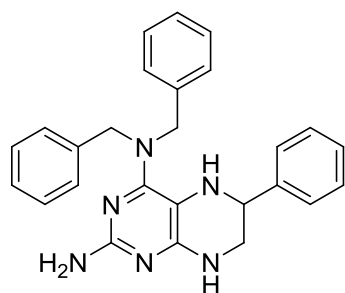
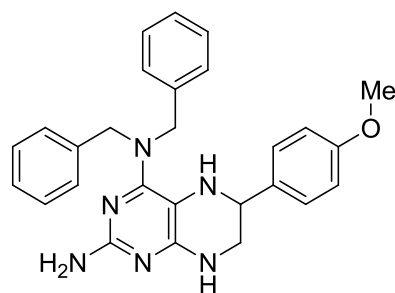
Scheme 1.13: A synthetically flexible Taylor synthesis<sup>160</sup>

## 1.4 Analogues of tetrahydrobiopterin for study in NOS programmes

### 1.4.1 Literature compounds

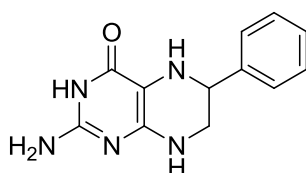
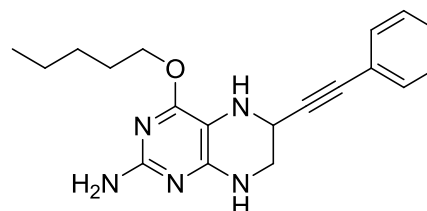
It has already been shown in the discussion above that NO has an important role to play in maintaining good health and, indeed, that BH<sub>4</sub> (**1.1**) has a central role to play in the production of NO from NOS. Moreover, it has been demonstrated that levels of NO significantly higher or lower than normal may lead to adverse and potentially serious side effects. As a result, a number of pteridine derivatives have been synthesised and tested for their activity at NOS as either an activator or an inhibitor. This section will give a brief overview of the state of the art in this field.

In 1999, Schmidt and his team published the results of a structure-activity relationship conducted into selected pteridines and their effect on the inhibition of NOS.<sup>3</sup> The study looked into variations at the 2-, 4-, 6- and 7-positions and the effect that structural variation had on NO production using nNOS. They found that substituents at the 2-, 6- and 7-positions had no discernable effect on NOS inhibition when the pteridine was tested in its fully oxidised state. However, in the corresponding reduced state (tetrahydro oxidation state), several hits were observed, with substituents at C6 showing the greatest effects. The most potent of these inhibitors are shown below with compound **1.74** having an IC<sub>50</sub> of 3 μM and compound **1.75** having an IC<sub>50</sub> of 5 μM (with BH<sub>4</sub> having a K<sub>m</sub> of 1 μM).<sup>161,162</sup>

**1.74****1.75**

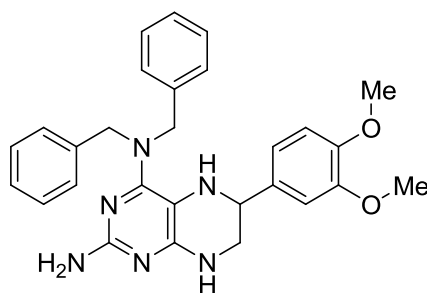
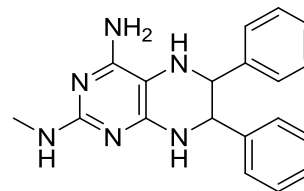
Interestingly, bulky benzyl groups were tolerated on the 4-amino position, suggesting that a significantly large amount of space is available in this region of the pterin binding site.

In 2001, Schmidt and his team published the results of another SAR with further variations at the 2-, 4-, 5-, 6- and 7-positions.<sup>162</sup> However, this SAR was primarily concerned with 4-oxo substituents and their derivatives as nNOS inhibitors. Again similar patterns around the pteridine nucleus emerged. The most potent inhibitors are shown below, with **1.76** having an  $IC_{50}$  of 7  $\mu M$  and **1.77** having an  $IC_{50}$  of 8  $\mu M$ . Interestingly, compound **1.76** has the potential to take part in the much debated proton exchange within the NOS molecular mechanism but remains an inhibitor of NOS anyway.

**1.76****1.77**

Finally, in 2002, Schmidt and his team released one final SAR, testing both 4-amino and 4-oxo pteridines.<sup>2,161</sup> In this study, the group discovered their most active inhibitor yet with compound **1.78** having an  $IC_{50}$  of 2  $\mu M$ . However, one compound which appears to have only moderate activity is of particular relevance when set in the context of this thesis (see **Chapter 3**). Compound **1.79** has a 2-NMe substituent

and retains a modest  $IC_{50}$  of  $30\ \mu\text{M}$ , suggesting that there is sufficient room within the pterin-binding site to accommodate such a substituent.

**1.78****1.79**

To date, perhaps unsurprisingly, the best pteridine-containing inhibitor of NOS is the 4-amino analogue of  $\text{BH}_4$  (**1.19**) with an  $IC_{50}$  of  $1\ \mu\text{M}$  ( $\text{BH}_4$  has a  $K_m$  of  $1\ \mu\text{M}$ ).<sup>53,54,162</sup> As alluded to earlier, the exact reason that the 4-amino analogue of  $\text{BH}_4$  is an inhibitor of NOS is unknown, although it has been suggested that, due to the lack of a proton at  $\text{N}^3$ , the analogue cannot take part in the presumed proton transfer, thus halting NO production. It should be noted that there has been no systematic study of pteridine derivatives as probes of the molecular mechanism of NOS; this is one of the major driving forces behind this thesis.

Very few compounds other than  $\text{BH}_4$  (**1.1**) that are NOS activators have been described. However there are two activators, studied by Werner and his team, which are of particular relevance to this thesis, 5-methyl- $\text{BH}_4$  (**1.17**) and 2-*N*-methyl- $\text{BH}_4$  (**1.80**).<sup>77</sup> 5-Methyl- $\text{BH}_4$  (**1.17**) has the ability to donate an electron to NOS more easily than  $\text{BH}_4$  (**1.1**), due to a positive inductive effect (**Figure 1.14**). 5-methyl- $\text{BH}_4$  has been used in several mechanistic studies and has helped confirm the redox role of  $\text{BH}_4$  (**1.1**) within the NOS enzymes.<sup>71,73-76,78,79,81</sup> 5-Methyl- $\text{BH}_4$  has a poorer affinity for NOS ( $\sim 20$  fold lower than  $\text{BH}_4$ <sup>63</sup>) and acts as a poorer coenzyme within the enzyme. However, when the enzyme is saturated with 5-methyl- $\text{BH}_4$  (**1.17**), the rate of NO production is actually higher than when  $\text{BH}_4$  (**1.1**) is used. When considering a purely electronic rationale, this makes sense; the higher the electron density in the pterin, the more readily it will donate an electron. This explains the faster rate of NO production at and above saturation levels. It can be suggested that the reason that 5-



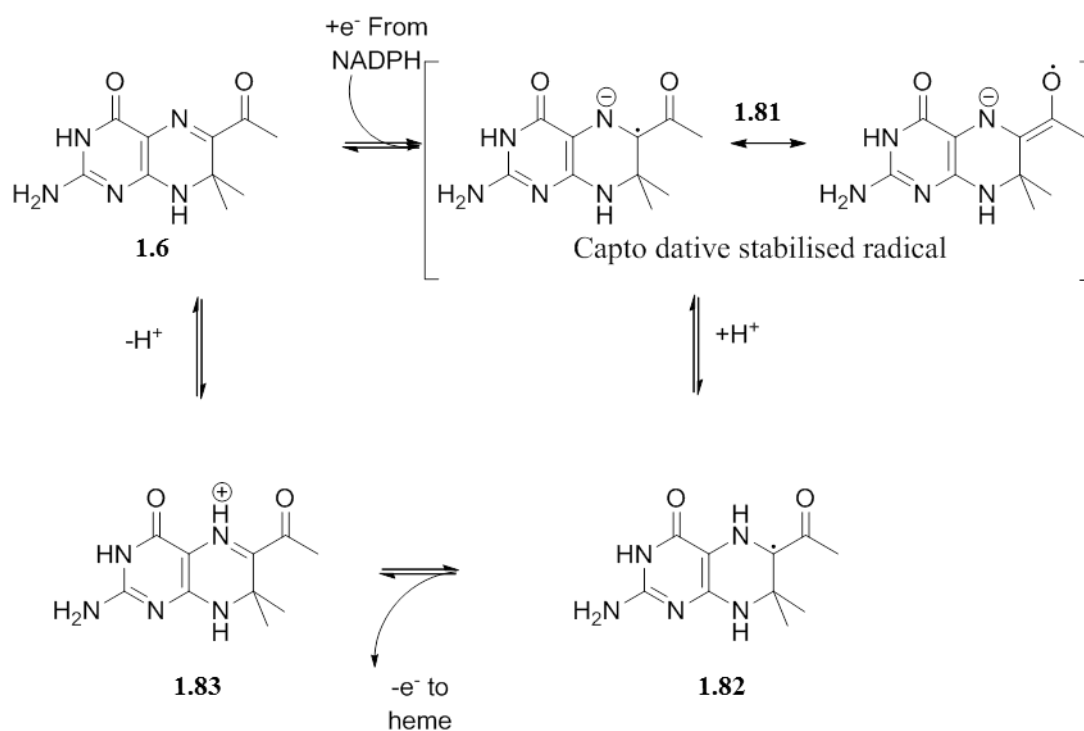
### 1.4.2 The WSG compounds and their biological activities

As previously mentioned, Wood and Suckling, along with their team, prepared a short series of blocked dihydropteridines.<sup>40</sup> The initial intention for this library of compounds was to test for 6-hydroxymethyl-7,8-pterin pyrophosphokinase inhibitors. The synthesis of these molecules followed an incomplete Boon synthesis. When these compounds were first made, it was not known that BH<sub>4</sub> (**1.1**) was a cofactor for NOS and these molecules were not studied for any NOS activity. When the roles of NO and BH<sub>4</sub> (**1.1**) within NOS were established, compounds from the library were tested in the appropriate biological assays.<sup>43-45</sup> One compound in particular was a significant hit in rat aorta tests, WSG1002 (**1.2**), and it was proven to be acting as an eNOS activator with properties similar to BH<sub>4</sub> (**1.1**).

At the time of the rat aorta tests,<sup>43,44</sup> WSG1002 (**1.6**) was administered in its dihydro oxidation state yet still produced activity in NOS. This caused some confusion as it was later proven to be activating NOS only in the tetrahydro oxidation state. At the time three possible explanations were put forward to address this matter:

- The compounds bind to NOS and engage in electron transfer *via* a captodative stabilised radical mechanism (**Scheme 1.14**)
- Dihydrofolate reductase (DHFR) was reducing the pterin **1.6** *in situ* to the tetrahydro oxidation level
- High levels of ascorbic acid were reducing the pterin in the assay itself.





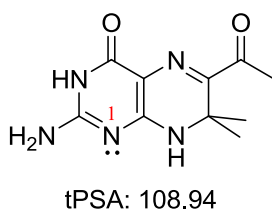
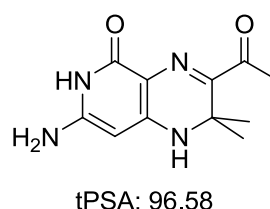
**Scheme 1.14: Proposed mechanism of donation of an electron to the haem via the capto-dative radical mechanism.**

The first suggestion has been discounted as a result of the work carried out in collaboration with Daff and his group.<sup>45</sup> This result is not entirely surprising as the mechanism by which it would have to work is inconsistent with the evidence in the literature. The final suggestion was not wholly unreasonable as cellular experiments and animal models suggested that high levels of ascorbic acid helped increase the concentration of  $BH_4$  (**1.1**) relative to  $BH_2$  (**1.13**).<sup>163,164</sup> A more detailed investigation of this mechanism, through work carried out in our laboratory, suggested that ascorbic acid did not reduce blocked dihydropterins such as **1.6**.<sup>165-167</sup> Instead, it was suggested that ascorbic acid may be limited to an anti-oxidant role. Consequently, the *in situ* reduction of the dihydropterin by DHFR seems to be the most likely explanation for the observed activity.

### 1.5 A brief look at another target molecule, pyridopyrazine

It has been demonstrated that pteridines possess a wide range of applications in medicinal chemistry and consequently have been used as a template in drug-

discovery programmes. However it is also widely accepted that having fewer nitrogen atoms in a heterocyclic core makes a candidate more “drug-like”. This can be seen by comparing compounds **1.6** and the deazapterin **1.84**; the total polar surface area (tPSA) of the deazapterin is lower. Having a lower tPSA will make the deazapterine more soluble than pterins and therefore more likely to cross biological membranes including the blood-brain barrier. Having the ability to cross the blood brain barrier enables these types of compounds to be targeted towards CNS-based disorders. Using these ideas, Suckling and his team have begun several synthetic strategies to improve the “drug-likeness” of pteridines to potentially find more suitable compounds.<sup>146</sup> The nitrogen at position 1 appeared to be the best candidate for removal as its lone pair of electrons did not appear to play a major role in binding within the active site of NOS. This can be seen in **Figure 1.15** showing the hydrogen bonds (highlighted in green) made by the pterin within the binding site. It can be seen that this nitrogen makes one hydrogen-bond with a water molecule and not the protein backbone itself. It is not known whether this interaction with the molecule of water is important and any result gained from testing pyrido[4,3-*b*]pyrazines as BH<sub>4</sub> mimetics would have to take this into account. As a result of this rationale, an investigation was begun to see if pyrido[4,3-*b*]pyrazines could act as NOS modulators. At the same time, the group held interests in other fields of biology such as antifungals, antibacterials, antiparasitics and antifolates. Due to this, it was deemed prudent to investigate the synthesis of pyrido[2,3-*b*]pyrazines also, in case these compounds displayed activity against these targets. With this in mind, a brief review of the state of the art with respect to synthesis and to medicinal chemistry of some deazapterins is appropriate.

**1.6****1.84**

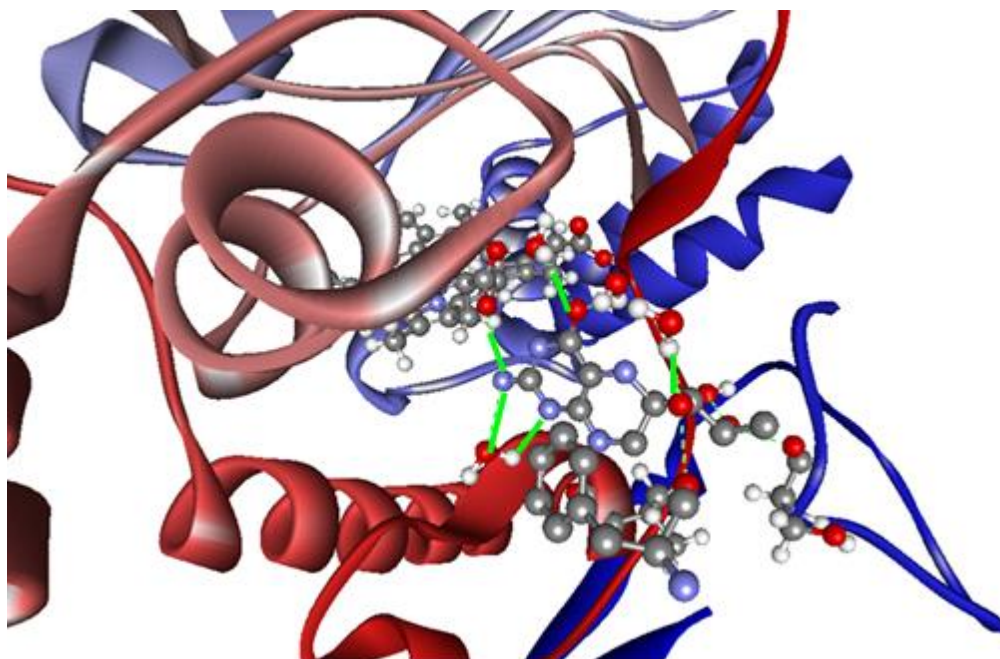


Figure 1.15: Showing hydrogen bonds made by BH<sub>4</sub> within its binding site. (H-Bonds in green)

### 1.5.1 The synthesis and application of pyridopyrazines

In 1968, Temple described the preparation of both pyrido[3,4-*b*]pyrazines (**1.84**) and pyrido[2,3-*b*]pyrazines (**1.85**) in a non-selective approach, using tetraaminopyridines (resulting in compounds **1.86** to **1.91**).<sup>168</sup> This work closely paralleled the work carried out by Gabriel, Coleman and Isay, by condensing diamines with  $\alpha$ -dicarbonyl compounds. The initial stages of this work were primarily concerned with the library synthesis of different isomeric forms of pyridopyrazines: a few examples are given below (**1.86** – **1.91**).

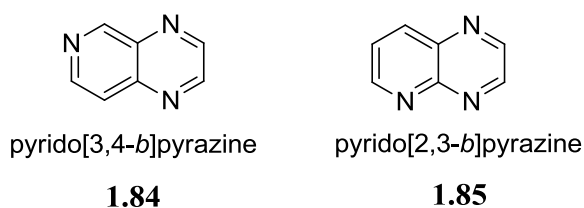
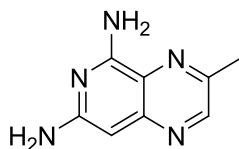
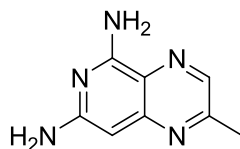
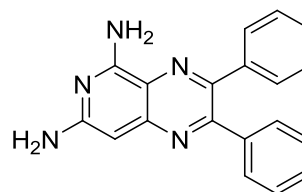
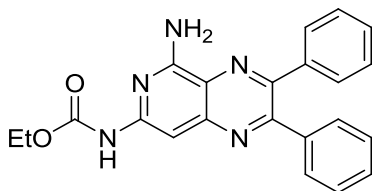
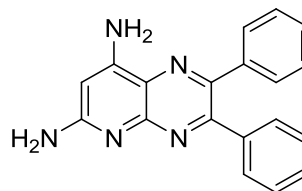
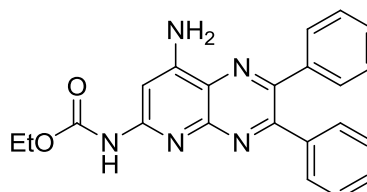
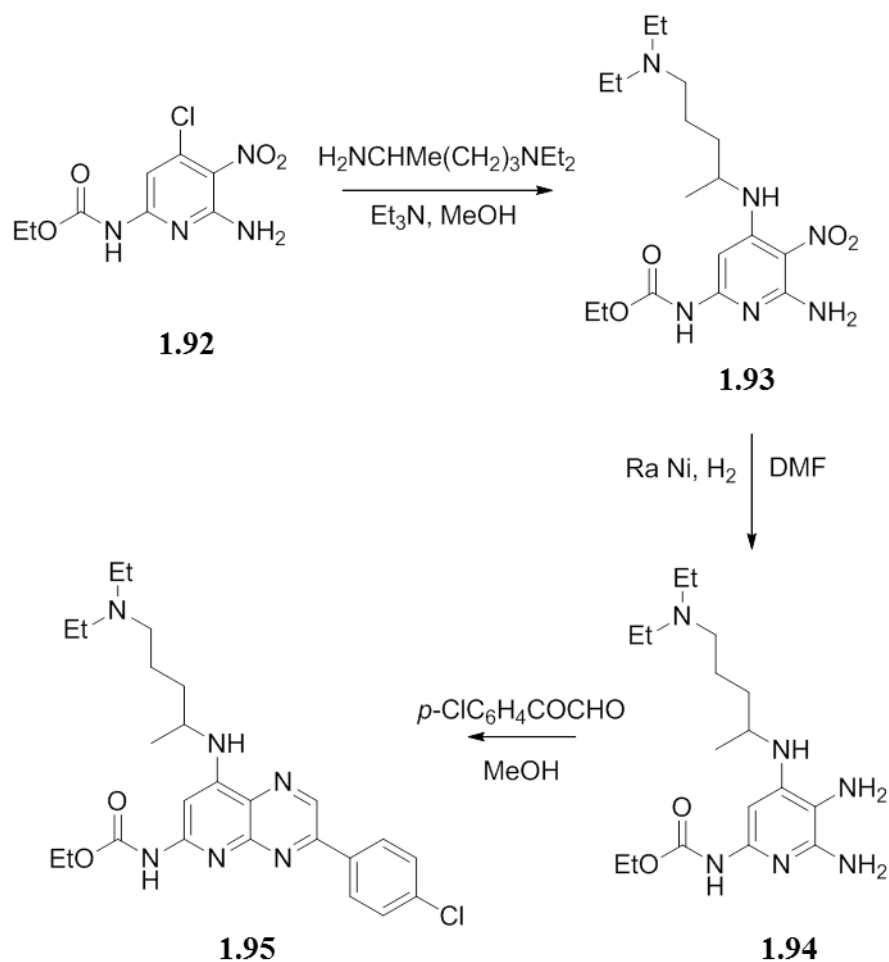


Figure 1.16: The ring structures for pyrido[3,4-*b*]pyrazine and pyrido[2,3-*b*]pyrazine.

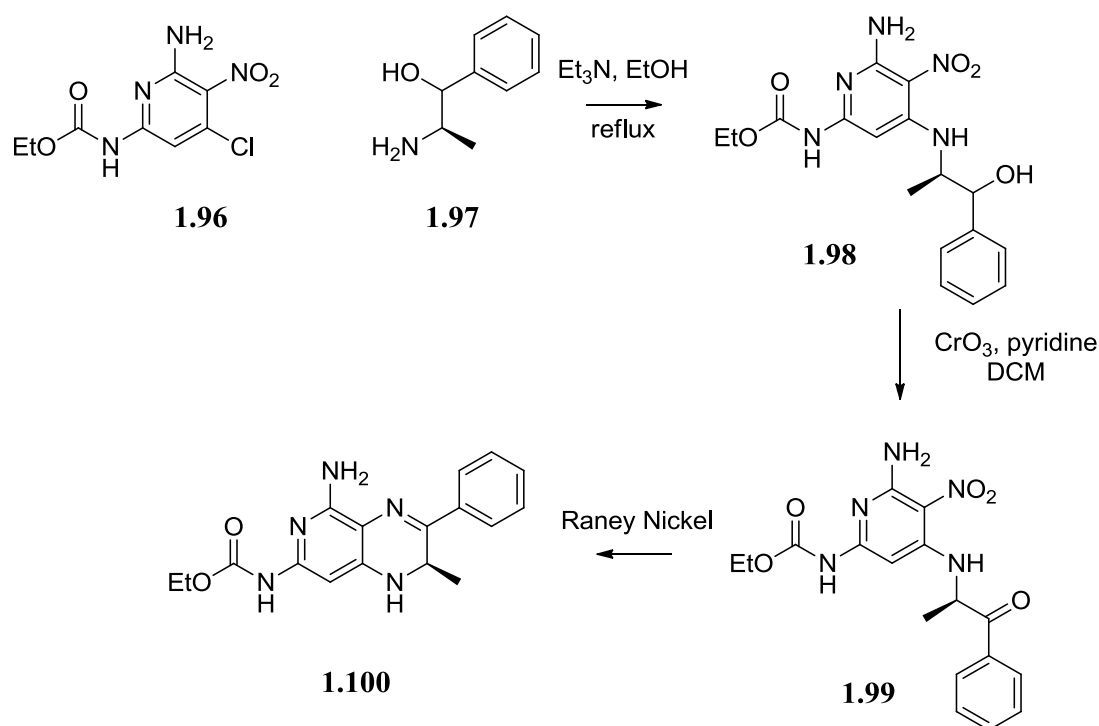
**1.86****1.87****1.88****1.89****1.90****1.91**

The synthesis of the library of compounds relied heavily on the ability to separate each isomer. Somewhat fortunately, there was only one occurrence where two isomers could not be separated completely. Again, the familiar problem of a mixture of structures was encountered when employing unsymmetrical dicarbonyl species, shown above with compounds **1.86** and **1.87**. That same year Temple published the results of testing this library for antimalarial properties.<sup>169</sup> Although a modest hit at best, structure **1.95** was the first example of a pyridopyrazine being used successfully in a biological context (**Scheme 1.15**). It can be seen that displacement of the chloro at the 4-position, aided by the electron-withdrawing nitro group, was carried out with a relatively large primary amine. Next reduction of the nitro to the corresponding amine using Raney nickel was carried out, facilitating the condensation with the appropriate dicarbonyl compound onto the least hindered amines.



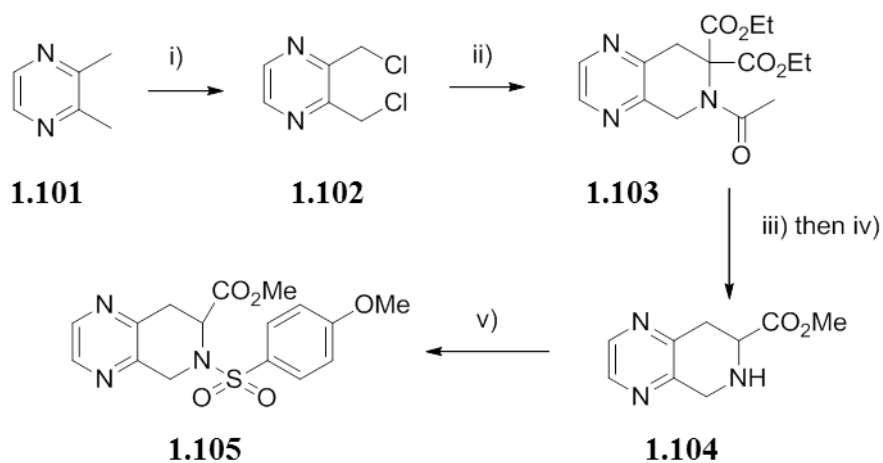
**Scheme 1.15:** The synthesis of Temple's first biologically relevant pyrido[2,3-*b*]pyrazine<sup>169</sup>

In 1970, Temple also began screening these types of compounds to assess their biological activity as antibacterials, antimalarials and antifolate drugs.<sup>170,171</sup> The vast majority of Temple's work focused on pyrido[2,3-*b*]pyrazines until the early 1980's.<sup>172</sup> Around this time focus shifted back towards the pyrido[4,3-*b*]pyrazines as antimetabolic agents for the treatment of cancer; this remained a significant interest for the Temple group over the following decade.<sup>173-180</sup> The syntheses of these compounds now closely paralleled the Boon approach. A stereoselective example of this is shown below in **Scheme 1.16** in which Temple's most active compound was discovered. Again, displacement of the chlorine at the 4-position was assisted by the electron-withdrawing nitro group. The alcohol was then oxidised to the corresponding ketone. This facilitated the following annulation reaction, which was initiated by the reduction of the nitro to the amine using Raney nickel.



Scheme 1.16: The synthesis of a pyrido[4,3-*b*]pyrazine<sup>177</sup>

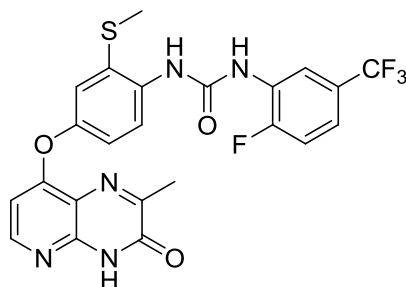
More recently, in 2003, Yoshiizumi and his team used a synthetic approach which closely paralleled that of the Taylor synthesis to prepare a tetrahydropyrido[4,3-*b*]pyrazine **1.105** that acts as a heparin-binding epidermal growth factor (HB-EGF) inhibitor (Scheme 1.17).<sup>181</sup>



Scheme 1.17: i) NCS, benzoyl peroxide; ii) diethyl acetamidomalonate, Cs<sub>2</sub>CO<sub>3</sub>; iii) 6M HCl<sub>(aq)</sub>; iv) SOCl<sub>2</sub> and MeOH; v) *p*-methoxybenzenesulfonyl chloride, DMAP<sup>181</sup>

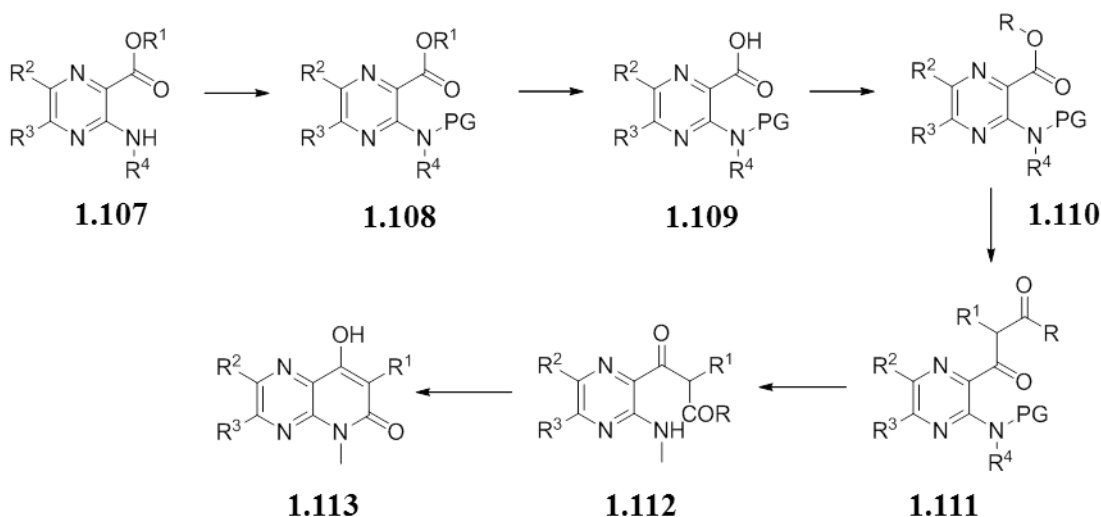
Even more recently, in 2010, Springer's team at the Institute of Cancer Research developed novel kinase inhibitors based on a pyrido[2,3-*b*]pyrazine nucleus. The

most potent compounds of this class are able to bind to the hinge region of a protein kinase called BRAF. Activation of the BRAF pathway has been linked to malignant melanomas as well as colorectal, thyroid and ovarian cancers.<sup>182,183</sup> The most active and kinase-selective compound **1.106** is shown below and is highly potent ( $IC_{50} = 9$  nM).



**1.106**<sup>182</sup>

The field of pyridopyrazines has undergone a relatively recent revival and its expansion into biological fields, other than folic acid synthesis antagonists, has spurred on a renewed enthusiasm towards this class of compound. This could not be exemplified much better than with the publication of Syngenta's interest in these compounds as herbicides, fungicides and safeners for crop protection (**Scheme 1.18**).<sup>184,185</sup> When large industrial companies take an interest in an unexplored heterocyclic system, it is reassuring for those venturing into the field.



**Scheme 1.18:** Syngenta's approach to pyrido[2,3-*b*]pyrazines

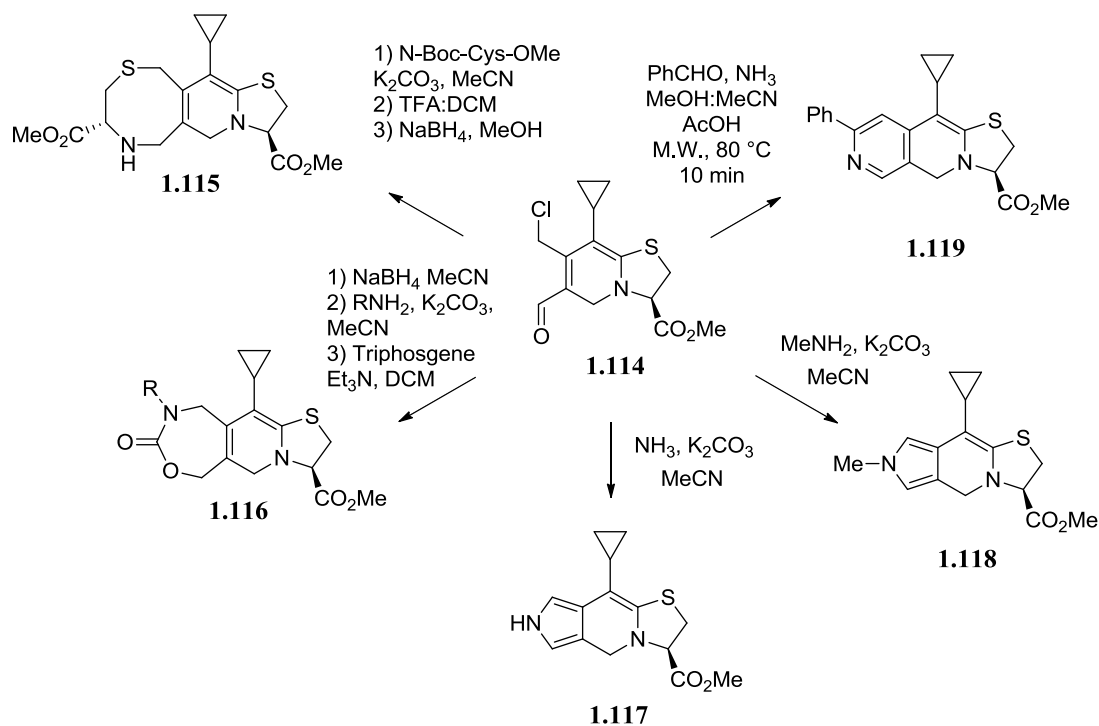
Pyridopyrazines have a wide range of biological applications and a number of possible routes by which they can be made, therefore they are an attractive nucleus for drug design.<sup>185-189</sup>

### 1.6 Syntheses with late-stage diversity

A common challenge for the modern medicinal chemist is the introduction of a diverse range of functional groups and motifs within a complex molecule. Introducing diversity into a chemical framework can take place early in the synthetic route or at a later stage. It is often advantageous to introduce this diversity at the latest possible point, giving access to the greatest diversity of related compounds. The concept of late-stage diversity has found great favour within drug discovery, as it allows the relatively easy preparation of large numbers of related compounds, generally for use in a structure-activity relationship (SAR) study. It is convenient to work from a stockpiled reactive intermediate, when making a diverse library, as opposed to a targeted synthesis for each related compound. Having a highly diverse library of compounds may also allow for the easier discovery of hits against several disease states.

One of the major driving forces behind this thesis was the development of a late-stage diversity oriented synthesis, akin to that of the Boon synthesis. This idea was developed from previous success within our laboratory concerning diversity at the  $C^2$ -position of a range of fused pyrimidines.<sup>146</sup> The development of a diversity-oriented methodology finds use in many different drug discovery programmes as it makes use of a speculative approach towards a large and diverse library of compounds.<sup>190</sup> One such example of a diversity-oriented synthetic approach to a compound library is shown below (**Scheme 1.19**) and highlights the variety of compounds that can be accessed from one reactive intermediate.<sup>191</sup>

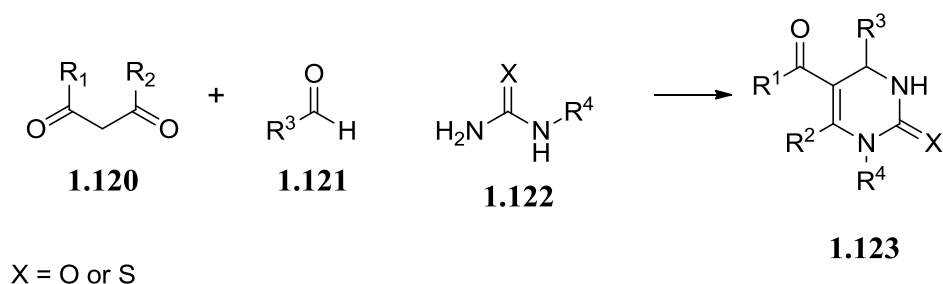




Scheme 1.19: An example of diversity-oriented synthesis.<sup>191</sup>

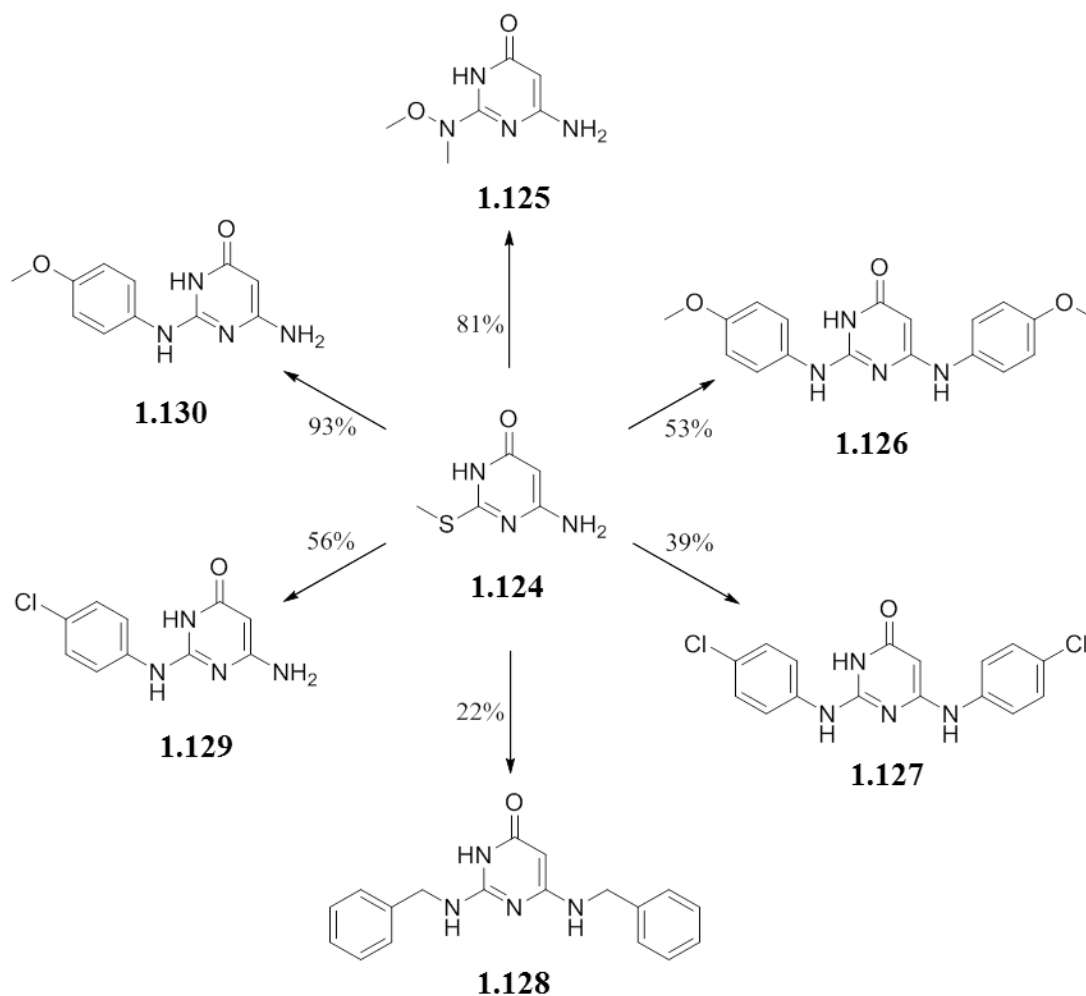
## 1.7 Aims and objectives

Developing a method to make use of late-stage diversity was the motivation behind some of the work described in this thesis. The primary aim of this project was to establish a synthetic route that would allow diversity to be introduced at the C<sup>2</sup>-position of a blocked dihydropteridine at as late a stage as possible. At the outset of this project, there were two established methods for introducing diversity at the C<sup>2</sup>-position of a pyrimidine and, consequently, in the fused systems derived from this molecule. The first of these approaches is the well-established Biginelli reaction.<sup>192</sup> The Biginelli reaction, frequently used with the Atwal modification,<sup>193</sup> is a multi-component reaction that gives access to functionalised dihydropyrimidinones. It is carried out using an aromatic aldehyde, urea or thiourea and ethyl acetoacetate in the presence of a catalytic amount of HCl (**Scheme 1.20**). The obvious limitations of this reaction are centred on the fact that only oxo or thio substituents can be at the C<sup>2</sup>-position and it does not lend itself well to late-stage diversity of fused pyrimidines.



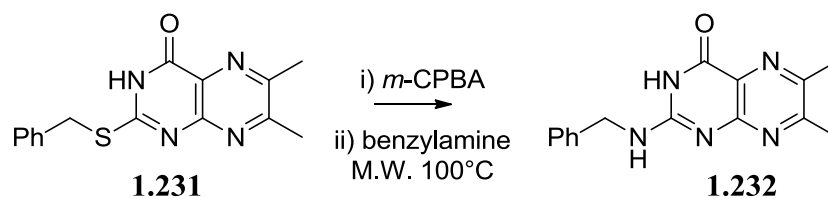
**Scheme 1.20: The Biginelli reaction**

To allow for a more diverse range of substituents at the  $C^2$ - position of a pyrimidine, our laboratory had previously developed a method of displacing a sulfur-containing substituent with an amine and a half an equivalent of acid, typically hydrochloric acid (**Scheme 1.21**). Displacement of the sulfur group, typically *S*-methyl, took place upon heating in a sealed tube and appropriate solvent. Unfortunately, this method suffered from poor yields, limited reactivity, unpredictable side reactions (seen with compounds **1.126** to **1.128**) and also did not lend itself to late-stage diversity of fused pyrimidines.<sup>194</sup> However, the suitability of an alkylthio leaving group was established and this reaction led the way for further development.



**Scheme 1.21:** Early stage diversity of pyrimidines bearing a sulfur group at  $C^2$ .<sup>194</sup>

Following the establishment of this general process, another method was developed which would lend itself to late-stage diversity in the synthesis of pteridines. Again utilising a sulfur-containing substituent as a leaving group, a variety of amines could be introduced at the  $C^2$ -position. This methodology required prior oxidation of the sulfide to the sulfone and the following substitution was preferably carried out using microwave heating in neat amine (**Scheme 1.22**).<sup>146</sup>



**Scheme 1.22:** Modified Isay approach to allow late-stage diversification<sup>146</sup>

However, this methodology was not conducive to the synthesis of blocked dihydropteridines as it used a modified Isay approach. To allow the facile synthesis of a library of blocked dihydropteridines, it is necessary to develop a modified Boon approach. This is something that has previously been attempted within our laboratory but with no success.<sup>195</sup>

It is worth noting that a large amount of industrial interest surrounded this project at the outset of this work. As WSG1002 (**1.6**) was such an efficient activator of all NOS isoforms, early collaborations were initiated to understand better the properties of the compound. Johnson & Johnson were responsible for the initial pharmacokinetic and toxicity studies and the results indicated that WSG1002 (**1.6**) was a compound with minimal innate toxicity problems. This result supported the main driving force behind the establishment of this project and accounts for the narrow structural scope within the overall aims and objectives. The over-arching aim of this project is to develop upon the success of WSG1002 (**1.6**) and discover a compound with a superior profile, specifically a better mimetic of BH<sub>4</sub> (**1.1**), in the context of NOS activators.

At the initial stages of this work, a number of objectives were set out, as questions, relating to both the synthesis and application of blocked dihydropteridines. It was hoped that answers to some, if not all, of these questions could be provided:

- Is it possible to establish a synthetic route specifically giving access to a blocked dihydropteridine that allows diversity to be introduced to the molecule at a late stage?
- Is it possible to introduce diversity to the C<sup>2</sup>-position using thioether chemistry, giving access to a diverse library of pteridines?
- Can the products of these reactions be further elaborated to introduce even more diversity to the library?
- How large a space is available within NOS to accommodate a pteridine that has been expanded at the C<sup>2</sup>-position?
- If there is sufficient space available to accommodate expanded pteridines, would these analogues be suitable activators of NOS and what will this add to the questions remaining about the molecular mechanism on NOS?

- Is it possible to synthesise a deaza-analogue of a dihydropteridine and, if so, does it also act as a NOS activator?
- Are there other dihydropteridines that would be more suitable as activators of NOS and, if so, is there anything in particular that makes them more suitable?
- Is it possible to design an isoform-selective NOS activator based on a synthetic pteridine?

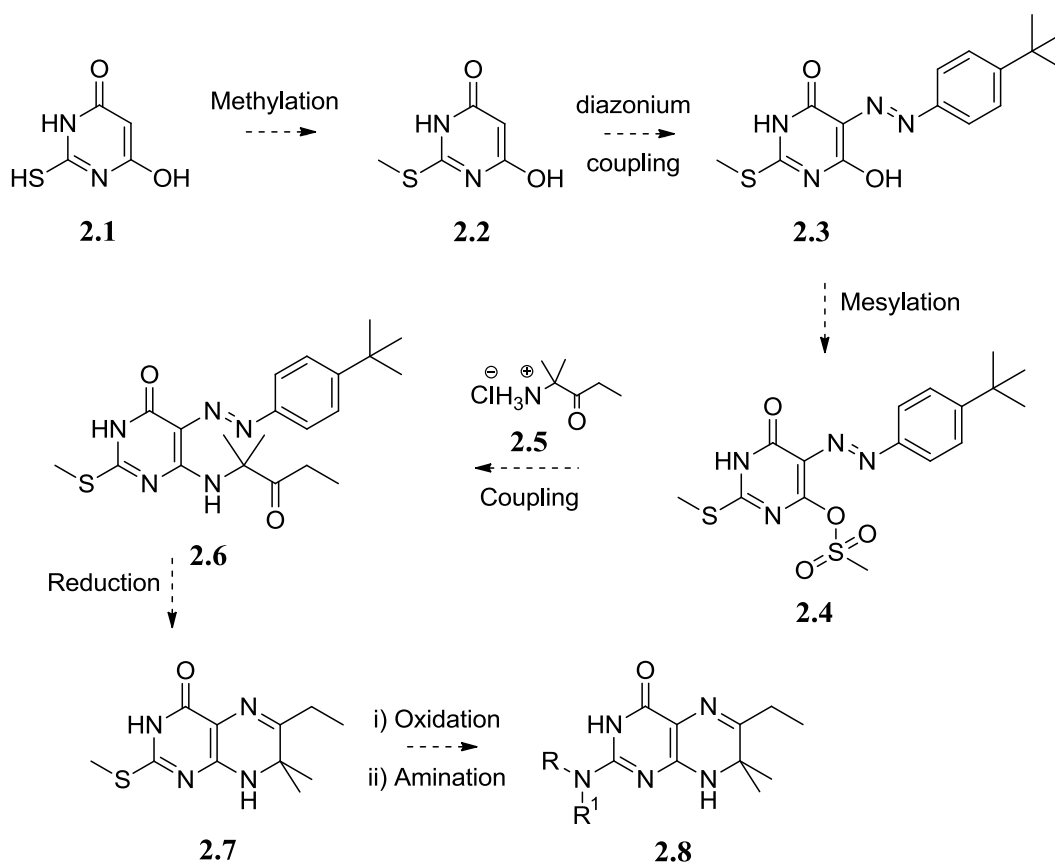
The following chapters describe efforts to answer these questions and delineate the conclusions that can be drawn.

# Chapter 2

## Results and discussion – diversity oriented synthesis

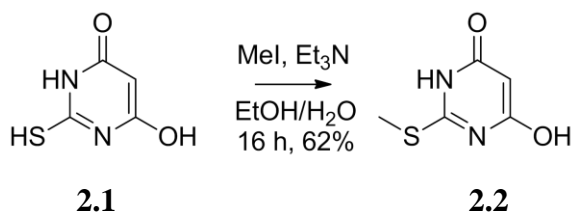
### 2.1 Mesityl leaving group

The first synthetic approaches involved a modified Boon synthesis. A typical Boon synthesis uses displacement of chloride at  $C^6$  from a 5-nitropyrimidinone. However, based on previous work performed within our laboratory, the decision was taken to attempt a modified Boon synthesis using a mesityl group as the leaving group.<sup>195</sup> It was also known from previous work that insertion of a nitro or nitroso group at  $C^5$  would produce unstable compounds and the decision was taken to use the less electron-withdrawing diazo derivative. **Scheme 2.1** displays the envisioned synthetic protocol to allow a late-stage diversity oriented synthesis.



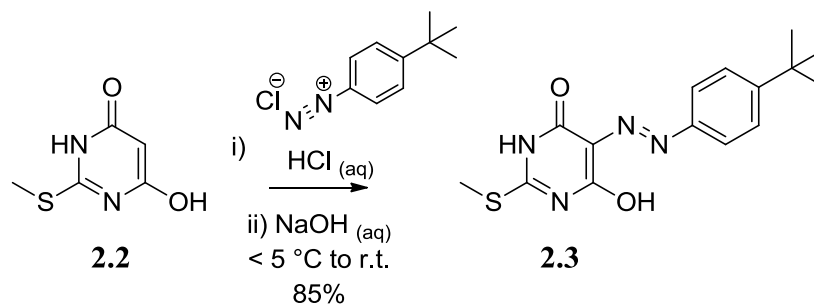
Scheme 2.1: Proposed diversity-oriented synthesis

The first step in the synthetic protocol followed the literature procedure and delivered a similar yield.<sup>195</sup> Treatment of 2-thiobarbituric acid **2.1** with iodomethane and triethylamine in a 2:1 ethanol-water mixture afforded the desired product **2.2** in 62% yield (**Scheme 2.2**).



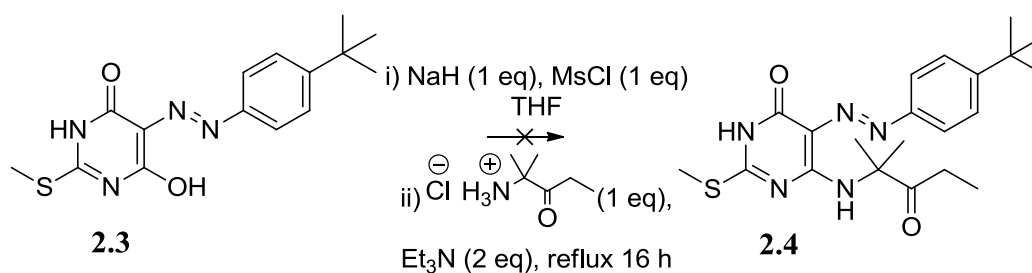
**Scheme 2.2: Methylation of 2.1 to give 2.2.**

Next, the coupling of the diazonium salt derived from *p-tert*-butylaniline was performed using freshly prepared diazonium salt under basic conditions, utilising the more reactive pyrimidinone anion; the product (**2.3**) precipitated upon complete addition of the diazonium salt. After crystallisation from ethanol, the desired product was obtained in 85% yield (**Scheme 2.3**).



**Scheme 2.3: Diazonium coupling to give 2.3.**

Previous experience within our laboratory advised avoiding the isolation of the mesylated pyrimidine (**2.4**), if possible, because it may react with traces of water. Therefore, mesylation of diazo compound **2.3** and displacement with the  $\alpha$ -aminoketone (**2.5**) were attempted in a one-pot reaction under strictly anhydrous conditions (**Scheme 2.4**). This approach was unsuccessful and the starting material was recovered.



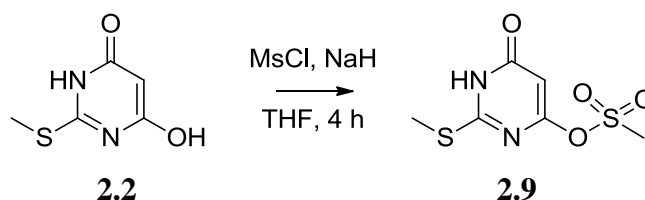
**Scheme 2.4:** Conditions used when attempting the coupling of **2.3** with an aminoketone.

In a diagnostic approach to solving this problem, a brief experimental study was conducted to try to assess whether the problem was arising from the mesylation or the subsequent substitution. **Table 2.1** displays the conditions used in addressing this issue. It appeared that the mesylation reaction had reached completion after 3 hours (monitored by tlc) but this could not be confirmed due to the reactive nature of this leaving group. The pyrimidine could not be trapped out of the reaction using either the  $\alpha$ -aminoketone or butylamine, suggesting the problem was with the displacement of the mesylate group and not its formation. To test this hypothesis further, the 5-unsubstituted 2-methylthiopyrimidine **2.2** (**Scheme 2.5**) was mesylated and the extent of reaction assessed by NMR. This compound was less reactive than **2.3** and could be isolated without the loss of the mesylate. It was found to be beneficial to have 2 equivalents of sodium hydride present at this stage of the reaction (**Table 2.2**).

Equivalents of NaH	Equivalents of MsCl	Equivalents of $\alpha$ -aminoketone <b>2.5</b>	Equivalents of triethylamine	comment
1	1	1 (HCl salt)	2	Starting material recovered
2.2	1	1 (free base)	0	Starting material recovered
1	1	0	0	Failed trapping with <i>n</i> -butylamine

**Table 2.1:** Conditions for the mesylation of **2.3** and displacement reactions using **2.5**.





Scheme 2.5: Successful mesylation of 2.2, confirming that the problem with the coupling of 2.3 and the aminoketone is with the displacement of the mesylate group.

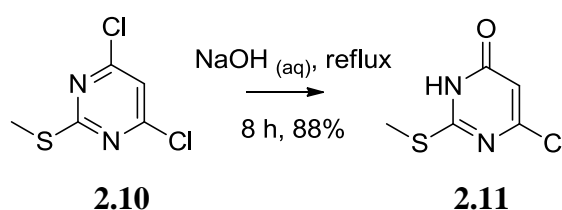
Equivalents of base	Equivalents of MsCl	Ratio of starting material: product
1	1	3:1
2	1	1:1
3	1	1:1
2	2	1:1

Table 2.2: Conditions to assess the extent of mesylation using 2.2 as the substrate

The data above confirm that it is possible to form the mesylated species but highlights the fact that it is unsuitable for use in a modified Boon approach.

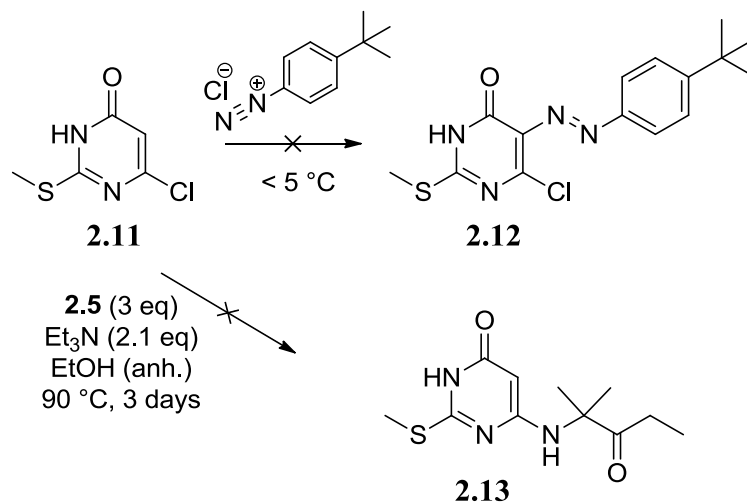
## 2.2 Halide leaving groups

As the typical Boon synthesis utilises a chloride leaving group, the possibility of a halogen-based leaving group was assessed within the modified approach. The facile substitution of a halide in a pyrimidinone is known to require the assistance of an electron-withdrawing group at  $C^5$ . The possibility of inserting a nitro or nitroso group at this position has already been excluded due to its incompatibility with the sulfide at  $C^2$ , as highlighted by previous work within our laboratory.<sup>195</sup> As a result, the possibility of inserting a diazo group was explored. Starting from the commercially available 2-methylthio-4,6-dichloropyrimidine (**2.10**), compound **2.11** was produced by hydrolysis with sodium hydroxide (Scheme 2.6) following a literature procedure.<sup>196</sup>



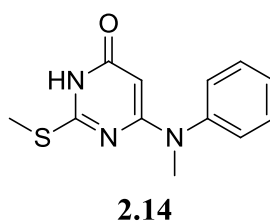
Scheme 2.6: Displacement of one chlorine to form 2.11

Next, an attempt was made to couple **2.11** with the diazonium salt derived from *p*-*tert*-butylaniline. As reported previously,<sup>195</sup> a black tar was recovered and neither starting material nor product could be obtained from the crude mixture (**Scheme 2.7**).



**Scheme 2.7:** Attempt to make use of **2.11** as the pyrimidine for the coupling reaction. Both diazonium coupling and coupling with **2.5** failed.

Following literature precedent, an attempt was made to displace the chlorine on **2.11** by prolonged heating with excess aminoketone (**2.5**).<sup>196</sup> **2.11** and **2.5** were heated in a sealed tube for three days at  $90\text{ }^\circ\text{C}$ . Unfortunately starting material was recovered from the crude mixture, suggesting that the highly sterically-hindered neopentyl-aminoketone was less able to displace the chlorine than other primary amines used in the published examples. Interestingly, secondary amines have been used successfully in the literature to couple with **2.11** but this is thought to be due to the increased nucleophilicity of the amine (see example **2.14**).<sup>197</sup>

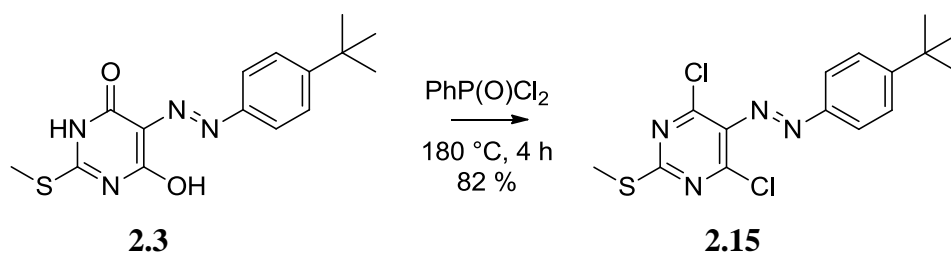


### 2.3 Electron-withdrawing group and chloride leaving-group

It was postulated that a chlorine leaving group could be introduced to the molecule after the insertion of an electron-withdrawing group. In order to achieve this, the decision was made to replace the hydroxyl groups of 5-diazo-2-methylthiopyrimidine

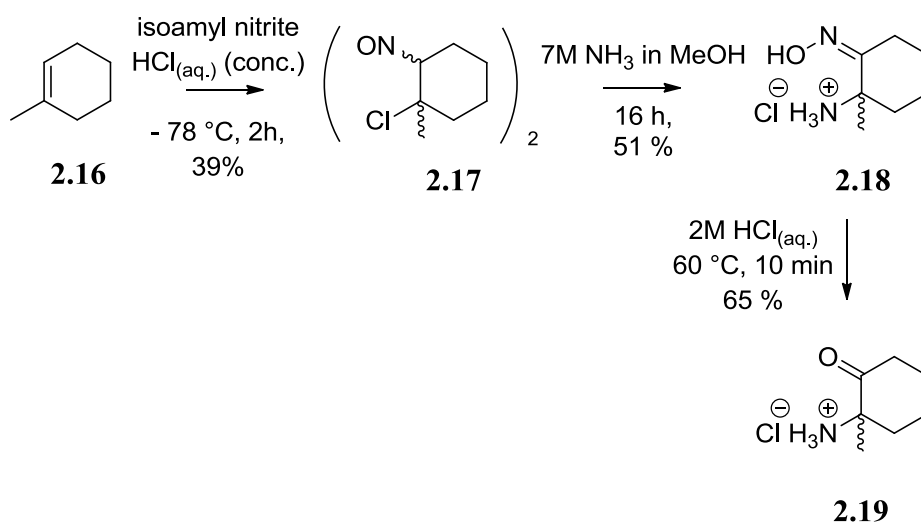
**2.3** with chlorine atoms. This was carried out in the hope of obtaining a molecule that was more likely to take part in the coupling reaction (**Scheme 2.8**).

Replacement of the oxygen atoms of **2.3** with chlorine atoms using phenylphosphinic dichloride was attempted at 180 °C. Upon work-up, the product was obtained in 82 % yield as a deep-red oil (**Scheme 2.8**). Two different solid state structures could be obtained depending upon the conditions used to initiate the phase change. If the product was left to stand for three days then a crystalline solid (small needles) was obtained but when sonicated with agitation an amorphous solid was obtained.



**Scheme 2.8:** Chlorination using phenylphosphinic dichloride

For reasons which will become evident in Chapter 6, the choice of aminoketone was changed. The synthesis of this cyclic aminoketone **2.19** (or amino-oxime **2.18**) had been described previously in the literature and the preparation of this compound followed that procedure (**Scheme 2.9**).<sup>40</sup>

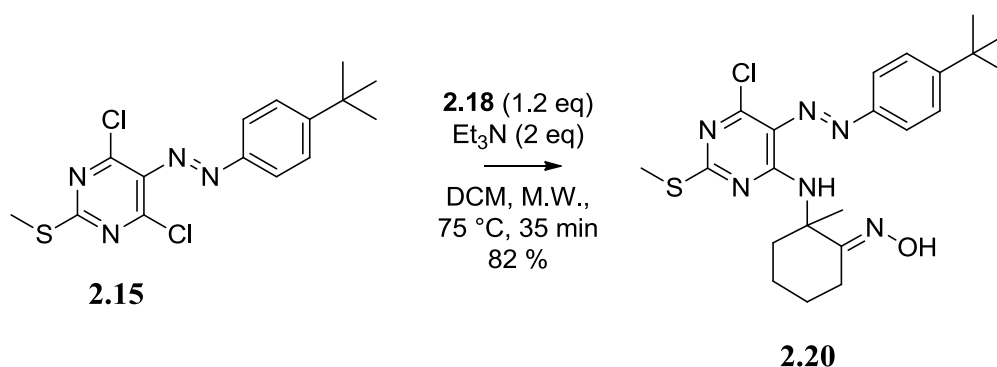


**Scheme 2.9:** Preparation of amino-oxime and the corresponding ketone

The first step involved the addition of nitrosyl chloride to **2.16**. The resulting chloro nitroso compound (**2.17**) was obtained as the dimer typically in about 39% yield. The amino-oxime (**2.18**) was produced in 51% yield by stirring **2.17** in a sealed tube with

methanolic ammonia and then subsequent work-up with hydrochloric acid and evaporation of solvents. It was also possible to produce the aminoketone (**2.19**) at the work-up stage. When removing the solvent from the previous reaction, if heat was used to aid removal of the solvent system, then cleavage of the oxime to the ketone was observed.

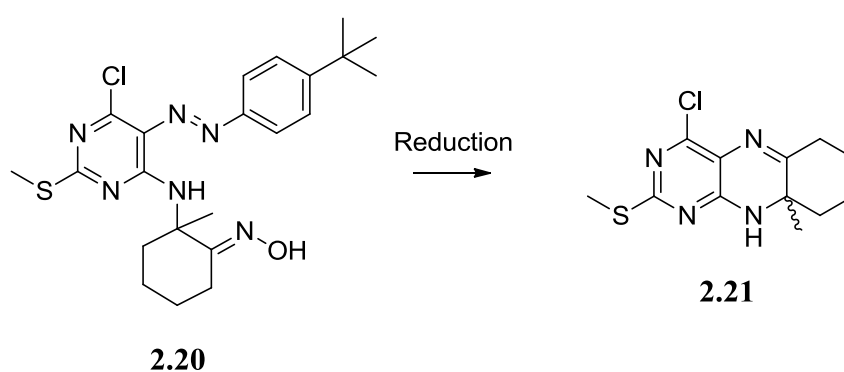
With the amino-oxime (**2.18**) available to couple to the pyrimidine (**2.15**), the reaction was attempted using microwave heating. DCM was chosen as a solvent in an attempt to improve the yield. In the typical Boon synthesis, the coupling reaction is low yielding and it was postulated that side reactions with ethanol, a more nucleophilic solvent, may be responsible. It was also thought that use of DCM would provide a less hydrogen-bonded environment for the amino-oxime, thus encouraging nucleophilic attack. Pleasingly, the desired product was obtained in 82 % yield after only 35 minutes reaction time (**Scheme 2.10**). This yield is much higher than one would expect when carrying out a typical Boon synthesis, as will be seen in **Chapter 4**.



**Scheme 2.10:** Microwave-assisted coupling reaction, making use of much milder conditions.

The reduction and *in situ* annulation reaction (**Scheme 2.11**) was attempted under a variety of conditions (**Table 2.3**). Reduction with sodium dithionite did not produce the desired product and it became a matter of necessity to resort alternative reduction reactions. The first set of conditions to be attempted made use of zinc metal and acetic acid, conditions which had been used previously within our laboratory.<sup>195</sup> Even after 15 hours, with heating, only a small amount of conversion to the product was observed and, upon fractionation *via* flash column chromatography, no product was obtained. This was attributed to very small amounts of pteridine being highly

fluorescent giving the impression of a larger amount of product being present. Next a palladium-catalysed hydrogenation was attempted on a small scale of 150 mg. Fortunately, the product (**2.21**) was obtained in a 79 % yield as a light yellow oil (**Scheme 2.11**). Repetition of this reaction on a larger scale, 600 mg, led to the discovery of new crystalline form of **2.20**. This form was completely insoluble in methanol and appeared as a yellow/orange fluffy solid which could not be carried forward in the synthetic route; DMF was the only solvent which would dissolve this compound and reaction within this system was not possible by conventional hydrogenation or flow hydrogenation. It was found that **2.20** was completely soluble in hot methanol and was much less likely to form the insoluble crystal structure. As a result the decision was taken to amass the cyclised product **2.21** from batch reactions performed in methanol at 60 °C. It was noted that yields from these reactions varied dramatically and on some occasions no product was recovered at all (see **Table 2.3**). It was postulated that the sulfide on the pyrimidine was binding to the palladium and halting the reaction. It was also feasible that sulfide on the pteridine was so well bound to the palladium that recovery of the product from the catalyst was impossible, leading to reduced yields. Nevertheless, the compound that was obtained from the parallel batches was combined with an eye to moving forward to diversification. At this point, comparison of the two batches highlighted another innate problem with the product. It appeared that the product obtained from the first successful reaction had started degrading (**Figure 2.1**) and it became apparent that it would not be possible to spend time amassing a stock.



**Scheme 2.11: Reduction and annulation reaction**

Reducing agent	Solvent	Conditions	Yield
Sodium dithionite	Dioxane and 2M NaOH <sub>(aq)</sub>	Room temperature 15 h	0 %
Zinc	Acetic acid: water (1:1)	30 °C, 2 h	0 %
Zinc	Acetic acid: water (1:1)	40 °C, 15 h	0%
Zinc	Acetic acid: water (1:1)	70 °C, 15 h	0%
Pd/C 50% wt/wt	Methanol	150 mg, room temperature, 8 h	79%
Pd/C 30% wt/wt	Methanol	600 mg, room temperature	Starting material precipitated as insoluble form
Pd/C 30% wt/wt	Methanol: DMF (10:1)	600 mg, room temperature	0%
Pd/C standard cartridge for H-Cube flow system	DMF	0.05 M solution, room temperature	0 %
Pd/C standard cartridge for H-Cube flow system	DMF	0.05 M solution, 35 °C	0%
Pd/C standard cartridge for H-Cube flow system	DMF	0.05 M solution, 45 °C	0 %

Pd/C standard cartridge for H-Cube flow system	DMF	0.05 M solution, 55 °C	0%
Pt/C low loading cartridge for H-Cube flow system	DMF	0.05 M solution, 55 °C	0%
Pd/C 15% wt/wt	Methanol: DMF (10:1)	600 mg, 60 °C	0%
Pd/C 30% wt/wt	Methanol	600 mg, 60 °C	46 %
Pd/C 30% wt/wt (repeated 15 times)	Methanol	600 mg, 60 °C	61% average yield

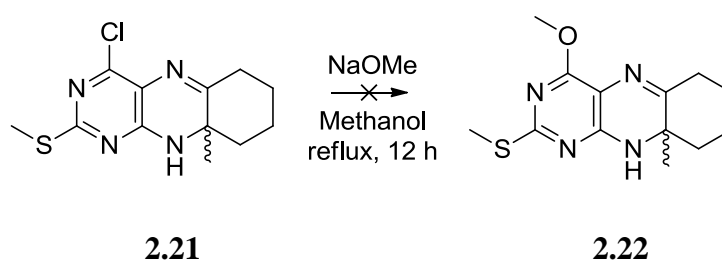
Table 2.3: Conditions for the reduction reaction in Scheme 2.19



Figure 2.1: Fresh 2.21 at the front and decomposing 2.21 behind

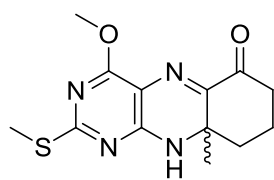
At this point, it was obvious that there were two points of diversity within the molecule; namely the chlorine, which could leave as a chloride, and the sulfide, which could be displaced upon oxidation to the sulfone. It appeared that there was an opportunity to displace one over the other selectively. It was speculated that the chloride would displace first as the carbon-chlorine bond is much more polarised than the carbon-sulfur bond. Instead of simply using sodium hydroxide to generate the pterin, the decision was taken to try this displacement with sodium methoxide. The resulting methoxy pteridine could possibly offer a route to the 2-amino derivative, which might act as a novel inhibitor of NOS (see **Section 1.2.2**).

The reaction of **2.21** with freshly prepared sodium methoxide (**Scheme 2.12**) was monitored by tlc, and the starting material had disappeared after 12 hours. Upon extraction then fractionation by flash column chromatography, a new compound was obtained. NMR spectroscopy suggested that the material was not a single compound but several peaks observed corresponded to what might be expected of the desired product (**2.22**). Mass spectroscopy suggested that the compound may have oxidised, although it was unclear whether this had happened on the third ring system or the sulfide (**2.23** and **2.24** respectively). Further purification was attempted by HPLC. Two peaks on the HPLC trace had a mass that corresponded to the oxidised product. Upon isolation, neither peak appeared to contain pure material or, indeed, the desired product. It is unclear as to whether the problem is arising from the instability of the starting material or the product.

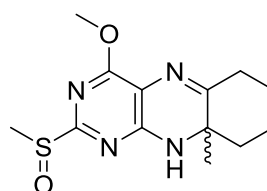


**Scheme 2.12:** Attempt at synthesising **2.22**. A complex mixture of products was obtained instead and isolation of the desired **2.22** was not possible.



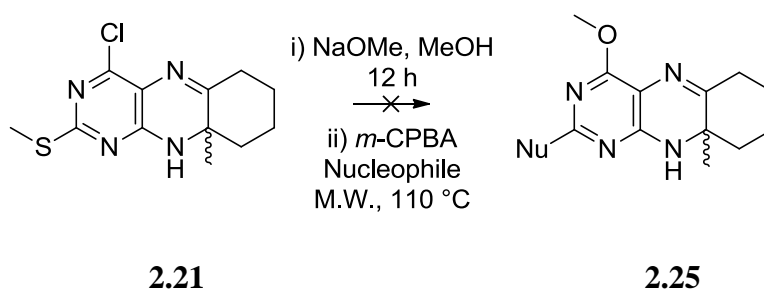


2.23



2.24

To address this issue, the decision was taken to telescope the reaction and attempt the two displacements in quick succession without any purification at the intermediate stage (**Scheme 2.13**).



2.21

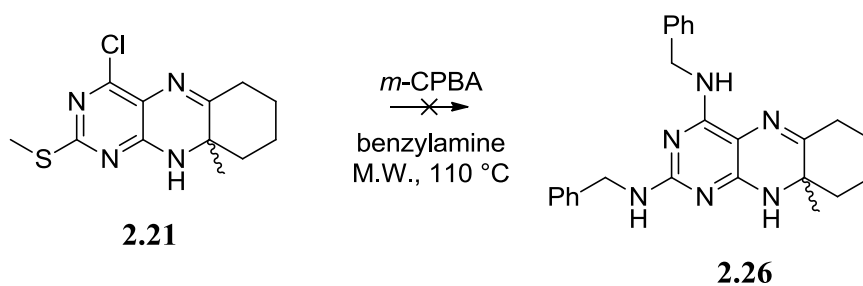
2.25

**Scheme 2.13:** Attempted double substitution with sodium methoxide and three different nucleophiles.

Nucleophile	Solvent
Methanolic ammonia	Methanol
Benzylamine	Benzylamine
Sodium azide	DMF

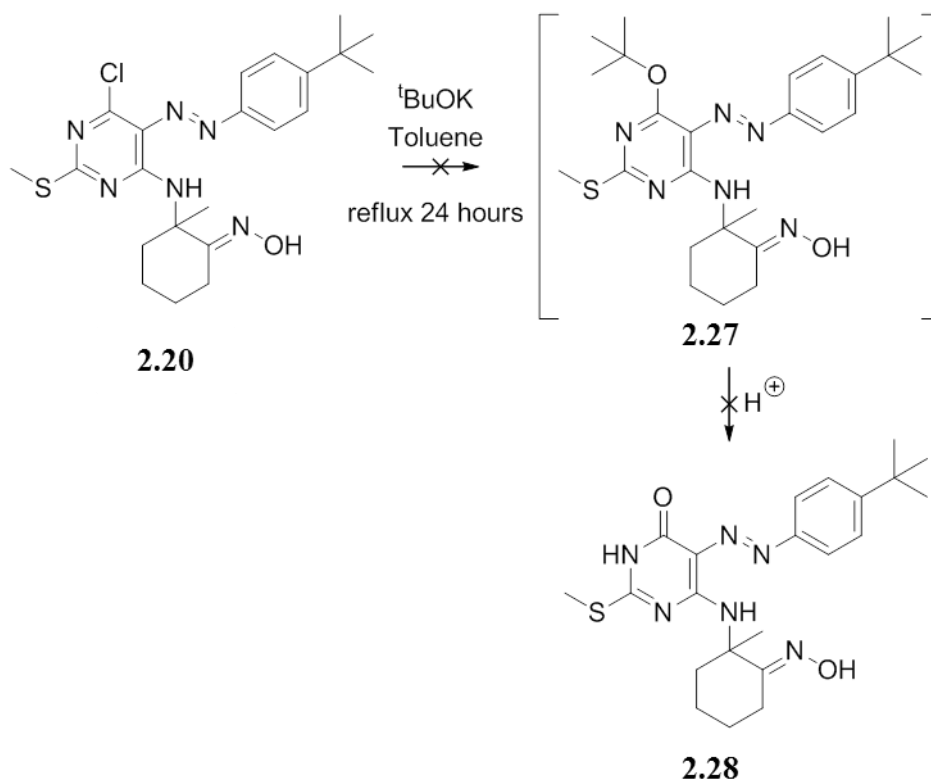
**Table 2.4:** Conditions for the unsuccessful nucleophilic displacement shown in Scheme 2.13.

Introduction of an amine group, benzylamine or azide was unsuccessful and no material could be recovered from the mixture (**Table 2.4**). It is suggested the starting material is insufficiently stable to allow a productive reaction to occur. To assess this suggestion, a double substitution was attempted. The sulfide was oxidised to the sulfone using *m*-CPBA and then heated in neat benzylamine by microwave irradiation. If the starting material is too unstable, it is conceivable that this reaction should have the same outcome as **Scheme 2.13**; this was in fact the case and no material was recovered from the reaction (**Scheme 2.14**).



**Scheme 2.14:** Attempt at synthesising a more stable pteridine (2.26) whilst avoiding instability problems.

In an attempt to reduce the innate reactivity of the pteridine, an approach to remove the chlorine earlier in the synthetic route was made (**Scheme 2.15**). Pyrimidine **2.20** was heated at reflux for 24 hours in toluene with potassium *tert*-butoxide. It was thought that the *tert*-butoxy group could function as a protecting group and allow access to the less reactive pyrimidinone upon an acidic work-up. Unfortunately, this was not the case, as when the crude mixture was analysed by NMR, no aliphatic protons were observed. This suggested that removal of the C<sup>6</sup> substituent was also taking place at the same time as the chlorine.



**Scheme 2.15:** Attempt to remove the instability from the pteridine earlier in the synthetic route. The desired intermediate (2.28) was not obtained.

## 2.4 Conclusions and further work

It was possible to proceed to an advanced intermediate with the synthetic approach that has been described. However the reactivity of this intermediate precluded the successful synthesis of the desired products. In response to the first two questions set out at the end of **Section 1.7**:

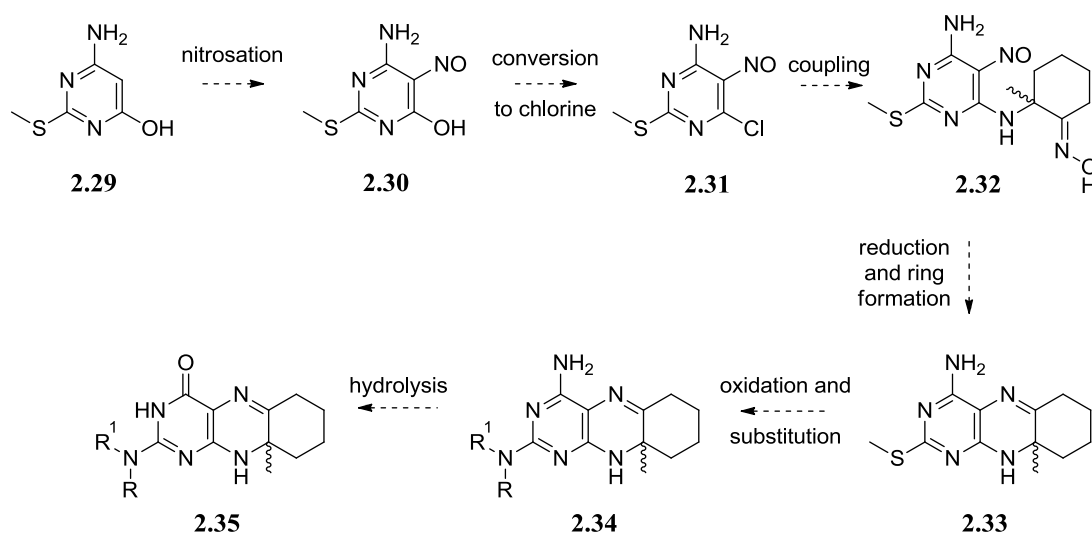
- Is it possible to establish a synthetic route specifically giving access to a blocked dihydropteridine that allows diversity to be introduced to the molecule at a late stage?
- Is it possible to introduce diversity to the  $C^2$ -position using thioether chemistry giving access to a diverse library of pteridines?

The results obtained indicate that these aims are not yet achievable. This apparent instability makes the third question at the end of **Section 1.7** currently not addressable:

- Can the products of these reactions be further elaborated upon to introduce even more diversity to the library?

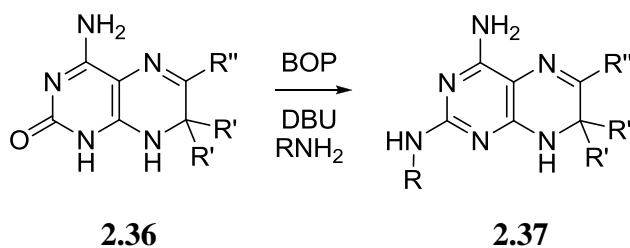
Nevertheless, many options have been explored and the reactivity of these systems is now better understood, albeit with an unsatisfactory outcome. With the current knowledge, it appears that the development of a modified Boon synthesis, based on the sulfur-chemistry explored here, is unlikely to succeed without further research and development.

A sensible place to start would be to capitalise upon the successes from this programme. It is now known how to couple a complex aminoketone to a sulfide-containing pyrimidine ring that has a nitrogen-based electron-withdrawing group attached to it. It may be possible to take advantage of this knowledge to synthesise a less reactive pteridine and avoid the instability problems encountered with **2.21**. **Scheme 2.16** displays one envisioned route to a useable library synthesis.



**Scheme 2.16:** Potential route to an advanced intermediate with altered reactivity (2.33) and further synthetic steps to allow completion of a library synthesis.

It has also been reported that the use of BOP can allow the introduction of a variety of amines at the  $C^4$  position on fused pyrimidines.<sup>146</sup> It appears possible that this could be expanded to 2-oxopteridines, allowing a late-stage diversity-oriented approach to blocked dihydropteridines (**Scheme 2.17**).



**Scheme 2.17:** A potential alternative route to a diversity oriented approach to blocked dihydropteridines.

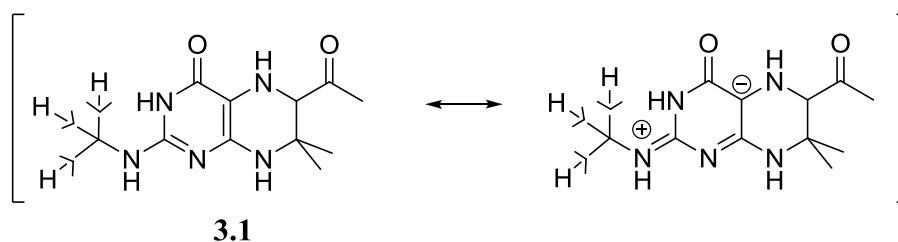
# Chapter 3

---

## Results and discussion – $C^2$ -expansion

### 3.1 Background

X-ray crystallographic studies of all of the isoforms of NOS have shown that the hydrogen-bonding interactions between the pyrimidine section of the pteridine and the haem ring propanoate groups were of high importance to binding.<sup>9,48</sup> In **Section 1.2.2**, it was stated that it is likely that the pterin plays an important role in the molecular mechanism of NOS as an electron shuttle and is essential to the redox chemistry carried out. With this in mind, the decision was made to probe these properties by expanding upon the exocyclic amine at  $C^2$  of the pteridine. This would allow a fuller understanding of the space available within the pterin-binding pocket and also presented an opportunity to modify the electronic characteristics of the analogues which could bind therein. It was proposed that having a more electron-rich pterin would allow a more thermodynamically stable radical at  $N^5$  to form and, by a logical extension, might affect the turnover rate of NOS. With this in mind, the most logical compound to make was an analogue of WSG1002 (**1.6**), with a methyl group attached to the exocyclic amine (**3.1**). The methyl group would not only be a small expansion towards the propanoate groups of the haem but should also have a positive inductive effect, thus subtly increasing the electron density on the pterin ring (**Scheme 3.1**). Not only would this compound possess the increased oxidative stability, when compared to  $BH_4$  (**1.1**), but the extra methyl group should significantly increase the solubility of the pterin in both organic and aqueous media by interrupting their hydrogen bonding network at this side of the molecule.<sup>198</sup> When this work began, it was assumed that adding a methyl group to the exocyclic amine would change its electronic properties and it was also assumed that the effect might be subtle. However, the conclusions that can be drawn from this chapter are not only unexpected but quite exceptional and have wider reaching consequences.



**Scheme 3.1:** *N*-Methyl analogue of WSG1002 with resonance stabilisation, highlighting the inductive effect which should increase the electron density of the pterin ring system

## 3.2 $C^2$ -Expansion

### 3.2.1 Compound evaluation

As the  $BH_4$ -binding pocket is limited in size, computational analysis was carried out to assess the possibility of an expanded pterin binding therein. This experiment was carried out using GOLD.<sup>200</sup> GOLD allows bond rotation of the ligand and flexible amino acid side chains during modelling but does not allow movement of the protein backbone. With this limitation in mind, it was necessary to inspect each result individually, assessing the likelihood of the binding pose, hydrogen bonds and steric interactions before a direct comparison was made with  $BH_4$  (**1.1**).

A suitable X-ray crystal structure for nNOS was chosen from the protein databank and loaded into GOLD; in this case 1OM4 was chosen as it is the structure with the highest resolution available to download. The starting point for ligand binding was chosen to be the pterin binding pocket and the scoring functions were tested with the active enantiomer of  $BH_4$  (**1.1**). To do this, the structure of  $BH_4$  (**1.1**) which was already present in the crystal was deleted and then reloaded into the model and given 20 iterations using all the scoring functions, whereupon it was noted that only one function (Gold.Chemscore.fitness) gave consistently sensible binding poses. Next, both enantiomers of **3.1** were modelled, minimised and loaded into GOLD and 20 iterations were run using the same scoring function. The highest scoring reasonable results were then visualised using DS Visualizer and the poses are shown below with the 6*S*-enantiomer (**3.1a**) in **Figures 3.1** and the 6*R*-enantiomer (**3.1b**) in **Figure 3.2**. The pose for the highest score of  $BH_4$  (**1.1**) is shown in **Figure 3.3** and all three Gold scores are shown in **Table 3.1**.

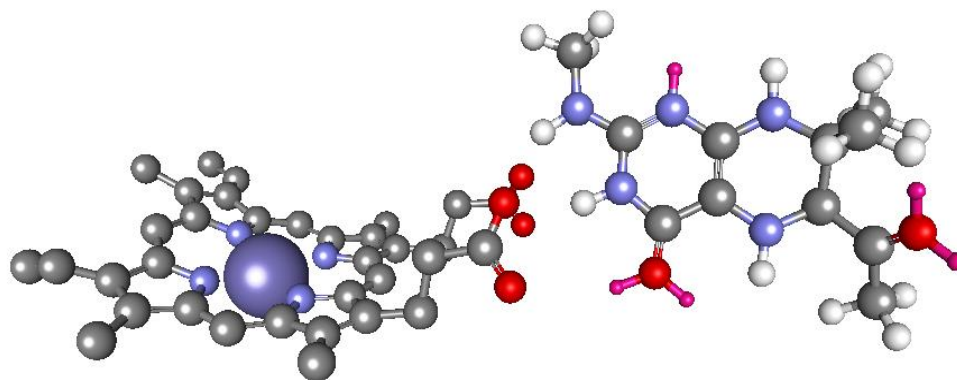


Figure 3.1: 6*S*-Enantiomer of the *N*-methyl analogue of WSG1002 (3.1a). The analogue can be seen adopting an inverted binding pose within the BH<sub>4</sub> binding pocket.

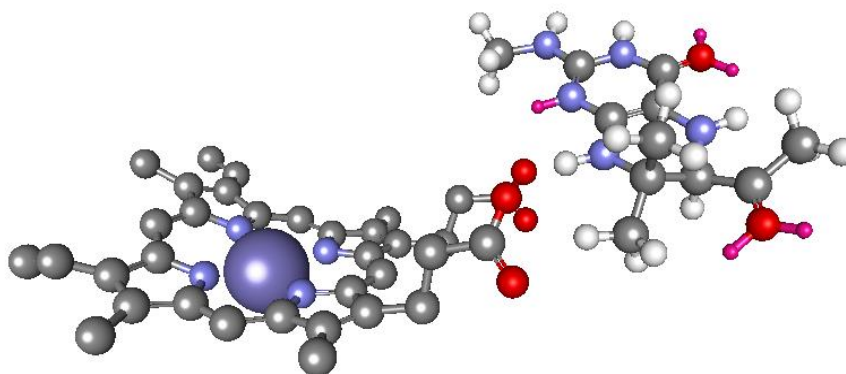


Figure 3.2: 6*R*-Enantiomer of the *N*-methyl analogue of WSG1002 (3.1b). The analogue can be seen adopting an unusual binding pose outwith the BH<sub>4</sub> binding pocket and it was known whether this was a valid binding pocket within NOS.

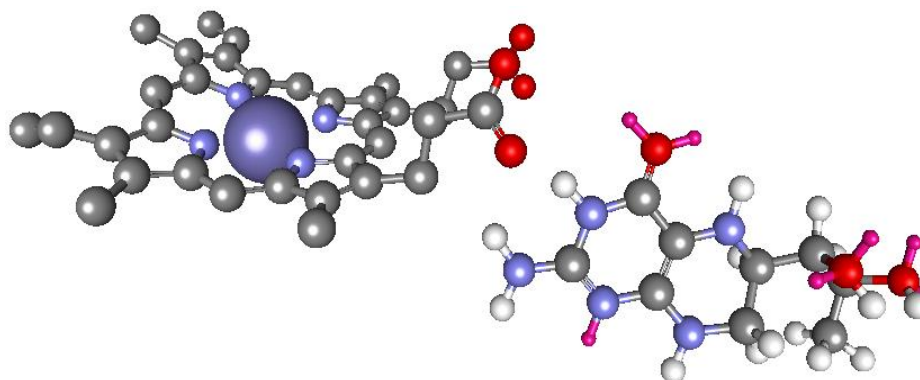


Figure 3.3: Active enantiomer of BH<sub>4</sub> (1.1) modelled using GOLD and is showing the correct orientation within NOS. Analogues that adopt this binding position within NOS could, potentially, act as BH<sub>4</sub>-mimetics.

Compound	Gold score
6 <i>S</i> -enantiomer ( <b>3.1a</b> )	18.47
6 <i>R</i> -enantiomer ( <b>3.1b</b> )	15.75
BH <sub>4</sub> ( <b>1.1</b> )	23.71

Table 3.1: The highest Gold scores for the compound **3.1**, **3.2b** and **1.1**

It appeared that binding within the enzyme was possible; however, one enantiomer (**3.1a**) seemed consistently to produce results that were closer to that of BH<sub>4</sub> (**1.1**). Although the location of **3.1a** was very close to that of BH<sub>4</sub> (**1.1**) the orientation adopted seemed to suggest that the space available was indeed limited. Methyl derivative **3.1a** had to flip by 180° through the x-axis to form the necessary hydrogen bonding interactions with the haem propionate group. The 6*R*-enantiomer (**3.1b**) consistently bound outside of the pterin-binding pocket but was close enough to the heme to form a hydrogen bond through the hydrogen on the *N*<sup>8</sup> position. This pterin is still close enough to the haem to donate an electron. However, it is conceivable that it may not be able to take part in the electron cascade with this altered location and orientation. With this in mind, it was not possible to rule out either enantiomer as a potential coenzyme mimetic and the racemic mixture was synthesised for further evaluation.

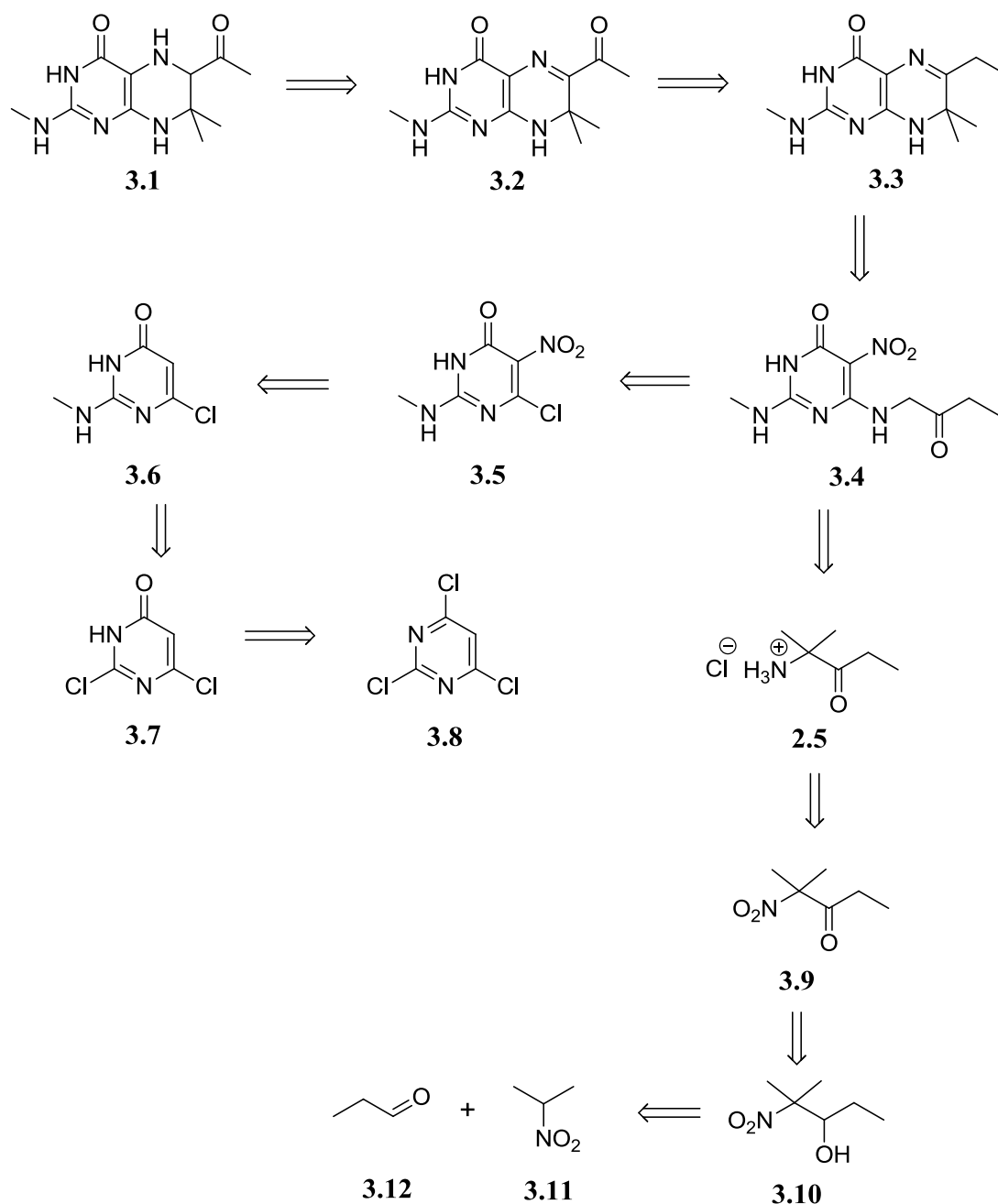
### 3.2.2 Retrosynthetic analysis

The synthesis of a racemic mixture of **3.1** was envisioned as following the classical “incomplete” Boon synthesis and a retrosynthetic analysis is given below in **Scheme 3.2**. The first disconnection takes the tetrahydropterin (**3.1**) to its corresponding dihydropterin (**3.2**). The forward reaction should be achieved by hydride reduction and is well documented.<sup>40,44</sup> The second disconnection takes place on the *C*<sup>6</sup> side chain by functional group interchange of the acetyl to an ethyl functionality. The forward reaction has been documented for these types of compounds and occurs *via* an aerial oxidative process.<sup>40,44</sup> The next disconnection takes place between *N*<sup>5</sup> and



$C^6$  and is typical of the Boon synthesis. The functionality that would result in disconnecting this imine bond would arise from an amine and a carbonyl group, and the forward reaction would be the corresponding condensation reaction. However this spontaneous reaction would be triggered after the reduction of a suitable nitrogen-based functional group (in a higher oxidation level) to the amine, thus our disconnection could proceed to the nitro group seen in compound **3.4**. The presence of this nitro group would greatly aid the installation of an  $\alpha$ -aminoketone group at the  $C^6$  position of the pyrimidine ring and it is typical of this approach to have a chloride leaving group in place, as seen in compound **3.5**.<sup>155</sup> Introduction of the nitro group should proceed *via* classical nitration conditions using concentrated sulfuric acid and fuming nitric acid.<sup>201,202</sup> Insertion of the methylamino group at  $C^2$  of the pyrimidine ring should be achievable by heating 2,6-dichloropyrimidin-4(3*H*)-one (**3.7**) in a sealed tube with methylamine, in a fashion similar to analogous reactions performed frequently within our laboratory.<sup>146,195</sup> 2,6-Dichloropyrimidin-4(3*H*)-one (**3.7**) can be prepared simply by the hydrolysis of 2,4,6-trichloropyrimidine (**3.8**) with sodium hydroxide.<sup>45,203</sup>

The synthesis of the  $\alpha$ -aminoketone (**2.5**) has been well documented and the nitro to amine transformation should be easily achieved *via* simple hydrogenation using palladium on activated carbon. The nitroketone (**3.9**) is disconnected to the nitroalcohol (**3.10**) and the forward reaction should take place using a Jones oxidation. Finally, the formation of the nitroalcohol should take place *via* a Henry reaction between nitropropane (**3.11**) and propanal (**3.12**).<sup>40</sup>

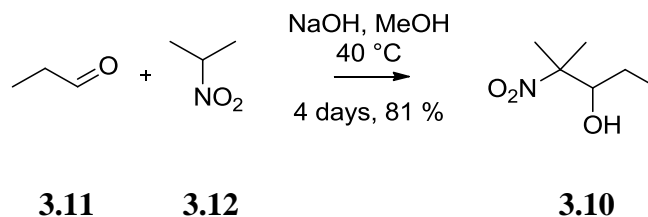


Scheme 3.2: The retrosynthetic analysis of compound 3.1

### 3.2.3 Preparation of $\alpha$ -aminoketone

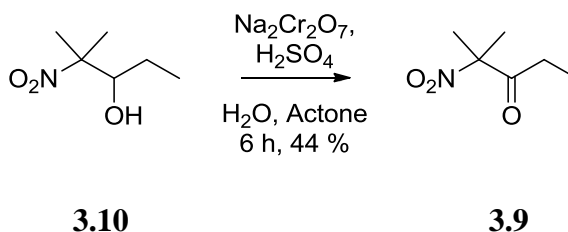
The Henry reaction followed the literature procedure and involved heating propanal (**3.12**) and nitropropane (**3.11**) with a catalytic amount of sodium hydroxide in

methanol at 40 °C for four days. The product was obtained in 81% yield and worked well on a gram and multigram scale.



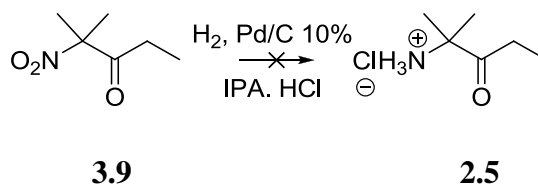
**Scheme 3.3: Henry reaction to form nitroalcohol**

The oxidation of the nitroalcohol (**3.10**) to the corresponding nitroketone (**3.9**) was carried out on both a milligram and multigram scale with comparable yields. The reaction was carried out using the Jones oxidation and was followed by observing the colour change throughout the reaction (orange to green).



**Scheme 3.4: Jones oxidation to form nitroketone**

The reduction of the nitroketone (**3.9**) to the aminoketone hydrochloride (**2.5**) proved to be impossible (**Scheme 3.5**). Several attempts were made on various different scales and using fresh batches of palladium, all without any success (**Table 3.2**). The uptake of hydrogen was monitored during these experiments and it appeared that no reaction was taking place. This result was most surprising as the reaction has been described previously in the literature.<sup>40</sup> One suggestion as to why this reaction did not take place centres on the source of palladium. Novák recently reported substantial variation between palladium sources when carrying out cross-coupling reactions with palladium on charcoal.<sup>204</sup> It is possible that the same problem has been encountered here and the specific source of palladium is preventing the reaction from taking place. Instead of screening a variety of palladium catalysts from various sources at a great cost, the decision was taken to obtain the aminoketone *via* a different route.

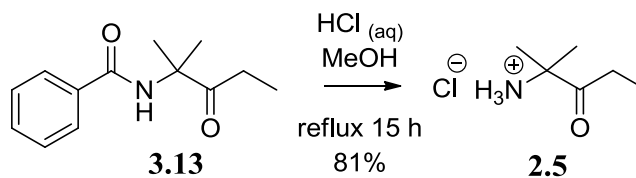


Scheme 3.5: Unsuccessful reduction of the nitroketone

Entry	Solvent system	Repeats	Comments
1	Methanol saturated with HCl	2	No material recovered
2	Methanol with dilute HCl added at work-up	1	No material recovered
3	IPA saturated with HCl	2	Traces of hydroxylamine recovered
4	IPA with dilute HCl added at work up	4	No material recovered

Table 3.2: Conditions for attempted reduction of nitroketone 3.9 to aminoketone 2.5

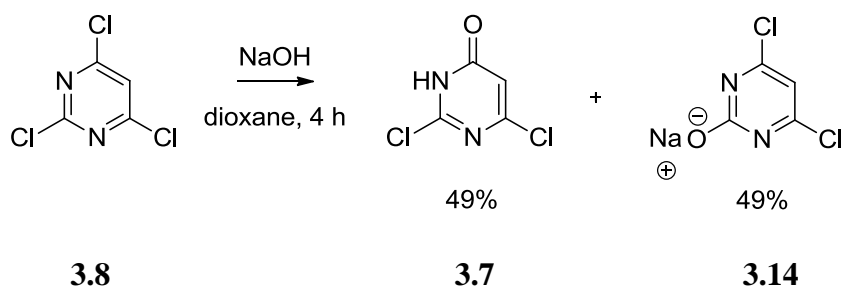
Fortunately a small supply of the benzoyl-protected aminoketone (**3.13**) was available within our laboratory's compound library and the deprotection reaction was carried out in 81% yield.



Scheme 3.6: Removal of the benzoyl protecting-group

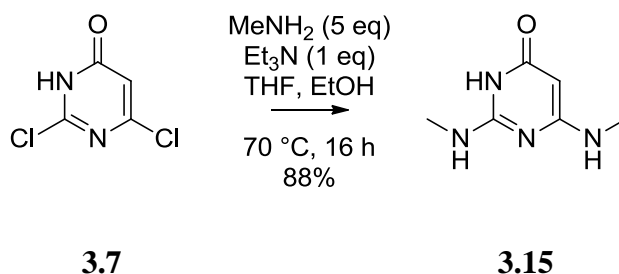
### 3.2.4 Preparation of the *N*-methylpyrimidine

The preparation of 2,6-dichloropyrimidin-4(3*H*)-one (**3.7**) from the commercially available 2,4,6-trichloropyrimidine (**3.8**) followed the literature precedent and the product was obtained in 49% yield along with 4,6-dichloro-2-pyrimidinolate (**3.14**) also in 49% yield.<sup>203</sup>



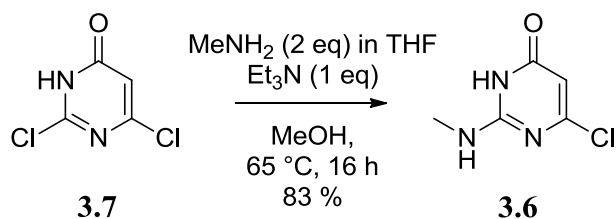
Scheme 3.7: Hydrolysis of 2,4,6-trichloropyrimidine

Insertion of the methylamino group at  $C^2$  required slightly milder conditions than those used in the formation of analogous compounds.<sup>195</sup> The bis-substituted compound (**3.15**) was isolated when heating temperatures reached or exceeded 70 °C. This result was surprising and holds some relevance to properties that will be discussed later in **Section 3.2.7**.



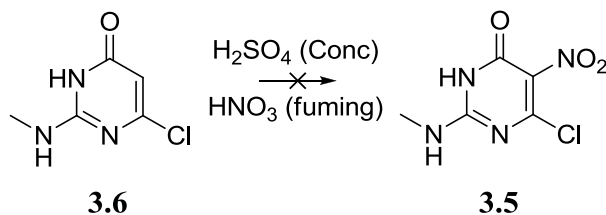
Scheme 3.8: Preparation of the bismethylamino pyrimidine

In an attempt to address this problem, the reaction was attempted again using 2 equivalents of methylamine and one equivalent of triethylamine and was heated at 65 °C for 16 hours. The mono-substituted pyrimidine (**3.6**) was obtained in good yield (83%).



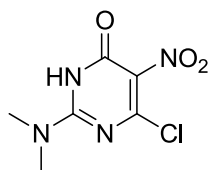
Scheme 3.9: Preparation of the mono-substituted pyrimidine

### 3.2.5 Nitration of 2-*N*-methylamino-6-chloropyrimidin-4(3*H*)-one



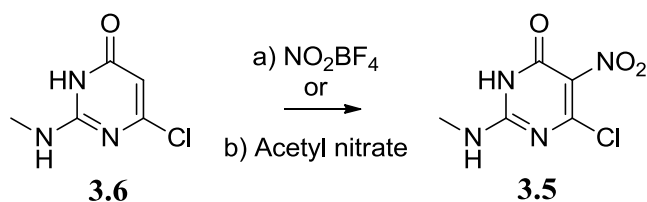
**Scheme 3.10:** Attempted nitration of *N*-methylpyrimidinone

Surprisingly, the nitration of 2-*N*-methyl-6-chloropyrimidin-4(3*H*)-one proved to be unachievable by classical methods (**Scheme 3.10**).<sup>40,201,205-208</sup> Each time the reaction was attempted, no material was recovered from the product isolation and it was postulated that this particular compound may have some inherent instability towards acid. It was initially thought that the extra methyl group was increasing the electron density on the lone pair of electrons for the nitrogen at *C*<sup>2</sup>. However, upon investigation of the literature, this appeared not to be the case, as Pfleiderer had previously reported the synthesis of the *N,N*-dimethyl analogue (**3.16**) which should be even more susceptible to protonation at this site.<sup>209</sup>



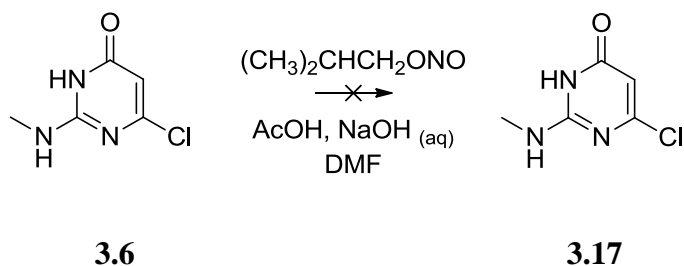
**3.16**

The decision was made to attempt the nitration *via* another method, in the hope that the product was present but was too difficult to obtain from acidic media. Nitronium tetrafluoroborate was chosen as the nitrating agent and was used in three different solvents, sulfolane, THF, and acetonitrile, all without any product being observed. Nitration with acetyl nitrate was then tried as this procedure was frequently carried out within our laboratory, again with no success (**Scheme 3.11**).

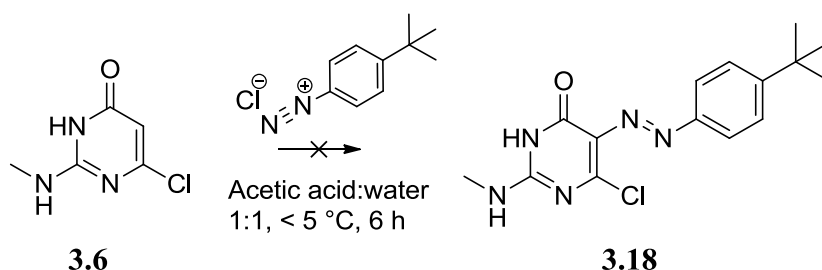


Scheme 3.11: Alternative conditions for nitration

It is also possible to use other nitrogen-based electron-withdrawing groups in pteridine synthesis and in light of the previous failed nitrations; this option was also explored. Nitrosation with isoamyl nitrite was attempted in a buffered solution of sodium acetate; however, no reaction took place and the starting material was recovered. The lack of reaction could be attributed to either the substrate's low reactivity or its low solubility. To assess this further, the reaction was carried out again but with the addition of DMF, ensuring that the substrate was in solution for the entirety of the reaction. Again, upon purification of the reaction mixture, starting material was recovered, suggesting a surprisingly low reactivity for **3.6**.

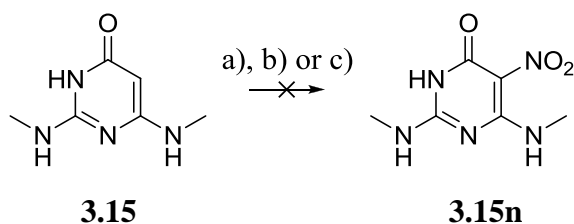
Scheme 3.12: Attempted nitrosation of *N*-methylpyrimidinone

A diazo-linked compound was also considered, as it is possible to obtain these types of compounds from weakly activated pyrimidines (**Section 2.2**). This was attempted using the diazonium salt derived from *p*-*tert*-butylaniline under standard conditions (**Scheme 3.13**).<sup>195</sup> Again, no reaction occurred.

Scheme 3.13: Attempted diazonium coupling of *N*-methylpyrimidinone

These results led us to believe that having one methyl group attached to the amine at  $C^2$ , was somehow paradoxically deactivating the pyrimidine towards electrophilic aromatic attack.

As the bis-substituted methylaminopyrimidine (**3.15**) was available, the decision was taken to see how its reactivity would compare to that of the monoaminomethyl pyrimidine **3.6** and other literature compounds.<sup>203,210,211</sup> It appeared from the literature that insertion of a nitrogen-based electron-withdrawing group was possible when an *N*-methyl substituent was present at  $C^6$  with a variety of substituents at  $C^2$  – including oxygen, sulfur and even carbon-based groups. However, once more, nitration did not occur by the classical method, using acetyl nitrate or nitronium tetrafluoroborate (**Scheme 3.14**) suggesting that there is something special about the *N*-methyl group at  $C^2$  which is altering the reactivity in an unexpected manner. Further mechanistic discussion will be presented later in **Section 3.2.7**. Despite these reactivity problems an alternative route to **3.1** was explored (**Section 3.2.6**).

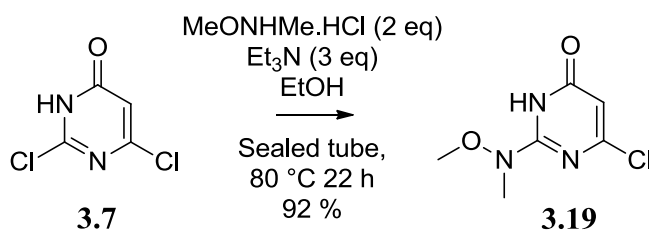


**Scheme 3.14:** Attempted nitration of bis-substituted pyrimidinone. a)  $\text{H}_2\text{SO}_4$  (conc.) and  $\text{HNO}_3$  (red fuming), b) acetyl nitrate, and c)  $\text{NO}_2\text{BF}_4$

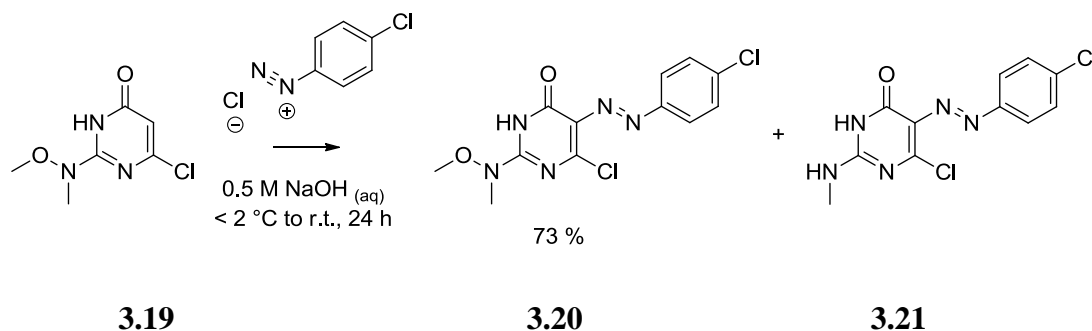
### 3.2.6 An alternative route to the *N*-methyl analogue of WSG1002

It was thought that utilising an activating protecting group could allow the insertion of a nitrogen-based electron-withdrawing substituent at  $C^5$ . From work carried out previously within the group, it was known that using an *N*-methoxy-*N*-methylamino substituent would sufficiently activate the pyrimidine ring towards electrophilic attack.<sup>195</sup> With this in mind, an alternative route to the desired product was initiated. The first step in this synthetic protocol was the insertion of the *N*-methoxy-*N*-methylamino group at the  $C^2$  position of the pyrimidine ring and followed the literature precedent giving the product in 92% yield (**Scheme 3.15**).



Scheme 3.15: Insertion of the *N*-methoxy-*N*-methyl group

The next step involved the electrophilic aromatic attack of the diazonium salt derived from *p*-chloroaniline, which proceeded in 73% yield (Scheme 3.16). Varying levels of the deprotected material (3.21) were observed by NMR each time the reaction was performed. However, this mixture was taken on without further purification, as the stability of the material was a concern. It appeared that the material was quickly degrading over the course of a few days to the deprotected material (3.21) and then to an unknown substance. It was speculated that the deprotection reaction may be initiated by N-O bond scission, which has been well documented in the literature under a variety of conditions.<sup>212,213</sup>

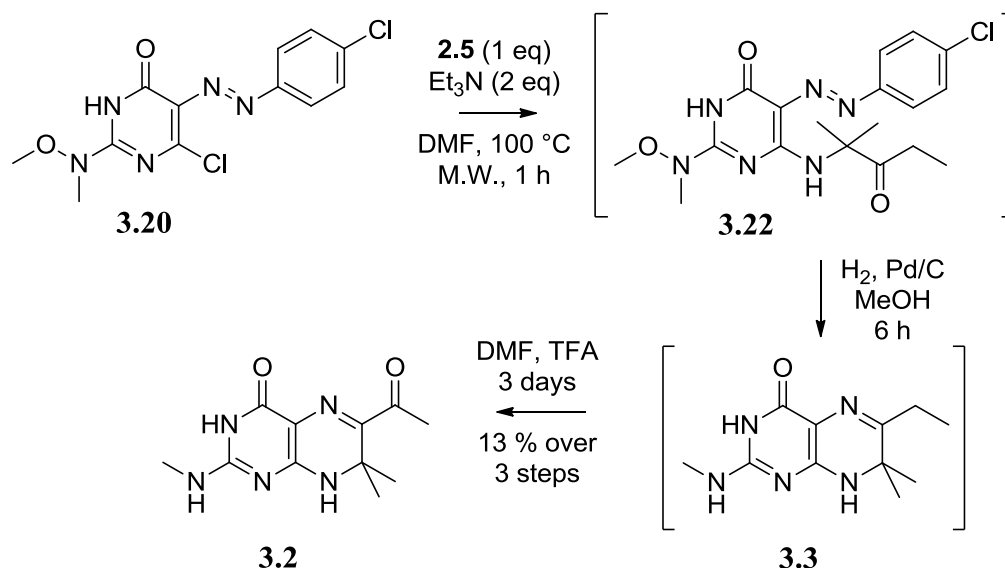


Scheme 3.16: Diazonium coupling giving 3.20 as the major product

With the stability issues of 3.20 being understood, the synthesis was moved forward as quickly as possible. To assist the synthesis through to the pteridine, microwave heating was utilised to couple the  $\alpha$ -aminoketone (2.5) to the pyrimidine. This was successfully carried out in DMF at 100 °C in 1 hour. The DMF was then removed and the crude solid was quickly carried forward to the palladium-catalysed hydrogenation reaction. This hydrogenation reaction facilitate three structural changes to the molecule: the reduction of the diazo group to the corresponding amine, the spontaneous cyclisation to form the pteridine and the deprotection reaction to give the *N*-methyl pteridine 3.3. The outcome of this synthetic step was

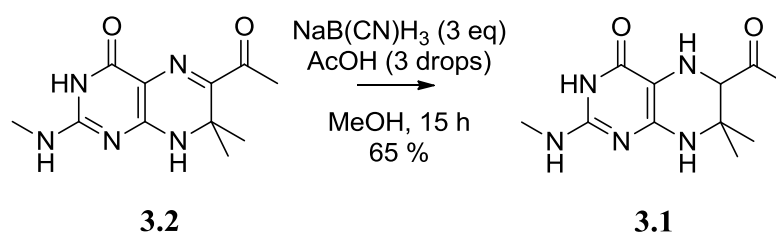
encouraging. When considering the general application of this chemistry, it appears that this route may be a novel method to make 2-*N*-alkyl pyrimidines and their derivatives, such as the corresponding blocked dihydropteridines.

At this point, it was necessary to purify the crude material by HPLC. During the purification process the appearance of another product was observed and upon characterisation it was noted that **3.3** was spontaneously oxidising to **3.2** (**Scheme 3.17**). This reaction was somewhat unexpected as it had previously been reported that this reaction occurred only in very specific conditions and had never been observed in DMF before.<sup>195</sup> It is reasonable to suggest that this oxidation is being catalysed by trace amounts of palladium from the previous hydrogenation reaction; the relative rates of oxidation will be discussed later in **Section 3.2.7**.



**Scheme 3.17:** The coupling, annulation, deprotection and oxidation steps

With the dihydropterin successfully made, the final step was to perform the reduction to the tetrahydro oxidation state. This was carried out using sodium cyanoborohydride following the typical literature fashion (**Scheme 3.18**).<sup>45</sup> The final product **3.1** was obtained in 65 % yield, was purified by HPLC and stored on dry ice for transport to the University of Edinburgh for evaluation as an activator of NOS.

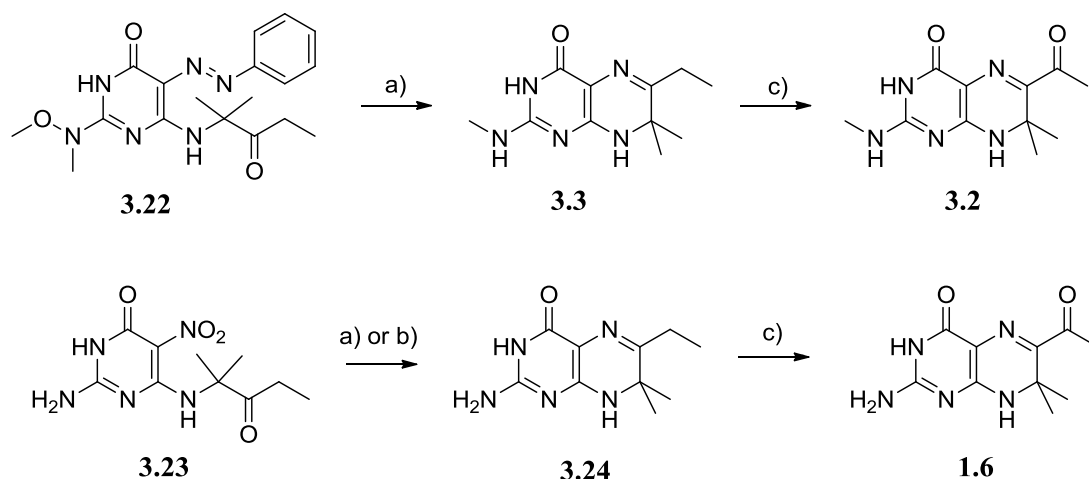


**Scheme 3.18:** The reduction of the dihydropterin

### 3.2.7 The peculiar properties of *N*-methylpyrimidines and fused pyrimidines

From the results obtained so far (Sections 3.2.5 and 3.2.6), it is apparent that pyrimidines and their derivatives that possess an *N*-methyl substituent at the  $C^2$ -position have unusual and unexpected reactivity. There was a small body of evidence suggesting that these compounds were unreactive to nitrogen electrophiles, which could be a result of a lower electron density in the ring than expected for a 2-aminopyrimidine. However, the unexpectedly-ready oxidation of **3.3** may present conflicting evidence, as oxidation usually takes place with electron-rich species; this might be expected with a weakly electron-donating methyl group. To address this problem, a comparative oxidation study was initiated to assess the relative rates of oxidation of the *N*-methylaminopteridine **3.3** and corresponding aminopteridine **3.24** (the synthesis of **3.24** is discussed later in Chapter 4).

It was assumed that the oxidative process that took place with **3.3** was a palladium-catalysed C-H activation. To confirm this, compound **3.23** was reduced twice, once with sodium dithionite and once with palladium and hydrogen (Scheme 3.19). Both compounds were then dissolved in DMF with 4-5 drops of TFA, placed in a total recovery vial and left in the HPLC auto sampler to recreate more fully the conditions that **3.3** was exposed to. After one day, an HPLC trace was run for both oxidations and it became apparent that not only were traces of palladium catalysing the oxidation reaction but that compound **3.24** underwent this reaction much more readily than **3.3** (Table 3.3).



Scheme 3.19: Comparative oxidation reactions. a) Pd/C, H<sub>2</sub>; b) Na<sub>2</sub>S<sub>2</sub>O<sub>4</sub>; c) DMF, TFA

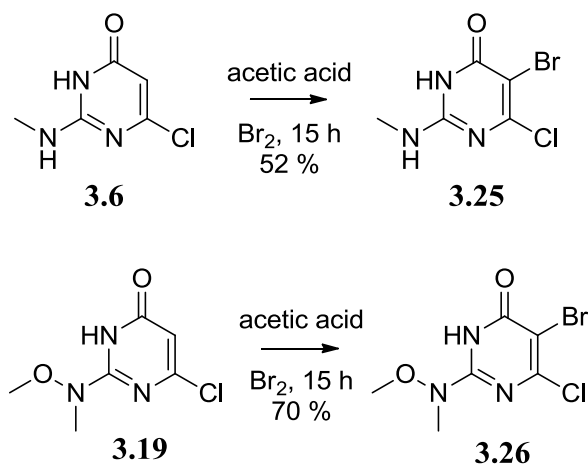
Compound	Extent of oxidation after 1 day
<b>3.3 (reduction method a)</b>	None observed
<b>3.24 (reduction method a)</b>	25%
<b>3.24 (reduction method b)</b>	9%

Table 3.3: Comparative oxidation rates between 3.3 and 3.24 as well as oxidation method

These results add further weight to the argument that 2-*N*-methylaminopyrimidines and their derivatives react as if they were more electron-deficient than their amino analogues. These results were unexpected and are the opposite of what one might predict in terms of electron density and reactivity. Considering the inability of **3.6** and **3.15** to react with some nitrogen electrophiles and the slower rate of oxidation of **3.3** when compared with **3.24**, a trend appeared to be emerging. An explanation was sought so that a deeper understanding of the chemistry may be obtained. This was important as *N*-methyl ketopterin **3.1** was to be taken on for enzymatic assay and understanding the chemistry could provide a deeper insight into the results obtained therein. Furthermore, understanding the processes behind this unexpected reactivity is a basic scientific endeavour and may help better inform future pyrimidine and fused pyrimidine work within the field.

This first hypothesis considered the idea that the methyl group was somehow forcing the lone pair of electrons out of the plane of the pyrimidine ring, thus reducing the pyrimidine electron density. To test this, an attempt was made to grow crystals of

pyrimidine systems which possess an *N*-methyl group. Two compounds were chosen (**3.6** and **3.19**) and were brominated at  $C^5$  to allow the structures to be easily solved (**Scheme 3.20**). Each product was then dissolved in hot methanol, placed in a fresh, clean vial, covered with aluminium foil and the solvent was allowed to slowly evaporate. When the solvent had almost totally evaporated, **3.26** had grown crystals suitable for X-ray diffraction whereas **3.25** consistently gave an amorphous solid. The crystal growth for **3.25** was attempted again in an NMR tube as well as using a DMSO:water diffusion technique, each with no success. However it is notable that bromination of these compounds occurred readily whereas substitution at  $C^5$  by nitrogen electrophiles did not (**Section 3.2.5**).



**Scheme 3.20: Bromination of *N*-methyl pyrimidine systems**

Compound **3.26** did not display any unusual geometry and it is reasonable to suggest that the lone pair is oriented correctly to allow overlap with the  $p$ - $\pi$  orbital on the  $C^2$  position of the pyrimidine ring (**Figures 3.4, 3.5** and appendix A). Even though **3.19** underwent electrophilic aromatic substitution, it did so relatively slowly compared to its amino analogue (**Chapter 4, 4.7**). If the rotation of the lone pair out of the ring plane was a likely explanation for the decreased reactivity, it would be reasonable to expect to see it in this crystal structure. The lack of any unusual geometry might suggest that this first hypothesis may be incorrect.

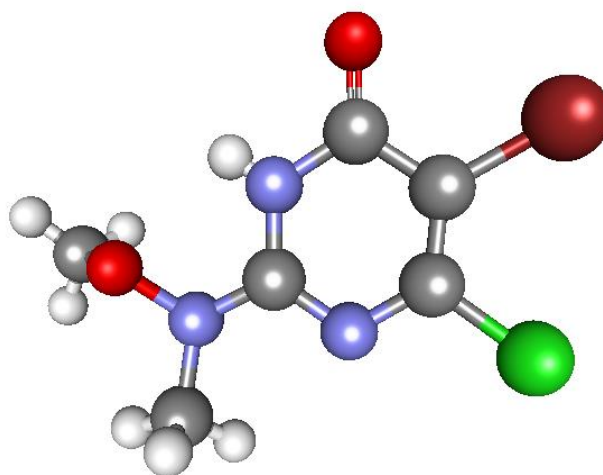


Figure 3.4: Face on view of X-ray structure of compound 3.26

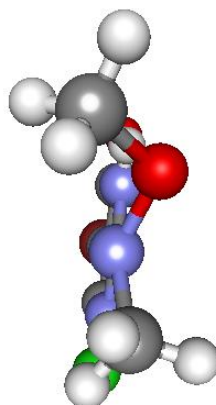


Figure 3.5: Side-on view of the X-ray structure of compound 3.26 - showing the expected geometry around the C<sup>2</sup> bond

As any crystal structure obtained might not necessarily reflect the correct geometry adopted by a compound in solution, it was important to balance this finding with spectroscopic data in the solution phase. To that end, a comparison of the <sup>13</sup>C NMR data was appropriate to inspect the relative chemical shifts of the carbon at C<sup>5</sup>.

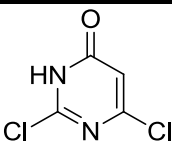
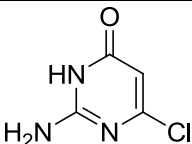
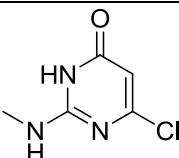
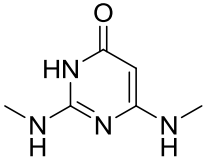
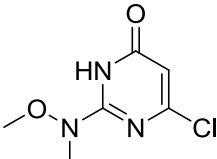
Compound	$C^5$ chemical shift ppm
 <p style="text-align: center;"><b>3.7</b></p>	99.9
 <p style="text-align: center;"><b>4.7</b></p>	99.4
 <p style="text-align: center;"><b>3.6</b></p>	99.4
 <p style="text-align: center;"><b>3.15</b></p>	74.4
 <p style="text-align: center;"><b>3.19</b></p>	101.4

Table 3.4:  $^{13}\text{C}$  NMR chemical shifts for  $C^5$  position of various pyrimidines

From the  $^{13}\text{C}$  NMR data (Table 3.4), it can be seen that there is surprisingly little difference in the electron-density at  $C^5$  when the substituent at  $C^2$  is changed. These results suggest that electron density at  $C^5$  may not be the source of the lowered reactivity. With both the X-ray and the NMR data suggesting that the lone pair of electrons from the amine at  $C^2$  are oriented in the usual manner, the hypothesis of unusual geometry has been discounted.

With the solid state and solution state studies discounting one hypothesis, further information was sought on the reactive intermediates that could influence the progress of these reactions. The decision was taken to investigate the HOMO energy levels of the pyrimidine systems, as a low energy HOMO could retard the electrophilic aromatic substitution. To investigate the energy levels of these pyrimidines, Spartan calculations were performed using two different basis sets, AM1 (semi-empirical calculations) and B3LYP 6-31G\* (DFT calculations). Whilst both basis sets would give different numerical values, the important piece of information which could be obtained would be a rank order of reactivity. The results are given below in **Table 3.5** and a representative picture of the orbital cloud is presented in **Figure 3.6**, the remaining diagrams are available in appendix B.

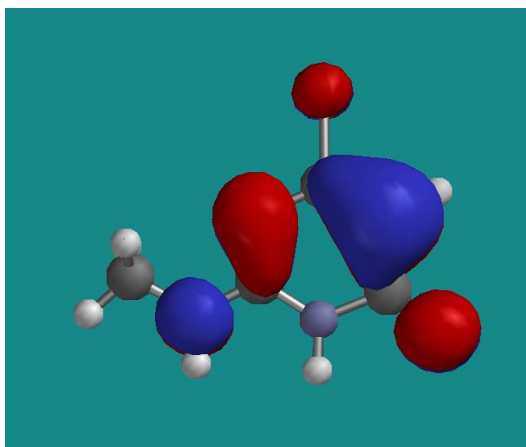


Figure 3.6: Orbital diagram for the DFT calculation of the *N*-methylpyrimidine 3.6.



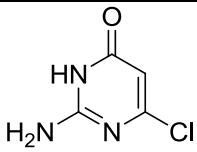
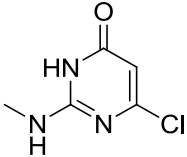
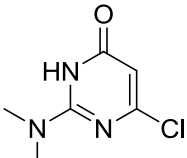
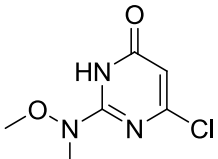
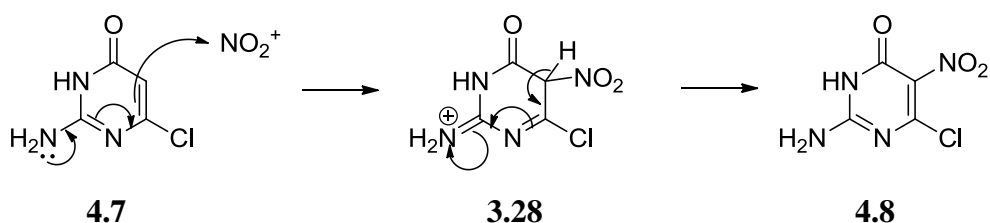
Compound	AM1 (kJ mol <sup>-1</sup> )	B3LYP 6-31 G* (kJ mol <sup>-1</sup> )
 <b>4.7</b>	-888.35	-603.57
 <b>3.6</b>	-880.25	-595.02
 <b>3.27</b>	-888.03	-580.77
 <b>3.19</b>	-915.67	-604.37

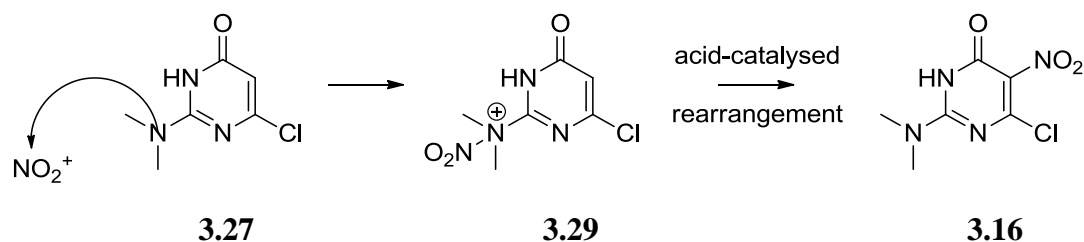
Table 3.5: Results from Spartan calculations of the HOMO energies of differently substituted pyrimidines

From the numerical data, it is clear that the semi-empirical calculations are adding no real insight to the situation, with the first three compounds having essentially the same value, within experimental error. When considering the DFT calculations, it appears that the order of reactivity follows  $\text{NMe}_2 > \text{NHMe} > \text{NH}_2$ . This is what might normally be expected when predicting the reactivity of such systems and adds no extra insight into the lack of reaction taking place. Interestingly, both the semi-empirical and the DFT calculations predicted a low reactivity for the *N*-methoxy-*N*-methyl compound. From the depiction of the HOMO location (**Figure 3.6**) it is clear to see that the majority of the electron density resides on the  $C^5$  position and this is consistent with the experimental results.

With every available avenue explored, within the skill-set of our laboratory, assistance was sought from a more experienced computer modelling collaborator. In collaboration with Tuttle and Idziak, one final hypothesis was placed under scrutiny. The idea is based on the possibility that the pyrimidine can attack the electrophile from different places on the molecule.<sup>195</sup> It is conceivable that one pyrimidine is proceeding *via* the classical electrophilic aromatic substitution mechanism (for example NH<sub>2</sub> at C<sup>2</sup> **Scheme 3.21**) and the other (for example NMe<sub>2</sub> at C<sup>2</sup> **Scheme 3.22**) is proceeding *via* another mechanism, for example, an acid-catalysed rearrangement. Several mechanisms are currently under evaluation and it is hoped that the results will provide more of an insight into the problem.



**Scheme 3.21: Direct electrophilic aromatic attack of 4.7**



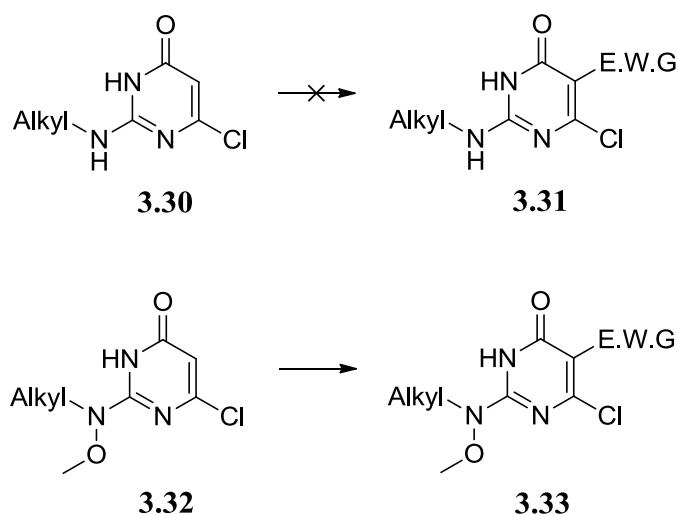
**Scheme 3.22: Acid-catalysed rearrangement nitration proposal for 3.27.**

So far, the Tuttle group has looked in great detail at many possible mechanisms for these nitrations and are still currently assessing these routes for a number of pyrimidines. As such, it is not possible for any conclusions to be drawn at this time.

### 3.3 Conclusion

The original synthetic approach employed that gave access to variation at the C<sup>2</sup>-position was unsuccessful in producing an analogue of WSG1002. However, this result was very surprising and provided some evidence that the monomethylated exocyclic amine on the pyrimidine was acting in an unexpected fashion. This route

provided the first insight into the strange properties of such systems. Next, a solution was found that would address the problem of the unreactive pyrimidine and an analogue of WSG1002 was prepared. This analogue will be used in **Chapter 6** to assess the suitability of extended pteridines within the nNOS enzyme. Upon preparation of this compound, some more unusual properties were observed with the monomethylated species – this time on the pteridine itself. An oxidation study was undertaken and further evidence was obtained to suggest that pyrimidines and fused-pyrimidines that possess the exocyclic monomethylated amine act as if they have been starved of electron-density when compared to expected reactivity. With the unusual characteristics of such systems now better understood, a reason for this behaviour was sought. However, at this point, no firm answer has been found. What can be said is that the reactivity of these monomethylated systems is quite exceptional and is entirely counter-intuitive in terms of reactivity. Finally and importantly in the context to the chemistry of 2-aminopyrimidines, a procedure for early-stage diversity-oriented synthesis of fused pyrimidines has been established. In principle, the chemistry developed using the *N*-methoxy-*N*-methylaminopyrimidine could be greatly expanded to provide a route to other *N*-alkylated pyrimidines (**Scheme 3.23**).



**Scheme 3.23:** A general route to mono-alkylated fused-pyrimidine precursors

# Chapter 4

---

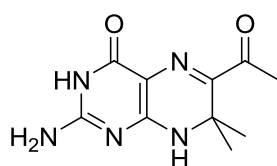
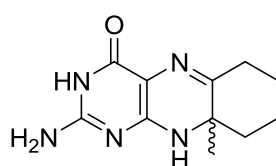
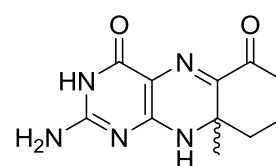
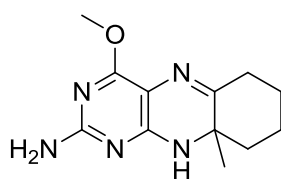
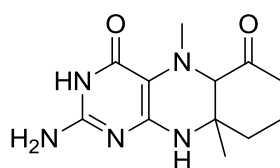
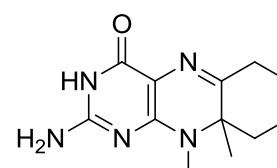
## Results and discussion – targeted syntheses

### 4.1 Background

The Boon synthesis has been used many times at Strathclyde to prepare blocked dihydropteridines and the resynthesis of some compounds was required to further our studies of nitric oxide synthase. These compounds were a part of the library collection and have been given a systematic name based on the type of fused pyrimidine they were and the order in which they were made. For this particular collection, there is a three letter, four number code, WSG1###. WSG refers to the main inventors behind this collection, the late and great Hamish Wood, Colin Suckling and Colin Gibson. The number 1 – the first number in this series – refers to the blocked pteridines and the three remaining numbers signify the chronological order with which the compounds were added to the library.

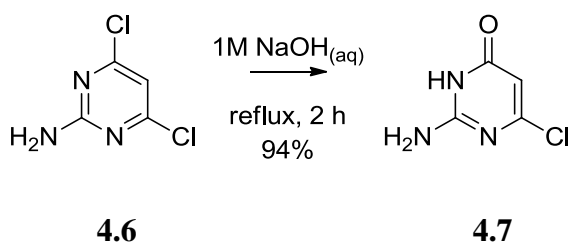
With the development of the enzyme-based assay and the potential application of active-compounds towards cardiovascular disease being a high priority for this project, it was necessary to resynthesise three particular compounds, WSG1002 (**1.6**), WSG1007 (**4.1**) and WSG1060 (**4.2**) for evaluation (**Chapter 6**). Unpublished data from previous cell-based assays suggested that compounds **4.1** and **4.2** may act as NOS activators; however, the data obtained from these assays proved to be unreliable and a definitive answer to this problem was sought.<sup>199</sup> It was also thought that these pteridines would add a further understanding to what makes a blocked dihydropteridine a good NOS activator. The resynthesis of these compounds also provided a good opportunity to attempt the new synthesis of related analogues using precursors and WSG compounds as potential intermediates for diversification (**4.3 – 4.5**). The motivation for attempting the synthesis of these compounds was to probe the available space within the NOS enzymes; the same rationale used in **Chapter 3**. In a fashion similar to the synthesis of **3.1**, the aim was to synthesise compounds that

were a one-carbon expansion upon an active- or potentially active-pteridine. With the product of the  $C^2$  extension already synthesised, products for  $C^4$ ,  $C^5$  and  $C^8$  extended pteridines were sought (**4.3** – **4.5**). Further to probing the available space within NOS, **4.3** could potentially act as a novel pterin-based inhibitor and would provide further evidence for or against the necessity of a proton at  $N^3$  (**Section 1.4.1**). Compound **4.4** would potentially be an example of a stable blocked tetrahydropterin, if active. However, it is worth noting that a facile route to these compounds was sought and a lengthy individual synthesis of each compounds was not suitable, as the development of the assay and assessing the suitability of **4.1** and **4.2** as activators was the main priority.

**1.6****4.1****4.2****4.3****4.4****4.5**

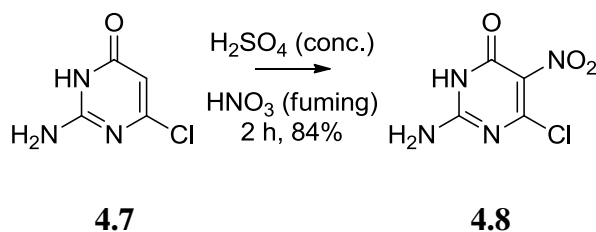
#### 4.2 Synthesis of a common precursor

All three pteridines make use of the reactive nitrochloropyrimidine (**4.8**). The synthesis of **4.4** follows literature precedent, starting from the commercially available 2-amino-4,6-dichloropyrimidine (**4.6**).<sup>214-216</sup> Hydrolysis of the first chlorine was accomplished by heating **4.6** at reflux in dilute aq. sodium hydroxide for 2 hours and was achieved in good yield (94%, **Scheme 4.1**).



Scheme 4.1: The hydrolysis of one chlorine to give selectively the aminochloropyrimidinone **4.7**

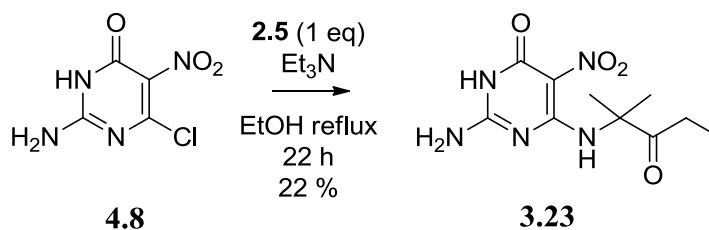
The nitration of aminochloropyrimidine **4.7** was carried out using concentrated sulfuric acid and red fuming nitric acid and, again, followed literature procedure (Scheme 4.2).<sup>195,205,207</sup> It was important to keep the initial temperature of the reaction low (*ca.* 5 °C) and the addition of the nitric acid drop-wise to achieve a high yield, in this case 84%.



Scheme 4.2: Nitration of **4.7** using the classical nitration technique.

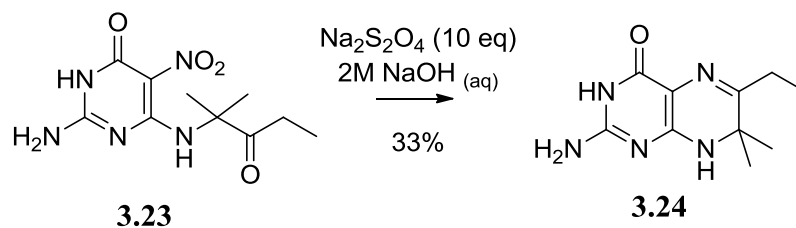
### 4.3 Preparation of WSG1002 (1.6)

The displacement of the chloride from chloronitropyrimidine **4.8** using the appropriate  $\alpha$ -aminoketone hydrochloride (**2.5**) was achieved by heating at reflux the two components together in strictly anhydrous ethanol with two equivalents of triethylamine. The product **3.23** was obtained in 22 % yield, with this level of reaction efficiency being typical of this type of coupling (Scheme 4.3).



Scheme 4.3: Coupling of aminoketone and pyrimidinone

The annulation was initiated by the reduction of the nitro to the corresponding amine, which was performed using an excess of sodium dithionite in aq. sodium hydroxide. The progress of the reaction was followed by a colour change from amber to red to yellow (**Figure 4.1**) and the product was isolated in 33 % yield (**Scheme 4.4**).

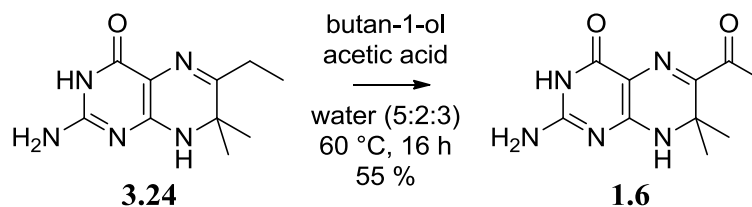


Scheme 4.4: Annulation reaction



Figure 4.1: Progress of annulation as monitored by colour change. Top left with sodium dithionite just added, top right showing the reaction progressing, bottom showing the reaction at completion

The final step in the preparation of WSG1002 (**1.6**) was the oxidation of the ethyl side-chain at C<sup>6</sup>. This oxidation has been well documented and preparation followed the literature precedent.<sup>195</sup> Oxidation was carried out by stirring dihydropterin **3.24** in a mixture of butan-1-ol, acetic acid and water at 60 °C overnight. After purification, WSG1002 (**1.6**) was obtained in 55 % yield (**Scheme 4.5**).

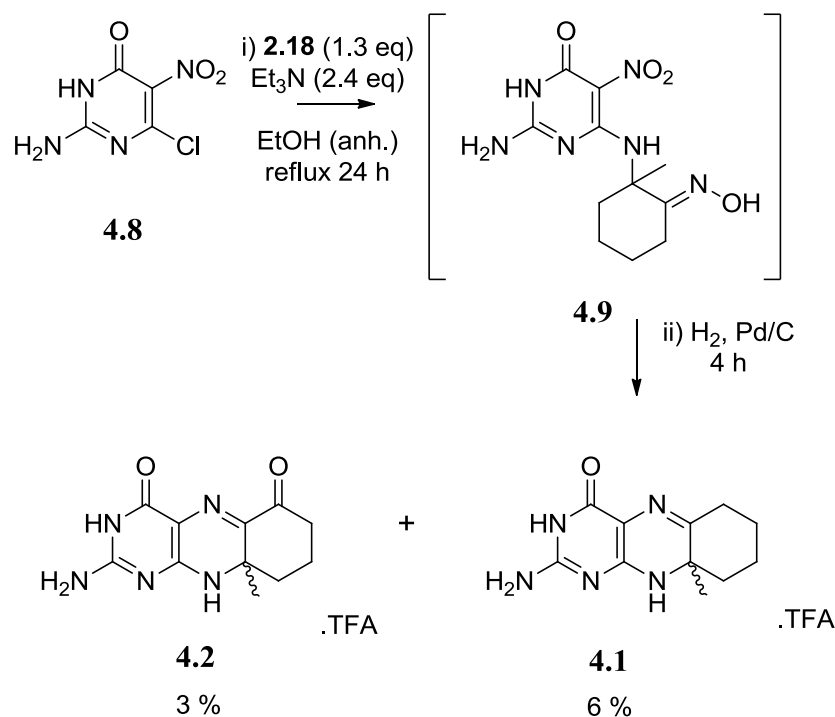


**Scheme 4.5: Final aerial-oxidation to give WSG1002**

#### 4.4 Preparation of WSG1007 (**4.1**) and WSG1060 (**4.2**)

When comparing the method of preparing WSG1002 (**1.6**) with its *N*-methyl analogue (**3.2** described in Chapter 3), it was quickly realised that the typical Boon synthesis was significantly more difficult than the telescoped one-pot coupling and annulation procedure. Consequently, the telescoped route was employed to synthesise both WSG1007 (**4.1**) and WSG1060 (**4.2**). It was well understood that the oxidation of the third ring would be relatively quick using this method and purification to separate **4.1** from **4.2** was carried out as a matter of urgency (**Scheme 4.6**).





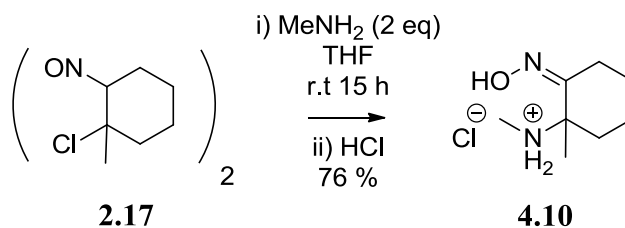
Scheme 4.6: Telescoped route to 4.1 and 4.2

As expected, upon purification both **4.1** and **4.2** were observed and the longer the purification took, the more **4.2** dominated the HPLC trace. Pleasingly, enough of **4.1** and **4.2** were obtained for further experiments.

#### 4.5 Analogues of WSG1060

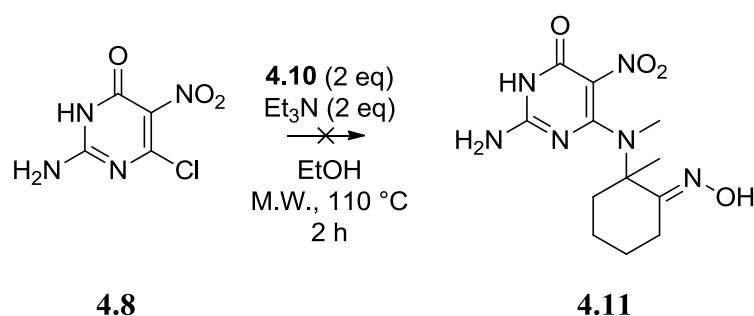
An opportunity to synthesise an analogue of WSG1060 (**4.2**) with an alkyl substituent at the  $N^8$  position (**4.5**) arose. In the context of NOS binding and activation, such an  $N^8$  alkyl analogue would be expected to be tolerated at the active site and, because of the electron-donating methyl group, might be a more active tetrahydrobiopterin than WSG1060 itself. With a slight alteration to the final step in the preparation of the cyclic  $\alpha$ -amino-oxime (**2.18**), it could be possible to use substituted amines, in place of ammonia, to introduce diversity to the pteridine. As these pteridines were ultimately being targeted as NOS activators, it seemed appropriate to expand at the  $N^8$  position in a conservative fashion; in this case, a one-carbon expansion was employed and an attempt was made to synthesise the cyclic  $\alpha$ -(methylamino)oxime (**4.10**) (Scheme 4.7). It was hoped that expanding out at this position in such a conservative fashion would allow the compounds to act as molecular probes. This could facilitate the exploration into the enzymatic pocket,

probing the space available and also testing the necessity of the hydrogen bonds at this position. Gratifyingly, **4.10** was synthesised in 76 % yield in a readily straightforward manner.



**Scheme 4.7: Diversification of nitrosochloro dimer (2.17)**

Next it was a matter of displacing the chloride on **4.8** to make the coupled pyrimidine (**4.11**). As this type of compound had never been made before, the reactivity of this system was unknown and it was uncertain as to whether a secondary amine would successfully displace the chloride. It was also known that the yield for the coupling step was poor for the Boon synthesis and it was suspected that this more sterically encumbered amine would further decrease the yield observed when compared with similar substrates. As a result of these suspicions and the fact that the coupled pyrimidine would itself be a novel compound, the typical Boon synthesis was selected over the telescoped version (**Scheme 4.8**). In an attempt to improve the likelihood of a good yield, microwave irradiation was selected as the preferred heating method.



**Scheme 4.8: Attempted coupling of a more hindered cyclic amino-oxime**

Unfortunately, even with microwave heating, this coupling did not occur and both starting materials were recovered. This reaction was attempted again but using conventional heating over a period of two days. No product was observed and neither starting materials could be recovered (**Table 4.1**). One last attempt was made at forcing this reaction to occur using silver carbonate. It was hoped that the formation

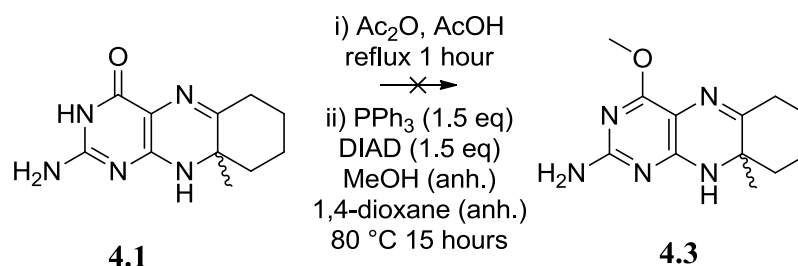
of the insoluble silver chloride would encourage the reaction to take place. Heating the reaction in a sealed tube containing DMF and the additive silver carbonate also failed to yield any of the desired product (**Table 4.1**).

Heating method	Reaction time	Solvent	Additive	Comment
Microwave	2 hours	Anhydrous ethanol	N/A	Starting material recovered
Conventional heating	2 days	Anhydrous ethanol	N/A	No starting material or product recovered
Conventional heating	3 days	Anhydrous DMF	Silver Carbonate	No starting material or product recovered.

**Table 4.1:** Conditions used for the attempted coupling of the *N*-methyl cyclic aminooxime, 4.10. Despite a number of different conditions this reaction was unsuccessful.

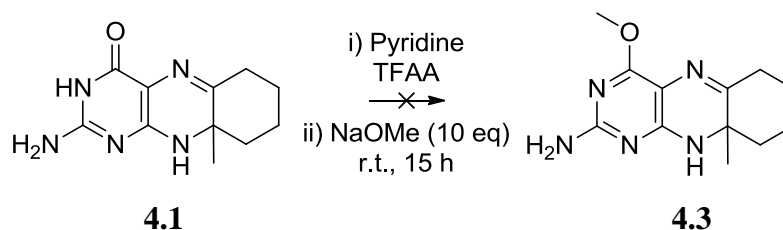
These were disappointing results; however, it is now apparent that there is a limited scope for coupling partners in the Boon synthesis. Although this approach utilised a more electron-rich cyclic  $\alpha$ -aminooxime, its increased steric bulk is the likely cause of its ultimate failure. The boundaries at which the Boon synthesis can operate are now further understood.

Moving on from this target, another analogue was deemed within reach, again following the strategy of expanding upon a compound of interest by one-carbon unit. As mentioned in Chapter 2, a pteridine with a methoxy substituent on  $C^4$  would be of great interest and could potentially aid in the elucidation of the molecular mechanism of NOS. In an attempt to access this type of compound, chemistry developed by Yao and Pfeleiderer was employed.<sup>198</sup> This chemistry involved the acetyl protection of a pterin followed by a Mitsunobu reaction. This reaction was attempted on WSG1007 (**4.1**), as it did not have the potential complication of the carbonyl group on the third ring (**Scheme 4.9**).



Scheme 4.9: Attempted Mitsunobu reaction on WSG1007

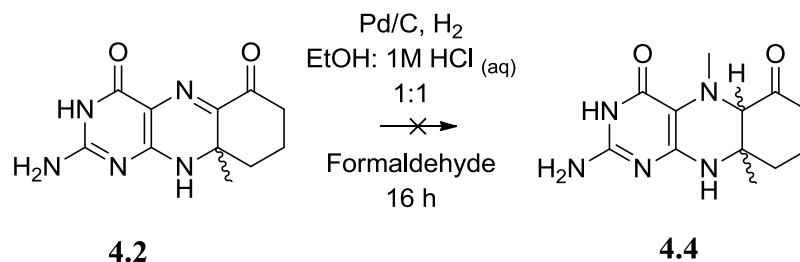
Upon fractionation *via* flash column chromatography (95:5 DCM:MeOH), neither product nor starting material was recovered. At the same time as this reaction was taking place, a colleague had successfully made a methoxy analogue of WSG1002. This method was adapted from an experimental procedure reported by the Jones group.<sup>217</sup> In this procedure, it was reported that the concentration of the sodium alkoxide was crucial in obtaining the optimum yield. It also appeared that this concentration differed with each alkoxide and substrate. With very little WSG1007 (**4.1**) and WSG1060 (**4.2**) available to work with, one attempt was made using the conditions that were successful in the lab. These pteridine-specific conditions were likely to be closer to optimum than the guanine chemistry that had been reported in the literature.<sup>217</sup> For this reaction, WSG1007 (**4.1**) was selected and ten equivalents of sodium methoxide in 5 ml of anhydrous methanol was used as the displacement reagent (**Scheme 4.10**). Disappointingly no product or starting material could be recovered *via* HPLC separation.

Scheme 4.10: Attempted S<sub>N</sub>Ar at C<sup>4</sup>

With the spare supply of WSG1007 (**4.1**) exhausted and only a small amount left of WSG1060 (**4.2**), one final reaction was attempted with an eye on one last diversified pteridine. As discussed earlier in Chapter 1 (**Section 1.2.2**) it is possible for an N<sup>5</sup> methylated version of BH<sub>4</sub> to function as a cofactor mimetic.<sup>79</sup> Moreover, the rate of nitric oxide production is higher than that of BH<sub>4</sub> when the mimetic is present at

saturation concentration. Therefore, it is conceivable that an  $N^5$  methylated synthetic pteridine might also act as a better mimetic at suitable concentrations. One other important feature of this type of compound is the potential for the pteridine to act as an oxidatively stable tetrahydropteridine. This would provide the first example of a blocked tetrahydropteridine and, if active, would tackle one of the major problems currently hampering  $BH_4$  (**1.1**) as a drug.<sup>38,39</sup>

Using a method previously described by *Eberlein et al.* and separately by *Temple et al.* for analogous systems, the methylation of WSG1060 (**4.2**) was attempted.<sup>218,219</sup> WSG1060 (**4.2**) was dissolved in a 1:1 mixture of ethanol and 1M hydrochloric acid and hydrogenated in the presence of palladium and two equivalents of formaldehyde (**Scheme 4.11**). An attempt was made at HPLC purification of the dry crude mixture. However, by mass spectroscopic analysis, it appeared that methylation had taken place at multiple sites on the pteridine as shown by **Figure 4.2** and separation of the products within the mixture was not possible.



**Scheme 4.11: Attempted methylation**

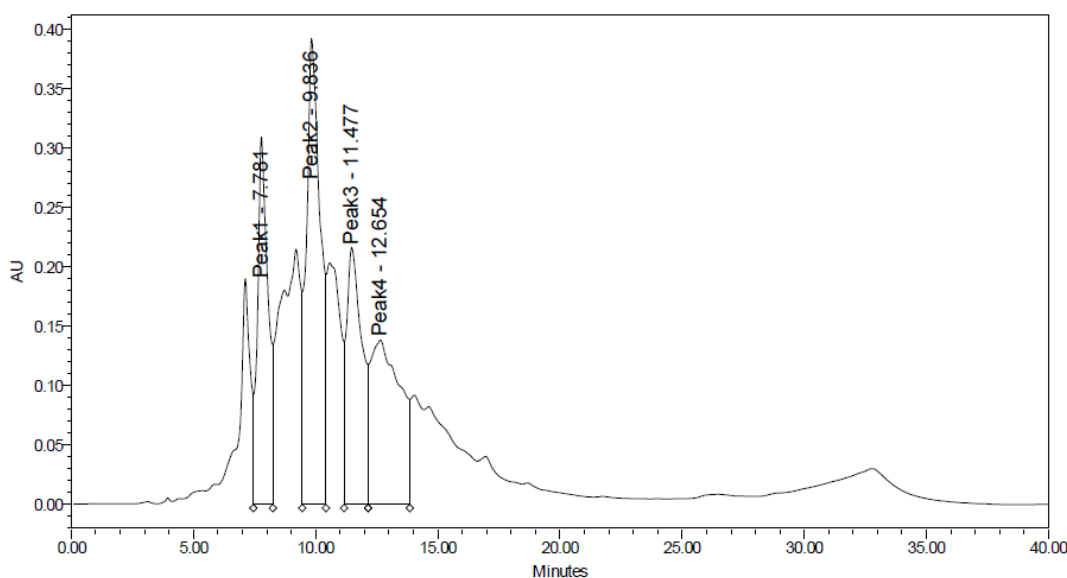
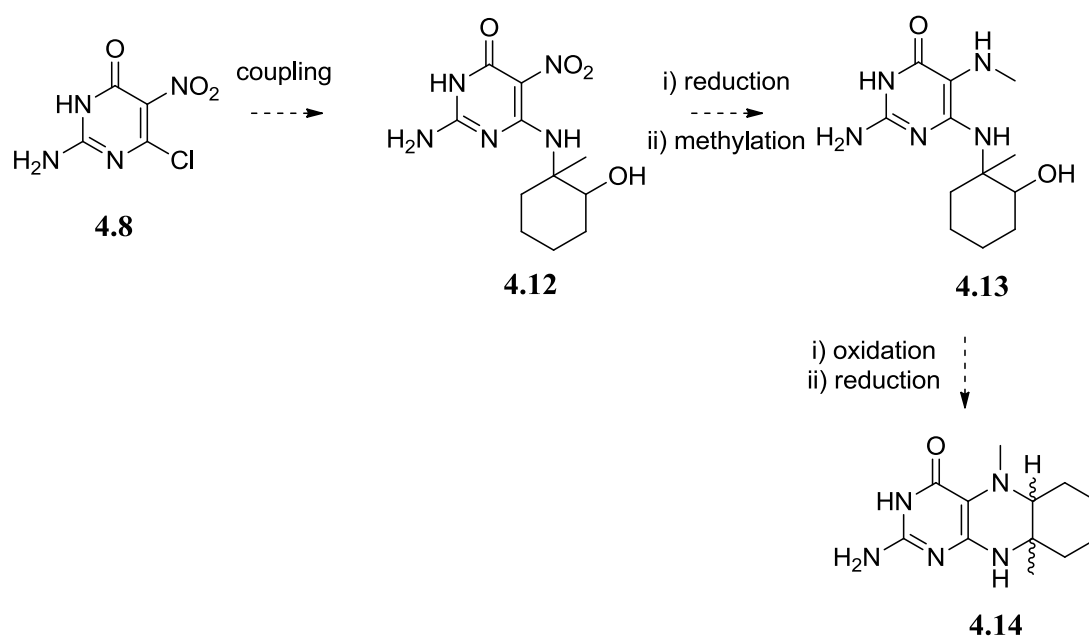


**Figure 4.2:** HPLC trace showing the difficulty in separating the crude mixture for the methylation of **4.2**. Several peaks show the addition of a methyl to the mass of the starting material.

This was thoroughly disappointing result; however, with hindsight, probably unsurprising. Not only are there multiple sites for methylation but the desired product would be present as a mixture of four different stereoisomers. It is possible that the HPLC trace contained two peaks which were different diastereoisomers of **4.4** as well as various differently methylated pteridines, further complicating the purification. The fact that this was coupled with a relatively small scale makes it understandable, if not predictable, that this reaction would not yield the desired product. As a suggestion for further work, another route to this desired product is presented in **Scheme 4.12**. Hopefully by making use of the high nucleophilicity of the amine at  $C^5$ , selective methylation could occur. It is also hoped the reduced number of steps would allow the preparation a reasonably large amount of material. Finally, this route would avoid the preparation of the oxidatively unstable tetrahydropteridine as an intermediate, assisting the synthesis of the desired product.



Scheme 4.12: Proposed route to a methylated pterin

#### 4.6 Conclusion

The preparation of two previously known dihydropteridines was carried out with the aim of ascertaining whether another dihydropteridine would be more suitable as a NOS activator than the lead compound, WSG1002. This question will be addressed in Chapter 6. Several reactions were attempted in an effort to synthesise novel dihydropteridines for further study. Unfortunately, these compounds could not be obtained in the available time. The priority of this work was to re-establish the enzymatic assay, ensure its reliability and evaluate the available blocked dihydropterins as NOS activators in detail (**Chapter 6**). There may be inherent limitations of this pteridine chemistry that are the cause of these disappointing results but the experience serves to better define what can and cannot be achieved with this series of compounds.

# Chapter 5

## Results and discussion – fused pyridines

### 5.1 Background

As stated in Chapter 1 (**Section 1.5**) one of the main interests within our laboratory was the development of a more “drug-like” pteridine analogue with particular reference to nitric oxide synthase in this thesis. This principle can be expanded to all of the fused pyrimidines that Suckling group researchers are currently involved in synthesising. Being able to reliably synthesise a reactive intermediate, based on a pyridine building block, and utilise it in the formation of a fused pyridine would be of great value to our whole laboratory. A target was sought (**Figure 5.1**) which would allow the development of a modified Boon synthesis (**Scheme 5.1**). This modified approach should allow the development of deaza analogues related to the lead compound in nitric oxide synthase activation, WSG1002 (**1.6**).

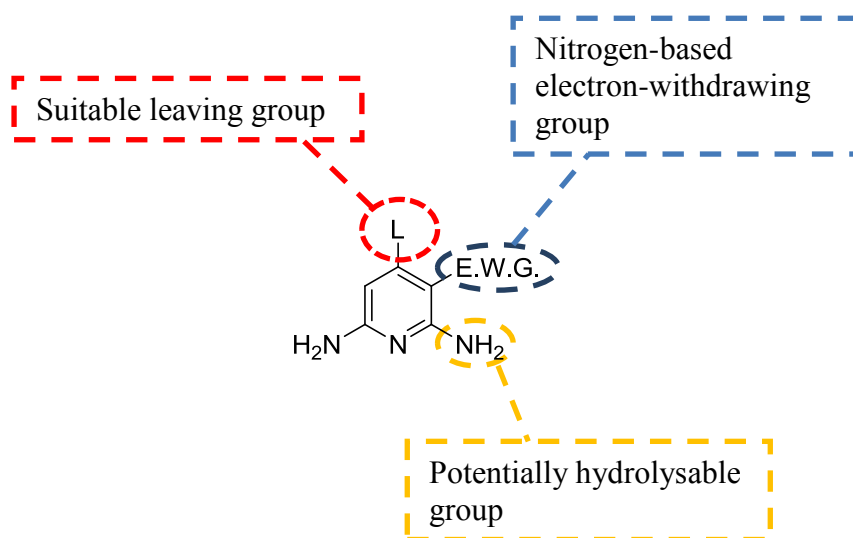
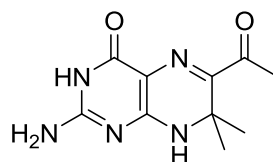


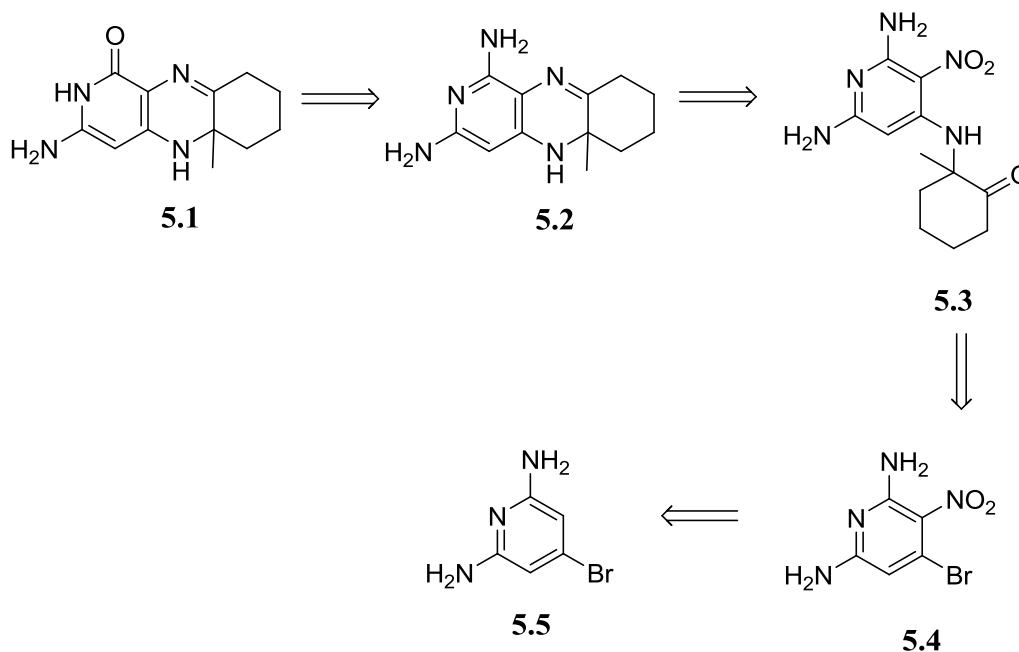
Figure 5.1: Synthetically useful pyridine





## 1.6

The selection of a suitable leaving group at  $C^4$  of the pyridine could be a critical decision and the choice was made to opt for bromide. This choice was based on the previous experience with the Boon synthesis and the knowledge that the coupling step was the bottleneck in these approaches. It was thought that having bromine present, as opposed to another halide, would allow the coupling to take place quicker and may improve the yield for this troublesome reaction. With that decision made, the choice of the electron-withdrawing group was now at the forefront of the mind. From work published by Temple *et al.*, it appeared possible to perform a nitration selectively at  $C^3$ .<sup>168-172,176,177</sup> With these key choices made, it is possible to arrive at a retrosynthetic analysis (**Scheme 5.1**) starting with the target of a blocked dihydrodeazapteridine (**5.1**) and returning to the aforementioned pyridine (**5.5**).



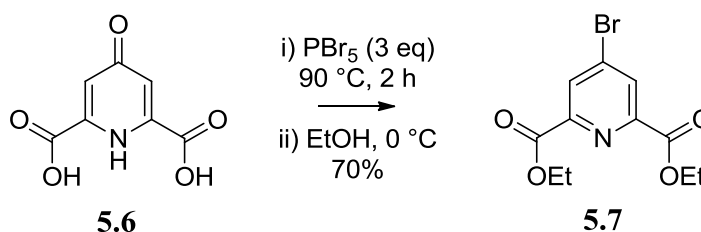
**Scheme 5.1:** Retrosynthetic analysis of the deazapteridine

It was envisioned that acid hydrolysis of one of the exocyclic amines, on compound **5.2**, should be possible in a manner similar to that seen in most pteridines.<sup>152,220</sup> It is,

however, also possible to carry this reaction out under basic conditions.<sup>221</sup> It can be seen that **5.2** could be made from reduction and *in situ* annulation of **5.3**. It was envisioned that displacement of the bromide would be assisted by the electron-withdrawing nitro group, giving **5.4**. Finally, nitration of **5.5** should give **5.4**.

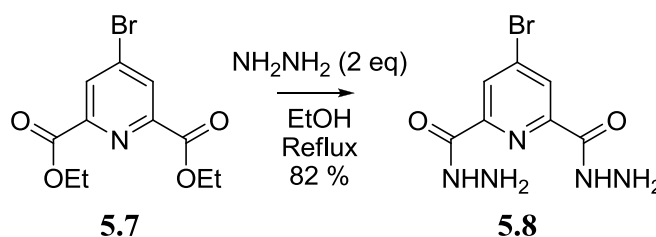
## 5.2 Preparation of 2,6-diamino-4-bromopyridine

Upon consultation of the literature there appeared to be a method, making use of the Curtius rearrangement, that could be adapted to allow the synthesis of bromodiaminopyridine precursor **5.5**.<sup>222</sup> Starting from the commercially available chelidamic acid (**5.6**), bromination and esterification was carried out in a one-pot two-step reaction (**Scheme 5.2**) using phosphorus pentabromide and ethanol to give the bromodiester **5.7** in 70% yield.



Scheme 5.2: Bromination and esterification

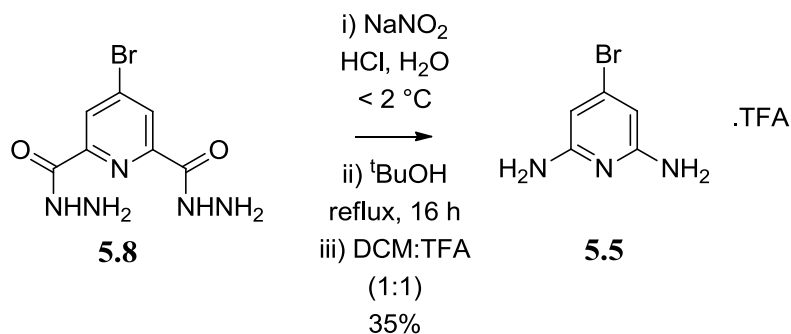
Next, the preparation of the bis-hydrazide (**5.8**) was carried out using hydrazine hydrate and ethanol. The reaction was heated at reflux until completion and was monitored by tlc. After work-up the desired product (**5.8**) was obtained in 82 % yield (**Scheme 5.3**).



Scheme 5.3: Formation of the hydrazide

Sodium nitrite was used in aqueous acidic media at a temperature below 2 °C to form the bis-acyl azide (**Scheme 5.4**). Great caution was taken when handling this compound as it could be potentially explosive. Following pH adjustment with a

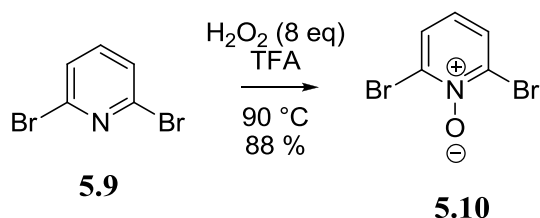
saturated aqueous solution of sodium bicarbonate, the material was extracted into DCM then dried and evaporated. The mixture was then heated at reflux in *tert*-butanol overnight to form the Boc-protected amine which was subsequently deprotected using DCM and TFA. The product (**5.5**) was obtained as the TFA salt in 35 % yield.



**Scheme 5.4:** The Curtius rearrangement to form the key pyridine

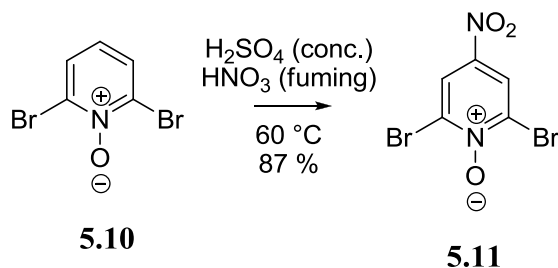
With an overall yield of 20 %, the amount of product obtained was disappointingly low. Moreover, proceeding through an acyl azide meant that there was limited scalability to tackle this problem. This material was set aside for later use and an alternative route was attempted. Nettekoven, from Roche, reported a synthesis of **5.5** on a kilogram scale in five steps and this preparation was settled on as the method to provide a larger amount of material.<sup>223</sup>

Starting with the commercially available 2,6-dibromopyridine (**5.9**), the *N*-oxide (**5.10**) was prepared in 88 % yield and on a 120 g scale (**Scheme 5.5**). This was carried out by heating the starting material in a mixture of TFA and hydrogen peroxide. Due to the potential risks involved with this process, specific precautions were taken to minimise damage in the event of an explosion: the reaction was carried out in an isolated special operations laboratory, behind a blast shield and in high dilution.



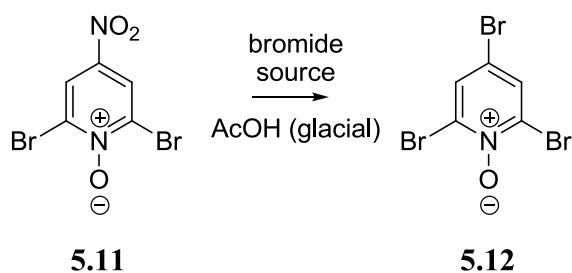
**Scheme 5.5: Formation of the *N*-oxide**

With the *N*-oxide directing the subsequent electrophilic aromatic attack, a nitration was carried out under relatively forcing conditions (**Scheme 5.6**). Dibromide **5.10** was heated over a 24 hour period at 60 °C in concentrated sulfuric acid and fuming nitric acid. It was noted that only fresh red fuming nitric acid would facilitate the reaction, as starting material was isolated when either an old bottle of red fuming nitric acid or 70 % nitric acid was used. In the successful cases, the nitrated product was isolated in good yield (87 % on the largest scale attempted).



**Scheme 5.6: Nitration of 5.10 using fresh red fuming nitric acid**

Formation of the tribromopyridine **5.12** could be approached in two different, but related, methods.<sup>223,224</sup> Both methods make use of a bromide anion that displaces the nitro group. However, the source of the bromide anion makes a large difference to the outcome of the reaction. Shetty reported that use of hydrobromic acid greatly increased the yields of an otherwise inconsistent bromination.<sup>224</sup> However, when attempted, this appeared not to be the case and higher yields were consistently obtained using acetyl bromide (**Scheme 5.7** and **Table 5.1**).

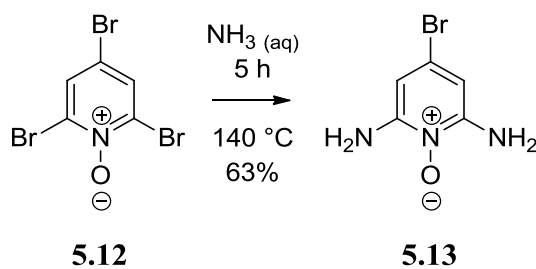
Scheme 5.7: Bromination to give the tribromopyridine *N*-oxide

Bromide source	Temperature	Reaction length	Comment
HBr	60 °C	2 days	Starting material recovered
AcBr	80 °C	5 hours	73 % yield

Table 5.1: Conditions for bromination of nitro dibromide 5.12

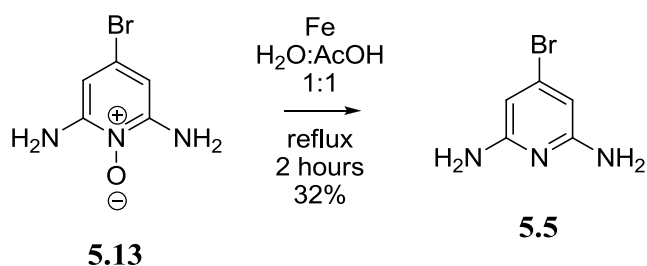
Special precautions were taken with **5.12** as it appeared to be light-sensitive, turning from a faint yellow to a deep red over a period of months. The large batch was wrapped in aluminium foil and stored in a dry and dark cupboard.

The amination of **5.12** was ultimately carried out using thick-walled Aldrich reaction tubes (Carius tubes, by another name) which were sealed using an oxy-acetylene blow-torch. This precaution was taken as critical damage to other reaction vessels was highly likely under the corrosive reaction conditions. The amination was performed in aqueous ammonia at 140 °C for a period of 5 hours (**Scheme 5.8**). The reaction scale never exceeded 5 g and it is suspected that an autoclave would be necessary on a kilogram preparation due to high internal pressure. The desired product was obtained in 63 % yield.



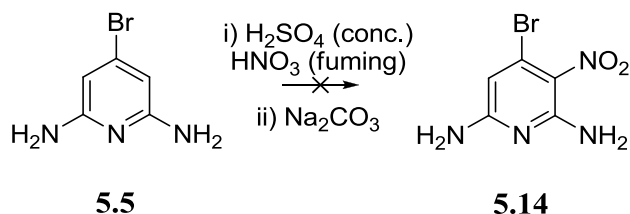
Scheme 5.8: Amination of 5.12

The final reaction in this series involved the reduction of the *N*-oxide to form **5.5**. This reaction was carried out using iron filings in a water and acetic acid mixture (1:1) and was heated at reflux for 2 hours (Scheme 5.9). After purification the material was isolated as a colourless solid in 32% yield.

Scheme 5.9: Reduction of the *N*-oxide

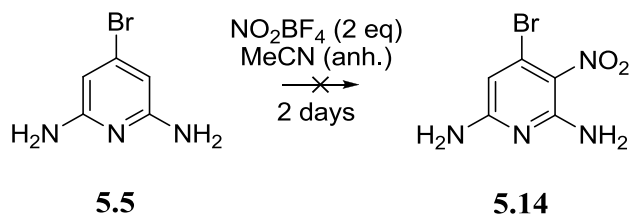
### 5.3 Insertion of a nitrogen-based electron-withdrawing group

Under classical nitrating conditions, concentrated sulfuric acid and red fuming nitric acid, an attempt was made to nitrate **5.5** at  $C^3$  (Scheme 5.10). The reaction was stirred for 3 hours at room temperature and then poured over a large excess of ice, however no material precipitated from the mixture. Even with neutralisation using solid sodium carbonate, no material could be recovered.



Scheme 5.10: Attempted nitration of 5.5 using classical nitration conditions but failing to provide 5.14

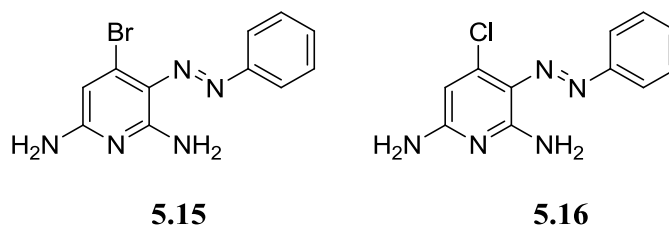
In a bid to overcome this problem, nitration using nitronium tetrafluoroborate was attempted in anhydrous acetonitrile (**Scheme 5.11**). This reaction could be more efficiently monitored using mass spectrometry and, if the product was formed, obtaining the crude solid should be much simpler than working with aqueous media.



**Scheme 5.11:** Attempted nitration reaction using  $\text{NO}_2\text{BF}_4$  as the nitrating agent. The reaction did not provide **5.14**

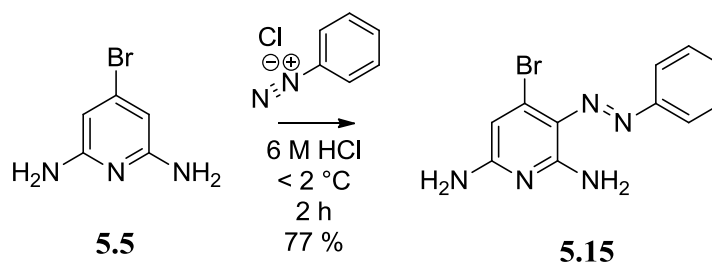
Initially one equivalent of nitronium tetrafluoroborate was used; however, it appeared that both the starting material and the product were still present (as monitored by mass spectrometry), so an extra equivalent of nitronium tetrafluoroborate was added to the reaction mixture. After two days, no more starting material was observed and solid sodium carbonate was added to the reaction mixture, filtered and the solvent removed. Surprisingly, the crude material showed no sign of the product.

It appeared that obtaining the nitrated product was more difficult than originally assumed. It was speculated that synthesising the diazo compound (**5.15**) might be easier than preparing the nitro compound **5.14**. This speculation was supported by previous work in the literature in which a similar 4-chloro compound had been prepared (**5.16**).<sup>222</sup>



The diazo coupling, using the diazonium salt derived from aniline, was attempted with **5.5** as substrate in 6 M hydrochloric acid at a temperature below 2 °C (**Scheme 5.12**). Gratifyingly, the product (**5.15**) was isolated easily in 77 % yield. Purification of this material was a relatively straightforward recrystallisation from aqueous

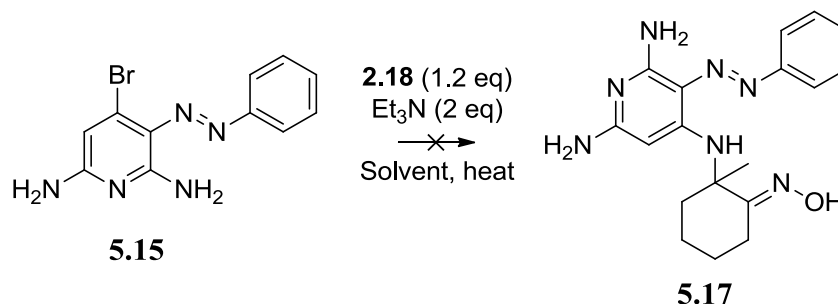
ethanol. However it was also possible to purify this material on a basic alumina column.



Scheme 5.12: Diazonium coupling of 5.5

#### 5.4 The coupling reaction

With the electron-withdrawing group in place, it was assumed that **5.15** was primed for coupling with an appropriate amine in this case, **2.18**. The diazo compound **5.15** and amine **2.18** were heated at reflux in anhydrous ethanol overnight (Scheme 5.13 and Table 5.2); however, only starting material was observed by alumina tlc, later confirmed by NMR. It was hypothesised that a strongly hydrogen-bonding solvent such as ethanol might be hindering the reaction by shielding the nucleophile from the pyridine. To test this hypothesis, the reaction was attempted again in DCM in the hope of providing a more exposed nucleophile (Table 5.2). Unfortunately only starting material was recovered from the reaction. In one final attempt at using a metal-free approach, more forcing conditions were tested. Microwave irradiation was utilised and the conditions used in Chapter 3 (Section 3.2.6) were directly transferred to this reaction set up (Table 5.2). Again, unfortunately no product was observed and the starting material was isolated.



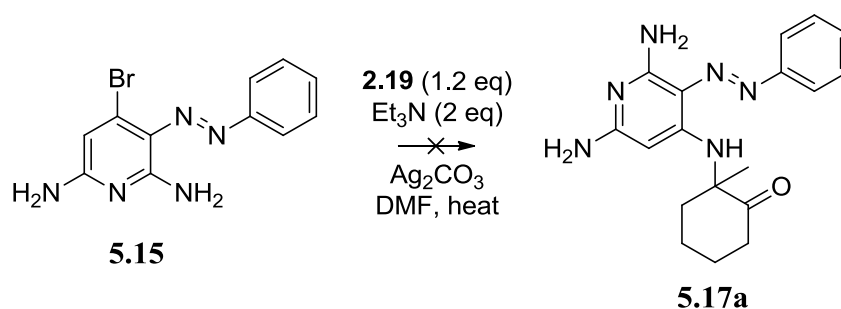
Scheme 5.13: Attempted coupling using analogous conditions to a classical Boon synthesis as well as microwave-assisted heating. All reaction conditions failed to produce 5.17



Solvent	Heating method	Temperature	Duration	Comment
Ethanol	Conventional	Reflux	15 hours	Starting material recovered
DCM	Conventional	Reflux	15 hours	Starting material recovered
DMF	Microwave	100 °C	1 hour	Starting material recovered

Table 5.2: Conditions for the attempted metal-free coupling shown in Scheme 5.13

It appeared that displacement of the bromine was much more difficult than initially anticipated and an explanation is offered at the end of this chapter. Nevertheless, it was thought possible to couple diazo compound **5.15** and amine **2.19** together under slightly more forcing conditions and primarily with metal-mediated reactions. Silver chemistry was initially employed in an attempt to force the reaction to proceed. Diazo compound **5.15** and amine **2.19** were heated in a sealed tube for three days with an excess of silver carbonate **Scheme 5.14**. The ketone was used instead of the oxime in an attempt to avoid metal-mediated ring-opening.<sup>225,226</sup> Disappointingly, only starting material was recovered and it appeared that the silver chemistry was not going to be of use in this case.



Scheme 5.14: Attempted silver-catalysed coupling

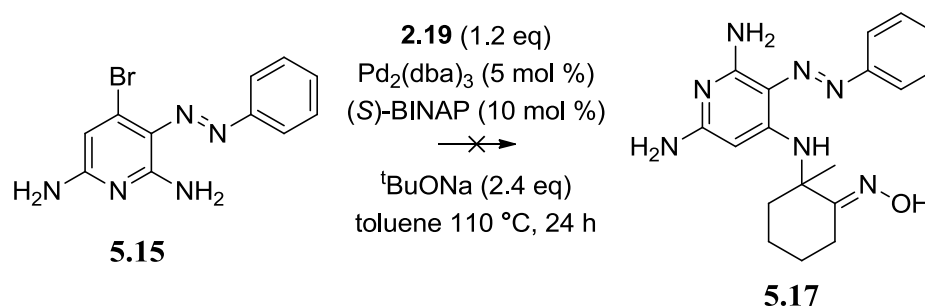
The next logical choice was to try to capitalise upon palladium-catalysed cross-couplings, specifically the chemistry developed in the laboratories of Buchwald and Hartwig.<sup>227-229</sup> When assessing the molecules for their suitability in this type of coupling, there were a number of factors to be considered.

- Substitution of a halide at the 4-position of a pyridine ring is notoriously difficult and suspiciously absent in many publications that deal with pyridine couplings.<sup>230-233</sup>
- Secondary amines are typically the coupling partners used for the displacement of the leaving group.

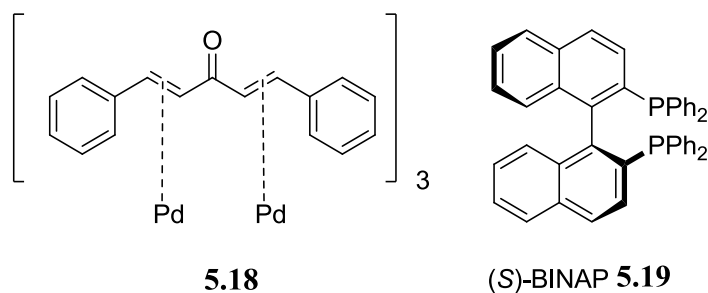
- Electron-deficient aromatic halides are favoured.
- Differing ligands produce differing results and often a small ligand screen is necessary.
- A bulky substituent *ortho* to the halide assists with the reductive elimination.

One final consideration is the possibility that the functional groups on the pyridine may act as ligating groups that could hinder the reaction. However, it was preferable not to make use of protecting groups unless it was absolutely necessary because they lengthen the synthesis and add two steps to the reaction sequence.

Utilising fresh  $\text{Pd}_2(\text{dba})_3$  **5.18**, diazo compound **5.15** and (*S*)-BINAP ((*S*)-(2,2'-bis(diphenylphosphino)-1,1'-binaphthyl) **5.19** to form the active catalyst and sodium *tert*-butoxide as a base the coupling was attempted in anhydrous and degassed toluene (**Scheme 5.15**).



**Scheme 5.15: First attempt at Buchwald-Hartwig amination**

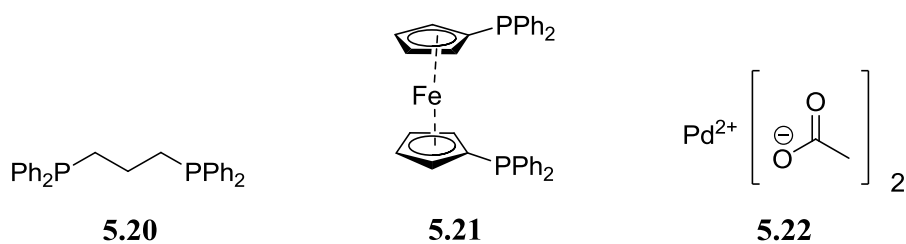


Upon fractionation through a basic alumina column (toluene:ethyl acetate 3:1), a large proportion of starting material was recovered with no sign of desired product **5.17**. Whilst this was a disappointing result, it was not entirely unsurprising. Alternative reaction conditions were investigated (**Table 5.3**). Initially BINAP (**5.19**) was changed for dppp (1,3-bis(diphenylphosphino)propane) **5.20** but to no avail. A

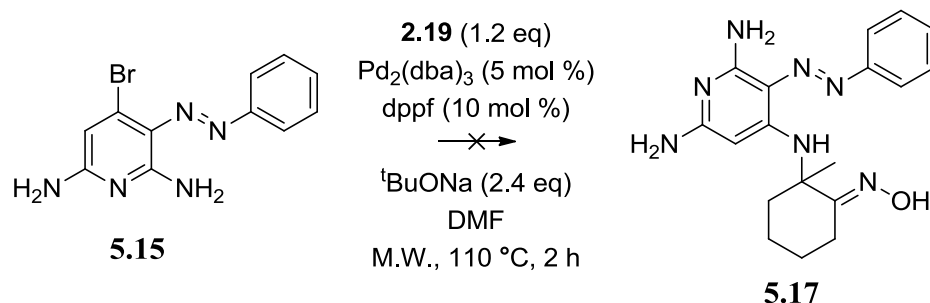
more electron-rich ligand set was then selected, dppf (1,1'-bis(diphenylphosphino)ferrocene) **5.21**, unfortunately also with no success.

Ligand	Catalyst	Solvent
Dppp <b>5.20</b>	Pd <sub>2</sub> (dba) <sub>3</sub>	Toluene
Dppf <b>5.21</b>	Pd <sub>2</sub> (dba) <sub>3</sub>	Toluene
Dppf	Pd(OAc) <sub>2</sub>	Toluene

Table 5.3: Differing conditions for the attempted amination reaction

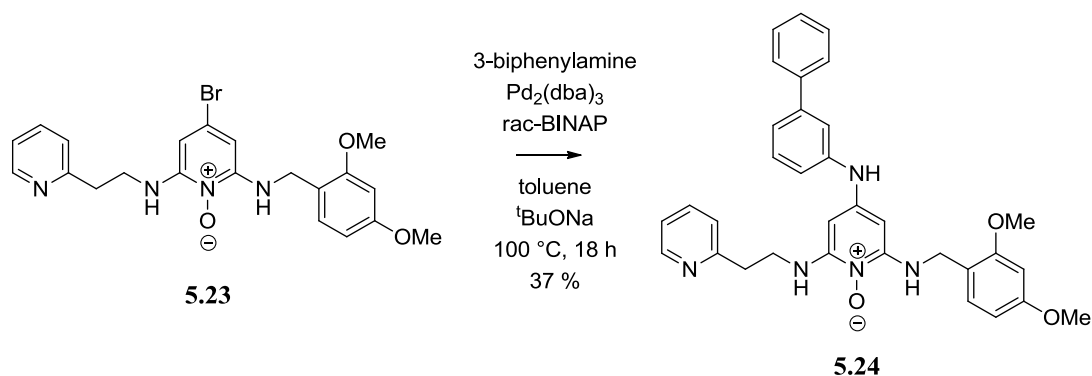


With no success thus far, it seemed appropriate to make use of the conditions popularised by Kappe and use microwave heating.<sup>234</sup> This method uses DMF in the reaction and therefore higher temperatures can be reached but it also negates the need for stringently dry or degassed solutions. Nevertheless, anhydrous DMF was available and was degassed prior to the reaction (**Scheme 5.16**).



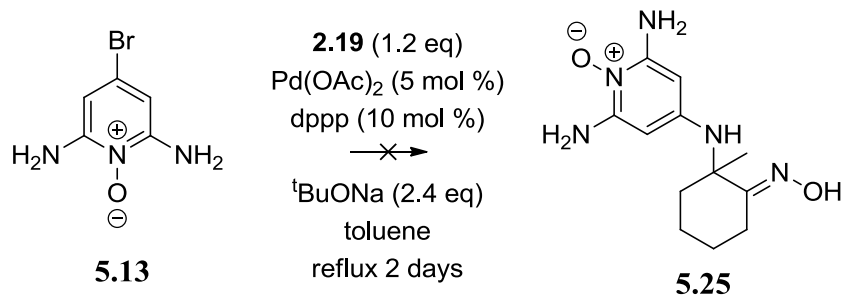
Scheme 5.16: Microwave conditions for Buchwald-Hartwig amination. The reaction was unsuccessful and the starting material was recovered

Again, starting material was recovered and it appeared that the reactants were not appropriate for the reasons stated earlier. However, encouraged by work published by Shetty, it appeared that a Buchwald-Hartwig amination was possible at the 4-position of a 2,6-disubstituted pyridine-*N*-oxide (**Scheme 5.17**).<sup>224</sup>

Scheme 5.17: Shetty's Buchwald-Hartwig amination<sup>224</sup>

As *N*-oxide **5.13** had been made previously and was available for use, the amination was attempted without the assistance of the diazo group. This decision was further supported by the recovery of starting material, from the failed Buchwald-Hartwig reactions, as opposed to the product of hydrodehalogenation. This suggested that the troublesome part of this reaction was with the oxidative insertion and not the reductive elimination – where a bulky *ortho*-substituent would be helpful.

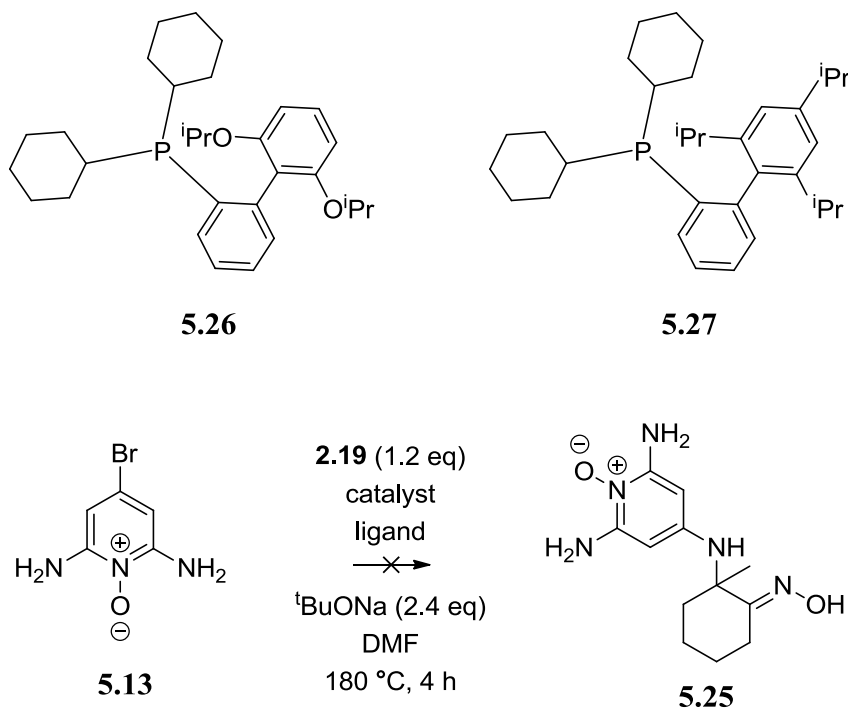
The *N*-oxide **5.13** was conventionally heated for two days at reflux with amine **2.19** using Pd(OAc)<sub>2</sub>, 1,3-bis(diphenylphosphino)propane (dppp), anhydrous and degassed toluene, and sodium *t*-butoxide (Scheme 5.18).



Scheme 5.18: Attempt at using Shetty's amination conditions. Again no product was observed and the starting material was recovered suggesting that no reaction was taking place

Again, a large proportion of starting material was recovered from the reaction, suggesting that oxidative insertion was the limiting factor. Again, in an attempt to provide more forcing conditions to initiate the reaction, microwave heating was employed and DMF was chosen as the solvent. As microwave reactions can be simply automated, the opportunity was taken to screen increasingly more electron-rich ligands: dppf (**5.21**), RuPhos (**5.26**) and XPhos (**5.27**). Finally, to ensure that the

ligand system had actually formed, a control was run using Pd(dppf)Cl<sub>2</sub>.DCM and extra base (**Scheme 5.19** and **Table 5.4**).



**Scheme 5.19:** General microwave conditions used when the catalyst and ligand system changes were investigated

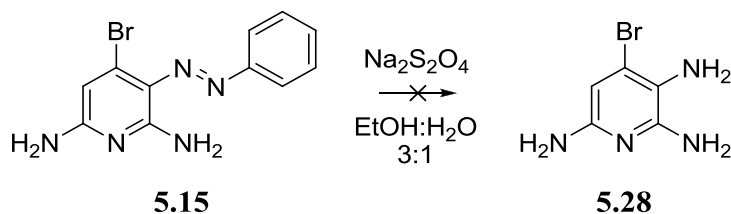
Catalyst	Ligand	Outcome
Pd(OAc) <sub>2</sub>	Dppf <b>5.21</b>	Starting material recovered
Pd(OAc) <sub>2</sub>	RuPhos <b>5.26</b>	Starting material recovered
Pd(OAc) <sub>2</sub>	XPhos <b>5.27</b>	Starting material recovered
Pd(dppf)Cl <sub>2</sub> .DCM	N/A	Starting material recovered

**Table 5.4:** Changes that were made to the amination reaction. Only the catalyst or ligand system were changed to investigate whether more electron-rich systems would facilitate oxidative addition

Again, a large proportion of starting material was recovered from each experiment and the decision was made to halt this chemistry and capitalise upon the in-built reactivity of diazo compound **5.15** to allow access to other fused pyridines. It is probable that the large primary amine is too hindered for the Buchwald-Hartwig amination and this reaction was not investigated further.

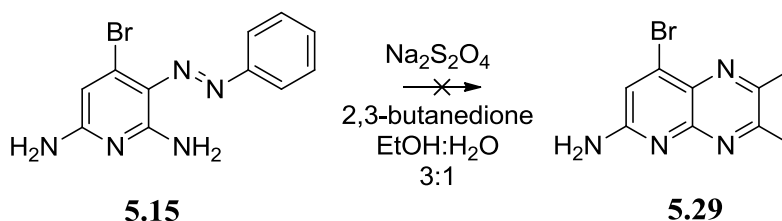
### 5.5 Other fused pyridines of interest

Although access to the blocked dihydrodeazapteridines was not possible by these methods, other deazapteridines could, in principle, be obtained from the available intermediates. It would be interesting, although not part of this project, to discover whether they had similar biological activity to their pteridine analogues. For example, a pyrido[2,3-*b*]pyrazine could be formed by reducing diazo compound **5.15** to the triamine **5.28** and condensing it with a dicarbonyl species, as described in Chapter 1 (**Section 1.5.1**). In a metal-free approach to forming these species, isolation of the triamine (**5.28**) was attempted by reducing diazo compound **5.15** with an excess of sodium dithionite in aqueous ethanol (**Scheme 5.20**) in a fashion similar to that reported by Markees.<sup>222</sup>



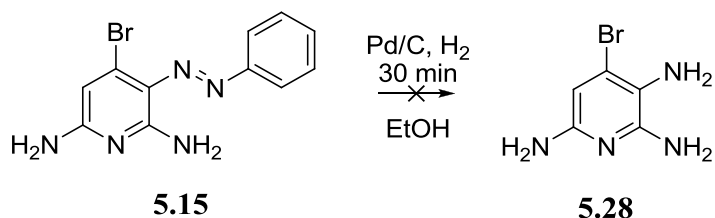
**Scheme 5.20:** Attempted reduction of **5.15** using sodium dithionite.

Disappointingly, no product was obtained from this reaction; however, the starting material was not recovered either. This suggested that, if the product was being formed, it could very well be degrading. To test this hypothesis, diazo compound **5.15** was reduced using sodium dithionite in the presence of 2,3-butanedione in the hope of trapping **5.28** out as the product from the next step **5.29** (**Scheme 5.21**).



**Scheme 5.21:** Unsuccessful synthesis of **5.29**.

No product or starting material was isolated. Reduction using palladium on charcoal was carried out and another attempt at isolating triamine **5.28** was made (**Scheme 5.22**).

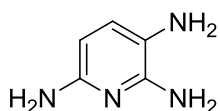


**Scheme 5.22: Unsuccessful synthesis of 5.28.**

A white solid was obtained after purification; however, when dissolved in DMSO- $d_6$  there were obvious visual signs of a reaction taking place (**Figure 5.2**). The NMR results indicated a complex mixture of materials were either isolated or forming in the NMR tube. Regardless of the negative outcome from this reaction, encouragement was taken from the result. It appeared that the white solid (seen in **Figure 5.2**) could have been the dehalogenated pyridine triamine **5.30** (however this was never isolated in its purified form).



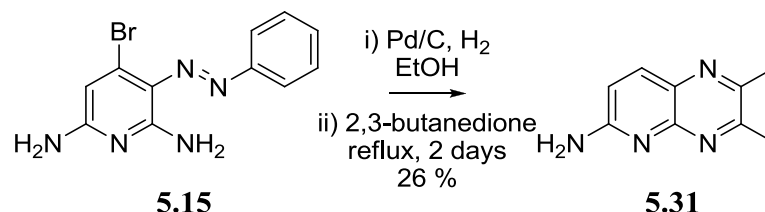
**Figure 5.2: (left) NMR tube with decomposing material, (middle) isolated white solid, (right) material being retested in DMSO- $d_6$**



**5.30**

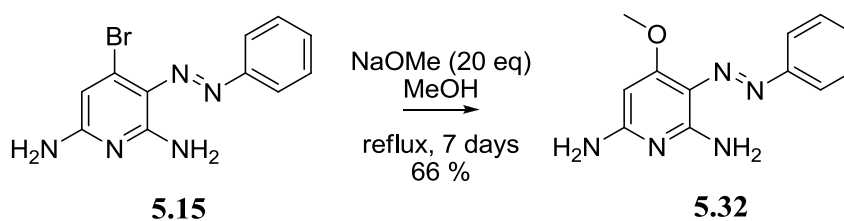
With data suggesting that it is possible to perform a reduction using palladium (Appendix C), the same approach as before was employed. The material was reduced using hydrogen over palladium on charcoal, then quickly filtered into a stirring

solution of 2,3-butanedione, whereupon it was heated at reflux for two days (**Scheme 5.23**).



**Scheme 5.23:** Formation of the dehalogenated pyridopyrazine

After HPLC purification, the dehalogenated pyrido[2,3-*b*]pyrazine **5.31** was isolated. The low yield and different colour changes throughout the course of the reaction suggested that there may well have been some decomposition or oxidation of triamino pyridine **5.30**. Nevertheless this was a good result and, although late-stage diversity was no longer possible, an attempt was made at diversifying diazo compound **5.15** with the aim of assessing the feasibility of synthesising a diverse library of pyrido[2,3-*b*]pyrazines. From work described earlier (**Section 5.4**), it was clear that a potent nucleophile would be needed to displace the bromide from compound **5.15**. It was assumed that relatively forcing conditions would also be required due to the low reactivity observed previously. With this in mind, a displacement with sodium methoxide was attempted (**Scheme 5.24**).

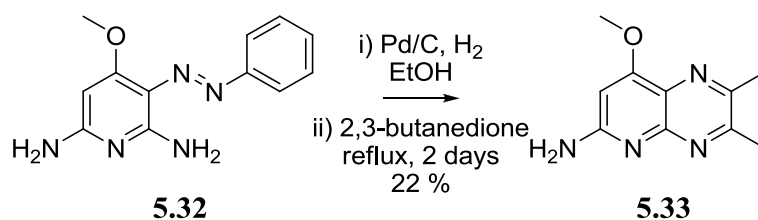


**Scheme 5.24:** Displacement of the bromide in **5.15** with methoxide to form **5.32**

A large excess and long reaction time was needed to convert **5.15** into **5.32**; on the small scale used, separation of the two materials was very difficult. Nevertheless, the required product **5.32** was obtained in 66% yield, a result that suggests that diversification at this stage is possible.



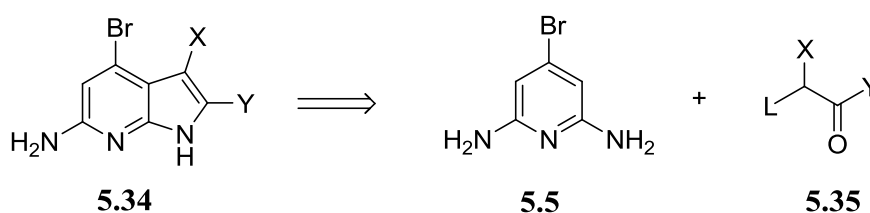
With limited resources and time remaining, a resynthesis of diazo compounds **5.15** and **5.32** was carried out and the corresponding methoxypyrido[2,3-*b*]pyrazine (**5.33**) was synthesised in a fashion similar to pyridopyrazine **5.31** (Scheme 5.25).



Scheme 5.25: Synthesis of **5.33** using a catalytic hydrogenation

Pleasingly, **5.33** was isolated in 22% yield after HPLC purification, showing that limited diversity might be introduced to diazo compound **5.15** and that the synthesis of a library of pyrido[2,3-*b*]pyrazines was possible.

A further application of the aminobromopyridine intermediates such as **5.5** is in the synthesis of 6-5 fused systems. In parallel to this work, other studies were also ongoing within our laboratory. With one of the main aims of this project being the design and synthesis of a library of 7-azaindoles **5.34**, it seemed appropriate to assess diaminopyridine **5.5** as a precursor to this material (Scheme 5.26). If suitable, this structural building block could allow access to deaza analogues of previously published compounds from our laboratory.<sup>147</sup>

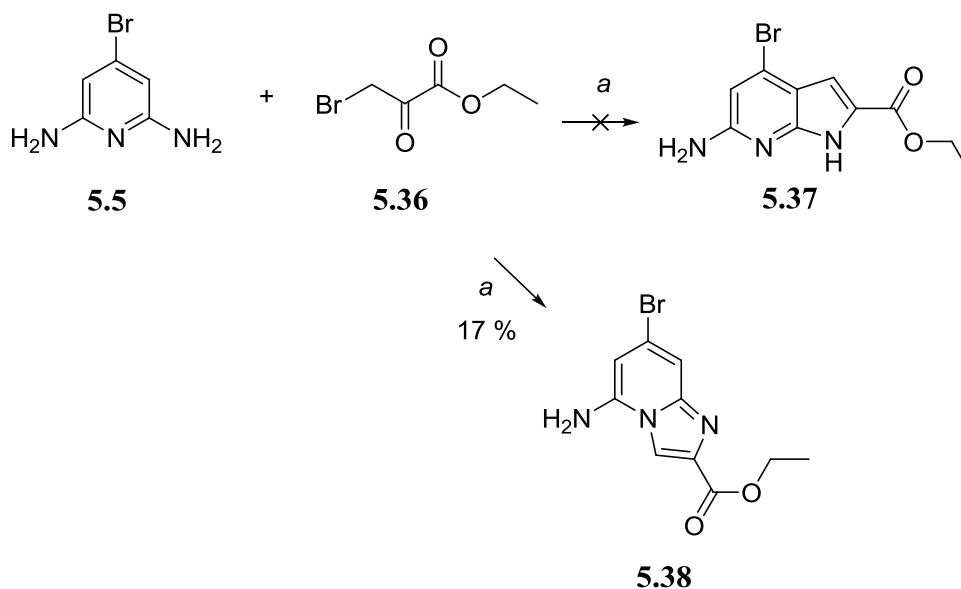


L = leaving group  
X & Y = in-built points of diversity

Scheme 5.26: Potential components for the synthesis of a deaza pyrrolopyrimidines

This approach would also make use of the chemistry, which has just been discussed; displacement of the bromide in pyridine **5.5** could be achieved using a suitably

powerful nucleophile but this time it could be achieved at a late stage. As many of the starting materials for this reaction were available, ethyl bromopyruvate was arbitrarily chosen from a selection of coupling partners. The pyridine **5.5** and ethyl bromopyruvate would serve as a pilot reaction, allowing the assessment of reactivity (Scheme 5.27).



Scheme 5.27: Formation of the imidazole and not the 7-azaindole. *a*) DMF, Et<sub>3</sub>N (1 eq), r.t., 2 days

The 7-azaindole (**5.37**) was not the product formed from this reaction but in fact it was ethyl 5-amino-7-bromoimidazo[1,2-*a*]pyridine-2-carboxylate (**5.38**), which was isolated in 17 % yield. With the benefit of hindsight, this is not a surprising result as the most nucleophilic site on the pyridine (**5.5**) is the lone pair of electrons residing on *N*<sup>1</sup> and not the  $\pi$ -electrons on *C*<sup>3</sup>. Upon searching the literature, it appeared that this compound was known and the analysis perfectly matched that of **5.38**.<sup>235</sup> To confirm the regiochemistry, a NOESY spectrum was obtained showing a positive interaction between the exocyclic amine protons and the aromatic proton alpha to the pyridyl nitrogen.

### 5.6 A serendipitous insight

When the diazonium coupling reaction was left unquenched for too long (12 hours) a deep orange/red compound was observed upon work-up. This served as the first indicator that something unusual had occurred, as **5.15** is a bright yellow compound.

NMR results suggested that there may be two compounds present in this isolated mixture. As the mixture was dissolved in deuterated chloroform, a test recrystallisation was performed in the NMR tube by slow evaporation of the solvent (**Figure 5.3**).

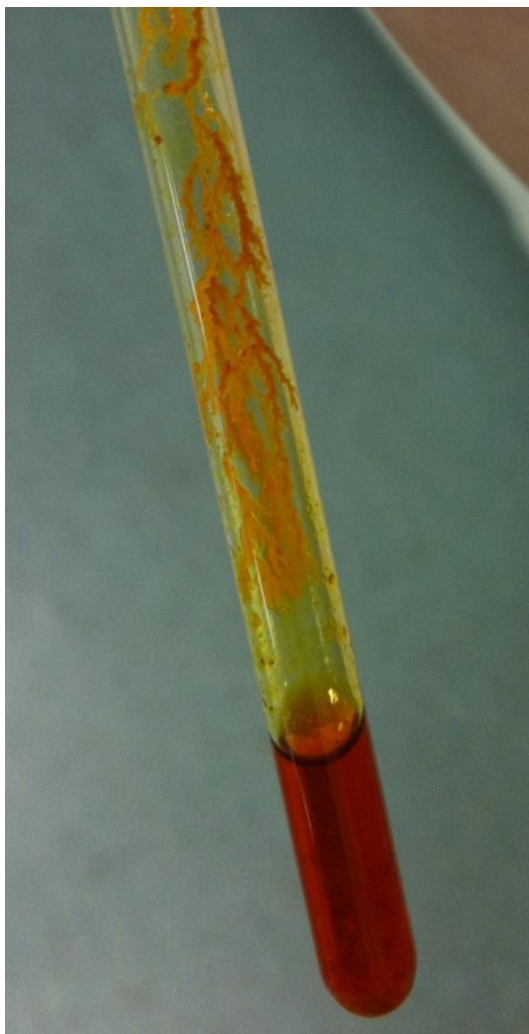


**Figure 5.3: Pilot recrystallisation from  $\text{CDCl}_3$**

It was noticed that a yellow precipitate formed at the bottom of the tube, which turned out to be **5.15**. However, orange and yellow crystals formed round the side of the tube and the mother liquor was brightly coloured (orange/red) indicating that another product was still present. After separating the orange/red compound from **5.15** crystallisation was attempted to obtain a definitive structure. Gratifyingly, this was performed successfully by slow evaporation from chloroform and the crystals were analysed by Dr. Alan Kennedy (Strathclyde University). A surprising result was

returned from this analysis (**Figure 5.4**) and it indicated that **5.5** had undergone a double diazonium coupling to give **5.39** (X-ray data in Appendix D).

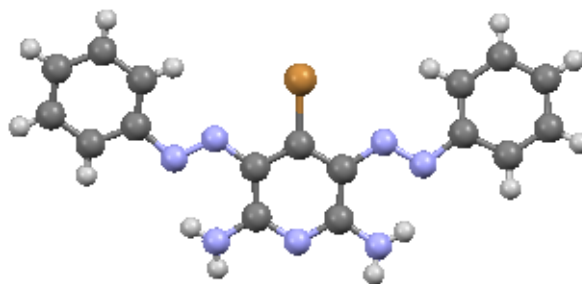
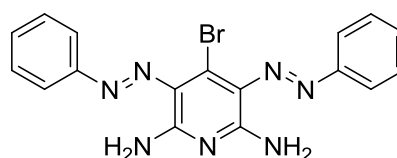


Figure 5.4: X-ray crystal structure of **5.39**



**5.39**

This surprising result actually serves to highlight what may have been hindering the coupling reactions attempted in **Section 5.4**. If pyridine **5.5** has enough electron density to undergo two consecutive diazonium couplings, then the ring system of **5.15** is not as electron-deficient as originally suspected. This would clearly hinder the attack of a nucleophile (in the classical coupling) or the oxidative insertion step (with the palladium-catalysed cross-coupling). Although at the final stages of the Buchwald-Hartwig chemistry it was suspected that the amino-oxime was unsuitable for this coupling, it appears that the aryl halide may also be insufficiently reactive for electronic reasons.

### 5.7 Conclusions and further work

In order to synthesise the original target compound, protection of **5.15** appears to be a route towards this compound that merits further consideration. An amide or carbamate protecting may reduce the electron density in the pyridine ring sufficiently to allow a Buchwald-Hartwig reaction to take place. With respect to the sixth question set out in Chapter 1 (**Section 1.7**):

- Is it possible to synthesise a deaza-analogue of a dihydropteridine and if so, does it also act as a NOS activator?

It was not possible to synthesise a blocked dihydrodeazapteridine using the methods outlined above.

The pyridine chemistry allowed the synthesis of two pyrido[2,3-*b*]pyrazines (**5.31** and **5.33**) in a strategy that incorporates a mid-stage diversity approach. This approach allows the synthesis of potentially biologically-active compounds. Surprising reactivity was observed with the 2,6-diamino-4-bromopyridine **5.5**, suggesting that it is more electron-rich than one might suspect. As a result, a new compound was isolated, the bis-diazopyridine (**5.39**) leading directly to a proposed alternative approach using Buchwald-Hartwig aminations. In an attempt to synthesise a 7-azaindole, ethyl 5-amino-7-bromoimidazo[1,2-*a*]pyridine-2-carboxylate (**5.38**) was isolated instead. This class of compound has potential applications in many areas including kinase inhibitors, antibiotics and preventing gastric acid secretions.<sup>235</sup>

# Chapter 6

---

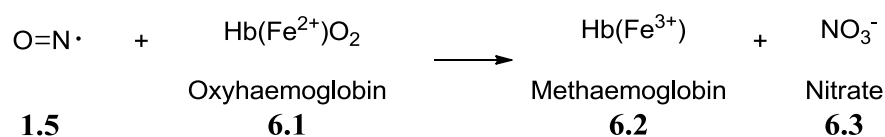
## Results and discussion – biological results and compound evaluation

### 6.1 Background

As described in **Chapter 1**, the main aim of this project was to design, synthesise and evaluate blocked dihydropteridines as nitric oxide synthase modulators, preferably activators. To assess these compounds' effectiveness as NOS activators, they were reduced using sodium cyanoborohydride (**Section 6.2**) and assessed at The University of Edinburgh in collaboration with the Daff group. It had already been established, in collaboration with the Daff group, that BH<sub>4</sub> analogues must be tested in their tetrahydro oxidation state.<sup>45,195</sup> One of the main questions at the outset of this project was, could increasing the electron-density of a pteridine improve its ability to act as a coenzyme mimetic? The other main questions were how much space is available within the BH<sub>4</sub>-binding pocket? Also, would expanding into these regions be beneficial in terms of developing potent BH<sub>4</sub> mimetics through better binding to NOS? Whilst these may be simple questions, they have remained largely unanswered by the community and need addressing. Lastly, while it has been shown previously that some blocked dihydropteridines can act as NOS activators, it was only assumed that they function in the same manner as BH<sub>4</sub> (**1.1**) and this hypothesis has never been tested. It was with these questions in mind that a selection of pteridines were taken to Edinburgh to be evaluated fully as BH<sub>4</sub> mimetics.

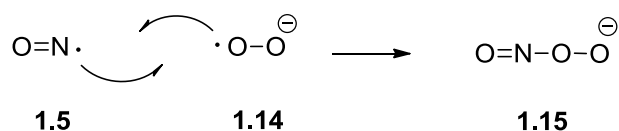
The *in vitro* assay used for the evaluation of these pteridines makes use of UV-Vis spectroscopic measurements to track the change of oxyhaemoglobin (OxyHb **6.1**) to methaemoglobin (MetHb **6.2**) caused by NO (**1.5**, **Scheme 6.1**). Nitric oxide is a highly reactive radical species with indiscriminate selectivity; however, this assay is designed in such a way as to have the statistical majority of NO reacting with OxyHb. This means that the conversion of OxyHb to MetHb is directly proportional to the levels of NO being produced.<sup>236-238</sup> OxyHb is added to the assay mixture at the

beginning of the experiment and is not to be confused with the haem that is resident within the NOS enzyme itself.



**Scheme 6.1: Indicator of nitric oxide levels within the assay. Nitric oxide reacts with a haem source and is monitored by a change in the UV-vis spectrum**

The rate at which NO (**1.5**) reacts with a haem depends upon the oxidation state of the iron. When the iron is in the  $2^+$  oxidation state, as with oxyhaemoglobin, the rate of reaction is  $3.7 \times 10^7 \text{ M}^{-1}\text{s}^{-1}$ . When the iron is in the  $3^+$  oxidation state the rate can range between  $10^2 - 10^7 \text{ M}^{-1}\text{s}^{-1}$ . Nitric oxide also reacts very quickly with superoxide (**Scheme 1.2**) to form peroxynitrite with a rate constant of  $7 \times 10^9 \text{ M}^{-1}\text{s}^{-1}$ . It is obvious that this reaction is around two orders of magnitude faster than the reaction of NO with OxyHb. If superoxide (**1.14**) was present, even at low concentrations within the assay, then the rate at which MetHb was produced would not be an accurate measure of NO concentration. To ensure that no superoxide was present within the assay, superoxide dismutase (SOD) was present in the buffer at all times. SOD reacts with superoxide at a rate of  $2 \times 10^9 \text{ M}^{-1} \text{ s}^{-1}$  effectively removing all traces of superoxide before NO is even produced.

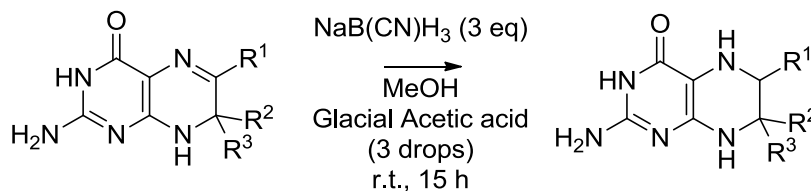


**Scheme 1.2: Formation of peroxynitrite from nitric oxide and superoxide.**

## 6.2 Reduction of the pteridines

The pteridines prepared thus far were reduced following a literature procedure<sup>45</sup> using three equivalents of sodium cyanoborohydride in acidified methanol (**Scheme 6.2** and **Table 6.1**). After HPLC purification and freeze drying, the solid products were stored at  $-23 \text{ }^\circ\text{C}$  and tested at Edinburgh within two days. One other pteridine known as WSG1017 (**6.4a**) was taken from the library collection and reduced for enzymatic assay. WSG1017 had previously shown promising activity in an iNOS cell-based assay; however, these results remain unpublished.<sup>215</sup> Finally, one

compound that had proven stable in its tetrahydro form for a number of years, known as WSG1010 (**6.5**), was also taken forward for testing. This particular compound possessed minimal structural complexity and was, in fact, not even a blocked dihydropteridine but a typical pterin in its fully reduced state. This was chosen as a baseline compound, enabling the assessment of the basic ability of a synthetic tetrahydropteridine to act as a NOS activator.



**Scheme 6.2: General scheme for the reduction of a pteridine**



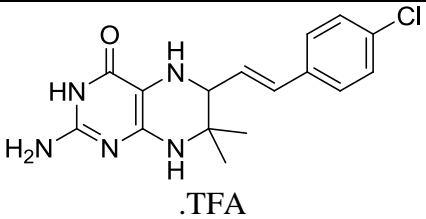
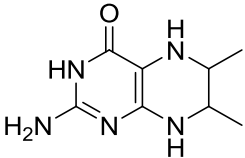
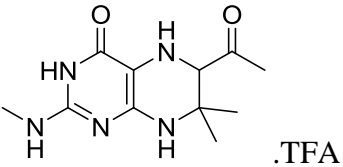
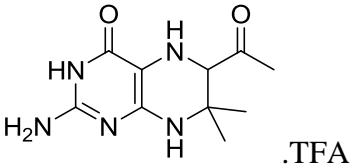
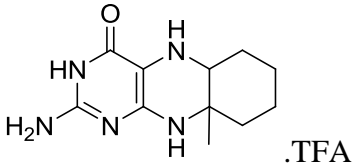
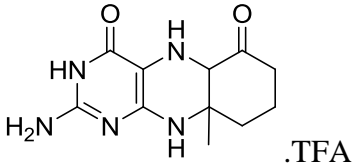
Compound structure	Compound number	Yield of reduction
 .TFA	<b>6.4</b>	44 %
 .TFA	<b>6.5</b>	N/A
 .TFA	<b>3.1</b>	N/A
 .TFA	<b>1.7</b>	42 %
 .TFA	<b>6.6</b>	58 %
 .TFA	<b>6.7</b>	36 %

Table 6.1: Yields for reduction of pteridines

### 6.3 Single-point turnover assay

All the compounds displayed in **Table 6.1** were dissolved into a standard 20  $\mu\text{M}$  solution in Tris/HCl buffer (pH 7.5) along with 1 mM of dithiothreitol (DTT), which retards the rate of oxidation.<sup>239</sup> The component parts of the assay (**Table 6.2**), excluding arginine, were combined together and allowed to equilibrate for 30 – 60

seconds at 25 °C, making sure that the reading was stable. The UV-Vis spectrophotometer was zeroed, the substrate, arginine, was added and the appearance of MetHb monitored by the increase in absorbance at 401 nm. The gradient of the slope was measured from the initial section of the spectrum, allowing the rate of the reaction to be obtained for each pterin. The assay was performed in triplicate for each pteridine tested and the rates are provided in **Table 6.3**. Final values were obtained in collaboration with Ben Gazur from the University of Edinburgh.

Reagent	Final concentration	Volume in Cuvette
Tris/ HCl (CaCl <sub>2</sub> + DTT)	50 mM	943 µl
Calmodulin/Ca <sup>2+</sup>	500 µg/ml and 5 mM	10 µl
NADPH	100 µM	5 µl
SOD/Catalase	20 µg/ml	2 µl
Oxyhaemoglobin	excess	10 µl
Pterin	20 µM	10 µl
NOS	500 nM	10 µl
Arginine	20 nM	10 µl

**Table 6.2: Conditions for NOS assay**

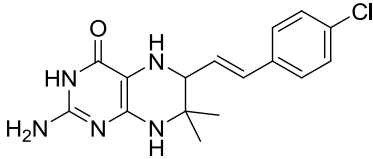
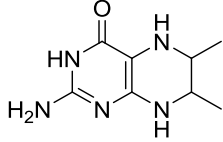
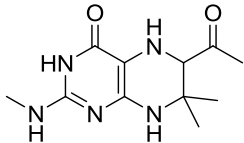
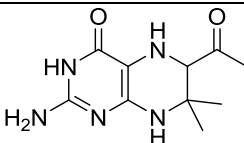
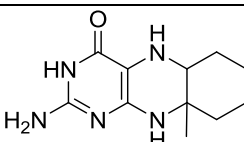
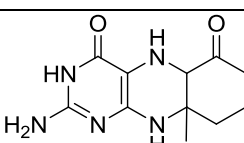
Compound	Rate min <sup>-1</sup> (standard deviation)
<b>BH<sub>4</sub></b>	18 (1.1)
 <b>6.4</b>	Inhibitor (apparent)
 <b>6.5</b>	1.3 (0.4)
 <b>3.1</b>	0.0 (0.0)
 <b>1.7</b>	3.4 (0.8)
 <b>6.6</b>	2.8 (0.4)
 <b>6.7</b>	8.2 (0.3)

Table 6.3: Single-point turnover assay rates

Previous studies had shown that the  $K_d$  of tetrahydropterin **1.7** was 151  $\mu\text{M}$ .<sup>45</sup> It was, therefore, not surprising to find such a low rate of nitric oxide production as the

enzyme was well below saturation point. As this compound has been well characterised in terms of its cofactor mimetic ability, it was important to use it as a synthetic pteridine standard with every batch of enzyme. Each batch had a natural variance in terms of rate and, in one case, led to tetrahydropterin **6.4** appearing as an inhibitor (**Table 6.3** entry 2). The results suggesting that **6.4** was an inhibitor were called into question when considered alongside unpublished cell-based data and initially prompted the use of two standards (BH<sub>4</sub> **1.1** and tetrahydroWSG1002 **1.7**). It was found that, upon retesting tetrahydroWSG1002 **1.7** with one particular batch of enzyme, the order of addition appeared to affect the outcome of the experiment. There were insufficient quantities of tetrahydropterin **6.4** left to perform further assays and the biological information available is largely inconclusive.

5,6-Dimethyltetrahydropterin **6.5** acted as an activator towards NOS (**Table 6.3**, entry 3), albeit a weak one, which was a surprising result. NOS has evolved an exquisite selectivity towards other naturally occurring pteridines, notably the closely related compound, neopterin (**Section 1.2.1**), probably associated with the specific hydrogen-bonding network. The fact that such a simple synthetic pteridine, which lacks side chain functional groups, can act as a coenzyme suggests that most of the important interactions for binding take place between the basic pteridine scaffold: this will be addressed later in **Section 6.7**.

*N*-Methylaminopterin **3.1** appeared not to bind with the enzyme (**Table 6.3**, entry 4) and, when compared to tetrahydroWSG1002 **1.7** and dimethyl tetrahydropterin **6.5**, the result clearly suggests that expansion at the C<sup>2</sup> position prevents the pterin from acting as a BH<sub>4</sub> mimetic in NOS. The result demonstrates that there is insufficient space available for binding these types of analogues and serves to further exemplify the importance of the hydrogen-bonding network present at this side of the pteridine. When considering this result along with the computer modelling, it appears that the unusual binding poses obtained are not genuine poses that the pterin can adopt within the NOS enzyme.

In contrast, high activity was found for the tricyclic pterins **6.6** and **6.7**. Interestingly, cyclohexyl derivative **6.6** and ketocyclohexyl reduced pterin **6.7** (**Table 6.3**, entries 6 and 7) have remarkably different levels of activation. Both compounds act as

activators of NOS and are comparably active to the original lead compound, WSG1002 (**1.6**). Impressively, ketocyclohexyl reduced pterin **6.7** had the highest rate of nitric oxide production observed with a synthetic cofactor at 20  $\mu\text{M}$ . Due to the significant activation observed, both cyclohexyl hydropterin **6.6** and ketocyclohexyl reduced pterin **6.7** were resynthesised and Michaelis-Menten kinetic studies were performed to determine formal kinetic parameters.

## 6.4 Michaelis-Menten kinetics

### 6.4.1 Background

Michaelis-Menten kinetics are used to ascertain specific pieces of information about an enzymatic process,  $k_{\text{cat}}$  and  $K_{\text{d}}$  (or in this case  $K_{\text{m}}$  as a resident coenzyme is being measured). By measuring the rate of reaction at varying concentrations of substrate (in this case the coenzyme concentration was altered), a hyperbolic plot of coenzyme concentration versus initial velocity can be constructed (see **Figure 6.1**).<sup>240,241</sup> Towards the higher end of concentrations tested, the plot should be essentially flat; this is known as the  $V_{\text{max}}$ . The concentration that produces half  $V_{\text{max}}$  is  $K_{\text{m}}$ ; this is a measure of the apparent dissociation constant, otherwise known as its binding affinity. Reliable values for the kinetic constants can be obtained directly from the Michaelis-Menten curve using software specifically designed for the task, which was “origin 8.1” (Origin lab’s software) for the experiments described in **Section 6.4.2**.

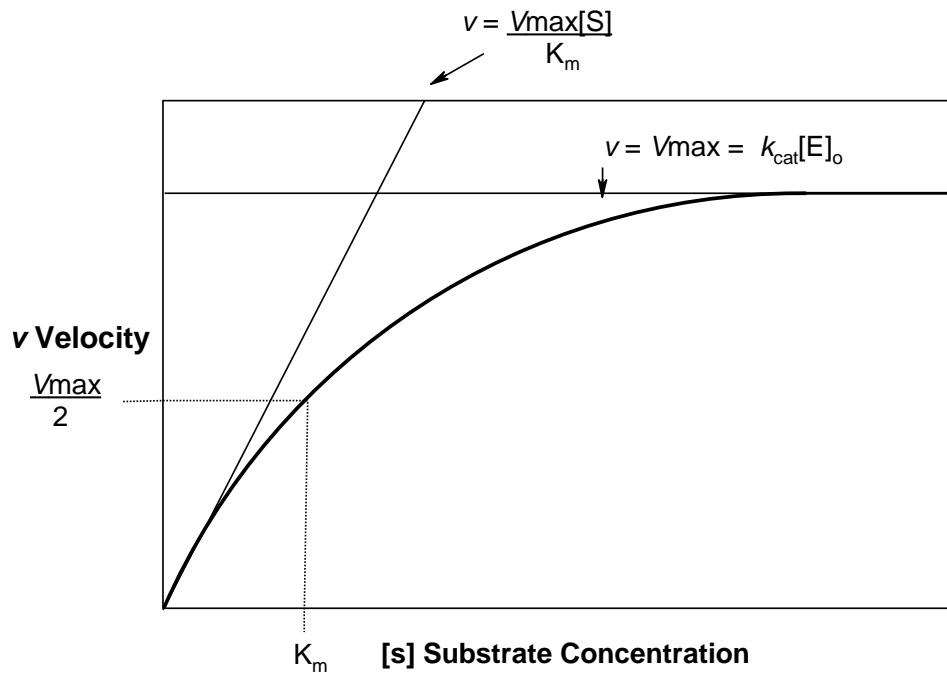
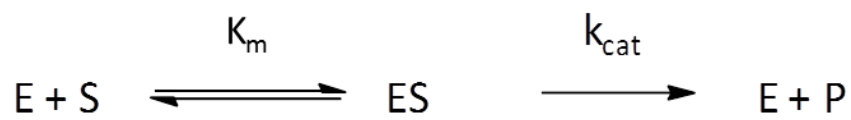


Figure 6.1: Sample Michaelis-Menten plot



$$K_m = \frac{[E][S]}{[ES]}$$

$$[E] = [E]_o - [ES]$$

$$V = k_{\text{cat}}[E]_o$$

$$V_{\max} = k_{\text{cat}}[E]_o$$

Equations 6.1: The key equations for Michaelis-Menten kinetics

Where:

$K_m$  is the dissociation constant

$[E]$  is the free enzyme concentration

$[E]_0$  is the total enzyme concentration (a known value)

$[ES]$  is the concentration of the enzyme-substrate complex

$[S]$  is the substrate concentration

$k_{cat}$  is the catalytic constant (also known as the “turnover constant”)

$V_{max}$  is the fastest reaction rate possible

$v$  is the velocity of the reaction at a set concentration of substrate

After solving for  $[ES]$ , the Michaelis-Menten equation can be obtained (**Equation 6.2**).<sup>240</sup>

$$v = \frac{V_{max}[S]}{K_m + [S]}$$

**Equation 6.2: The Michaelis-Menten equation**

Although specific computer software is available to assist in the interpretation of these data sets, it is also possible to interpret the data by using a Lineweaver-Burk plot **Figure 6.2**.<sup>241-243</sup> This double reciprocal plot has  $1/v$  on the y-axis and  $1/[S]$  on the x-axis and produces a straight line. The intercept with the y-axis gives  $1/V_{max}$ , the slope has a gradient of  $K_m/V_{max}$  and the intercept with the x-axis gives  $-1/K_m$ .

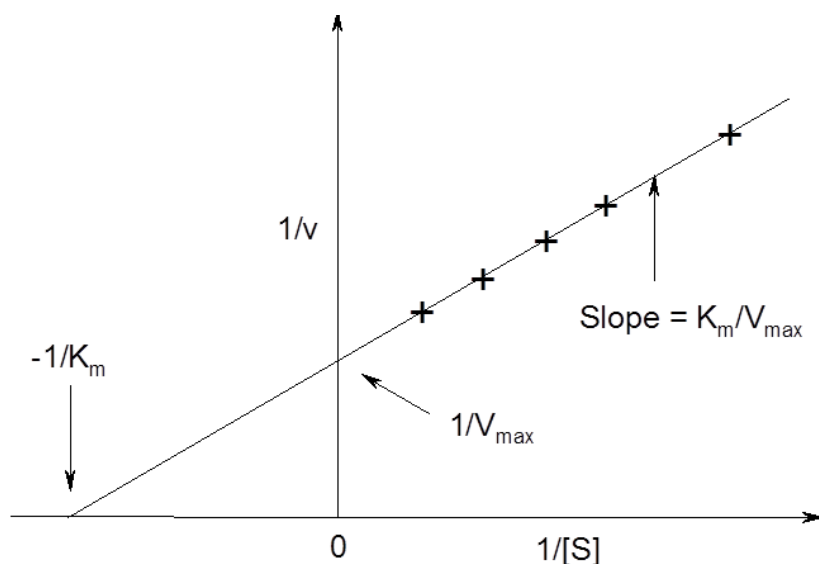


Figure 6.2: Representation of a Lineweaver-Burk plot

#### 6.4.2 Michaelis-Menten kinetic results

A concentration study was carried out, to determine the  $K_m$  and  $k_{\text{cat}}$  values for compounds cyclohexyl derivative **6.6** and ketocyclohexyl tetrahydropterin **6.7**. Values for  $K_m$  and  $k_{\text{cat}}$  were obtained for tetrahydro WSG1002 **1.7** again to ensure consistency across batches of enzyme. The Michaelis-Menten plots for cyclohexyl derivative **6.6** and ketocyclohexyl tetrahydropterin **6.7** are shown in **Figure 6.3** and **Figure 6.4**, respectively, and the numerical values for all three compounds are given in **Table 6.4**.



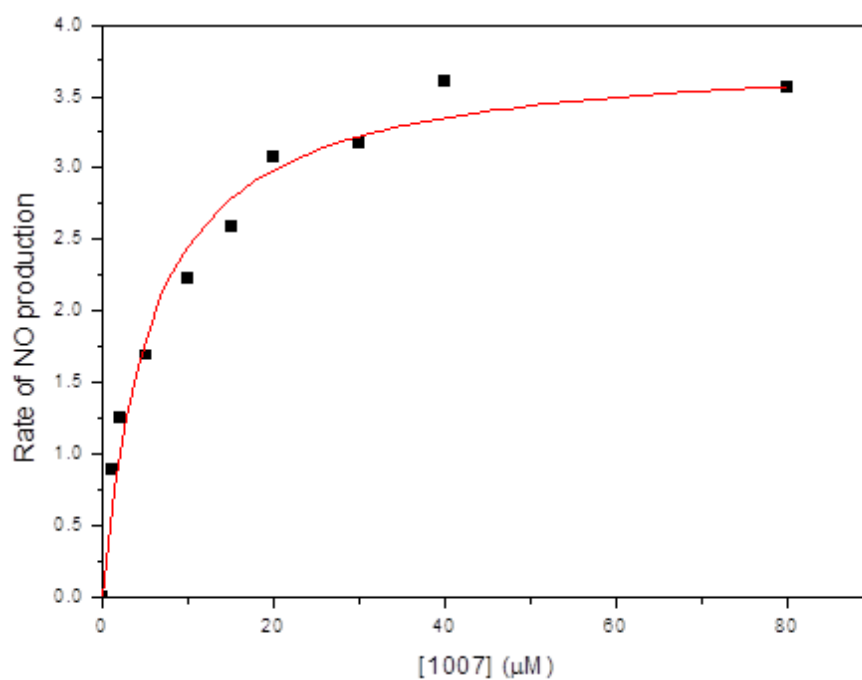


Figure 6.3: Concentration study for cyclohexyltetrahydropterin 6.6

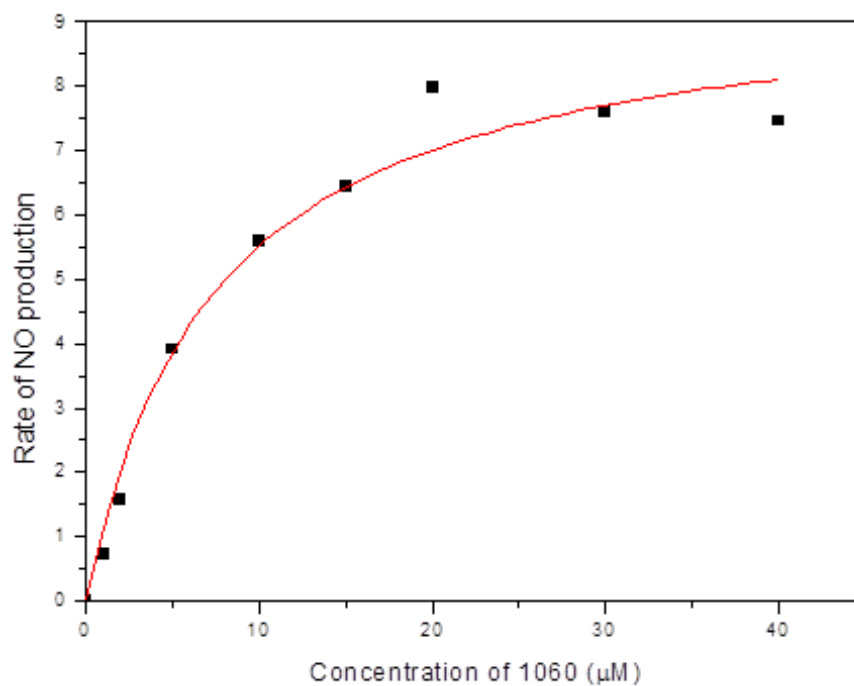


Figure 6.4: Concentration study for ketocyclohexyltetrahydropterin 6.7 (note different scales from figure 6.3)

Compound	$k_{\text{cat}} \text{ min}^{-1}$	$K_{\text{m}}$
<b>BH<sub>4</sub></b>	13	1
<b>1.7</b>	$5.27 \pm 0.36$	$151 \pm 22$
<b>6.6</b>	$3.8 \pm 0.20$	$5.57 \pm 1.00$
<b>6.7</b>	$9.61 \pm 0.67$	$7.41 \pm 1.63$

Table 6.4: Turnover rate and binding affinity of tetrahydropterins 1.7, 6.6 and 6.7

These results suggest that, within experimental error, the cyclohexyl tetrahydropterin (**6.6**) and the ketocyclohexyl tetrahydropterin (**6.7**) had essentially the same affinity for nNOS (Table 6.4, entries 3 and 4). This is hardly surprising, due to the high similarity between structures. Pleasingly, these numbers are vastly improved upon when compared to tetrahydro WSG1002 (**1.7**) and represent a much higher affinity for NOS than has been seen previously within our laboratory. Interestingly, the rate of turnover varied quite significantly. The cyclohexyl tetrahydropterin (**6.6**) had a lower turnover rate than tetrahydro WSG1002 **1.7** but is still very close; this result in itself is quite significant in supporting the structural range of synthetic pteridines that can act as BH<sub>4</sub> mimetics. Impressively though, the ketocyclohexyl tetrahydropterin (**6.7**) has a truly remarkable turnover rate ( $9.61 \pm 0.67 \text{ min}^{-1}$ , Table 6.4 entry 4) and is very close to the value achieved by BH<sub>4</sub> ( $13 \text{ min}^{-1}$ , Table 6.4 entry 1). When both values for ketocyclohexyl tetrahydropterin **6.7** are taken into consideration it is apparent that it is an exceptional example of a synthetic pteridine acting as a BH<sub>4</sub> mimetic. With these excellent results in hand, it was easy to find the motivation to investigate the mechanism of action further through a more detailed kinetic study, stopped flow kinetics, on all three compounds.

### 6.5 Stopped-flow kinetics

The aim of the stopped-flow kinetic study was to obtain a numerical value for the rate-limiting step of the molecular mechanism of NOS; the decay of the oxyferrous species (Figure 6.5). It was hoped that with these data, the differences between the compounds would become apparent (with different compounds having different rates for this step) and an explanation could be offered for the different levels of activity observed from previous assays. Once more, the compounds were resynthesised and

transported to Edinburgh. This time the experiments were carried out only by Simon Daff and Ben Gazur and it is with great thanks to them that these data can be reported.

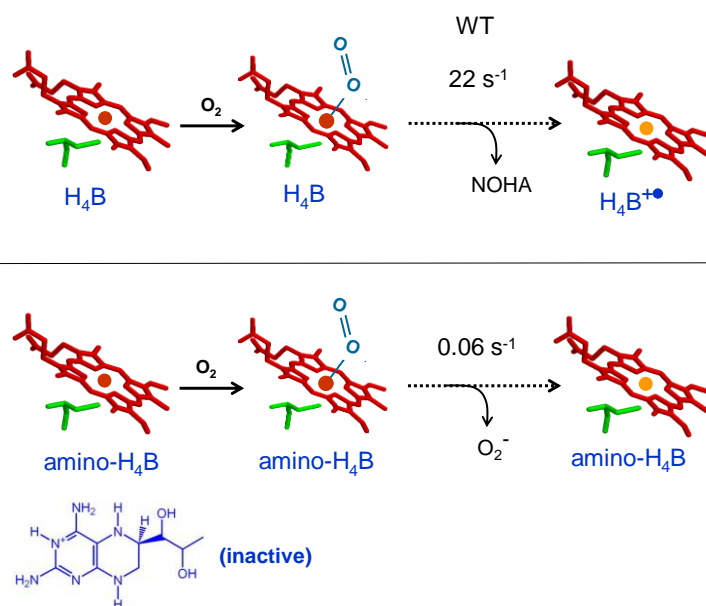


Figure 6.5: Pre-steady state kinetic diagram, courtesy of Ben Gazur

It can be seen from **Figure 6.5** that the decay of the oxyferrous complex (the rate-limiting step) cannot be studied without oxygen present, due to molecular oxygen participating in the reaction. All stopped-flow kinetic studies were carried out in a glove-box with an oxygen level of less than 10 ppm. A simple cartoon of the apparatus is presented in **Figure 6.6**. The component parts of the assay (Pump A), which were thoroughly degassed, were allowed to equilibrate in deoxygenated buffer. To initiate the experiment, this degassed mixture was transferred to Cell C and mixed with oxygenated buffer from pump B. The spectrophotometric changes were monitored in cell C using Pro-Kineticist 4.21 software and around 400 spectra were recorded over a period of 1 second.

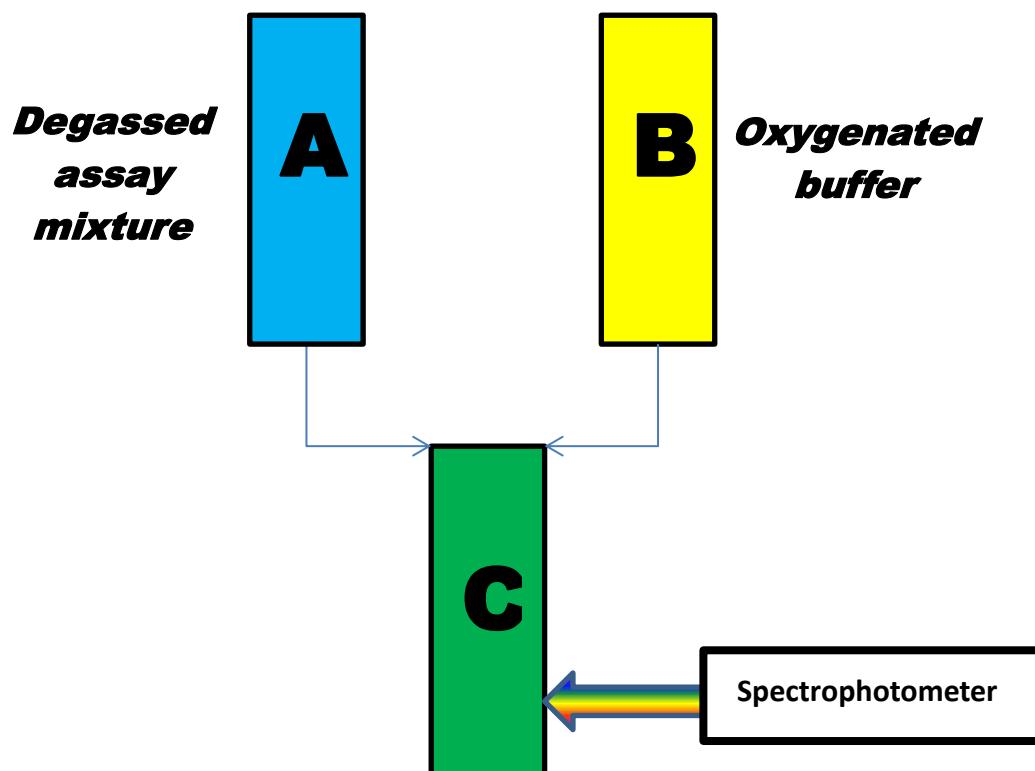


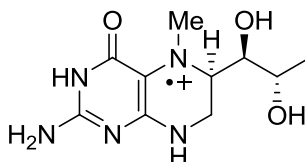
Figure 6.6: Cartoon depiction of stopped-flow kinetic instrument

The results of stopped-flow experiments for compounds **1.7**, **6.6** and **6.7** are presented in **Table 6.5** along with values for  $\text{BH}_4$  (**1.1**) and 4-amino $\text{BH}_4$  (**1.19**). The rate limiting step involves the donation of an electron from the pteridine and it was expected that differing rates of electron-transfer would be observed.

Compound	Rate s <sup>-1</sup> (error s <sup>-1</sup> )
BH <sub>4</sub>	27.8 (± 0.2)
<b>1.19</b>	< 1
<b>1.7</b>	25.2 (± 0.3)
<b>6.6</b>	24.5 (± 0.2)
<b>6.7</b>	24.7 (± 0.2)

Table 6.5

Surprisingly, the rates of electron transfer, for the activating pterins, were very similar within experimental error. These rates are so similar as to be virtually identical, demonstrated with graphical representations in **Figures 6.7 to 6.10** (OxyHb in red, MetHb in blue). These data suggest that the rate of electron transfer within the enzyme is the same regardless of the activating pteridine used; this was a very interesting but surprising result. It was assumed that if one were to alter the electronic properties of a pterin-based NOS activator, then one would expect to see the appropriate difference in turnover rate, this appears not to be the case. This calls into question the argument used to explain the increased activity of 5-methylBH<sub>4</sub> (**1.17**) at saturation concentrations; a more stable radical cation may not be the cause of the observed increased activity compared with BH<sub>4</sub> itself.

**1.17**

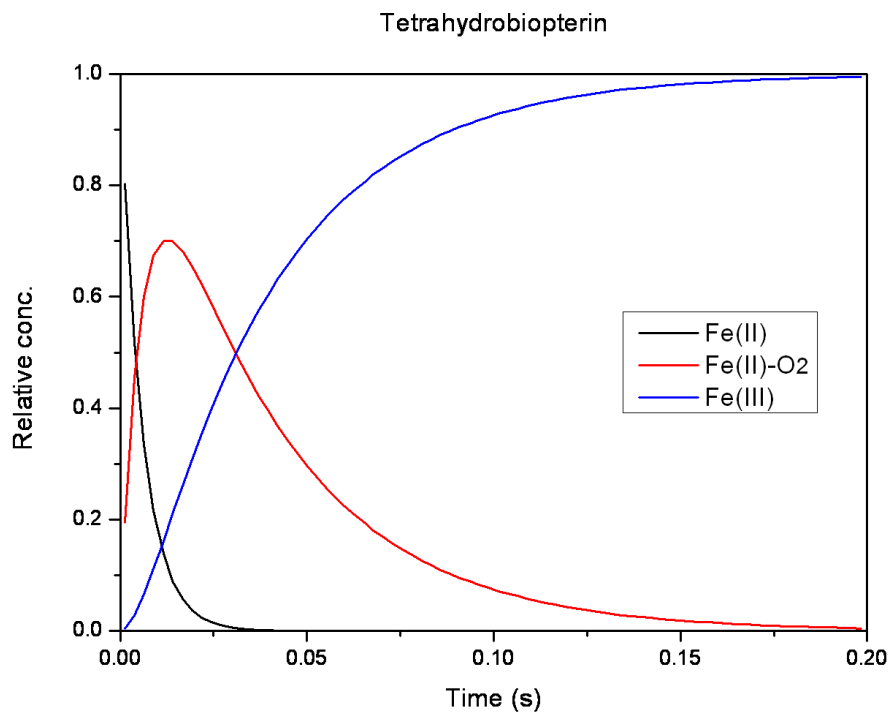


Figure 6.7: Graphical representation of rates for stopped-flow kinetics of BH<sub>4</sub> (1.1)

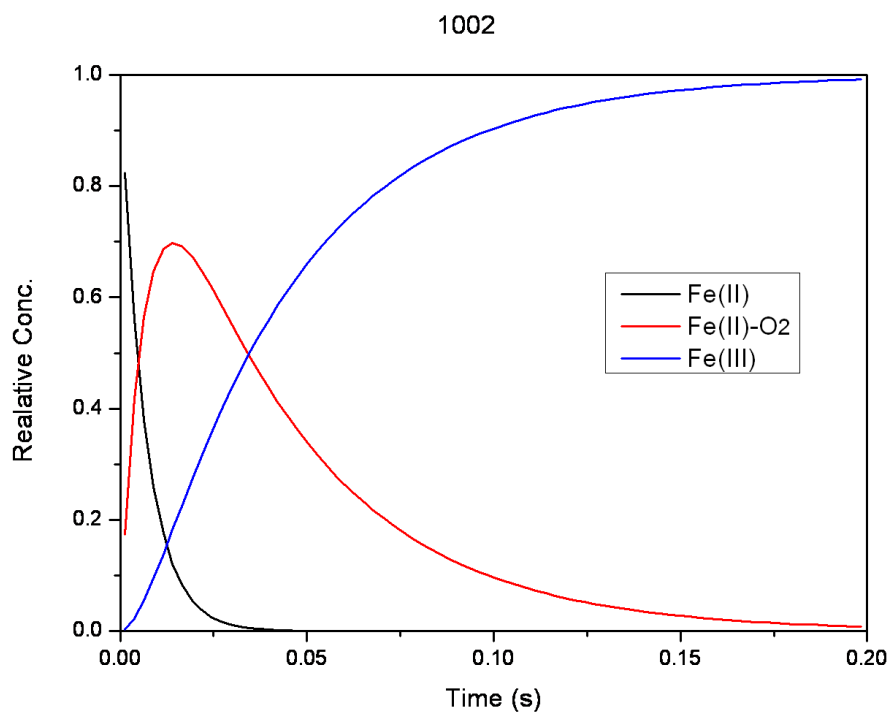


Figure 6.8: Graphical representation of rates for stopped-flow kinetics of 1.7

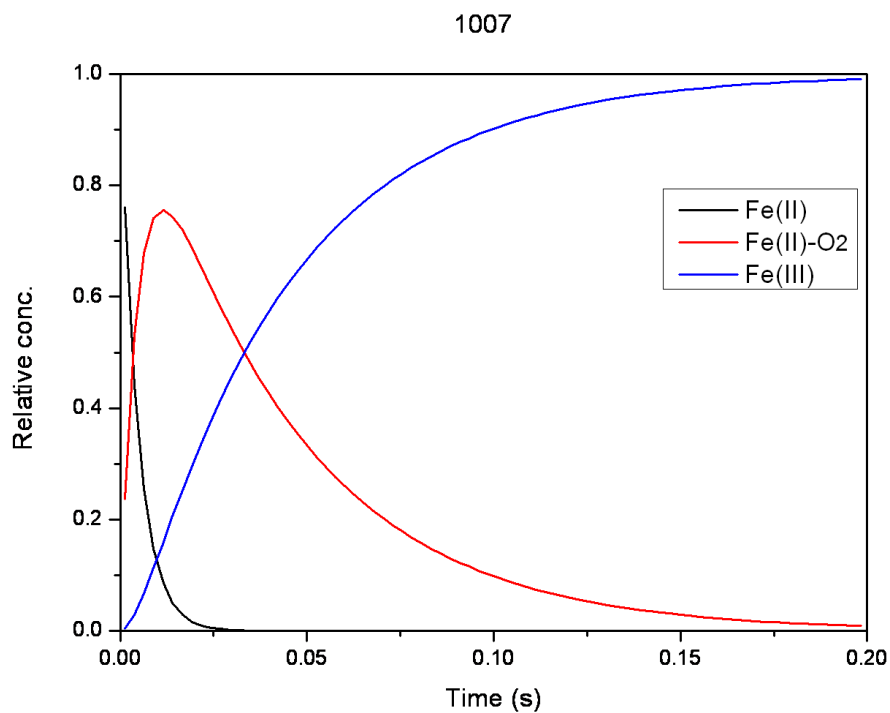


Figure 6.9: Graphical representation of stopped-flow kinetics for 6.6

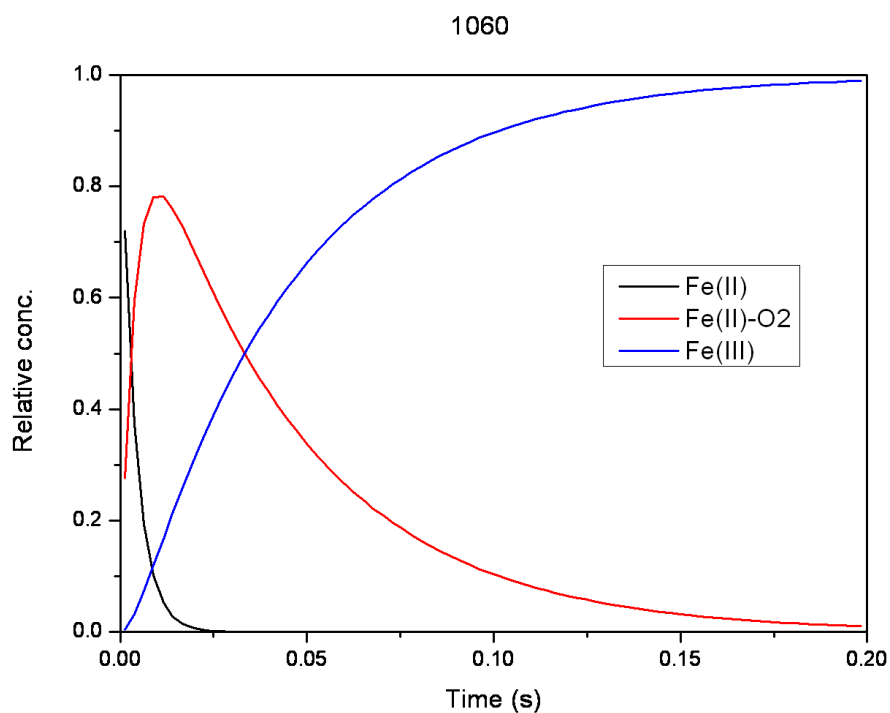


Figure 6.10: Graphical representation of stopped-flow kinetics for 6.7

With no evidence to suggest a reason as to why turnover rates vary between pteridines but the rate of electron-transfer is the same, some computer modelling was

carried out to quantify the HOMO and SOMO energy levels of the natural and non-natural cofactors.

### 6.6 Spartan calculations

It was hoped that by obtaining the HOMO and SOMO energy levels using both semi-empirical and DFT calculations, some insight into the differences of reactivity across the pteridines series might be obtained. If there was no difference in energy levels then this might suggest that the difference in turnover rate was not an electronic phenomenon. However, if there was an appreciable difference in energy levels, and hence in the pterins' ability to donate an electron to the haem, then there are implications for the mechanism of action of NOS. Spartan calculations were carried out for  $\text{BH}_4$  (**1.1**), tetrahydro WSG1002 **1.7** and the two diastereoisomers of cyclohexyl hydropterin **6.6** and keto cyclohexyl hydropterin **6.7** and the data for the HOMO calculations are displayed in **Table 6.6** with the SOMO in **Table 6.7**.



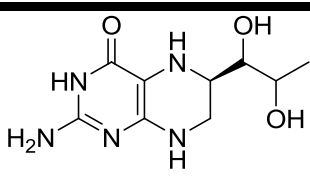
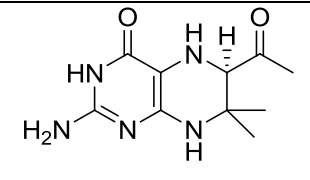
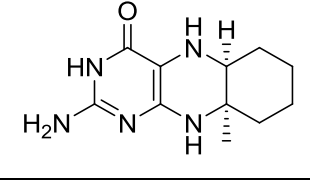
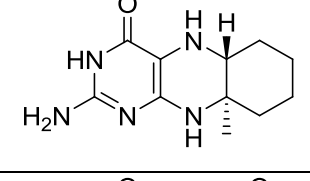
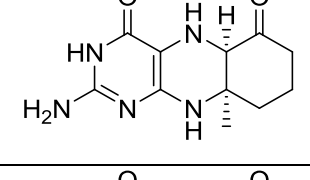
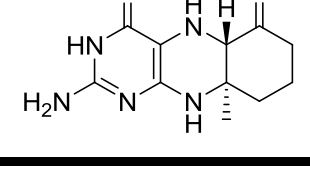
Compound	AM1 (kJ mol <sup>-1</sup> )	B3LYP 6-31 G* (kJ mol <sup>-1</sup> )
	-773.77	-446.86
	-773.94	-449.02
	-750.47	-410.24
	-751.41	-419.06
	-764.08	-441.43
	-764.59	-431.83

Table 6.6: HOMO energy levels

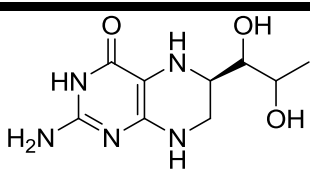
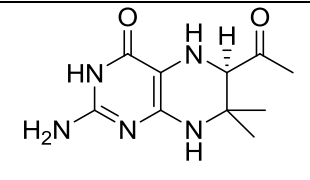
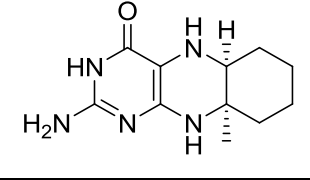
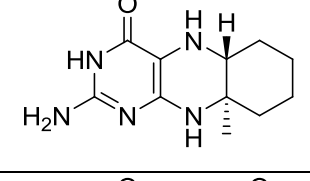
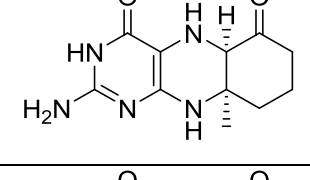
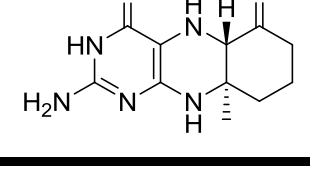
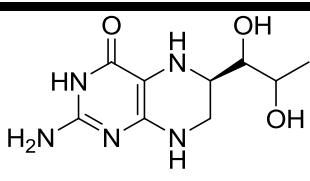
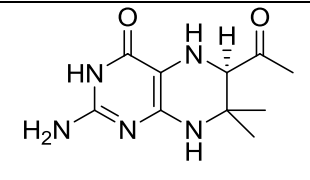
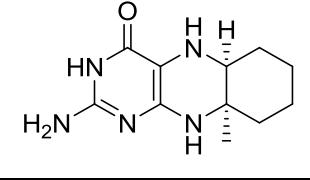
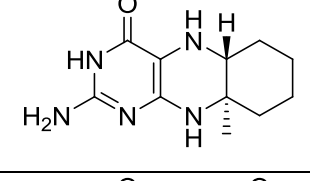
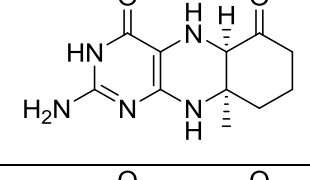
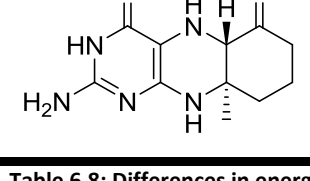
Compound	AM1 (kJ mol <sup>-1</sup> )	B3LYP 6-31 G* (kJ mol <sup>-1</sup> )
	-1219.07	-888.51
	-1225.83	-911.31
	-1216.49	-880.69
	-1212.25	-886.69
	-1221.99	-886.35
	-1221.36	-897.44

Table 6.7: SOMO energy levels

Compound	$\Delta E$ AM1 (kJ mol <sup>-1</sup> )	$\Delta E$ B3LYP 6-31 G* (kJ mol <sup>-1</sup> )
	445.30	436.65
	451.89	462.29
	466.02	470.45
	460.84	467.63
	457.91	444.92
	456.77	465.61

**Table 6.8:** Differences in energy between HOMO and SOMO. This shows that there is only relatively small differences in stability between the three main compounds. Interestingly, there is a notable difference in stability between the two diastereomers of WSG1060.

It appears that there is no systematic trend emerging from these data ( $\Delta E$ , **Table 6.6 - Table 6.8**), suggesting that the difference in turnover rate is less affected by their electron density than originally anticipated. Another explanation is required to account for the differences in turnover rate. It appeared that we had ruled out the coenzymes' electronic properties as the factor that affected the difference in turnover rate. This led us to investigate the ability of a pteridine to stabilise the NOS dimer as possibly being the factor that alters the turnover rate. Biological experiments are ongoing with regards to this question but, in a bid to shed some light on the subject,

computational analysis was performed on the pteridines' adopted binding mode within NOS.

### 6.7 GOLD analysis

GOLD<sup>200</sup> was again used to assess the potential binding orientations adopted by the pteridines within NOS (see **Chapter 3** for a previous example). In this case each all stereoisomer of the selected pteridines were modelled and the highest scoring feasible binding orientation for each is overlaid below in **Figures 6.11 to 6.14**. Each enantiomer's Goldscore is given in **Table 6.9**.

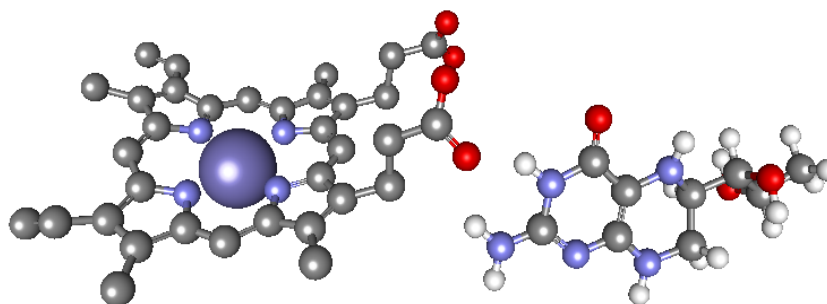


Figure 6.11: BH<sub>4</sub>'s (1.1) natural binding mode

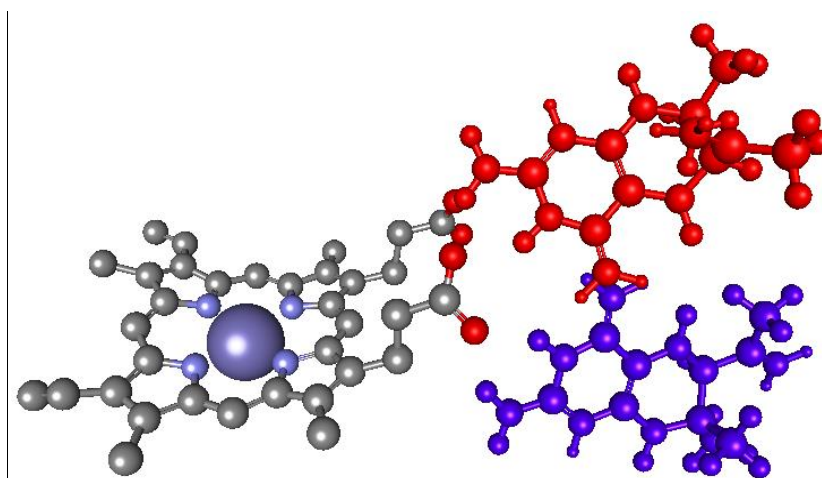


Figure 6.12: (6S)-1.7 in red, (6R)-1.7 in blue

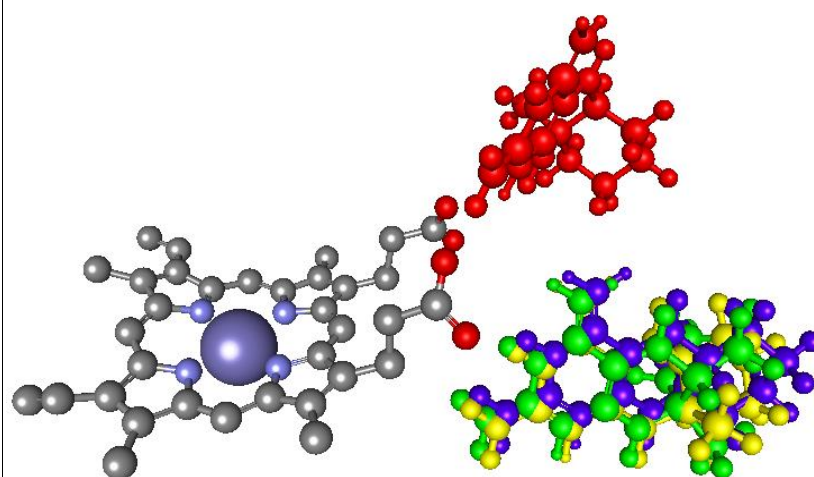


Figure 6.13: (6*S*,7*R*)-6.6 in red, (6*R*,7*R*)-6.6 in blue, (6*R*,7*S*)-6.6 in green, (6*S*,7*S*)-6.6 in yellow

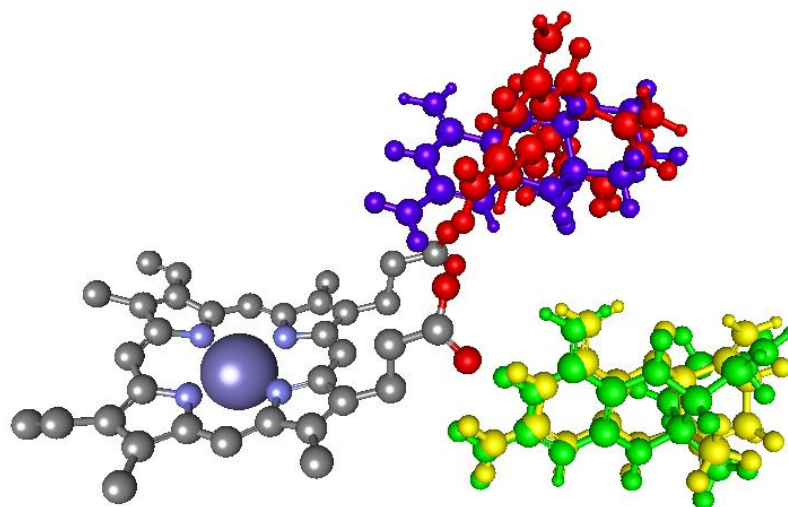


Figure 6.14: (6*R*,7*R*)-6.7 in red, (6*S*,7*R*)-6.7 in blue, (6*S*,7*S*)-6.7 in green, (6*R*,7*S*)-6.7 in yellow

Compound	goldscore
BH <sub>4</sub>	23.71
(6 <i>S</i> )- <b>1.7</b>	15.44
(6 <i>R</i> )- <b>1.7</b>	16.92
(6 <i>S</i> ,7 <i>R</i> )- <b>6.6</b>	20.05
(6 <i>R</i> ,7 <i>R</i> )- <b>6.6</b>	24.09
(6 <i>R</i> ,7 <i>S</i> )- <b>6.6</b>	25.95
(6 <i>S</i> ,7 <i>S</i> )- <b>6.6</b>	22.97
(6 <i>R</i> ,7 <i>R</i> )- <b>6.7</b>	18.51
(6 <i>S</i> ,7 <i>R</i> )- <b>6.7</b>	18.42
(6 <i>S</i> ,7 <i>S</i> )- <b>6.7</b>	22.75
(6 <i>R</i> ,7 <i>S</i> )- <b>6.7</b>	20.99

Table 6.9: Goldscores for each tetrahydropterin showing activity.

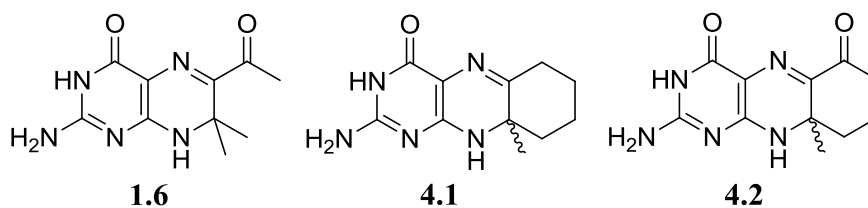
The results for the binding orientations tell an interesting story. It appears that not every stereoisomer adopts the BH<sub>4</sub> binding pose, with some stereoisomers consistently preferring to bind in a space above the BH<sub>4</sub> binding pocket. As the point at which these calculations were initiated starts within the BH<sub>4</sub> pocket, the results suggest that there is insufficient space available for these stereoisomers ((6*S*,7*R*)-**6.6**, (6*R*,7*R*)-**6.7** and (6*S*,7*R*)-**6.7**). These results should be taken into consideration along with the fact that GOLD does not allow flexibility of the protein-backbone during modelling. It may still be possible for these stereoisomers to be accommodated within the BH<sub>4</sub> pocket. However this is currently thought to be less likely as it would require further movement of the protein backbone and would alter the highly conserved dimer interface. The Goldscores also suggest that this new binding pose is relatively unfavourable when compared to binding within the BH<sub>4</sub> pocket. Both the visual and the numerical data together may be suggesting that not every stereoisomer of each synthetic pteridine is involved in binding and NOS activation.

There is also a distinct possibility that this new binding pose actually facilitates electron transfer within the enzyme, due to its proximity to the haem, and it could be a functional binding pose: this could account for the difference in turnover rate.

Whilst this again seems unlikely, there is insufficient evidence to rule this out completely. What seems most likely, however, is that the third ring system on cyclohexyl tetrahydropterin **6.6** and ketocyclohexyl tetrahydropterin **6.7**, which are protruding into a lipophilic region of the opposite dimer, are engaging in hydrophobic interactions and further stabilising the NOS dimer. This could account for the differences in binding affinity between the bicyclic and tricyclic systems. It is clear that more data are needed to answer this question.

### 6.8 X-Ray crystallographic studies

Several attempts were made at crystallising nNOS with compounds **6.6** and **6.7** by Ben Gazur at The University of Edinburgh and, although crystals were obtained, in both circumstances neither refracted to give useful data sets. However, in collaboration with the Poulos group at The University of California, Irvine, co-crystallisation experiments were performed with compounds **1.6**, **4.1** and **4.2** using bovine eNOS. Taking into consideration the results reported in **Section 6.7** it would be of obvious benefit to have data to confirm the binding mode of these analogues. Fortunately, in each case, good data sets were obtained and selected views are shown below in Figures **6.15** through to **6.23**.



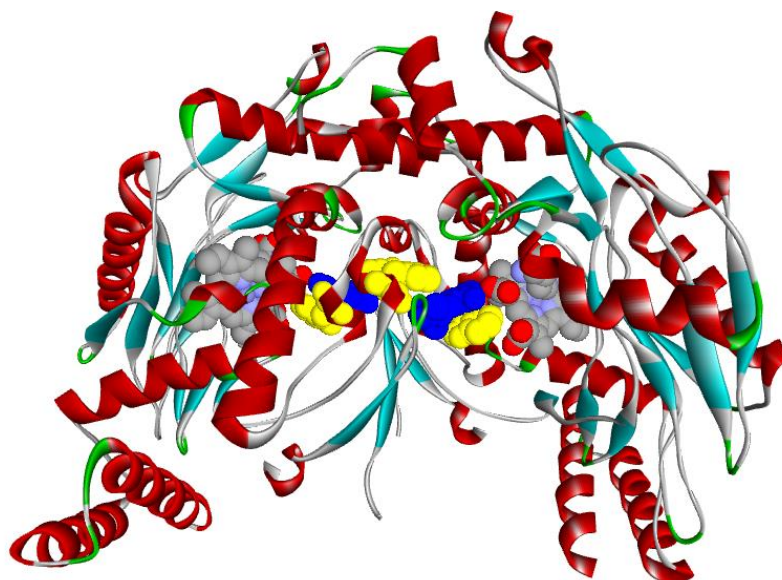


Figure 6.15: Full view of eNOS dimer with compound 1.6 (blue) bound between phenylalanine and tryptophan (both in yellow) and next to the haem (coloured according to atoms). Compound 1.6 can be seen adopting the typical binding pose of  $\text{BH}_4$

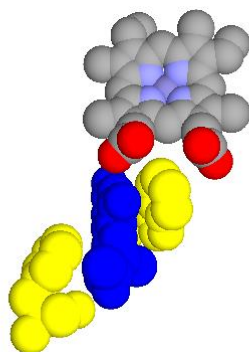


Figure 6.16: A view from above showing, in more detail, compound 1.6 (blue) bound between phenylalanine (yellow molecule on the left) and tryptophan (yellow molecule on the right) in the typical binding pose of  $\text{BH}_4$

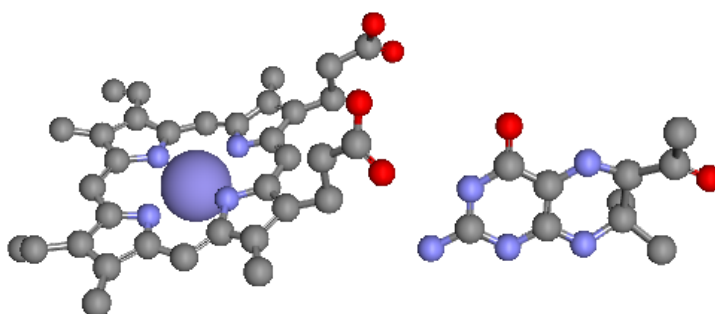


Figure 6.17: A side-on view explicitly showing the orientation of 1.6 relative to the haem

It can be seen from Figures 6.15 to 6.17 that 1.6 adopts the same binding pose as  $\text{BH}_4$ ,  $\pi$ -stacked between the phenylalanine and tryptophan residues and hydrogen-bonded to the haem. What is less obvious from these figures is the complete lack of a



$\text{Zn}^{2+}$  bridge stabilising the dimer. NOS has been observed to form a stable dimer in the absence of zinc before;<sup>51</sup> however, it is noteworthy that this has only happened with compound **1.6**, which has a lower affinity for nNOS than **4.1** and **4.2**. It is reasonable to speculate that the smaller size of **1.6**, in comparison to other pteridine-based NOS activators, is distorting the dimer and preventing the zinc from binding. It may also be reasonable to suggest that the lack of zinc is one possible reason that **1.6** has a lowered affinity for nNOS than **4.1** or **4.2**.

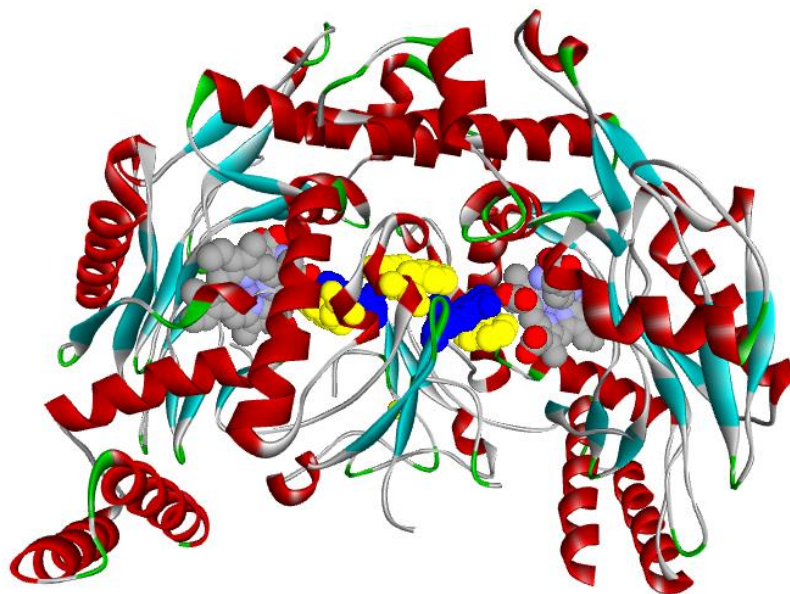


Figure 6.18: Full view of eNOS dimer with compound **4.1** (blue) bound between phenyl alanine and tryptophan (both in yellow) and next to the haem (coloured according to atoms). Compound **4.1** can be seen adopting the typical binding pose of  $\text{BH}_4$

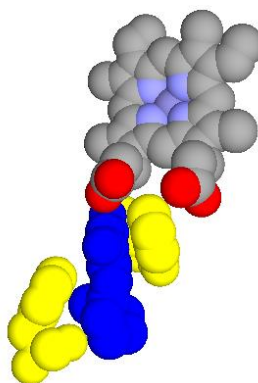


Figure 6.19: A view from above showing, in more detail, compound **4.1** (blue) bound between phenylalanine (yellow molecule on the left) and tryptophan (yellow molecule on the right) in the typical binding pose of  $\text{BH}_4$

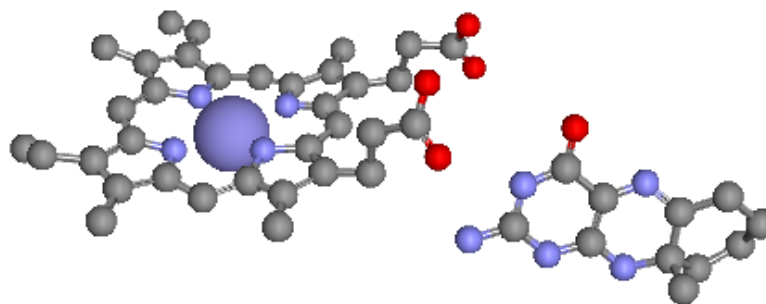


Figure 6.20: A side-on view explicitly showing the orientation of 4.1 relative to the haem

From Figures 6.18 to 6.20 it can be seen that compound 4.1 adopts the same binding pose as  $\text{BH}_4$ .



Figure 6.21: Full view of eNOS dimer with compound 4.2 (blue) bound between phenyl alanine and tryptophan (both in yellow) and next to the haem (coloured according to atoms). Compound 4.2 can be seen adopting the typical binding pose of  $\text{BH}_4$

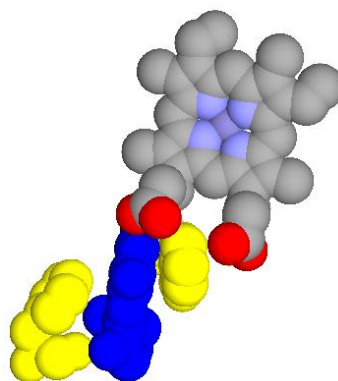


Figure 6.22: A view from above showing, in more detail, compound 4.2 (blue) bound between phenylalanine (yellow molecule on the left) and tryptophan (yellow molecule on the right) in the typical binding pose of  $\text{BH}_4$

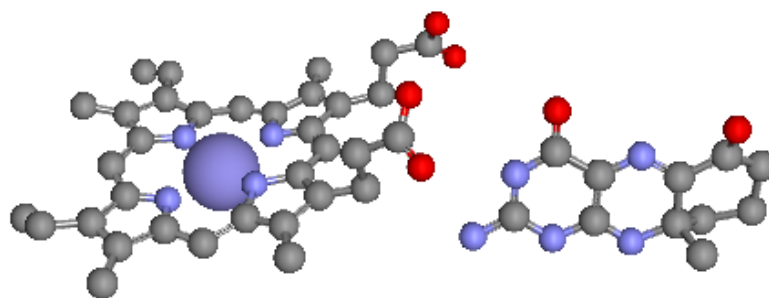


Figure 6.23: A side-on view explicitly showing the orientation of 4.2 relative to the haem

From Figures 6.21 to 6.23 it can be seen that 4.2 also adopts the same binding pose as  $\text{BH}_4$ .

These data provide a useful insight into how synthetic pteridines are acting as NOS activators. Comparing these results with those obtained for the computational chemistry, reported in Section 6.7, some important speculations can be made regarding binding modes. It is unlikely that the synthetic pteridines are binding in an unusual manner and that they are more likely to be binding in the typical  $\text{BH}_4$  binding pose. Coupling this evidence with the computational studies, it appears that the tetrahydro form of 1.6 (1.7) would only be active if it contained the 6*R* stereocentre. As 1.7 was tested as a mixture of enantiomers it appears likely that the active enantiomer will have a greater affinity for NOS (twice that of the racemic mixture) than that which has been previously reported. From the X-ray data, it can be seen that compounds 4.1 and 4.2 had to be in the 7*S* configuration to retain binding. This suggests that the tetrahydropteridines (6.6 and 6.7) should also contain the 7*S*-stereocentre to retain activity. The results from the computational analysis suggest that either the 6*R*,7*S*- or the 6*S*,7*S*-stereoisomers could potentially bind in the  $\text{BH}_4$  binding mode but suggest that (6*R*,7*S*) 6.5 and (6*S*,7*S*) 6.6 could have a higher affinity for NOS due to their higher GOLD score. In this respect, the prediction of GOLD modelling is consistent with experiment and serves to highlight the quality of these predictions.

Combining the knowledge from the existing enzymatic assays, the stopped-flow kinetic experimentation and the computational work discussed so far, it is likely that the synthetic pteridines are functioning as coenzyme mimetics in a fashion exactly

the same as BH<sub>4</sub>. To the best of our knowledge this level of detail has not been provided for synthetic pteridines before and provides a useful insight for further compound design.

### 6.9 eNOS enzymatic assay

Following the successes in obtaining the X-ray crystal data, the Poulos group agreed to assay our tetrahydropteridines with eNOS. This was performed using an enzymatic assay similar to that used with nNOS. To date only the result has been obtained for the tetrahydro WSG1002 (**1.7**) and further work is on-going to obtain the remaining data for the final two compounds. The results obtained so far are very encouraging (see **Figure 6.24** and **6.25**) and suggest that **1.7** is not only functioning as an eNOS activator but that it is out-performing BH<sub>4</sub> in terms of the maximum turnover rate. **Figure 6.24** shows the normal activation of eNOS with BH<sub>4</sub> following normal Michaelis-Menten kinetics. **Figure 6.25** shows activation of eNOS using **1.7** and it can be seen that the plateau of the curve has not yet been reached. This strongly suggests that the maximal activation-level for **1.7** has not been reached; indeed the maximum rate might be limited by the solubility of this compound. Significantly more material would be needed to assess this. Consequently reliable figures for  $K_m$  and  $k_{cat}$  could not be obtained. It is however, clear to see that eNOS has a higher affinity for BH<sub>4</sub> than **1.7** and provides us with a relative order of preference. Furthermore, it can be stated that **1.7** is a weakly binding compound within eNOS.

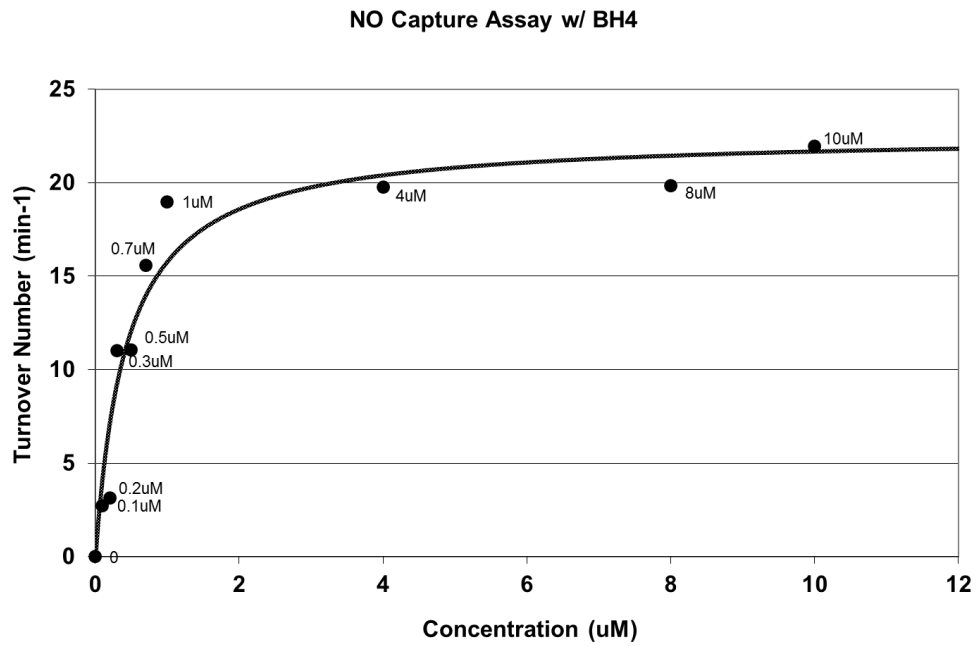


Figure 6.24: Michaelis-Menten plot for BH<sub>4</sub> and eNOS.

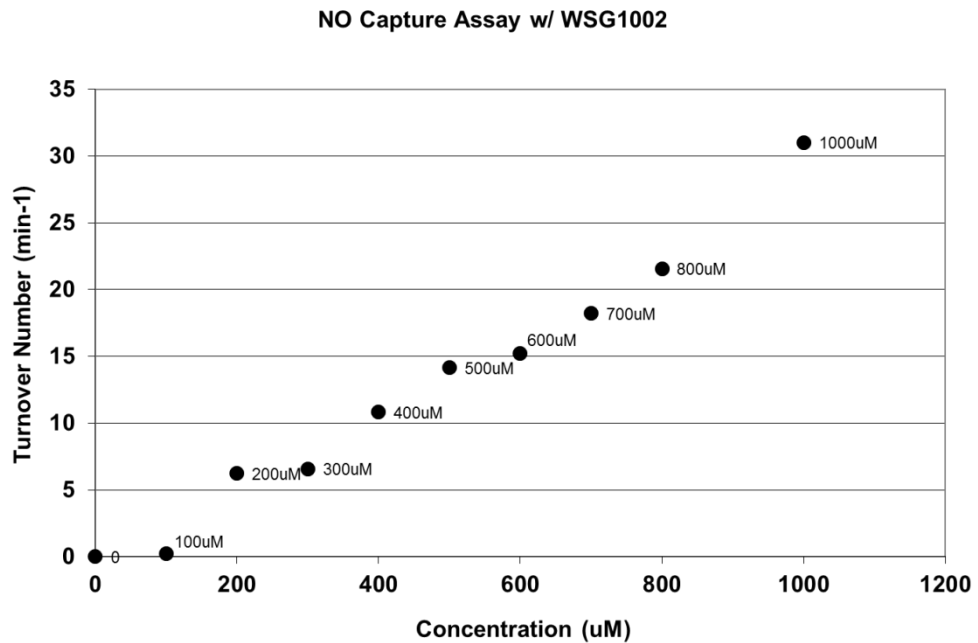


Figure 6.25: Michaelis-Menten plot for tetrahydro WSG1002 (1.7) and eNOS. (Note the difference in scale.)

These data lead to a further interesting conclusion that the tetrahydro WSG1002 would be well suited to activating eNOS when it is lacking BH<sub>4</sub> but that it could not compete with BH<sub>4</sub> for the pterin binding-pocket. Such a situation is just as required for a selectively acting BH<sub>4</sub>-mimetic drug. This suggests that **1.7** is a very suitable

candidate for development as a drug in treating conditions that are affected by low BH<sub>4</sub> bioavailability.

### 6.10 Conclusion and further work

Expansion at the C<sup>2</sup> position was counterproductive and it seems likely that this is due to the inability of the *N*-methyltetrahydropteridine (**3.1**) to fit into the BH<sub>4</sub> binding pocket. In a direct response to questions four and five from Chapter 1 (**Section 1.7**):

- How large a space is available within NOS to accommodate a pteridine that has been expanded at the C<sup>2</sup>-position?
- If there is sufficient space available to accommodate expanded pteridines, would these analogues be suitable activators of NOS and what will this add to the questions remaining about the molecular mechanism on NOS?

It appears that any expansion at the C<sup>2</sup>-position would appear to be a poor strategy for further developing NOS activators as the small expansion of a single methyl group removed all activity. **6.5** was able to activate NOS, albeit with a very low turnover rate and suggests that the basic hydrogen bonding interactions between NOS and the basic pteridine scaffold are of high importance to retain activity, when designing coenzyme mimetics. This adds further evidence to the necessity of retaining important hydrogen-bonds between the propionate groups of the haem and the pyrimidine section of the pteridine. The successful binding of this compound was a surprise but provides a baseline binding strength for all pteridines.

The differences between batches of NOS provided unreliable data for 6-alkenyl tetrahydropterin **6.4** and further evaluation is necessary to confirm or refute its ability to act as an activator.

In a direct response to question seven from Chapter 1 (**Section 1.7**):

- Are there other dihydropteridines that would be more suitable as activators of NOS and if so, is there anything in particular that makes them more suitable?

There are other blocked dihydropteridines that act as a better coenzyme mimetics than the original lead compound. Two examples of synthetic pteridines acting as excellent NOS activators have been assessed, with one being of particular interest ketocyclohexyl tetrahydropterin (**6.7**). This pteridine is, as far as is known, the best example of a synthetic pteridine acting as a NOS activator to-date and is truly remarkable when taken into account with the selectivity of NOS for natural pteridines. Not only does this pteridine act as competent NOS cofactor and function in a manner identical to BH<sub>4</sub>, it is significantly more soluble than BH<sub>4</sub> (**1.1**) making it more attractive as a candidate for drug development.

Further work is required to explain the difference in turnover rate between compounds and, whilst this is on-going, there is mounting evidence to suggest that these differences are caused by dimer-stabilisation. What is clear from the work performed so far is that differences in electronic profile, between pteridines, appears to have much less of an impact upon coenzyme mimetic suitability than originally anticipated.

Although the synthesis of ketocyclohexyl tetrahydropterin **6.7** has been described in the literature previously, its application here is entirely novel and has the potential to become a medicinal compound for specific disease states; something which is a thoroughly exciting prospect.

# Chapter 7

---

## Experimental

### 7.1 General experimental

Dry reaction solvents were freshly distilled prior to use, as follows: triethylamine over KOH; pyridine over KOH; methanol and ethanol from the corresponding magnesium alkoxide generated from Mg turnings and iodine crystals. Commercially available dry DMF and acetonitrile were used as supplied from Aldrich. DCM, toluene, hexane, THF and Et<sub>2</sub>O were provided by standard operating procedure for Innovative Technology Solvent Purification System. All other reagents were used as supplied. Compounds; **2.2**, **2.10**, **2.16**, **3.11**, **3.12**, **3.8**, **4.6**, **5.6** and **5.9** were all commercially available at the time of this research.

Removal of solvents was carried out by evaporation using the rotary evaporator at reduced pressure (*ca.* 70 mbar) unless otherwise stated.

Thin layer chromatography (TLC) was carried out using pre-coated silica plates (Alugram<sup>®</sup> Sil G/UV<sub>254</sub>). Visualisation of TLC plates was achieved by UV (254 nm).

Flash column chromatography was performed according to the procedure of Still *et al.* using silica gel (230-400 mesh).<sup>244</sup>

Melting points were performed on Reichert 7905 hot stage melting point apparatus and are uncorrected.



Nuclear magnetic resonance ( $^1\text{H}$ ,  $^{13}\text{C}$ ) spectra were recorded on a Bruker Spectrospin 400 MHz or 500 MHz spectrometer for  $^1\text{H}$  and 100 MHz or 125 MHz for  $^{13}\text{C}$ . Chemical shifts are quoted relative to the solvent in parts per million. Coupling constants ( $J$ ) are given in Hz. The following abbreviations were used: s = singlet; d = doublet; t = triplet; q = quartet; m = multiplet; dd = doublet of doublets; tt = triplet of triplets; bs = broad singlet.

Infra red (IR) spectra were recorded on a Nicolet Impact 400 D FTIR spectrometer as KBr discs. Frequencies are quoted in  $\text{cm}^{-1}$ .

Mass spectra were recorded at the University of Strathclyde using a Jeol JMS AX505 mass spectrometer in low resolution mass spectrometry (LRMS) or high resolution mass spectrometry (HRMS) by Orbitrap. Both methods use Electrospray ionisation (ES).

HPLC purification was carried out using a Waters 1525 binary HPLC pump, Waters 717 plus autosampler, Waters 2487 dual  $\lambda$  absorbance detector and breeze 2 software using a Vydac protein and peptide reverse phase C18 column;  $\lambda = 254 \text{ nm}$ , gradient elution with water/acetonitrile containing 0.1% TFA. The gradient elution is shown below **Table 7.1**.

X-ray crystal structures were visualised using Mercury 2.4; free to download from the Cambridge Crystallographic Data Centre.

Entry	Time (min)	Flow (ml/min)	Water (%)	Acetonitrile (%)	Curve <sup>a</sup>
1	0.0	6	75	25	6
2	25.0	6	50	50	6
3	30.0	6	30	70	6
4	35.0	6	70	30	6
5	40.0	6	70	30	11
6	40.1	0	70	30	11

Table 7.1: HPLC gradient flow conditions. <sup>a</sup> Curve 6 is a continue run command, curve 11 is a stop command

Continuous flow hydrogenation was carried out using a ThalesNano H-Cube continuous flow hydrogenation reactor on full hydrogen mode at standard pressure unless otherwise stated. All reaction concentrations were standard at 0.05 M and had a flow rate of 2 ml min<sup>-1</sup>.

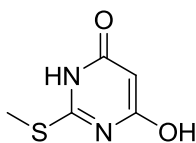
Biological Spectrophotometry was recorded on a Shimadzu UV-2101PC.

Microwave reactions were run using a Biotage Initiator Eight with the absorption level set to “normal” unless the solvent being used is 1,4-dioxane; in this case the absorption level is set to “low”.

.pdb files were downloaded from the protein databank ([www.rcsb.org](http://www.rcsb.org) at the time of this work October 2007 to November 2012).

## 7.2 Experimental

### 6-Hydroxy-2-(methylsulfanyl)-4(3H)-pyrimidinone (2.2)<sup>195</sup>



To a suspension of 2-thiobarbuturic acid (**2.1**, 5.18 g, 35.8 mmol) in ethanol (50 ml) and water (25 ml) was added triethylamine (4.99 ml, 35.8 mmol). The solution was then cooled in an ice bath and iodomethane (2.64 ml, 42.4 mmol) was added. The solution was then stirred for 16 hours at room temperature. A precipitate was collected by filtration and washed with cold water (50 ml) and cold diethyl ether (50 ml) to give the title product as an off-white solid, which was dried at 40 °C under reduced pressure overnight (3.52 g, 62 %).

**M.P:** > 230°C; **lit** = >350 °C.<sup>245</sup>

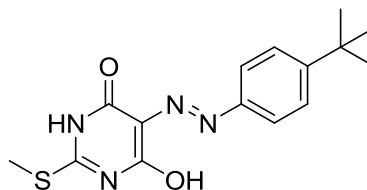
**$\nu_{\max}$**  (KBr,  $\text{cm}^{-1}$ ): 3438, 3010, 2935, 2571, 1643, 1498, 1454, 1420, 1343, 1264, 1221, 1190, 1015, 994, 873, 814

**$^1\text{H}$**  (DMSO- $d_6$ ) 400 MHz: 2.46 (s, 3H, S- $\text{CH}_3$ ), 5.13 (s, 1H,  $\text{C}^5\text{H}$ ), 11.73 (bs, 2H, amide NH and OH)

**$^{13}\text{C}$**  (DMSO- $d_6$ ) 100 MHz: 12.7 (S- $\text{CH}_3$ ), 85.5 ( $\text{C}^5$ ), 163.5 ( $\text{C}^2$ ), 167.2 ( $\text{C}^6$  and  $\text{C}^4$ )

**LC-HRMS:**  $\text{C}_5\text{H}_7\text{N}_2\text{O}_2\text{S}$  Expected (M+H) 159.0221; found (M+H) 159.0223. >99% pure by LC

**5-[(E)-(4-tert-Butylphenyl)diazenyl]-6-hydroxy-2-(methylsulfanyl)-4(3H)-pyrimidinone (2.3)**



*Preparation of the diazonium salt*

4-Tert-butylaniline (684 mg, 4.58 mmol) was dissolved in acetic acid:water (10 ml, 1:1) and cooled to -5 °C. Sodium nitrite (334 mg, 4.58 mmol) in water (5 ml) was added drop-wise with stirring, ensuring that the temperature stayed between -5 °C and 0 °C throughout. The mixture was stirred for 15 minutes.

*Coupling of the diazonium salt*

6-Hydroxy-2-(methylsulfanyl)-4(3H)-pyrimidinone (**2.2**, 500 mg, 3.16 mmol) was dissolved in 2M aq. sodium hydroxide (10 ml) and cooled to -5 °C. To this mixture, the diazonium salt was added drop-wise ensuring that the temperature did not rise above 5 °C. Once all the diazonium salt had been added, the reaction was stirred for 30 minutes at -5 °C and then 1 hour at room temperature. The solid was filtered off, washed with cold water (30 ml) and cold diethyl ether (30 ml) to give a dark yellow solid which was then recrystallised from ethanol. The solid was collected by filtration and dried at 40 °C under reduced pressure overnight to give the title product as a bright yellow solid (859 mg, 85 %).

**M.P:** > 230 °C

$\nu_{\max}$  (KBr,  $\text{cm}^{-1}$ ): 2956, 1701, 1614, 1549, 1471, 1417, 1250

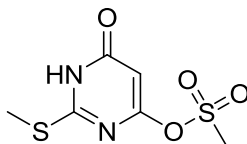
$^1\text{H}$  (DMSO- $d_6$ ) 500 MHz: 1.29 (s, 9H,  $^t\text{Bu}$ ), 2.50 (singlet overlapping DMSO signal, S- $\text{CH}_3$ ), 7.50 (2H, d,  $^3J = 8.8$  Hz,  $\text{C}^3\text{H}$  &  $\text{C}^3'\text{H}$  on diazo coupled ring), 7.55 (2H, d,  $^3J = 8.8$  Hz,  $\text{C}^2\text{H}$  &  $\text{C}^2'\text{H}$  on diazo coupled ring), 12.53 (bs, 1H, NH), 15.38 (bs, 1H, OH)

$^{13}\text{C}$  (DMSO- $d_6$ ) 125 MHz: 13.4 (S-CH<sub>3</sub>), 31.0 (3 x CH<sub>3</sub>), 34.4 (C(CH<sub>3</sub>)<sub>3</sub>), 117.0 (C<sup>3</sup> & C<sup>3'</sup> from diazo coupled ring), 121.0 (C<sup>5</sup>), 126.6 (C<sup>2</sup> & C<sup>2'</sup> from diazo coupled ring), 138.7 (C<sup>1</sup> from diazo coupled ring), 149.7 (C<sup>4</sup> from diazo coupled ring), 160.0 (C<sup>2</sup>), 167.7 (C<sup>4</sup>), 169.6 (C<sup>6</sup>)

**LRMS:** C<sub>15</sub>H<sub>19</sub>N<sub>4</sub>O<sub>2</sub>S Expected (M+H) 319; found (M+H) 319 (100%)

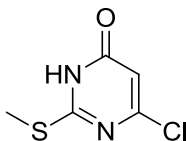
**C<sub>15</sub>H<sub>18</sub>N<sub>4</sub>O<sub>2</sub>S** Requires (%) C 56.6; H 5.7; N 17.6; S 10.1; Found (%) C 57.0; H 5.3; N 18.0; S 10.1

**2-(Methylsulfanyl)-6-oxo-1,6-dihydro-4-pyrimidinyl methanesulfonate (2.9)**



6-Hydroxy-2-(methylsulfanyl)-4(3*H*)-pyrimidinone (**2.2**, 200 mg, 1.24 mmol) was placed in a flame-dried round-bottomed flask containing anhydrous THF (15 ml) with stirring. Fresh 60 % sodium hydride in mineral oil (102 mg, 2.48 mmol) was then added and the solution was stirred for 15 minutes. Methanesulfonyl chloride (98  $\mu\text{l}$ , 1.24 mmol) was then added and the reaction mixture was left to stir for 4 hours. The solvent was then removed by rotary evaporation and a crude NMR was taken to observe the percentage conversion. Only *ca.* 50% conversion was ever observed.

$^1\text{H}$  (DMSO- $d_6$ ) 400 MHz: 2.31 (3H, s, CH<sub>3</sub>SO<sub>3</sub>), 2.43 (3H, s, CH<sub>3</sub>S), 5.05 (1H, s, C<sup>5</sup>H), 11.87 (1H, bs, amide NH)

**6-Chloro-2-(methylthio)pyrimidin-4(3H)-one (2.11)**

4,6-Dichloro-2-methylthiopyrimidine (**2.10**, 3.1 g, 16.06 mmol) was suspended in 2M aqueous NaOH (30 ml) and heated to reflux for 8 h. During this time the suspension became clear. The reaction mixture was then cooled to room temperature and glacial acetic acid was added dropwise with stirring until a white precipitate appeared. The solid was collected by filtration and washed with cold water (50 ml) and cold diethyl ether (50 ml). The solid was dried at 40 °C under reduced pressure overnight to give the title product as a glossy white solid (2.50 g, 88 %).

**M.P:** 209 – 212 °C; Lit = 208 °C,<sup>246</sup> 210 – 212 °C.<sup>197</sup>

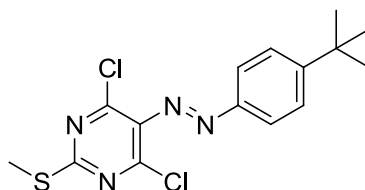
$\nu_{\max}$  (KBr,  $\text{cm}^{-1}$ ): 3440, 3018, 2935, 1650, 1548, 1100, 982

$^1\text{H}$  (CDCl<sub>3</sub>) 500 MHz: 2.59 (3H, s, CH<sub>3</sub>S), 6.28 (1H, s, C<sup>5</sup>H), 13.10 (1H, bs, amide NH)

$^{13}\text{C}$  (DMSO-*d*<sub>6</sub>) 125 MHz: 13.48 (S-CH<sub>3</sub>), 107.01 (C<sup>5</sup>), 157.81 (C<sup>2</sup>), 164.51 (C<sup>6</sup>), 166.13 (C<sup>4</sup>)

**LRMS:** C<sub>5</sub>H<sub>6</sub>ClN<sub>2</sub>OS Expected (M+H) 177 (100 %) 179 (30 %); Found (M+H) 177 (100%) 179 (30 %).

**5-[(E)-(4-Tert-butylphenyl)diazenyl]-4,6-dichloro-2-(methylsulfanyl)pyrimidine**  
**(2.15)**



5-[(E)-(4-Tert-butylphenyl)diazenyl]-6-hydroxy-2-(methylsulfanyl)-4(3H)-pyrimidinone (**2.3**, 2.34 g, 7.35 mmol) was suspended in phenylphosphonic dichloride (25 ml, 178 mmol) and heated under reflux at 180 °C for 4 hours. The mixture was then poured over ice (50 ml) with stirring. This layer was then extracted with diethyl ether (3 × 200 ml). The organic layer was then washed with saturated aqueous sodium hydrogen carbonate solution (3 × 200 ml). The organic layer was then dried using sodium sulfate, filtered and the solvent removed using rotary evaporation. The title product was recovered as a dark red oil which crystallised upon standing for three days or upon sonication (2.14 g, 82 %).

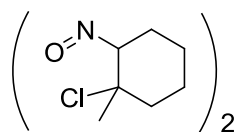
**M.P:** 87 – 91 °C (amorphous solid) or 97 °C (crystalline material formed at 3 days)

$\nu_{\max}$  (KBr,  $\text{cm}^{-1}$ ): 3058, 2964, 2931, 2905, 2869, 1739, 1601, 1535, 1482, 1337, 1317, 1239, 1159, 867, 845, 814

$^1\text{H}$  (DMSO- $d_6$ ) 400 MHz: 1.34 (s, 9H,  $\text{C}(\text{CH}_3)_3$ ), 2.61 (s, 3H,  $\text{SCH}_3$ ), 7.67 (2H, d,  $^3J = 8.8$  Hz,  $\text{C}^3\text{H}$  &  $\text{C}^5\text{H}$  on diazo coupled ring), 7.86 (2H, d,  $^3J = 8.8$  Hz,  $\text{C}^2\text{H}$  &  $\text{C}^6\text{H}$  on diazo coupled ring)

$^{13}\text{C}$  (DMSO- $d_6$ ) 100 MHz: 14.0 ( $\text{SCH}_3$ ), 30.8 ( $\text{C}(\text{CH}_3)_3$ ), 35.0 ( $\text{C}(\text{CH}_3)_3$ ), 122.8 ( $\text{C}^3\text{H}$  &  $\text{C}^5\text{H}$  on diazo coupled ring), 126.6 ( $\text{C}^2\text{H}$  &  $\text{C}^6\text{H}$  on diazo coupled ring), 136.8 ( $\text{C}^1$  on diazo coupled ring), 149.9 ( $\text{C}^5$ ), 152.8 ( $\text{C}^4$  and  $\text{C}^6$ ), 156.9 ( $\text{C}^4$  on diazo coupled ring), 170.6 ( $\text{C}^2$ )

**HRMS:**  $\text{C}_{15}\text{H}_{17}\text{Cl}_2\text{N}_4\text{S}$  Expected (M+H) 355.0546, found (M+H) 355.0546

**1-Chloro-1-methyl-2-nitrosocyclohexane (dimer) (2.17)**<sup>40</sup>

1-Methylcyclohexene (**2.16**, 16 ml, 151 mmol) and isoamyl nitrite (16 ml, 119 mmol) were stirred together in a 100 ml round bottomed flask at  $-78\text{ }^{\circ}\text{C}$ . To this solution concentrated (12 M) aqueous hydrochloric acid (16 ml, 192 mmol) was added drop-wise over a period of half an hour. The reaction was stirred at this temperature for a further 2 hours, whereupon a blue paste had formed. Ice-cold methanol (30 ml) was then added and the solution was allowed to rest at around  $0\text{ }^{\circ}\text{C}$  whilst a precipitate formed. This precipitate was collected by filtration and washed with excesses of ice-cold methanol to give the title product as a colourless solid (8.37g, 39 %).

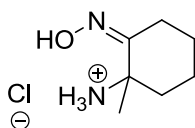
**M.P:** Decomposed at  $84\text{--}85\text{ }^{\circ}\text{C}$

$\nu_{\text{max}}$  (KBr,  $\text{cm}^{-1}$ ): 3544, 3467, 3414, 2937, 2868, 1638, 1618, 1412, 1381

$^1\text{H}$  ( $\text{CDCl}_3$ ) 400 MHz: 1.49 – 1.75 (6H, m, 3 x  $\text{CH}_2$ ), 1.74 (6H, s, 2 x  $\text{CH}_3$ ), 1.82 – 2.00 (8H, m, 4 x  $\text{CH}_2$ ), 2.29 – 2.31 (2H, m, 2 x  $\text{CH}$ ), 5.78 – 5.86 (2H, m, 2x  $\text{CH}$ )

$^{13}\text{C}$  ( $\text{DMSO-}d_6$ ) 125 MHz: 21.9 ( $\text{CH}_2$ ), 22.3 ( $\text{CH}_2$ ), 22.4 ( $\text{CH}_2$ ), 22.5 ( $\text{CH}_2$ ), 26.5 ( $\text{CH}_3$ ), 26.7 ( $\text{CH}_3$ ), 26.8 ( $\text{CH}_2$ ), 27.4 ( $\text{CH}_2$ ), 41.0 ( $\text{CH}_2$ ), 41.5 ( $\text{CH}_2$ ), 69.0 ( $\text{ClCCH}_3$ ), 69.0 ( $\text{ClCCH}_3$ ), 70.3 ( $\text{HCNO}$ ), 70.4 ( $\text{HCNO}$ )



**2-Amino-2-methylcyclohexanone oxime hydrochloride (2.18)**<sup>40</sup>

1-Chloro-1-methyl-2-nitrosocyclohexane (**2.17**, 3.13 g, 19.4 mmol) was dissolved in 7 M methanolic ammonia (50 ml) and stirred overnight in a sealed tube. The solvent was then removed by rotary evaporation and the residual oil dissolved in a small volume of water. The pH was adjusted to 7 with concentrated hydrochloric acid. The solvent was then removed by azeotropic evaporation with ethanol three times, ensuring that all traces of water were removed. The residue was then scratched in acetone to crystallise the material. The product was then recrystallised with a small volume of hot ethanol and a large excess of acetone to give the title product as a white solid (1.78 g, 51 %).

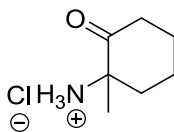
**M.P:** 217 – 219 °C, **Lit:** 219 – 220 °C<sup>40</sup>

$\nu_{\max}$  (KBr,  $\text{cm}^{-1}$ ): 3377, 3115, 3000, 2951, 2868, 1651, 1606, 1515, 1461, 1441, 969, 956,

$^1\text{H}$  (DMSO- $d_6$ ) 400 MHz: 1.22 – 1.25 (1H, m, CHH), 1.44 (3H, s,  $\text{CH}_3$ ), 1.57 – 1.71 (4H, m, 2 X  $\text{CH}_2$ ), 1.91 – 1.99 (2H, m,  $\text{CH}_2$ ), 3.06 – 3.10 (1H, m, CH), 8.30 (bs, 3H, + $\text{NH}_3$ ), 11.11 (s, 1H, NOH)

$^{13}\text{C}$  (DMSO- $d_6$ , 100 MHz): 20.4 ( $\text{CH}_2$ ), 20.7 ( $\text{CH}_2$ ), 22.4 ( $\text{CH}_3$ ), 24.7( $\text{CH}_2$ ), 37.1 ( $\text{CH}_2$ ), 56.0 ( $\text{CH}_3\text{CNH}_3$ ), 156.5 (CNOH)

**LRMS:**  $\text{C}_7\text{H}_{15}\text{N}_2\text{O}$  Expected (M+H) 143; found (M+H) 143

**2-Amino-2-methylcyclohexanone hydrochloride (2.19)**<sup>40</sup>

2-Amino-2-methylcyclohexanone oxime hydrochloride (**2.18**, 1.3 g, 7.28 mmol) was heated under reflux in 2 M hydrochloric acid (20 ml) for 10 minutes. The solution was then allowed to cool and the solvent was removed by azeotropic evaporation with toluene three times. The solid residue was then recrystallised with hot ethanol and a large excess of acetone to give the title product as a white solid (774 mg, 65% yield).

**M.P:** > 230 °C

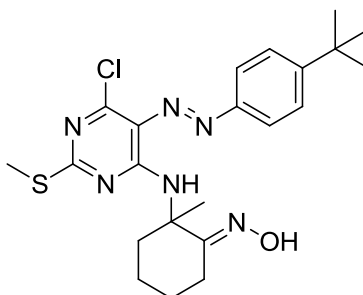
$\nu_{\max}$  (KBr,  $\text{cm}^{-1}$ ): 3428, 3025, 2953, 2846, 2882, 1725, 1587, 1511, 1474, 1359, 1147, 1126, 1000

$^1\text{H}$  (DMSO- $d_6$ ) 500 MHz: 1.49 (3H, s,  $\text{CH}_3$ ), 1.49 – 1.60 (1H, m,  $\text{CHH}$ ), 1.75 – 1.85 (3H, m,  $\text{CH}_2$  and  $\text{CHH}$ ), 2.00 – 2.04 (1H, m,  $\text{CHH}$ ), 2.12 – 2.15 (1H, m,  $\text{CHH}$ ), 2.26 – 2.30 (1H, m,  $\text{CHH}$ ), 2.74 – 2.81 (1H, m,  $\text{CHH}$ ), 8.43 (3H, bs,  $+\text{NH}_3$ )

$^{13}\text{C}$  (DMSO- $d_6$ ) 125 MHz: 20.4 ( $\text{CH}_2$ ), 20.6 ( $\text{CH}_3$ ), 26.6 ( $\text{CH}_2$ ), 36.9 ( $\text{CH}_2$ ), 37.3 ( $\text{CH}_2$ ), 61.7 (C), 207.9 (CO)

**HRMS:**  $\text{C}_7\text{H}_{14}\text{NO}$  Expected (M+H) 128.1070, Found (M+H) 128.1068

**(1E)-2-{{5-[(E)-(4-Tert-butylphenyl)diazenyl]-6-chloro-2-(methylsulfanyl)-4-pyrimidinyl}amino}-2-methylcyclohexanone oxime (2.20)**



5-[(E)-(4-Tert-butylphenyl)diazenyl]-4,6-dichloro-2-(methylsulfanyl)pyrimidine (**2.15**, 600 mg, 1.69 mmol), 2-amino-2-methylcyclohexanone oxime hydrochloride (**2.18**, 363 mg, 2.03 mmol) and triethylamine (495  $\mu$ l, 3.54 mmol) were placed in a 20 ml microwave vial and the contents were dissolved in DCM (12 ml). The vial was then sealed and irradiated in the microwave at the default power setting for 35 minutes at 75 °C with stirring. The organic layer was then diluted with DCM (15 ml) and washed with water (3  $\times$  15 ml), brine (15 ml), dried with sodium sulfate, filtered and the solvent removed by rotary evaporation. The dark orange solid was then triturated in hot hexane and collected by filtration to give the title product as a bright orange solid (640 mg, 82 %).

**M.P:** 188 – 190 °C

$\nu_{\max}$  (KBr,  $\text{cm}^{-1}$ ): 3422, 2930, 1583, 1546, 1410, 1379, 1263, 1143, 1130, 944

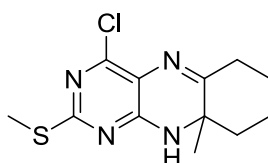
$^1\text{H}$  ( $\text{CDCl}_3$ ) 400 MHz: 1.28 – 3.12 (8H, m, 4  $\times$   $\text{CH}_2$ ), 1.38 (9H, s,  $\text{C}(\text{CH}_3)_3$ ), 1.71 (3H, s,  $\text{C}(\text{CH}_3)$ ), 2.53 (3H, s,  $\text{SCH}_3$ ), 7.23 (1H, s,  $\text{NH}$ ), 7.54 (2H, d,  $^3J = 8.8$  Hz,  $\text{C}^3\text{H}$  &  $\text{C}^5\text{H}$  on diazo coupled ring), 7.78 (2H, d,  $^3J = 8.8$  Hz,  $\text{C}^2\text{H}$  &  $\text{C}^6\text{H}$  on diazo coupled ring), 11.09 (1H, bs,  $\text{NOH}$ )

$^{13}\text{C}$  NMR ( $\text{DMSO-}d_6$ ) 100 MHz: 14.2 ( $\text{SCH}_3$ ), 20.6 ( $\text{CH}_2$ ), 21.2 ( $\text{CH}_2$ ), 23.0 ( $\text{CH}_2$ ), 25.3 ( $\text{CH}_2$ ), 30.8 ( $\text{CH}_3$ ), 30.9 ( $\text{C}(\text{CH}_3)_3$ ), 34.8 ( $\text{C}(\text{CH}_3)_3$ ), 48.6 ( $\text{CCH}_3$ ), 121.5 ( $\text{C}^1$  on diazo coupled ring), 121.9 ( $\text{C}^3\text{H}$  &  $\text{C}^5\text{H}$  on diazo coupled ring), 125.8 ( $\text{C}^5$ ), 126.4

(C<sup>2</sup>H & C<sup>6</sup>H on diazo coupled ring), 149.6 (C<sup>4</sup>), 154.2 (C<sup>4</sup> on diazo coupled ring), 158.6 (CNOH), 162.1 (C<sup>6</sup>), 171.2 (C<sup>2</sup>).

**HRMS:** C<sub>22</sub>H<sub>30</sub><sup>35</sup>ClN<sub>6</sub>OS Expected (M+H) = 461.1885, found (M+H) = 461.1881

**4-Chloro-9a-methyl-2-(methylsulfanyl)-6,7,8,9a,10-hexahydrobenzo[g]pteridine (2.21)**



**Method A**

(1*E*)-2-{[5-[(*E*)-(4-*Tert*-butylphenyl)diazenyl]-6-chloro-2-(methylsulfanyl)-4-pyrimidinyl]amino}-2-methylcyclohexanone oxime (**2.20**, 150 mg, 0.325 mmol) was placed in a 100 ml round-bottomed flask and dissolved in methanol (40 ml). The flask was then placed in an ice bath and the neck of the flask was placed under a constant stream of nitrogen. To the solution was added 10% w/w Pd/C (20 mg). The reaction flask was then hydrogenated for 8 hours using a balloon filled with hydrogen. The solution was then filtered through celite and the solvent removed by rotary evaporation to give a dark brown oil. The oil was purified by flash column chromatography (5:1 hexane: ethyl acetate) which afforded a light yellow oil (73 mg, 79 % yield). This method was only successful on one occasion and Method B was used to overcome solubility problems.

**Method B**

(1*E*)-2-{[5-[(*E*)-(4-*Tert*-butylphenyl)diazenyl]-6-chloro-2-(methylsulfanyl)-4-pyrimidinyl]amino}-2-methylcyclohexanone oxime (**2.20**, 600 mg, 1.30 mmol) was placed in a 250 ml round-bottomed flask and dissolved in methanol (180 ml). The flask was then placed in an ice bath and the neck of the flask was placed under a constant stream of nitrogen. To the solution was added 10% w/w Pd/C (80 mg). The

reaction mixture was then hydrogenated for 8 hours at 60 °C using a balloon filled with hydrogen. The solution was then filtered through celite and the solvent was removed by rotary evaporation to give a dark brown oil. The oil was purified by flash column chromatography (5:1 hexane: ethyl acetate) which afforded a light yellow oil (224 mg, 61% average yield). It was not possible to purify large quantities of the product completely and up to 50% para tertiary butyl aniline by-product was observed by NMR. An analytical sample was purified by HPLC ( $R_f = 25$  minutes) to give a light yellow solid.

The product must be stored away from light, under an atmosphere of nitrogen and used as quickly as possible.

$\nu_{\max}$  (KBr,  $\text{cm}^{-1}$ ): 3102, 3055, 2919, 1580, 1539, 1414, 1379, 1259, 957

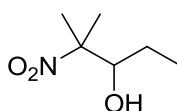
$^1\text{H}$  ( $\text{CDCl}_3$ ) 400 MHz: 1.51 (3H, s,  $\text{CCH}_3$ ), 1.61 – 2.62 (8H, m, 4x  $\text{CH}_2$ ), 2.49 (3H, s,  $\text{SCH}_3$ ), 5.08 (1H, bs,  $\text{NH}$ )

$^{13}\text{C}$  ( $\text{CDCl}_3$ ) 100 MHz: 14.5 ( $\text{SCH}_3$ ), 22.5 ( $\text{CH}_2$ ), 26.7 ( $\text{CH}_2$ ), 27.0 ( $\text{CH}_3$ ), 35.1 ( $\text{CH}_2$ ), 42.3 ( $\text{CH}_2$ ), 57.0 ( $\text{C}^8$ ), 116.7 ( $\text{C}^{4a}$ ), 153.4 ( $\text{C}^4$ ), 154.0 ( $\text{C}^{8a}$ ), 169.4 ( $\text{C}^7$ ), 170.3 ( $\text{C}^2$ )

**HRMS:**  $\text{C}_{12}\text{H}_{16}^{35}\text{ClN}_4\text{S}$  Expected (M+H) = 283.0779, found (M+H) = 283.0777

>95% purity by HPLC

### 2-Methyl-2-nitro-3-pentanol (3.10)<sup>44</sup>



2-Nitropropane (**3.12**, 16.6 g, 0.186 mol) and propanal (**3.11**, 11.70 g, 0.201 mol) were placed in a 250 ml round-bottomed flask and mixed with methanol (50 ml). To

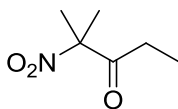
this stirring mixture, aqueous sodium hydroxide (1.0 ml, 10 M) was added and the reaction mixture was heated at 40 °C for 4 days. The solvent was then removed by rotary evaporation and the title product purified by distillation at 33 °C at  $4.9 \times 10^{-2}$  mbar to give a colourless clear oil (22.3 g, 81 %).

$\nu_{\max}$  (ATR,  $\text{cm}^{-1}$ ): 3450, 2972, 2939, 2881, 1716, 1535, 1460, 1400, 1373, 1346, 1111, 1097, 980, 856

$^1\text{H}$  ( $\text{CDCl}_3$ ) 400 MHz: 1.04 (3H, t,  $^3J = 5.8$  Hz,  $\text{CH}_3$ ), 1.28 (1H, m,  $\text{CHH}$ ), 1.51 (1H, m,  $\text{CHH}$ ) 1.52 (3H, s,  $\text{CH}_3$ ), 1.53 (3H, s,  $\text{CH}_3$ ), 2.56 (1H, bs,  $\text{OH}$ ), 3.90 (1H, dd,  $^3J = 8.4$  Hz,  $^3J = 1.6$  Hz,  $\text{CH}$ )

$^{13}\text{C}$  ( $\text{CDCl}_3$ ) 100 MHz: 11.1 ( $\text{CH}_3$ ), 20.4 ( $\text{CH}_2$ ), 23.8 ( $\text{CCH}_3$ ), 24.6 ( $\text{CCH}_3$ ), 77.7 ( $\text{CH}$ ), 92.4 ( $\text{CNO}_2$ )

### 2-Methyl-2-nitro-3-pentanone (3.9)<sup>44</sup>



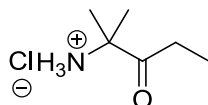
2-Methyl-2-nitro-3-pentanol (**3.10**, 9.95 g, 68.5 mmol) was stirred into acetone (10 ml). To this solution, sodium dichromate (18.37 g, 68.5 mmol) in water (10 ml) was added, along with concentrated sulfuric acid (9 ml) in water (5 ml). The reaction was stirred for 6 hours where upon the colour had changed from orange to green. The reaction mixture diluted with water and extracted with diethyl ether (100 ml) and washed with brine ( $3 \times 100$  ml). The aqueous layer was then back extracted with diethyl ether ( $2 \times 100$  ml) and the organic layers were combined, dried with sodium sulfate, filtered and the solvent removed by rotary evaporation. The crude material was then purified by vacuum distillation (44 °C at 3 mbar) or sublimation (22 °C at  $5.2 \times 10^{-2}$  mbar) to give a colourless oil which crystallised upon standing (4.35 g, 44 %).

**M.P.:** < 40 °C

$\nu_{\max}$  (ATR,  $\text{cm}^{-1}$ ): 3022, 1726, 1541, 1458, 1396, 1371, 1344, 1099

$^1\text{H}$  ( $\text{CDCl}_3$ ) 400 MHz: 1.11 (3H, t,  $^3J = 4.0$  Hz,  $\text{CH}_3$ ), 1.75 (6H, s,  $2 \times \text{CH}_3$ ), 2.52 (2H, q,  $^3J = 4.0$  Hz,  $\text{CH}_2$ )

$^{13}\text{C}$  ( $\text{CDCl}_3$ ) 100 MHz: 8.1 ( $\text{CH}_3$ ), 23.5 ( $2 \times \text{CH}_3$ ), 29.8 ( $\text{CH}_2$ ), 94.3 ( $\text{C}(\text{CH}_3)_2$ ), 202.9 (CO)

**2-Amino-2-methyl-3-pentanone hydrochloride (2.5)**<sup>44</sup>

2-(Benzoylamino)-2-methyl-3-pentanone (**3.13**, 1.38 g, 6.71 mmol) was dissolved in methanol (20 ml) and concentrated hydrochloric acid (50 ml) was added. The solution was heated at reflux for 15 hours and then allowed to cool. The methanol was evaporated using rotary evaporation and the aqueous layer was washed with ethyl acetate (3 × 30 ml). The aqueous layer was then lyophilised to give a clear oil which solidified upon trituration in diethyl ether to give the title product as a hygroscopic solid (768 mg, 81 %).

**M.P:** 138 – 140 °C; **lit** = 145 – 147 °C<sup>195</sup>

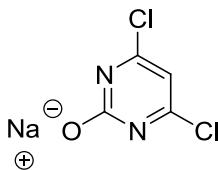
**v<sub>max</sub>** (ATR, cm<sup>-1</sup>): 3024, 1628, 1130, 827

**<sup>1</sup>H** (DMSO-*d*<sub>6</sub>) 400 MHz: 0.95 (3H, t, <sup>3</sup>*J* = 7.1 Hz, CH<sub>3</sub>), 1.46 (6H, s, 2 × CH<sub>3</sub>), 2.68 (2H, q, <sup>3</sup>*J* = 7.1 Hz, CH<sub>2</sub>), 8.57 (3H, bs, +NH<sub>3</sub>)

**<sup>13</sup>C** (DMSO-*d*<sub>6</sub>) 100 MHz: 7.5 (CH<sub>3</sub>), 22.4 (2 × CH<sub>3</sub>), 28.6 (CH<sub>2</sub>), 60.9 (C(CH<sub>3</sub>)<sub>2</sub>), 209.1 (CO)

**LRMS:** C<sub>6</sub>H<sub>14</sub>NO: Expected (M) = 116; Found (M) = 116



**Sodium salt of 4,6-dichloro-2-pyrimidinolate (3.14)**<sup>203</sup>

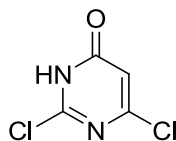
2,4,6-Trichloropyrimidine (**3.8**, 5 g, 27.3 mmol) was added to a stirring solution of 1,4-dioxane (90 ml) and left to stir for 10 minutes. Aqueous sodium hydroxide (2.6 g in 20 ml of water) was added to the solution, which was stirred for 4 hours, where upon white needles had precipitated out of solution. The majority of solvent was then evaporated under reduced pressure to leave a thick white paste, which was then dissolved in hot water and slowly allowed to cool to 0 °C to give colourless needles. The product was collected by filtration and dried at 40 °C under reduced pressure (2.52 g, 49 %).

**M.P:** 179-180 °C; **lit** = > 200 °C,<sup>195</sup> Lit M.P = 180 °C<sup>203</sup>

$\nu_{\max}$  (KBr,  $\text{cm}^{-1}$ ): 3632, 3471, 3235, 3122, 1644, 1592, 1511, 1496, 1238, 1082, 1019, 821, 797, 767

<sup>1</sup>H (DMSO-*d*<sub>6</sub>) 500 MHz: 6.05 (s, 1H, C<sup>5</sup>H)

<sup>13</sup>C (DMSO-*d*<sub>6</sub>) 125 MHz: 99.9 (C<sup>5</sup>), 159.5 (C<sup>4</sup>/C<sup>6</sup>), 165.0 (C<sup>2</sup>).

**2,6-Dichloro-4(3H)-pyrimidinone (3.7)**<sup>203</sup>

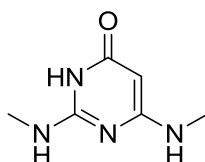
The filtrate of the preceding reaction was cooled to 0 °C with stirring, the pH was then adjusted to 2 by slow addition of 2 M hydrochloric acid. The solution was then allowed to stir for 1 hour at this temperature, during which time the product precipitated out of solution. The product was collected by filtration and recrystallised from water to give the title product as a colourless powder (2.23 g, 49 %).

**M.P:** decomposed at 174°C; **lit** = 173 – 174 °C<sup>195</sup>

$\nu_{\max}$  (KBr,  $\text{cm}^{-1}$ ): 3439, 3095, 3022, 2914, 2807, 1729, 1654, 1598, 1492, 1438, 1412, 1129, 1030, 1000, 840, 545

$^1\text{H}$  (DMSO- $d_6$ ) 500 MHz: 5.74 (1H, s,  $\text{C}^5\text{H}$ ), 12.04 (1H, bs, amide NH)

$^{13}\text{C}$  (DMSO- $d_6$ ) 125 MHz: 99.9 ( $\text{C}^5$ ), 144.7 ( $\text{C}^2$ ), 150.3 ( $\text{C}^6$ ), 162.6 ( $\text{C}^4$ )

**2,6-Bis(methylamino)-4(3H)-pyrimidinone (3.15)**

2,6-Dichloro-4(3H)-pyrimidinone (**3.7**, 500 mg, 3.03 mmol) in ethanol (3 ml) was placed in a sealed tube and cooled in an ice bath to 0 °C. Methylamine in THF (2M,

7.6 ml, 15.2 mmol) was added with stirring followed by triethylamine (422  $\mu$ l, 3.03 mmol). The tube was then sealed and heated to 70 °C for 16 hours. The solvent was then evaporated under reduced pressure and the solid residue was triturated in a small amount of water. The product was collected by filtration and washed with cold diethyl ether (5 ml). The solid was dried under reduced pressure at 40 °C to give the title product as a light yellow solid (413 mg, 88 %).

**M.P:** > 230°C

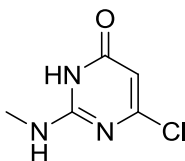
**$\nu_{\max}$**  (KBr,  $\text{cm}^{-1}$ ): 3423, 3096, 2970, 2924, 2818, 1716, 1687, 1497, 1446, 1428

**$^1\text{H}$**  (DMSO- $d_6$ ) 400 MHz: 2.61 (3H, d,  $^3J = 4.8$  Hz,  $\text{C}^2\text{NHCH}_3$ ), 2.71 (3H, d,  $^3J = 4.0$  Hz,  $\text{C}^6\text{NHCH}_3$ ), 4.36 (1H, s,  $\text{C}^5\text{H}$ ), 6.29 (1H, bs,  $\text{C}^2\text{NH}$ ), 6.74 (1H, bs,  $\text{C}^6\text{NH}$ ), 10.38 (1H, bs, amide NH)

**$^{13}\text{C}$**  (DMSO- $d_6$ ) 100 MHz: 27.1 ( $\text{C}^2\text{NHCH}_3$ ), 27.9 ( $\text{C}^6\text{NHCH}_3$ ), 74.4 ( $\text{C}^5$ ), 154.7 ( $\text{C}^2$ ), 163.8 ( $\text{C}^6$ ), 164.5 ( $\text{C}^4$ )

**LRMS:**  $\text{C}_6\text{H}_{11}\text{N}_4\text{O}$  Expected (M+H) 155; found (M+H) 155 (100%)

**HRMS:**  $\text{C}_6\text{H}_{11}\text{N}_4\text{O}$  Expected (M+H) 155.0927; found (M+H) 155.0927.

**2-(Methylamino)-6-chloro-4(3H)-pyrimidinone (3.6)**<sup>247</sup>

2,6-Dichloro-4(3H)-pyrimidinone (**3.7**, 500 mg, 3.03 mmol) was placed in a sealed tube and dissolved using methanol (3 ml). The vessel was then cooled to 0 °C in an ice bath and methylamine in THF (2 M, 3 ml, 6.00 mmol) was added along with triethylamine (421  $\mu$ l, 3.03 mmol). The tube was then sealed and heated at 65 °C for 16 hours. The reaction was then allowed to cool to room temperature, whereupon a white precipitate formed. The solvent was evaporated under reduced pressure and the solid was triturated in water (3 ml). The solid was then collected by filtration and dried at 40 °C under reduced pressure to give the title product as a colourless powder (436 mg, 83 %).

**M.P:** decomposed at 158 °C, Lit = 265 °C<sup>247</sup> It is suspected that due to the amorphous nature of this particular batch that a different melting point was obtained when compared to the crystalline material.

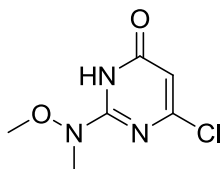
$\nu_{\max}$  (KBr,  $\text{cm}^{-1}$ ): 3436, 3137, 2959, 1672, 1633, 1537, 1474, 1390, 1335, 1150, 1042, 991

$^1\text{H}$  (DMSO- $d_6$ ) 400 MHz: 2.76 (3H, d,  $^3J = 4.8$  NHCH<sub>3</sub>), 5.60 (1H, s, C<sup>5</sup>H), 6.84 (1H, bs, CH<sub>3</sub>NH), 11.14 (1H, bs, amide NH)

$^{13}\text{C}$  (DMSO- $d_6$ ) 100 MHz: 27.5 (NHCH<sub>3</sub>), 99.4 (C<sup>5</sup>), 154.5 (C<sup>6</sup>), 159.2 (C<sup>2</sup>), 162.4 (C<sup>4</sup>)

**LRMS:** C<sub>5</sub>H<sub>7</sub>ClN<sub>3</sub>O Expected (M+H) 160 (100%), 162 (30%); found 160 (100 %) 162 (30 %)

**HRMS:** C<sub>5</sub>H<sub>7</sub><sup>35</sup>ClN<sub>3</sub>O Expected (M+H) 160.0272, found (M+H) 160.0274

**6-Chloro-2-(*N*-methoxy-*N*-methylamino)-4(3*H*)-pyrimidinone (3.19)**<sup>195</sup>

2,6-Dichloro-4(3*H*)-pyrimidinone (**3.7**, 500 mg, 3.03 mmol) was placed in a sealable tube along with *N,O*-dimethylhydroxylamine hydrochloride (569 mg, 6.06 mmol) which was then dissolved in ethanol (10 ml). The solution was then cooled to 0 °C and triethylamine (1.92 ml, 9.09 mmol) was added with stirring. The tube was then sealed and heated (*ca.* 80 °C) for 22 hours. The reaction vessel was then allowed to cool to room temperature, whereupon colourless needles precipitated out of solution. This solid was collected by filtration. The solvent was then removed under reduced pressure and the remaining solid was triturated with water (5 ml). The solid was then collected by filtration, washed with diethyl ether (5ml), combined with the other solid and dried at 40 °C under reduced pressure to give the title product as colourless needles (525 mg, 92 %).

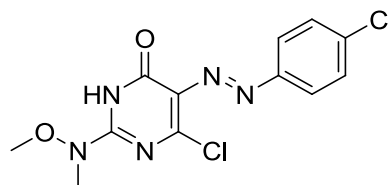
**M.P:** 192 – 194 °C, **Lit:** 193 – 194 °C<sup>195</sup>

$\nu_{\max}$  (KBr,  $\text{cm}^{-1}$ ): 3437, 2942, 1676, 1607, 1556, 1504, 1359, 1220, 1111, 978, 960

<sup>1</sup>H (DMSO-*d*<sub>6</sub>) 400 MHz: 3.22 (3H, s, NCH<sub>3</sub>), 3.67 (3H, s, OCH<sub>3</sub>), 5.80 (1H, s, C<sup>5</sup>H), 11.96 (1H, bs, amide NH)

<sup>13</sup>C (DMSO-*d*<sub>6</sub>) 100 MHz: 35.3 (NCH<sub>3</sub>), 61.5 (OCH<sub>3</sub>), 101.4 (C<sup>5</sup>), 155.8 (broad C<sup>6</sup>), 158.2 (C<sup>2</sup>), 162.4 (broad C<sup>4</sup>)

**6-Chloro-5-[(E)-(4-chlorophenyl)diazenyl]-2-[methoxy(methyl)amino]-4(3H)-pyrimidinone (3.20)**<sup>195</sup>



*Preparation of the diazonium salt*

*p*-Chloroaniline (470 mg, 3.68 mmol) was dissolved in 1 M hydrochloric acid (5 ml) and cooled to -5 °C. Sodium nitrite (260 mg, 3.77 mmol) in water (1 ml) was added drop-wise with stirring, ensuring that the internal temperature did not rise above 0 °C at any point. When all the sodium nitrite had been added, the mixture was stirred for 15 minutes below 0 °C.

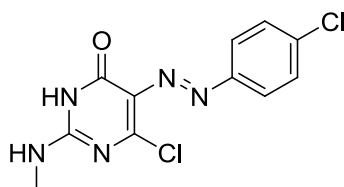
*Coupling of the diazonium salt*

In another flask, 6-chloro-2-(*N*-methoxy-*N*-methylamino)-4(3*H*)-pyrimidinone (**3.19**, 580 mg, 3.06 mmol) was dissolved in 0.5 M aq. sodium hydroxide (10 ml) at room temperature and the solution was then cooled to -5 °C. To this solution, the above diazonium salt solution was added very slowly, taking great care to keep the salt below 0 °C and the reaction mixture below 2 °C. Once the addition of the diazonium salt had been completed, the reaction mixture was stirred for 2 hours maintaining a temperature of 0 °C and then gradually allowed to warm to room temperature. The mixture was then stirred for 24 hours. The resulting precipitate was then filtered off and washed with cold water (2 × 10 ml). The solid was then boiled in ethanol/water (1:1) (20 ml) for 5 minutes and then allowed to cool to room temperature, where upon the resulting solid was collected by filtration and dried under reduced pressure to give 730 mg of the title compound as a dark orange/ brown solid (73% yield). The product was found to be unstable when stored at room temperature for a period of 7 days or more or in the presence of diethyl ether. This gave **3.21** and then further degraded which could not be analyzed further.

$^1\text{H}$  (DMSO- $d_6$ ) 400 MHz: 3.40 (3H, s,  $\text{NCH}_3$ ), 3.74 (3H, s,  $\text{OCH}_3$ ), 7.58 (2H, d,  $^3J = 8.7$  Hz,  $\text{C}^2\text{H}$  &  $\text{C}^6\text{H}$  on diazo coupled ring), 7.72 (2H, d,  $^3J = 8.7$  Hz,  $\text{C}^3\text{H}$  &  $\text{C}^5\text{H}$  on diazo coupled ring), 12.66 (bs, 1H, amide  $\text{NH}$ )

$^{13}\text{C}$  (DMSO- $d_6$ ) 100 MHz: 34.4 ( $\text{NCH}_3$ ), 62.0 ( $\text{OCH}_3$ ), 118.2 ( $\text{C}^5$ ), 127.7 ( $\text{C}^3$  &  $\text{C}^5$  on diazo coupled ring), 129.6 ( $\text{C}^2$  &  $\text{C}^6$  on diazo coupled ring), 132.7 ( $\text{C}^4$  on diazo coupled ring), 140.5 ( $\text{C}^1$  on diazo coupled ring), 155.5 ( $\text{C}^2$ ), 159.1 ( $\text{C}^4$ ) (the  $\text{C}^6$  signal could not be seen despite an increase in quantity, scan number and delay time.)

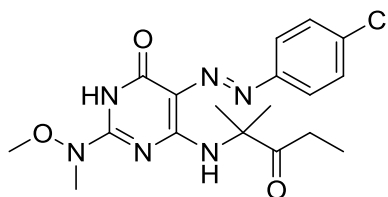
**6-Chloro-5-[(E)-(4-chlorophenyl)diazenyl]-2-(methylamino)-4(3H)-pyrimidinone (3.21)**



Traces of the above compound were observed by NMR when compound **3.20** degraded.

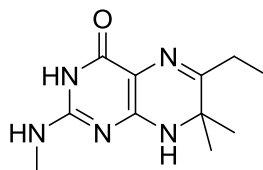
$^1\text{H}$  (DMSO- $d_6$ ) 400 MHz: 2.80 (3H, d  $^3J = 4.8$  Hz,  $\text{NHCH}_3$ ), 7.28 (2H, d,  $^3J = 8.5$  Hz,  $\text{C}^2\text{H}$  &  $\text{C}^2'\text{H}$  on diazo coupled ring), 7.40 (2H, d  $^3J = 8.5$  Hz,  $\text{C}^3\text{H}$  &  $\text{C}^3'\text{H}$  on diazo coupled ring).

**5-(4-Chlorophenyldiazenyl)-6-(2-methyl-3-oxopent-2-ylamino)-2-(N-methoxy-N-methylamino)-4(3H)-pyrimidinone (3.22)**



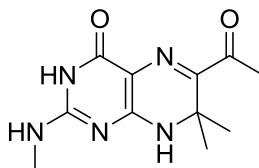
6-Chloro-5-(4-chlorophenyldiazenyl)-2-(*N*-methoxy-*N*-methylamino)-4(3*H*)-pyrimidinone (**3.21**, 250 mg, 0.76 mmol) was suspended in *N,N*-dimethylformamide (5 ml) in a suitable microwave vial. To this solution 2-amino-2-methyl-3-pentanone hydrochloride **2.5** (116 mg, 0.76 mmol) was added with stirring along with freshly distilled triethylamine (212  $\mu$ l, 1.53 mmol). The tube was then sealed and irradiated in the microwave for 1 hour at 100 °C. The solvent was then evaporated under high vacuum rotary evaporation at 60 °C. The product proved to be unstable and was taken straight through to the next step of the reaction sequence without further purification (crude yield 410 mg, 137%).



**6-Ethyl-7,7-dimethyl-2-(methylamino)-7,8-dihydro-4(3H)-pteridinone (3.3)**

The crude 5-(4-chlorophenyldiazenyl)-6-(2-methyl-3-oxopent-2-ylamino)-2-(*N*-methoxy-*N*-methylamino)-4(3*H*)-pyrimidinone (**3.22**) from the previous reaction (crude 410 mg) was dissolved in methanol and the solution was cooled to 0 °C. Palladium on charcoal (10% w/w, 200 mg) was then added to the solution with stirring. The reaction mixture was then hydrogenated using a balloon filled with hydrogen at room temperature for 6 hours. The resulting solution was then filtered through kieselguhr and the solvent was removed by rotary evaporation to give a sticky brown oil. The oil was triturated in diethyl ether (10 ml) to give a dark brown solid which was collected by filtration. The resulting product was taken up in *N,N*-dimethylformamide (1 ml) together with 5 drops of trifluoroacetic acid then purified by HPLC. The product was found to be unstable when left in solution for any time period above 1 day so no analysis other than LRMS could be obtained. The title compound **3.3** oxidised to 6-acetyl-7,7-dimethyl-2-(methylamino)-7,8-dihydro-4(3*H*)-pteridinone (**3.2**) over this period.

**LRMS:** Expected  $C_{11}H_{18}N_5O$  (M+H) = 236, found (M+H) 236

**6-Acetyl-7,7-dimethyl-2-(methylamino)-7,8-dihydro-4(3H)-pteridinone (3.2)**

6-Ethyl-7,7-dimethyl-2-(methylamino)-7,8-dihydro-4(3H)-pteridinone (**3.3**) from the previous reaction was left in DMF, with 5 drops of trifluoroacetic acid, for a period of 3 days and monitored by HPLC. Upon complete conversion to the title product the mixture was purified by HPLC and the fractions were lyophilised to give the title product as a light yellow solid (24 mg, 13 % over 3 steps).

$\nu_{\max}$  (KBr,  $\text{cm}^{-1}$ ): 3430, 2923, 1632, 1567, 1424, 1379, 1354, 1293, 1183

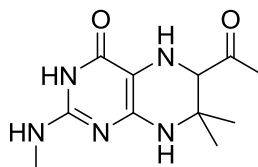
$^1\text{H}$  ( $\text{CD}_3\text{OD}$ ) 500 MHz: 1.52 (6H, s, 2 x  $\text{CH}_3$ ), 2.42 (3H, s,  $\text{C}(\text{O})\text{CH}_3$ ), 2.90 (3H, s,  $\text{NHCH}_3$ ).

$^{13}\text{C}$  ( $\text{CD}_3\text{OD}$ ) 125 MHz: 26.6 ( $\text{NHCH}_3$ ), 28.2 ( $\text{C}(\text{O})\text{CH}_3$ ), 28.7 (2 x  $\text{CH}_3$ ), 55.6 ( $\text{C}^7$ ), 103.45 ( $\text{C}^{4a}$ ), 149.41 ( $\text{C}^{8a}$ ), 156.15 ( $\text{C}^2$ ), 156.55 ( $\text{C}^6$ ), 161.83 ( $\text{C}^4$ ), 200.33 ( $\text{CO}$ )

**HRMS:**  $\text{C}_{11}\text{H}_{16}\text{N}_5\text{O}_2$  Expected (M+H) = 250.1299, found (M+H) = 250.1297

>95% purity by HPLC

**6-Acetyl-7,7-dimethyl-2-(methylamino)-5,6,7,8-tetrahydro-4(3H)-pteridinone**  
**(3.1)**

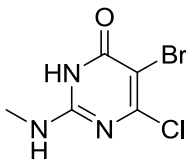


6-Acetyl-7,7-dimethyl-2-(methylamino)-7,8-dihydro-4(3H)-pteridinone (**3.2**, 32 mg, 0.13 mmol) was placed in a round bottomed flask and dissolved in anhydrous methanol (10 ml) under an atmosphere of nitrogen. Sodium cyanoborohydride (24 mg, 0.38 mmol) was then added with vigorous stirring. To this mixture, 3 drops of glacial acetic acid was then added, before the flask was wrapped in aluminium foil. The mixture was stirred for 15 hours. The reaction was quenched with concentrated hydrochloric acid (1 ml) and the solvent was removed under reduced pressure. The solid was purified by HPLC and combined fractions were stored on dry ice before being lyophilised. This gave the title product as a colourless solid (TFA salt) (21 mg, 65 % yield).

The product must be stored under nitrogen and away from light and used as soon as possible.

The material was not stable enough for fuller analysis.

**LRMS:**  $C_{11}H_{18}N_5O_2$  Expected (M+H) 252; Found (M+H) 252

**5-Bromo-6-chloro-2-(methylamino)-4(3H)-pyrimidinone (3.25)**

2-(Methylamino)-6-chloro-4(3H)-pyrimidinone (**3.6**, 500 mg, 2.10 mmol) was dissolved in glacial acetic acid (20 ml) and bromine (112  $\mu$ l, 2.20 mmol) was added drop-wise at room temperature. The solution was allowed to stir for 15 hours. The precipitate was collected by filtration and washed with water and diethyl ether then dried overnight at 40 °C under reduced pressure to give the title compound as a lightly yellow coloured solid (260 mg, 52%).

**M.P:** formed needles at 180 °C, melts > 230 °C

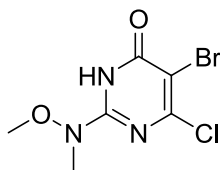
$\nu_{\max}$  (KBr,  $\text{cm}^{-1}$ ): 3420, 3272, 2945, 2646, 1679, 1662, 1621, 1557, 1298

$^1\text{H}$  (DMSO- $d_6$ ) 500 MHz: 2.75 (3H, d,  $^3J = 1.5$  Hz,  $\text{CH}_3\text{NH}$ ), 6.91 (1H, bs,  $\text{NHCH}_3$ ), 11.65 (1H, bs, amide  $\text{NH}$ )

$^{13}\text{C}$  (DMSO- $d_6$ ) 125 MHz: 27.7 ( $\text{CH}_3\text{N}$ ), 95.3 ( $\text{C}^5$ ), 152.9 ( $\text{C}^2$ ), 157.7 ( $\text{C}^6$ ), 158.7 ( $\text{C}^4$ )

**LRMS:** The equipment used will not allow for traces of DMSO to be used when dissolving the compound. As a result, only the HRMS was obtained, as small quantities of DMSO can be used with this equipment.

**LC-HRMS:**  $\text{C}_5\text{H}_6^{79}\text{Br}^{35}\text{ClN}_3\text{O}$  Expected (M+H) 237.9376; found (M+H) 237.9377.  
89.6% purity by LC

**5-Bromo-6-chloro-2-(*N*-methoxy-*N*-methylamino)-4(3*H*)-pyrimidinone (3.26)**

6-Chloro-2-(*N*-methoxy-*N*-methylamino)-4(3*H*)-pyrimidinone (**3.19**, 500 mg, 2.64 mmol) was dissolved in glacial acetic acid (20 ml) and bromine (143  $\mu$ l, 2.77 mmol) was added drop-wise at room temperature. The solution was allowed to stir for 15 hours. The precipitate was collected by filtration and washed with water (10 ml) and diethyl ether (10 ml) then dried over night at 40 °C under reduced pressure to give the title compound as a lightly yellow coloured solid (496 mg, 70%).

**M.P:** > 230 °C

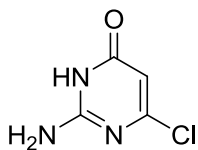
$\nu_{\max}$  (KBr,  $\text{cm}^{-1}$ ): 3466, 3094, 3006, 2955, 1663, 1611, 1539, 1315, 1222, 1016

$^1\text{H}$  (DMSO- $d_6$ ) 500 MHz: 3.22 (3H, s,  $\text{CH}_3\text{N}$ ), 3.67 (3H, s,  $\text{CH}_3\text{O}$ ), 12.41 (1H, bs, amide NH)

$^{13}\text{C}$  (DMSO- $d_6$ ) 125 MHz: 35.3 ( $\text{CH}_3\text{N}$ ), 61.6 ( $\text{CH}_3\text{O}$ ) 97.5 ( $\text{C}^5$ ), 153.9 ( $\text{C}^2$ ), 156.8 ( $\text{C}^6$ ), 158.9 ( $\text{C}^4$ )

**LC-HRMS:**  $\text{C}_6\text{H}_8^{79}\text{Br}^{35}\text{ClN}_3\text{O}_2$  Expected (M+H) 267.9481; found (M+H) 267.9483. >99% purity by LC.

X-Ray data available in appendix section.

**2-Amino-6-chloro-4(3H)-pyrimidinone (4.7)**<sup>196</sup>

4,6-Dichloro-2-pyrimidinamine (**4.6**, 10 g, 61.0 mmol) was suspended in aqueous sodium hydroxide solution (150 ml, 1 M) and heated at reflux with stirring for 2 hours. The reaction was then cooled to room temperature and the pH adjusted to 4 using glacial acetic acid and the mixture was left to cool in the fridge for 2 hours. The product was then collected by filtration, washed with cold water (30 ml) and cold diethyl ether (30 ml) and was dried in a vacuum oven at 40 °C for 2 days to give the title compound as a white solid (8.32 g, 94%).

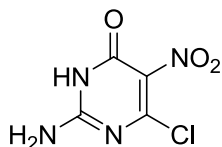
**M.P:** > 230°C; **lit** = 260 – 261 °C<sup>196</sup>

$\nu_{\max}$  (KBr,  $\text{cm}^{-1}$ ): 3114, 2924, 2774, 1659, 1561, 1488, 1376, 1231, 1162, 986, 796

$^1\text{H}$  (DMSO- $d_6$ ) 500 MHz: 5.52 (1H, s,  $\text{C}^5\text{H}$ ), 7.34 (2H, bs,  $\text{NH}_2$ ), 11.90 (1H, bs,  $\text{NH}$ )

$^{13}\text{C}$  (DMSO- $d_6$ ) 125 MHz: 99.0 ( $\text{C}^5$ ), 156.7 ( $\text{C}^6$ ), 159.2 ( $\text{C}^2$ ), 164.0 ( $\text{C}^4$ )

**LC-HRMS:**  $\text{C}_4\text{H}_5^{35}\text{ClN}_3\text{O}$  Expected (M+H) 146.0115; found (M+H) 146.0116.  
89.1% purity by LC.

**2-Amino-6-chloro-5-nitro-4(3H)-pyrimidinone (4.8)**<sup>40,195</sup>

2-Amino-6-chloro-4(3H)-pyrimidinone **4.7** (5.4 g, 34.4 mmol) was dissolved in concentrated sulfuric acid (10 ml) with slight heating and stirring. The solution was then treated drop-wise with red fuming nitric acid (10 ml), ensuring the temperature of the reaction did not rise above *ca.* 5 °C. The resulting solution was stirred for 2 hours at room temperature after which the solution was poured onto crushed ice (30 g), and filtered. The solid obtained was washed with cold water (30 ml), cold ethanol (30 ml), and cold diethyl ether (30 ml), then dried under reduced pressure overnight to give the title compound as a yellow solid (5.9 g, 84 %). The material was used without further purification, stored in a dark cupboard and used within a month of preparation.

**M.P:** > 230°C; **lit** = > 320 °C<sup>195</sup>

$\nu_{\max}$  (KBr,  $\text{cm}^{-1}$ ): 3408, 3314, 3188, 1689, 1561, 1450, 1374, 1279, 1128, 1063

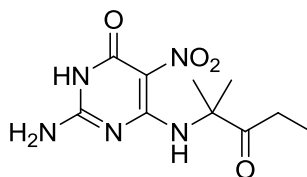
$^{13}\text{C}$  (DMSO- $d_6$ ) 125 MHz: 126.7 ( $C^5$ ), 153.2 ( $C^6$ ), 154.2 ( $C^2$ ), 155.0 ( $C^4$ )

**LRMS:**  $C_4H_4ClN_4O_3$  Expected (M) 190; found (M) 190

66.3% purity by LC.

**2-Amino-6-[(1,1-dimethyl-2-oxobutyl)amino]-5-nitro-4(3H)-pyrimidinone (3.23)**

40,195



2-Amino-5-nitro-6-chloro-4(3H)-pyrimidinone (**4.8**, 765 mg, 4.02 mmol) and 2-amino-2-methyl-3-pentanone hydrochloride (**2.5**, 406 mg, 4.02 mmol) were suspended in freshly distilled ethanol (25 ml). Triethylamine (1.12 ml, 8.04 mmol) was then added, with stirring, whilst under an atmosphere of nitrogen. The suspension was heated at reflux for 22 hours, then allowed to cool and refrigerated for 2 hours to allow the product to precipitate out of solution. The product was collected by filtration, washed with cold water ( $2 \times 10$  ml) and then dried at 40 °C under reduced pressure overnight to give the title product as a yellow solid (269 mg, 22% yield).

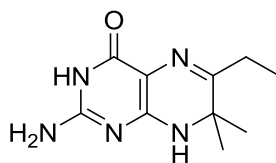
**M.P:** > 230°C; **lit** = > 320 °C<sup>40</sup>

$\nu_{\max}$  (ATR,  $\text{cm}^{-1}$ ): 1682, 1653, 1558, 1516, 1435, 1327, 1276, 1232, 1155, 1045, 781

<sup>1</sup>H (DMSO-*d*<sub>6</sub>) 400 MHz: 0.92 (3H, t, <sup>3</sup>J = 8.0 Hz, CH<sub>3</sub>), 1.48 (6H, s, 2 × CH<sub>3</sub>), 2.56 (2H, q, <sup>3</sup>J = 8.0 Hz, CH<sub>2</sub>), 6.92 (1H, bs, NH), 7.76 (2H, bs, NH<sub>2</sub>), 10.99 (1H, bs, amide NH)

<sup>13</sup>C (DMSO-*d*<sub>6</sub>) 100 MHz: 8.3 (CH<sub>3</sub>), 24.5 (CH<sub>2</sub>), 28.3 (2 × CH<sub>3</sub>), 61.7 (C(CH<sub>3</sub>)<sub>2</sub>), 110.6 (C<sup>5</sup>), 153.6 (C<sup>6</sup>), 156.2 (C<sup>2</sup>), 158.2 (C<sup>4</sup>) 210.3 (CO)



**2-Amino-6-ethyl-7,7-dimethyl-7,8-dihydro-4(3H)-pteridinone (3.24)**<sup>40,195</sup>**Method A**

2-Amino-6-(2-methyl-3-oxopentan-2-ylamino)-5-nitro-4(3H)-pyrimidinone (**3.23**, 256 mg, 0.95 mmol) was dissolved in aq. sodium hydroxide solution (2 M, 5 ml) with stirring and some heating (*ca.* 60 °C) in a 50 ml round-bottomed flask. Once the material was fully dissolved, the solution was allowed to cool to room temperature. Sodium dithionite (1.65 g, 9.50 mmol) was then added portion-wise to the mixture and the solution changed colour through a dark amber colour, to dark red and then to a pale yellow. Upon the final colour change, one more portion of sodium dithionite (*ca.* 100 mg) was added. The pH was then adjusted to 8 using glacial acetic acid and the mixture was left to stand for 2 hours at room temperature. The product was collected by filtration, dissolved in hot aqueous sodium hydroxide (0.5 M) and then recrystallised by adjusting the pH to 4 with acetic acid:water (1:1) and allowing the solution to cool to give the title product as a colourless solid (69 mg, 33 % yield).

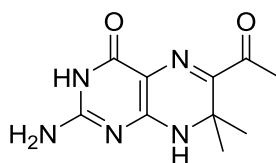
**Method B**

2-Amino-6-(2-methyl-3-oxopentan-2-ylamino)-5-nitro-4(3H)-pyrimidinone (**3.23**, 112 mg, 0.42 mmol) was dissolved in methanol (20 ml) in a 50 ml round-bottomed flask and cooled in an ice bath. Under a steady stream of nitrogen, 10 % w/w Pd/C (60 mg) was added to the stirring solution. The reaction was then hydrogenated for 4 hours using a balloon. The mixture was then filtered through celite and the solvent removed by rotary evaporation to give a clear oil which was triturated in ether to give the title compound as a colourless solid. This compound was immediately dissolved in DMF (2 ml) with 3 drops of TFA for use in the oxidation study.

**M.P.:** > 230 °C; **lit** = 280-284 °C<sup>40</sup>

$^1\text{H}$  (DMSO- $d_6$ ) 400 MHz: 1.04 (3H, t,  $^3J = 8.0$  Hz,  $\text{CH}_3$ ), 1.18 (6H, s,  $2 \times \text{CH}_3$ ), 2.23 (2H, q,  $^3J = 8.0$  Hz,  $\text{CH}_2$ ), 6.24 (2H, bs,  $\text{NH}_2$ ), 6.73 (1H, bs,  $\text{NH}$ ), 10.06 (1H, bs,  $\text{NH}$ )  
 $^{13}\text{C}$  (DMSO- $d_6$ ) 125 MHz: 11.3 ( $\text{CH}_2\text{CH}_3$ ), 25.8 ( $\text{CH}_2\text{CH}_3$ ), 26.0 ( $2 \times \text{CH}_3$ ), 53.4 ( $\text{C}^7$ ), 102.3 ( $\text{C}^{4a}$ ), 154.0 ( $\text{C}^{8a}$ ), 154.6 ( $\text{C}^2$ ), 156.6 ( $\text{C}^4$ ), 158.5 ( $\text{C}^6$ ),

**6-Acetyl-2-amino-7,7-dimethyl-7,8-dihydro-4(3H)-pteridinone (1.6)**<sup>40,195</sup>



**Method A**

2-Amino-6-ethyl-7,7-dimethyl-7,8-dihydro-4(3H)-pteridinone (**3.24**, 63 mg, 0.25 mmol) was placed in a round-bottomed flask and completely wrapped in aluminium foil and, through a small hole in the foil, a fresh mixture of butan-1-ol (5 ml), glacial acetic acid (2 ml) and water (3 ml) was slowly added. Once the material had dissolved, the foil surrounding the lid of the flask was removed to ensure free flow of oxygen throughout. The mixture was stirred for 16 hours at 60 °C in an atmosphere of air. The solvent was then evaporated and the remaining material was triturated in ether (5 ml). The product was collected by filtration and reprecipitated from 0.5 M aqueous sodium hydroxide by the slow addition of acetic acid:water (1:1) to give the title product as a bright yellow solid (32 mg, 55 %).

**Method B**

2-Amino-6-ethyl-7,7-dimethyl-7,8-dihydro-4(3H)-pteridinone (**3.24**) from method B in the previous reaction was dissolved in DMF (2 ml) with 3 drops of TFA. The flask was wrapped in aluminium foil but left open to an atmosphere of air. The reaction was monitored by HPLC for the appearance of another peak corresponding to a bright yellow solution. 25% conversion was observed after the first day.

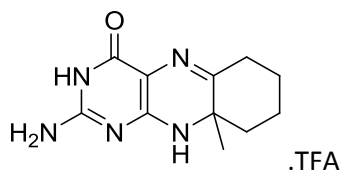
**M.P:** > 230°C; **Lit** = > 320 °C<sup>40</sup>

$\nu_{\max}$  (KBr,  $\text{cm}^{-1}$ ): 3444, 3228, 2886, 2742, 1655, 1574, 1536, 1456, 1354, 1292, 1181.

$^1\text{H}$  (DMSO- $d_6$ ) 500 MHz: 1.41 (6H, s,  $2 \times \text{CH}_3$ ), 2.26 (3H, s,  $\text{CH}_3\text{CO}$ ), 6.67 (2H, bs,  $\text{NH}_2$ ), 7.49 (1H, bs,  $\text{NH}$ ), 10.15 (bs, 1H, amide  $\text{NH}$ )

$^{13}\text{C}$  (DMSO- $d_6$ ) 125 MHz: 25.8 ( $\text{C}(\text{O})\text{CH}_3$ ), 27.7 ( $2 \times \text{CH}_3$ ), 53.3 ( $\text{C}^7$ ), 102.0 ( $\text{C}^{4a}$ ), 145.7 ( $\text{C}^{8a}$ ), 155.0 ( $\text{C}^2$ ), 155.5 ( $\text{C}^6$ ), 157.9 ( $\text{C}^4$ ), 197.0 ( $\text{CO}$ )

**2-Amino-9a-methyl-6,7,8,9,9a,10-hexahydrobenzo[g]pteridin-4(3H)-one TFA salt (4.1)**<sup>40</sup>



2-Amino-6-chloro-5-nitro-4(3H)-pyrimidinone (**4.8**, 500 mg, 2.62 mmol) was suspended in anhydrous ethanol (30 ml). To this suspension, 2-amino-2-methylcyclohexanone oxime hydrochloride **2.18** (565 mg, 3.45 mmol) was added along with anhydrous triethylamine (878  $\mu\text{l}$ , 6.29 mmol) under an atmosphere of nitrogen and the suspension was heated to reflux for 24 hours. The reaction vessel was then cooled in an ice bath and the open neck of the flask was placed under a constant stream of nitrogen. To the solution, Pd/C (10% w/w, 250 mg) was added. The reaction flask was then hydrogenated for 4 hours using a balloon filled with hydrogen. The solution was filtered through celite and the solvent was removed by rotary evaporation to give a dark red oil. The material was purified by HPLC ( $R_t = 5$  min) to give the title product as a light yellow solid (51 mg, 6%).

**M.P:** > 230 °C; **Lit** = > 320 °C<sup>40</sup>

$\nu_{\max}$  (KBr,  $\text{cm}^{-1}$ ): 3434, 1639, 1574, 1202, 1139, 576

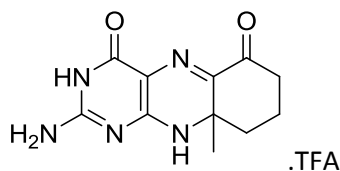
$^1\text{H}$  (CD<sub>3</sub>OD) 500 MHz: 1.59 (3H, s, CH<sub>3</sub>), 1.60 – 2.20 (6H, m, 3 X CH<sub>2</sub>), 2.78 – 2.95 (2H, m, CH<sub>2</sub>)

$^{13}\text{C}$  (CD<sub>3</sub>OD) 125 MHz: 22.4 (CH<sub>2</sub>), 25.1 (CH<sub>3</sub>), 26.3 (CH<sub>2</sub>), 26.4 (CH<sub>2</sub>), 41.7 (CH<sub>2</sub>), 57.7 (CCH<sub>3</sub>) 94.7 (C<sup>4a</sup>), 157.1 (C<sup>8a</sup>), 157.2 (C<sup>2</sup>), 157.5 (C<sup>4</sup>), 167.8 (C<sup>6</sup>)

**LRMS:** C<sub>13</sub>H<sub>16</sub>N<sub>5</sub>O Expected (M+H) 234; found (M+H) 234

> 95% purity by HPLC

**2-Amino-9a-methyl-8,9,9a,10-tetrahydrobenzo[g]pteridine-4,6(3H,7H)-dione**  
**TFA salt (4.2)**<sup>40</sup>



2-Amino-9a-methyl-6,7,8,9,9a,10-hexahydrobenzo[g]pteridin-4(3H)-one (**4.1**) from the previous reaction was left in DMF and 5 drops of trifluoroacetic acid for 15 hours. Upon conversion to the title product, the mixture was purified by HPLC (R<sub>t</sub> = 8 min). The fractions were then combined and lyophilised to give the title product as a dark orange solid (20 mg, 3 %).

**M.P:** > 230 °C; **Lit** = > 320 °C<sup>40</sup>

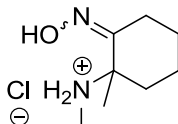
**v<sub>max</sub>** (KBr, cm<sup>-1</sup>): 3426, 3264, 2956, 2926, 2852, 1651, 1641, 1575, 1437, 1384, 1203, 1140

$^1\text{H}$  (CD<sub>3</sub>OD) 500 MHz: 1.40 (3H, s, CH<sub>3</sub>), 2.09 – 2.18 (4H, m, 2 X CH<sub>2</sub>), 2.41 – 2.56 (2H, m, CH<sub>2</sub>)

$^{13}\text{C}$  (CD<sub>3</sub>OD) 125 MHz: Material is too insoluble for analysis

**LRMS:** C<sub>11</sub>H<sub>13</sub>N<sub>5</sub>O<sub>2</sub> expected (M+H) 248; found (M+H) 248

>95% purity by HPLC

**2-Methyl-2-(methylamino)cyclohexanone oxime hydrochloride (4.10)**

1-Chloro-1-methyl-2-nitrosocyclohexane (**2.17**, 5 g, 30.9 mmol) was dissolved in 2M methylamine in THF (30 ml, 60 mmol) and stirred overnight. The solvent was then removed by rotary evaporation, the residual oil was dissolved in a small volume of water and the pH adjusted to 7 with concentrated hydrochloric acid. The water was then removed by rotary evaporation and the residue was scratched in toluene to crystallise the material. The product was then reprecipitated with a small volume of hot ethanol and a large excess of acetone to give the title product as a white solid (4.55 g, 76 %).

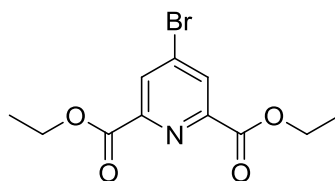
**M.P:** 228-230 °C

$\nu_{\max}$  (ATR,  $\text{cm}^{-1}$ ): 3188, 2981, 2940, 1601, 1550, 1469, 1410, 1350, 970, 692

$^1\text{H}$  (DMSO- $d_6$ ) 500 MHz: 1.35 – 1.40 (1H, m, CHH), 1.41 (3H, s,  $\text{CH}_3$ ), 1.53 – 1.65 (2H, m,  $\text{CH}_2$ ), 1.80 – 1.86 (2H, m,  $\text{CH}_2$ ), 1.88 – 1.93 (1H, m, CHH), 2.20 – 2.27 (1H, m, CHH), 2.42 (3H, bs,  $+\text{NH}_2\text{CH}_3$ ), 2.86 – 2.91 (1H, m, CHH), 9.11 (1H, bs,  $+\text{NHH}$ ), 9.30 (1H, bs,  $+\text{NHH}$ ), 11.27 (1H, s, NOH)

$^{13}\text{C}$  (DMSO- $d_6$ ) 125 MHz: 20.0 ( $\text{CH}_2$ ), 20.3 ( $\text{CCH}_3$ ), 20.5 ( $\text{CH}_2$ ), 24.5 ( $\text{CH}_2$ ), 26.5 ( $+\text{NH}_2\text{CH}_3$ ), 34.7 ( $\text{CH}_2$ ), 60.4 ( $\text{CH}_3\text{CNH}_2$ ), 155.4 (CNOH)

**LC-HRMS:**  $\text{C}_8\text{H}_{17}\text{N}_2\text{O}$  Expected (M+H) 157.1335; found (M+H) 157.1335. 79.0% purity by LC.

**Diethyl 4-bromopyridine-2,6-dicarboxylate (5.7)**<sup>223,248</sup>

4-Hydroxypyridine-2,6-dicarboxylic acid (**5.6**, 3.54 g, 19.4 mmol) and phosphorus pentabromide (25 g, 58.1 mmol) were stirred at 90 °C for 2 hours as a melt. The melt was then allowed to cool to room temperature whereupon it formed a purple solid. This solid was taken up in dichloromethane (10 ml) and filtered. The filtrate was then chilled to around 0 °C and ethanol was carefully added, taking care to ensure that the reaction temperature did not get excessively high (*ca.* 40 °C). The solvent was then evaporated under reduced pressure and the product was recrystallised twice from ethanol to give the title compound as off-white needles (3.31 g, 70 %).

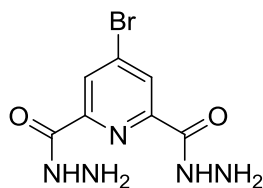
**M.P:** 97 – 98 °C, Lit = 95 – 96 °C<sup>248</sup>

$\nu_{\max}$  (ATR,  $\text{cm}^{-1}$ ): 3131, 2978, 1714, 1562, 1367, 1321, 1261, 1242, 1150, 1016, 876, 779, 723, 687

$^1\text{H}$  (DMSO- $d_6$ ) 400 MHz: 1.35 (6H, t,  $^3J = 8.0$  Hz,  $\text{CH}_3$ ), 4.39 (4H, q,  $^3J = 8.0$  Hz,  $\text{CH}_2$ ), 8.41 (2H, s,  $\text{C}^3\text{H}$  &  $\text{C}^5\text{H}$ )

$^{13}\text{C}$  (DMSO- $d_6$ ) 100 MHz: 14.0 ( $\text{CH}_3$ ), 62.0 ( $\text{CH}_2$ ), 130.6 ( $\text{C}^3$ ), 134.3 ( $\text{C}^4$ ), 149.1 ( $\text{C}^2$ ), 163.0 ( $\text{CO}_2\text{Et}$ )

**LC-HRMS:**  $\text{C}_{11}\text{H}_{13}^{79}\text{BrNO}_4$  Expected (M+H) 302.0019; found (M+H) 302.0022. >99% purity by LC.

**4-Bromopyridine-2,6-dicarbohydrazide (5.8)**<sup>223</sup>

Diethyl 4-bromopyridine-2,6-dicarboxylate (**5.7**, 3.28 g, 10.8 mmol) was dissolved in ethanol (30 ml) with stirring. To this solution, hydrazine hydrate (3.38 ml, 21.7 mmol) was added drop-wise and the mixture was left to stir for 15 minutes. The solution was then heated to reflux for 4 hours and the progress of the reaction was monitored by TLC. Upon the completion of the reaction, the solution was cooled and the solvent evaporated under reduced pressure. The product was then recrystallised from methanol to give the title product as a white solid (2.45 g, 82 %).

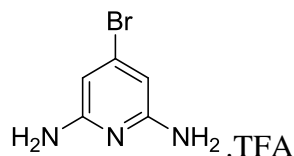
**M.P.:** > 230°C, Lit > 240°C<sup>223</sup>

$\nu_{\max}$  (KBr,  $\text{cm}^{-1}$ ): 3341, 3307, 3082, 1689, 1651, 1631, 1513, 1405, 1315, 1268, 1122, 977, 904, 744, 638

$^1\text{H}$  (DMSO- $d_6$ ) 400 MHz: 4.68 (4H, bs,  $\text{NH}_2$ ), 8.24 (2H, s, aromatic CH), 10.67 (2H, s, NH)

$^{13}\text{C}$  (DMSO- $d_6$ ) 100 MHz: 126.38 ( $\text{C}^3$ ), 134.96 ( $\text{C}^4$ ), 149.73 ( $\text{C}^2$ ), 160.59 (CO)

**LC-HRMS:**  $\text{C}_7\text{H}_7^{79}\text{BrN}_5\text{O}_2$  Expected (M-H) 271.9789; found (M+H) 271.9793. 83.6% purity by LC.

**2,6-Diamino-4-bromopyridine TFA salt (5.5)**<sup>223</sup>

4-Bromopyridine-2,6-dicarbohydrazide (**5.8**, 2 g, 7.30 mmol) was suspended in water (64 ml) which was then treated with concentrated hydrochloric acid (3.2 ml). The reaction mixture was then cooled to 0 °C and sodium nitrite (1.1 g in 5 ml of water) was added drop-wise, ensuring that the reaction temperature stayed below 2 °C throughout. The reaction was stirred for 15 minutes. Saturated aqueous sodium hydrogen carbonate solution was then added to adjust the pH to 8. The precipitate was filtered off and washed with cold water (5 ml). This was then taken up in the minimum volume of dichloromethane and dried using magnesium sulfate, filtered and the solvent was removed under reduced pressure at 20 °C. The solid obtained was then heated at reflux immediately in *t*-butanol for 16 hours. The solvent was then evaporated under reduced pressure to give a clear oil which was left for 2 hours to crystallise as a glassy solid, giving the Boc-protected product which was then deprotected by stirring in dichloromethane:trifluoroacetic acid 1:1 (10 ml) for 4 hours. The solvent was then evaporated under reduced pressure, and the material was recrystallised using ethyl acetate and hexane, to give the trifluoroacetic acid salt of the title product as a white powder (770 mg, 35%).

**M.P:** forms needles at 163 °C, melts at 179 - 180°C

$\nu_{\max}$  (KBr,  $\text{cm}^{-1}$ ): 3351, 3207, 1656, 1496, 1426, 1201, 1140, 985, 838, 799, 724

$^1\text{H}$  (DMSO- $d_6$ ) 400 MHz: 6.07 (2H, s,  $\text{C}^3\text{H}$ ), 7.45 (4H, bs,  $\text{NH}_2$ )

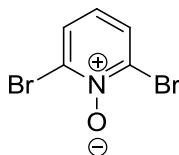
$^{13}\text{C}$  (DMSO- $d_6$ ) 100 MHz: 97.5 ( $\text{C}^3$ ), 138.9 ( $\text{C}^4$ ), 152.7 ( $\text{C}^2$ )

**LRMS:**  $\text{C}_5\text{H}_7\text{BrN}_3$  Expected (M+H) 188 (100%), 190 (100%); found (M+H) 188 (100%), 190 (100%)



**HRMS:**  $C_5H_7^{79}BrN_3$  Expected (M+H) 187.9819; found (M+H) 187.9829.

**2,6-Dibromopyridine 1-oxide (5.10)**<sup>223</sup>



The following reaction was carried out in the special operations laboratory. 2,6-Dibromopyridine (**5.9**, 120 g, 0.51 mol) was placed in a 2 litre round-bottomed flask, dissolved in TFA (500 ml) and heated with stirring at 60 °C. Hydrogen peroxide (33 % aqueous solution, 128 ml, 4.18 mol) was then added portion-wise to the solution which was then heated at 90 °C for 5 hours behind a blast shield. The solution was then allowed to cool, DCM (500 ml) was then added to the solution and a precipitate formed which was confirmed to be residual starting material. The solution was placed in a 2 litre separating funnel and 200 ml of water was slowly added and after agitation a tri-phasic mixture formed. The bottom layer (aqueous TFA) was removed and stored. The organic layer was then separated and washed a further two times with water (200 ml), then a saturated aqueous solution of sodium hydrogen carbonate (3 × 300 ml). The organic layer was then dried with sodium sulphate and filtered and the solvent was removed by rotary evaporation. The crude material was then re-precipitated with DCM:hexane to afford the title compound as a white powdery solid (113 g, 88 %).

**M.P.:** 118 – 120 °C, Lit = 186 – 187 °C<sup>223</sup>

$\nu_{\max}$  (KBr,  $\text{cm}^{-1}$ ): 3436, 1632, 1525, 1438, 1359, 1256, 840, 767, 748

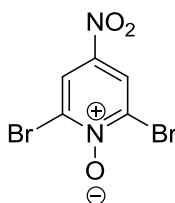
$^1\text{H}$  ( $\text{CDCl}_3$ ) 400 MHz: 6.94 (1H, t,  $^3J = 8.0$  Hz,  $\text{C}^4\text{H}$ ), 7.65 (2H, d,  $^3J = 8.0$  Hz,  $\text{C}^3\text{H}$  &  $\text{C}^5\text{H}$ ).

$^{13}\text{C}$  ( $\text{CDCl}_3$ ) 100 MHz: 125.1 ( $\text{C}^3$  &  $\text{C}^5$ ), 129.8 ( $\text{C}^4$ ), 134.0 ( $\text{C}^2$  &  $\text{C}^6$ )

**LRMS:**  $C_5H_4Br_2NO$  Expected (M+H) 252 (50%), 254 (100%), 256 (50%); found (M+H) 252 (50%), 254 (100%), 256 (50%)

**LC-HRMS:**  $C_5H_4^{79}Br^{81}BrNO$  Expected (M+H) 253.8634; found (M+H) 253.8630. 92.7% purity by LC.

**2,6-Dibromo-4-nitropyridine-1-oxide (5.11)**<sup>223</sup>



2,6-Dibromopyridine-1-oxide (**5.10**, 52.5 g, 0.176 mol) was dissolved slowly and with cooling in concentrated sulfuric acid (175 ml). To this stirring solution, fresh red fuming nitric acid (74 ml) was added drop-wise and the reaction mixture was heated at 60 °C for 24 hours. The reaction was then allowed to cool to room temperature and was very carefully added to a 2 litre conical flask containing 35 % aqueous ammonia (300 ml) and ice (200 ml). The content of the flask was then stirred for 15 minutes to ensure that all the material had precipitated. The solid was then collected by filtration, washed with water (100 ml) and dried to give the title product as a light green fluffy powder (54 g, 87 %).

**M.P:** 113 - 115°C

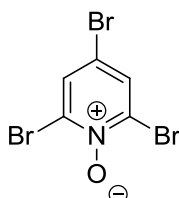
$\nu_{\max}$  (KBr,  $\text{cm}^{-1}$ ): 3422, 3089, 1520, 1412, 1330, 1283, 1155, 884, 710

$^1\text{H}$  (DMSO- $d_6$ ) 400 MHz: 8.79 (2H, s,  $\text{C}^3\text{H}$  &  $\text{C}^5\text{H}$ )

$^{13}\text{C}$  (DMSO- $d_6$ , 100 MHz): 123.9 ( $\text{C}^3\text{H}$  &  $\text{C}^5\text{H}$ ), 133.4 ( $\text{C}^2\text{H}$  &  $\text{C}^6\text{H}$ ), 140.8 ( $\text{C}^4\text{H}$ )

**LRMS:**  $C_5H_3Br_2N_2O_3$  Expected (M+H) 297 (50%), 299 (100%), 301 (50%); found (M+H) 297 (50%), 299 (100%), 301 (50%)

**2,4,6-Tribromopyridine 1-oxide (5.12)**<sup>223</sup>



2,6-Dibromo-4-nitropyridine-1-oxide (**5.11**, 20 g, 0.067 mol) was suspended in glacial acetic acid (125 ml) and was heated with stirring to 60 °C. To this mixture, acetyl bromide (6.6 ml, 0.089 mol) was added and the temperature was increased to 80 °C for 5 hours. The reaction was cooled to 20 °C whereupon a precipitate formed. This was collected by filtration and washed with diethyl ether (50 ml) to give the title product as a faintly yellow solid (16.25 g, 73 %).

**M.P:** decomposed at 138 °C

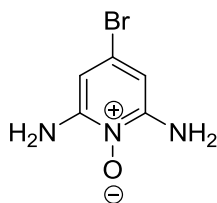
$\nu_{\max}$  (KBr,  $\text{cm}^{-1}$ ): 3422, 3103, 3010, 2694, 2302, 1567, 1522, 1492, 1381, 1330, 1286, 1226, 1194, 1155, 914, 878

$^1\text{H}$  (DMSO- $d_6$ ) 400 MHz: 8.30 (2H, s,  $\text{C}^3\text{H}$  &  $\text{C}^5\text{H}$ )

$^{13}\text{C}$  (DMSO- $d_6$ ) 100 MHz: 116.5 ( $\text{C}^4$ ), 132.1 ( $\text{C}^3\text{H}$  &  $\text{C}^5\text{H}$ ), 133.3 ( $\text{C}^2$  &  $\text{C}^6$ )

**LRMS:**  $C_5H_3Br_3NO$  Expected (M+H) = 330 (35%), 332 (100%), 334 (100%), 336 (32%); found (M+H) = 330 (30%), 332 (100%), 334 (100%), 336 (30%)

**LC-HRMS:**  $C_5H_3Br_3NO$  Expected (M+H) 331.7739; found (M+H) 331.7737. >99% purity by LC.

**4-Bromo-2,6-pyridinediamine-1-oxide (5.13)**<sup>223</sup>

2,4,6-Tribromopyridine-1-oxide (**5.12**, 5g, 0.012 mol) was placed in a mortar along with aqueous ammonia (15 ml, 35% w/v) which spontaneously forms a brick-hard solid. Using the pestle, the material was ground into a fine suspension which was, in turn, transferred to a 50 ml Aldrich reaction tube. The mortar was then washed with aqueous ammonia (15 ml) and transferred to the reaction tube. The tube and its contents were then frozen with dry ice to allow the top of the tube to be sealed using an oxy-acetylene torch. The reaction was then heated to 140 °C with stirring for 5 hours. The reaction was then cooled using dry ice to allow the removal of the top of the reaction tube, which was scored with a sharp blade and carefully broken off (caution high pressure inside). The tube was allowed to reach 0 °C in an ice bath and the precipitate was then collected by filtration, washed with cold water (20 ml) and dried to give the title product as dark brown needles (1.56 g, 63 %).

Care must be taken when performing this reaction to ensure that the proper glassware is used as an extremely high pressure is generated during the course of the reaction.

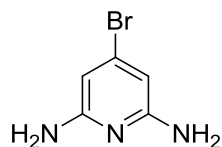
**M.P.:** reordered at 128 °C, decomposed at 157 °C

$\nu_{\max}$  (KBr,  $\text{cm}^{-1}$ ): 3436, 1638, 1529, 1197, 791

$^1\text{H}$  (DMSO- $d_6$ ) 400 MHz: 6.12 (2H, s,  $\text{C}^3\text{H}$  &  $\text{C}^5\text{H}$ ), 6.78 (4H, bs, 2 x  $\text{NH}_2$ )

$^{13}\text{C}$  (DMSO- $d_6$ ) 100 MHz: 96.5 ( $\text{C}^3\text{H}$  &  $\text{C}^5\text{H}$ ), 119.8 ( $\text{C}^4$ ), 150.1 ( $\text{C}^2$  &  $\text{C}^6$ )

**LC-HRMS:**  $\text{C}_5\text{H}_7\text{BrN}_3\text{O}$  Expected (M+H) 203.9767; found (M+H) 203.9767. 84.6% purity by LC.

**4-Bromo-2,6-pyridinediamine (5.5)**<sup>223</sup>

4-Bromo-2,6-pyridinediamine-1-oxide (**5.13**, 4.94 g, 24.2 mmol) was suspended in a 1:1 mixture of water and acetic acid (25 ml). To this suspension, iron filings (1.63 g, 29.2 mmol) were added and the reaction was heated at reflux with stirring for 2 hours. The reaction mixture was then allowed to cool to room temperature and was neutralised using 28% aqueous sodium hydroxide. This solution was then filtered under reduced pressure to remove the solid residue. This residue was then washed with ethyl acetate (90 ml). The aqueous layer was extracted with ethyl acetate (3 × 30 ml) and all the organic layers were combined. The combined organic layer was then washed with brine, dried using sodium sulfate, filtered and the solvent removed using rotary evaporation to give a light brown solid. The solid was re-precipitated twice from ether:hexane to give a colourless solid (1.46 g, 32 %).

**M.P:** 122-124 °C Lit = 124.5 °C<sup>223</sup>

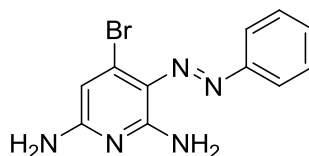
$\nu_{\max}$  (KBr,  $\text{cm}^{-1}$ ): 3447, 3418, 1631, 1581, 1428, 1236, 1104, 839, 803, 756

$^1\text{H}$  (DMSO- $d_6$ ) 400 MHz: 5.66 (4H, bs, 2 x  $\text{NH}_2$ ), 5.78 (2H, s,  $\text{C}^3\text{H}$  &  $\text{C}^5\text{H}$ )

$^{13}\text{C}$  (DMSO- $d_6$ ) 100 MHz: 97.3 ( $\text{C}^3\text{H}$  &  $\text{C}^5\text{H}$ ), 132.4 ( $\text{C}^4$ ), 159.7 ( $\text{C}^2$  &  $\text{C}^6$ )

**LRMS:**  $\text{C}_5\text{H}_7\text{BrN}_3$  Expected (M+H) 188 (100%), 190 (100%); found (M+H) 188 (100%), 190 (100%)

**HRMS:**  $\text{C}_5\text{H}_7\text{BrN}_3$  Expected (M+H) 187.9819; found (M+H) 187.9819.

**4-Bromo-3-[(E)-phenyldiazenyl]-2,6-pyridinediamine (5.15)***Preparation of the diazonium salt*

Aniline (120  $\mu$ l, 1.32 mmol) was suspended in water (1 ml) with stirring. To this suspension concentrated hydrochloric acid (700  $\mu$ l, 8.4 mmol) was added to dissolve the aniline. This solution was cooled to  $-5\text{ }^{\circ}\text{C}$  with an ice bath containing a small amount of acetone. Sodium nitrite (93 mg, 1.35 mmol in 1.5 ml of water) was added to the solution drop-wise, taking great care not to allow the internal temperature to rise above  $0\text{ }^{\circ}\text{C}$  at any point. Once the addition was complete the solution was stirred below  $0\text{ }^{\circ}\text{C}$  for 15 minutes.

*Coupling the diazonium salt*

In a separate flask, 4-bromo-2,6-pyridinediamine (**5.5**, 250 mg, 0.86 mmol) was dissolved in 6 M hydrochloric acid (2 ml) and cooled to  $0\text{ }^{\circ}\text{C}$  in an ice bath. To this solution, the diazonium salt was added drop-wise, ensuring that the internal temperature did not rise above  $2\text{ }^{\circ}\text{C}$ . The solution was stirred for 2 hours at or below this temperature. The solution was then diluted with water (10 ml) and allowed to stand for 12 hours. Anhydrous sodium acetate (2.56 g in 4 ml water) was then added to precipitate the product. This was then recrystallised from ethanol: water, collected by filtration and dried to give the title product as a bright yellow solid (300 mg, 77 %).

**M.P:** formed needles at  $155\text{ }^{\circ}\text{C}$ , melted at  $176 - 177\text{ }^{\circ}\text{C}$

$\nu_{\text{max}}$  (KBr,  $\text{cm}^{-1}$ ): 3436, 2923, 2852, 1698, 1637, 1580, 1382, 1288, 1245, 1209

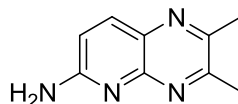
$^1\text{H}$  (DMSO- $d_6$ ) 400 MHz: 5.32 (2H, bs,  $\text{NH}_2$ ), 5.64 (2H, bs,  $\text{NH}_2$ ), 6.40 (1H, s,  $\text{C}^5\text{H}$ ), 7.36 (1H, m\*,  $\text{C}^4\text{H}$  on diazo linked ring), 7.46 (2H, m\*,  $\text{C}^3\text{H}$  &  $\text{C}^5\text{H}$  on diazo linked ring), 7.81 (2H, m\*,  $\text{C}^2\text{H}$  &  $\text{C}^6\text{H}$  on diazo linked ring)

m\* is used here as the pattern for either the *ortho* or *meta* protons (2 and 2' on the ring or 3 and 3' on the ring) is more complex than expected. This is due to twisting of the rings giving non-equivalent protons (2 and 2' being non-equivalent or 3 and 3' being non-equivalent) which would otherwise be equivalent.

$^{13}\text{C}$  (DMSO- $d_6$ ) 100 MHz: 103.9 ( $\text{C}^3$ ), 122.2 ( $\text{C}^3$  &  $\text{C}^5$  on diazo linked ring), 129.3 ( $\text{C}^1$  on diazo linked ring), 129.4 ( $\text{C}^2$  &  $\text{C}^6\text{H}$  on diazo linked ring), 143.0 ( $\text{C}^4\text{H}$  on diazo linked ring), 150.9 ( $\text{C}^5$ ), 153.1 ( $\text{C}^4$ ), 158.4 ( $\text{C}^2$ ), 176.5 ( $\text{C}^6$ )

**HRMS:**  $\text{C}_{11}\text{H}_{11}\text{BrN}_5$  Expected (M+H) 292.0192 (100%), 294.0192 (100%); found (M+H) 292.0190 (100%), 294.0190 (100%)

### 2,3-Dimethylpyridido[2,3-*b*]pyrazin-6-amine (5.31)



4-Bromo-3-[(*E*)-phenyldiazenyl]-2,6-pyridinediamine (**5.15**, 150 mg, 0.51 mmol) was dissolved in anhydrous ethanol (20 ml) and cooled in an ice bath. Under a constant stream of nitrogen, 10% w/w Pd/C (37 mg) was added and the solution was hydrogenated for 2 hours. The solution was filtered through celite and the solution placed into a round-bottomed flask containing 2,3-butanedione (68  $\mu\text{l}$ , 0.78 mmol) and heated at reflux for two days where colour had changed from green to pale yellow. The solvent was then removed by rotary evaporation and the residue was recrystallised from ether/hexane to give the title product as a colourless solid (23 mg, 26 %). An analytical sample was purified by HPLC.

M.P: 225 – 226 °C

$\nu_{\max}$  (KBr,  $\text{cm}^{-1}$ ): 3421, 3191, 2922, 1551, 1506, 1412, 1385, 1348

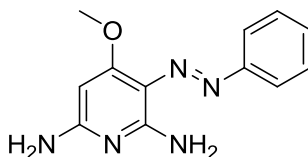
$^1\text{H}$  (DMSO- $d_6$ ) 500 MHz: 2.55 (3H, s,  $\text{CH}_3$ ), 2.57 (3H, s,  $\text{CH}_3$ ), 7.00 (1H, d,  $^3J = 9.0$  Hz,  $\text{C}^7\text{H}$ ), 7.21 (2H, bs,  $\text{NH}_2$ ), 7.96 (1H, d  $^3J = 9.0$  Hz,  $\text{C}^8\text{H}$ )

$^{13}\text{C}$  (DMSO- $d_6$ ) 125 MHz: 21.7 ( $\text{CH}_3$ ), 22.7 ( $\text{CH}_3$ ), 114.2, 115.8, 128.8, 131.0, 138.3, 155.0 ( $\text{C}^7$ ), 159.2 ( $\text{C}^8$ )

**HRMS:**  $\text{C}_9\text{H}_{11}\text{N}_4$  Expected (M+H) 175.0978; found (M+H) 175.0978

>95% purity by HPLC.

#### **4-Methoxy-3-[(*E*)-phenyldiazenyl]-2,6-pyridinediamine (5.32)**



Anhydrous methanol (50 ml) was stirred in a flame-dried flask under an atmosphere of nitrogen. Sodium metal (156 mg, 6.80 mmol) was added and allowed to dissolve. This solution was then stirred for 15 minutes. 4-Bromo-3-[(*E*)-phenyldiazenyl]-2,6-pyridinediamine (**5.15**, 100 mg, 0.34 mmol) was then added to the sodium methoxide solution and this was heated at reflux for 7 days. The reaction mixture was then allowed to cool to room temperature and the solvent was removed by rotary evaporation. The residue was triturated in 1 M hydrochloric acid and collected by filtration. The product was precipitated from a small volume of diethyl ether and a large volume of hexane to give the title product as a bright red solid (55 mg, 66 %).

M.P: 85 – 87 °C

$\nu_{\max}$  (KBr,  $\text{cm}^{-1}$ ): 3431, 1621, 1455, 1364, 1200



$^1\text{H}$  (DMSO- $d_6$ ) 500 MHz: 3.97 (3H, s,  $\text{OCH}_3$ ), 4.69 (2H, bs,  $\text{NH}_2$ ), 5.59 (1H, s,  $\text{C}^5\text{H}$ ), 7.29 (1H, m\*,  $\text{C}^4\text{H}$  on diazo linked ring), 7.43 (2H, m\*,  $\text{C}^3\text{H}$  &  $\text{C}^5\text{H}$  on diazo linked ring), 7.73 (2H, m\*,  $\text{C}^2\text{H}$  &  $\text{C}^6\text{H}$  on diazo linked ring)

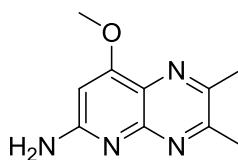
m\* is used here as the pattern for either the *ortho* or *meta* protons (2 and 2' on the ring or 3 and 3' on the ring) is more complex than expected. This is due to twisting of the rings giving non-equivalent protons (2 and 2' being non-equivalent or 3 and 3' being non-equivalent) which would otherwise be equivalent.

$^{13}\text{C}$  (DMSO- $d_6$ ) 125 MHz: 56.4 ( $\text{OCH}_3$ ), 82.3 ( $\text{C}^5$ ), 117.2 ( $\text{C}^3$ ), 121.7 ( $\text{C}^3$  &  $\text{C}^5$  on diazo linked ring), 128.4 ( $\text{C}^4$  on diazo linked ring), 129.2 ( $\text{C}^2$  &  $\text{C}^6$  on diazo linked ring), 151.9 ( $\text{C}^1$  on diazo linked ring), 153.7 ( $\text{C}^2$ ), 160.8 ( $\text{C}^6$ ), 167.2 ( $\text{C}^4$ )

**LRMS:**  $\text{C}_{12}\text{H}_{14}\text{N}_5\text{O}$  Expected (M+H) 244, found (M+H) 244

**HRMS:**  $\text{C}_{12}\text{H}_{14}\text{N}_5\text{O}$  Expected (M+H) 244.1190, found (M+H) 244.1193

### **8-Methoxy-2,3-dimethylpyrido[2,3-*b*]pyrazin-6-amine (5.33)**



4-Methoxy-3-[(*E*)-phenyldiazenyl]-2,6-pyridinediamine (**5.32**, 55 mg, 0.23 mmol) was dissolved in anhydrous ethanol (20 ml) and cooled in an ice bath. Under a constant stream of nitrogen, Pd/C (10% w/w 20 mg) was added and the solution was hydrogenated for 2 hours. The solution was then filtered through celite and placed into a round bottomed flask containing 2,3-butanedione (24  $\mu\text{l}$ , 0.28 mmol) and then heated at reflux for two days when the colour had changed from red to brown. The

solvent was then removed by rotary evaporation and the residue was purified by HPLC to give the title compound as a colourless solid (10 mg, 22 %).

**M.P:** > 230 °C

$\nu_{\max}$  (KBr,  $\text{cm}^{-1}$ ): 3360, 3318, 2965, 1687, 1651, 1601, 1567, 1494, 1436, 1391, 1254, 1205, 1182, 1130, 1049, 831, 799, 721

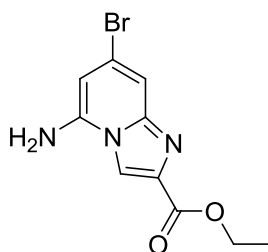
$^1\text{H}$  NMR ( $\text{CDCl}_3$ ) 400 MHz: 2.70 (6H, s,  $2 \times \text{CH}_3$ ), 4.17 (3H, s,  $\text{OCH}_3$ ), 6.54 (1H, bs, CH),  $\text{NH}_2$  could not be observed

$^{13}\text{C}$  NMR ( $\text{CDCl}_3$ ) 100 MHz: 22.5 ( $\text{CH}_3$ ), 23.1 ( $\text{CH}_3$ ), 58.0 ( $\text{OCH}_3$ ), 93.4 ( $\text{C}^7$ ), 125.0 ( $\text{C}^{8a}$ ), 143.2 ( $\text{C}^{4a}$ ), 151.7 ( $\text{C}^6$ ), 157.7 ( $\text{C}^2$ ), 158.3 ( $\text{C}^3$ ), 165.4 ( $\text{C}^8$ )

**LRMS:**  $\text{C}_{10}\text{H}_{13}\text{N}_4\text{O}$  Expected (M+H) 205; found (M+H) 205

**LC-HRMS:**  $\text{C}_{10}\text{H}_{13}\text{N}_4\text{O}$  Expected (M+H) 205.1083; found (M+H) 205.1084. 89.5% purity by LC.

**Ethyl 5-amino-7-bromoimidazo[1,2-*a*]pyridine-2-carboxylate (5.38)**<sup>235</sup>



4-Bromo-2,6-pyridinediamine (**5.5**, 200 mg, 1.06 mmol) was dissolved in anhydrous DMF (10 ml) under an atmosphere of nitrogen. To this, ethyl bromopyruvate (134  $\mu\text{l}$ , 1.07 mmol) was added, along with triethylamine (148  $\mu\text{l}$ , 1.06 mmol). The reaction was stirred for 2 days at room temperature. The solvent was then removed by high vacuum rotary evaporation. The residue was triturated in acetone ( $2 \times 5$  ml) and a saturated aqueous solution of sodium hydrogen carbonate (5 ml). The solid

suspension was collected by filtration and washed with water and ether. The solid was dried to give the title product as a white solid (52 mg, 17 %). An analytical sample was purified by HPLC.

**M.P.:** > 230 °C,

$\nu_{\max}$  (KBr,  $\text{cm}^{-1}$ ): 3404, 3139, 2924, 2551, 1926, 1712, 1660, 1623, 1555, 1525, 1497, 1340, 1219, 999, 834

$^1\text{H}$  (DMSO- $d_6$ ) 500 MHz: 1.32 (3H, t,  $^3J = 7.0$  Hz,  $\text{CH}_2\text{CH}_3$ ), 4.31 (2H, q,  $^3J = 7.0$  Hz  $\text{CH}_2\text{CH}_3$ ), 6.12 (1H, s,  $\text{C}^6\text{H}$ ), 7.08 (1H, s,  $\text{C}^8\text{H}$ ), 7.16 (2H, bs,  $\text{NH}_2$ ), 8.56 (1H, s,  $\text{C}^3\text{H}$ )

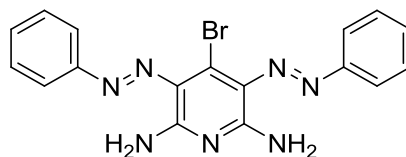
$^{13}\text{C}$  (DMSO- $d_6$ ) 125 MHz: 14.2 ( $\text{CH}_2\text{CH}_3$ ), 60.2 ( $\text{CH}_2\text{CH}_3$ ), 93.2 ( $\text{C}^6$ ), 105.1 ( $\text{C}^8$ ), 113.4 ( $\text{C}^3$ ), 122.3 ( $\text{C}^7$ ), 135.6 ( $\text{C}^2$ ), 143.3 ( $\text{C}^9$ ), 145.9 ( $\text{C}^5$ ), 163.6 ( $\text{COCH}_2\text{CH}_3$ )

**LRMS:**  $\text{C}_{10}\text{H}_{11}\text{BrN}_3\text{O}_2$  Expected (M+H) 284 (100%), 286 (100%); found (M+H) = 284 (100%), 286 (100%)

> 95 % purity by HPLC

**NOESY:** positive correlation observed between the protons on the amine and  $\text{C}^3\text{H}$ , confirming the structure as the title compound.

$^{15}\text{N}$   $^{13}\text{C}$  HMBC data could not be obtained due to low abundance of  $^{15}\text{N}$ .

**4-Bromo-3,5-bis[(E)-phenyldiazenyl]-2,6-pyridinediamine (5.39)***Preparation of the diazonium salt*

Aniline (240  $\mu$ l, 2.64 mmol) was suspended in water (2 ml) with stirring. To this suspension concentrated hydrochloric acid (1.4 ml) was added to dissolve the aniline. This solution was cooled to  $-5\text{ }^{\circ}\text{C}$  with an ice bath containing a small amount of acetone. Sodium nitrite (186 mg 2.70 mmol) in water (3 ml) was added to the solution drop-wise, taking great care not to allow the internal temperature to rise above  $0\text{ }^{\circ}\text{C}$  at any point. Once the addition was complete, the solution was stirred below  $0\text{ }^{\circ}\text{C}$  for 15 minutes.

*Coupling the diazonium salt*

In a separate flask, 4-bromo-2,6-pyridinediamine (**5.5**, 500 mg, 1.72 mmol) was dissolved in 6 M hydrochloric acid (4 ml) and cooled to  $0\text{ }^{\circ}\text{C}$  in an ice bath. To this solution, the diazonium salt was added drop-wise, ensuring that the internal temperature did not rise above  $2\text{ }^{\circ}\text{C}$ . The solution was stirred for 2 hours at or below this temperature. The solution was stirred for 12 hours. Anhydrous sodium acetate (2.56 g in 4 ml water) was then added to precipitate a mixture of 4-bromo-3-[(E)-phenyldiazenyl]-2,6-pyridinediamine (**5.15**) and the title product (**5.39**) as a bright red solid. This was then dissolved in the minimum amount of hot chloroform and allowed to crystallise. The bright yellow crystalline product was removed by filtration and the chloroform was allowed to evaporate slowly in a cold dark cupboard. This gave the title product as small orange crystals which were subjected to x-ray analysis.

**MP:** signs of decomposition at  $208 - 210\text{ }^{\circ}\text{C}$ , melts  $> 230\text{ }^{\circ}\text{C}$

$\nu_{\max}$  (ATR,  $\text{cm}^{-1}$ ): 3352, 3152, 1622, 1573, 1527, 1454, 1404, 1260, 1151, 1068, 1016, 796, 754, 684

$^1\text{H}$  ( $\text{CDCl}_3$ ) 500 MHz: 7.41 (2H, tt,  $^3J = 7.5$  Hz,  $^4J = 1.0$  Hz,  $\text{C}^4\text{H}$  on diazo linked ring), 7.51 (4H, m\*,  $\text{C}^3\text{H}$  and  $\text{C}^5\text{H}$  on diazo linked ring), 7.90 (4H, m\*,  $\text{C}^2\text{H}$  and  $\text{C}^6\text{H}$  on diazo linked ring), 10.09 (4H, bs, 2 x  $\text{NH}_2$ )

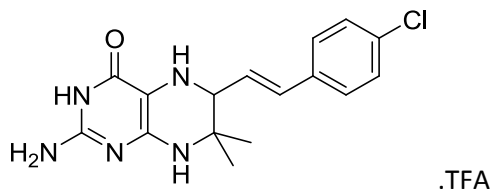
$^{13}\text{C}$  ( $\text{CDCl}_3$ ) 125 MHz: 122.6 ( $\text{C}^3$  and  $\text{C}^5$  on diazo linked ring), 124.3 ( $\text{C}^1$  on diazo linked ring), 129.3 ( $\text{C}^2$  and  $\text{C}^6$  on diazo linked ring), 142.3 ( $\text{C}^4$  on diazo linked ring), 151.1 ( $\text{C}^3$ ), 151.9 ( $\text{C}^4$ ), 152.9 ( $\text{C}^2$ )

**LC-HRMS:**  $\text{C}_{17}\text{H}_{15}^{79}\text{BrN}_7$  Expected (M+H) 396.0563; found (M+H) 396.0567. 64.6% pure by LC.

See Appendix D for x-ray data.

m\* is used here as the pattern for either the *ortho* or *meta* protons (2 and 6 on the ring or 3 and 5 on the ring) is more complex than expected. This is due to twisting of the rings giving non-equivalent protons (2 and 6 being non-equivalent or 3 and 5 being non-equivalent) which would otherwise be equivalent.

**2-Amino-6-[(E)-2-(4-chlorophenyl)ethenyl]-7,7-dimethyl-5,6,7,8-tetrahydro-4(3H)-pteridinone (6.4) TFA salt**

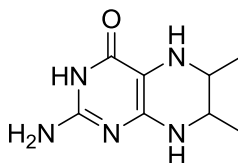


2-Amino-6-[(E)-2-(4-chlorophenyl)ethenyl]-7,7-dimethyl-7,8-dihydro-4(3H)-pteridinone (10 mg, 0.03 mmol), which was available from the laboratory's compound library, was placed in a round-bottomed flask and dissolved in anhydrous methanol (10 ml) under an atmosphere of nitrogen. Sodium cyanoborohydride (6 mg, 0.09 mmol) was then added with vigorous stirring. To this mixture, 3 drops of glacial acetic acid was then added before the flask was wrapped in aluminium foil. The mixture was stirred for 15 hours. The reaction was then quenched with concentrated hydrochloric acid (1 ml) and the solvent was removed under reduced pressure. The solid was purified by HPLC and combined fractions were stored on dry ice before being lyophilised. This gave the title product as a colourless powder (TFA salt) (6 mg, 44 %).

The product must be stored under nitrogen and away from light and used as soon as possible.

The material was not stable enough for fuller analysis.

**LRMS:**  $C_{16}H_{19}ClN_5O$  Expected (M+) 332; Found (M+) 332

**2-Amino-6,7-dimethyl-5,6,7,8-tetrahydro-4(3H)-pteridinone (6.5)**<sup>196</sup>

Compound taken from the pteridine library.<sup>196</sup> Analysis obtained to confirm that the compound was stable in the tetrahydro oxidation state.

**M.P:** > 230 °C

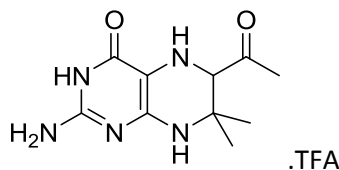
$\nu_{\max}$  (KBr,  $\text{cm}^{-1}$ ): 3454, 3372, 3243, 2953, 2831, 2705, 2521, 1720, 1663, 1562, 1442, 1342, 1173,

$^1\text{H}$  (DMSO- $d_6$ ) 500 MHz: 1.10 (3H, d,  $^3J = 7.0$  Hz,  $\text{CH}_3$ ), 1.12 (3H, d,  $^3J = 7.0$  Hz  $\text{CH}_3$ ), 3.45 (1H, m,  $\text{C}^6\text{H}$ ), 3.71 (1H, m,  $\text{C}^7\text{H}$ ), 7.21 (2H, bs,  $\text{NH}_2$ ), 7.69 (1H, bs,  $\text{N}^5\text{H}$ ), 9.84 (1H, bs,  $\text{N}^8\text{H}$ ), 11.14 (1H, bs, amide  $\text{NH}$ )

$^{13}\text{C}$  (DMSO- $d_6$ ) 125 MHz: 10.9 ( $\text{C}^6\text{HCH}_3$ ), 15.1 ( $\text{C}^7\text{HCH}_3$ ), 46.5 ( $\text{C}^6\text{HCH}_3$ ), 49.6 ( $\text{C}^7\text{HCH}_3$ ), 83.3 ( $\text{C}^{4a}$ ), 152.8 ( $\text{C}^2$ ), 153.6 ( $\text{C}^{8a}$ ), 157.3 ( $\text{C}^4$ )

**LRMS:**  $\text{C}_8\text{H}_{14}\text{N}_5\text{O}$  Expected (M+) 196; found (M+) 196

**6-Acetyl-2-amino-7,7-dimethyl-5,6,7,8-tetrahydro-4(3H)-pteridinone (1.7) TFA salt**



6-Acetyl-2-amino-7,7-dimethyl-7,8-dihydro-4(3H)-pteridinone (**1.6**, 30 mg, 0.13 mmol) was placed in a round-bottomed flask and dissolved in anhydrous methanol (20 ml) under an atmosphere of nitrogen. Sodium cyanoborohydride (24 mg, 0.38 mmol) was then added with vigorous stirring. To this mixture, 3 drops of glacial acetic acid was then added before the flask was wrapped in aluminium foil. The mixture was stirred for 15 hours. The reaction was quenched with concentrated hydrochloric acid (1 ml) and the solvent was removed under reduced pressure. The solid was purified by HPLC and combined fractions were stored on dry ice before being lyophilised. This gave the title product as a colourless solid (TFA salt) (19 mg, 42 %).

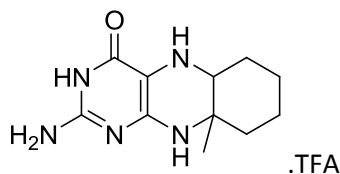
The product must be stored under nitrogen and away from light and used as soon as possible.

The material was not stable enough for fuller analysis.

**LRMS:**  $C_{10}H_{16}N_5O_2$  Expected (M+) 238; Found (M+) 238



**2-Amino-9a-methyl-5,5a,6,7,8,9,9a,10-octahydrobenzo[g]pteridin-4(3H)-one**  
**(6.6) TFA salt**



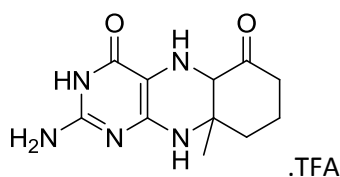
2-Amino-9a-methyl-6,7,8,9,9a,10-hexahydrobenzo[g]pteridin-4(3H)-one (**4.1**, 32 mg, 0.14 mmol) was placed in a round-bottomed flask and dissolved in anhydrous methanol (20 ml) under an atmosphere of nitrogen. Sodium cyanoborohydride (26 mg, 0.41 mmol) was then added with vigorous stirring. To this mixture, 3 drops of glacial acetic acid was then added before the flask was wrapped in aluminium foil. The mixture was stirred for 15 hours. The reaction was quenched with concentrated hydrochloric acid (1 ml) and the solvent was removed under reduced pressure. The solid was purified by HPLC and combined fractions were stored on dry ice before being lyophilised. This gave the title product as a colourless solid (TFA salt) (28 mg, 58 %).

The product must be stored under nitrogen and away from light and used as soon as possible.

The material was not stable enough for fuller analysis.

**LRMS:**  $C_{11}H_{18}N_5O$  Expected (M+) 236; Found (M+) 236

**2-Amino-9a-methyl-5,7,8,9a,10-hexahydrobenzo[g]pteridine-4,6(3H,5aH)-dione (6.7) TFA salt**



2-Amino-9a-methyl-8,9,9a,10-tetrahydrobenzo[g]pteridine-4,6(3H,7H)-dione (**4.2**, 30 mg, 0.12 mmol) was placed in a round-bottomed flask and dissolved in anhydrous methanol (20 ml) under an atmosphere of nitrogen. Sodium cyanoborohydride (23 mg, 0.36 mmol) was then added with vigorous stirring. To this mixture, 3 drops of glacial acetic acid was then added before the flask was wrapped in aluminium foil. The mixture was stirred for 15 hours. The reaction was quenched with concentrated hydrochloric acid (1 ml) and the solvent was removed under reduced pressure. The solid was purified by HPLC and combined fractions were stored on dry ice before being lyophilised. This gave the title product as a colourless solid (TFA salt) (16 mg, 36 %).

The product must be stored under nitrogen and away from light and used as soon as possible.

The material was not stable enough for fuller analysis.

**LRMS:**  $C_{11}H_{16}N_5O_2$  Expected (M+H) 250; Found (M+H) 250

### **General procedure for enzymatic assay**

All the following materials were obtained from Sigma chemical company, unless otherwise stated. The rate of NO formation was determined from the NO-mediated conversion of oxyhaemoglobin to methaemoglobin, monitored at 401 nm using a methaemoglobin minus oxyhemoglobin extinction coefficient of  $49 \text{ mM}^{-1} \text{ cm}^{-1}$ . Assay mixes containing 1 ml of 50 mM Tris/HCl buffer pH 7.5, 10  $\mu\text{M}$  oxyhemoglobin (prepared from bovine methaemoglobin), 0.1 mM NADPH, 1 mM L-arginine, 10 units/ml superoxide dismutase, 100 units/ml catalase, 10  $\mu\text{g/ml}$  calmodulin (prepared from recombinantly expressed protein), 1 mM  $\text{Ca}^{2+}$  were incubated at 25 °C before addition of  $\text{BH}_4$  (**1.1**) (Schricks Laboratories) or analogue and enzyme, typically 5  $\mu\text{l}$  of 10  $\mu\text{M}$ . All samples of tetrahydrobiopterin, or analogues, were dissolved in 50 mM Tris/HCl buffer pH 7.5 containing 1mM dithiothreitol to prevent oxidation and stored on ice during use.

### **General procedure for Spartan analysis**

The molecule under investigation was drawn out in ChemDraw Ultra 11.0 and saved as a .mol file. This file was then imported into ChemDraw 3D Pro 11.0 where an energy minimisation was performed using an MM2 minimisation protocol. When the calculation was complete the file was saved as a .mol2 file. The .mol2 file was then imported into Spartan '04 for Windows and the following operations carried out.

1. Further energy minimisation was performed using the protocol native to Spartan.
2. Next from the “set up” dropdown menu the “surfaces” option was selected. Within the pop-up box the option to visualise the HOMO surface was selected and should read as “pending” in the status box.
3. Subsequently, from the “set up” menu the “calculations” option was selected. Either a semi-empirical calculation (AM1) or a density functional calculation (B3LYP 6-31 G\*) was selected using the appropriate conditions (below) and the calculation was submitted.

**Conditions:** Calculate – Equilibrium geometry at the ground state. Start from – Initial geometry. Print – Orbitals and energies. Total charge – neutral, multiplicity – Singlet (for HOMO); Total charge – cation, multiplicity – doublet (for SOMO).

4. Upon completion of the calculation the spreadsheet option was selected from the “display” dropdown menu where the option to obtain the HOMO energy was selected in ( $\text{kJ mol}^{-1}$ ).

5. Next to visualise the orbitals the “surfaces” option was selected from the “display” dropdown menu. The HOMO check-box was selected and the image was saved as a jpeg file.

The files containing the Spartan calculation data can be found in the appendix section

### **General procedure for Gold docking.**

#### Preparation of ligands

1. The molecule to be docked was drawn using ChemDraw Ultra 11.0 with the stereochemistry explicitly assigned. This file was then saved as a .mol file type.

2. The ligand file was then opened using Accelrys Discovery Studio 2.5 wherein the hydrogens were added to the compound by selecting “add hydrogens” from then “chemistry” dropdown menu. The molecule was then set to its lowest energy conformation by selecting “structure” then “clean geometry”. The file was now saved as a .mol2 file.

#### Docking

1. From the PDB the appropriate enzyme crystal structure was downloaded and saved as a .pdb file – in this case 1om4 was chosen.

2. Using the program Hermes, the aforementioned .pdb file was opened and loaded into the visualizer. The structure was inspected to find the appropriate domain containing  $\text{BH}_4$  and the haem, which was kept clearly in view thereby allowing the binding site to be easily defined.

3. Using the “gold” dropdown menu the gold wizard was selected and the protein loading confirmed. All the waters in the protein were then deleted and all the hydrogens added. Next the binding site was defined as carboxylic acid attached to the haem (O1A, HEM750). The following options were then selected:

- Detect cavity
- Restrict atom selection to solvent accessible surface
- Chemscore kinase – csd
- Load template

4. The ligands were then queued and loaded as .mol2 files, the scoring function was selected as goldscore. The value of 20 iterations were selected and early termination was disallowed. The native cofactor residing in the binding site was then extracted and reloaded to define the starting point for the docking experiment and the program was allowed to run.

5. The results were then displayed and each result was inspected in the visualizer to assess the binding mode. Results with similar binding modes were grouped together and an average of their goldscores was taken. Improbable binding modes were discounted.

6. Each sensible binding mode was then exported as a complex into Accelrys discovery studio and a 10 Å pocket was selected for closer inspection. The display style was set as ball and stick, and the visualisation was set to publication quality. The complex was then saved as an image file (.jpeg).

# References

---

1. A. B. Knott and E. Bossy-Wetzel, *Diabetes, Obes. Metab.*, 2010, **12**, 126-133.
2. H. Matter, P. Kotsonis, O. Klingler, H. Strobel, L. G. Fröhlich, A. Frey, W. Pfleiderer and H. H. H. W. Schmidt, *J. Med. Chem.*, 2002, **45**, 2923-2941.
3. L. G. Fröhlich, P. Kotsonis, H. Traub, S. Taghavi-Moghadam, N. Al-Masoudi, H. Hofmann, H. Strobel, H. Matter, W. Pfleiderer and H. H. H. W. Schmidt, *J. Med. Chem.*, 1999, **42**, 4108-4121.
4. J.-H. Park, B.-H. Kim, S.-J. Park, J.-K. Jin, Y. C. Jeon, G. Y. Wen, H.-Y. Shin, R. I. Carp and Y.-S. Kim, *Hippocampus*, 2011, **21**, 319-333.
5. A. F. Rubio-Guerra, H. Vargas-Robles, L. M. Ramos-Brizuela and B. A. Escalante-Acosta, *Integr. Blood Press. Control*, 2010, **3**, 125-132.
6. Y. K. Choi and F. I. Tarazi, *BMB Rep.*, 2010, **43**, 593-598.
7. M. Tsutsui, H. Shimokawa, Y. Otsuji and N. Yanagihara, *Pharmacol. Ther.*, 2010, **128**, 499-508.
8. J. J. Sampson and M. D. Cheitlin, *Prog. Cardiovasc. Dis.*, 1971, **13**, 507-531.
9. C. S. Raman, H. Li, P. Martásek, V. Král, B. S. S. Masters and T. L. Poulos, *Cell*, 1998, **95**, 939-950.
10. D. K. Ghosh, C. Wu, E. Pitters, M. Moloney, E. R. Werner, B. Mayer and D. J. Stuehr, *Biochemistry*, 1997, **36**, 10609-10619.
11. A. C. F. Gorren, B. M. List, A. Schrammel, E. Pitters, B. Hemmens, E. R. Werner, K. Schmidt and B. Mayer, *Biochemistry*, 1996, **35**, 16735-16745.
12. D. J. Stuehr, H. J. Cho, N. S. Kwon, M. F. Weise and C. F. Nathan, *Proc. Natl. Acad. Sci. USA*, 1991, **88**, 7773-7777.
13. M. B. A. Oldstone, S. Dales, A. Tishon, H. Lewicki and L. Martin, *J. Exp. Med.*, 2005, **202**, 1185-1190.
14. V. Grau, O. Stehling, H. Garn and B. Steiniger, *Transplantation*, 2001, **71**, 37-46.
15. J. O. Koglin, T. Glysing-Jensen, J. S. Mudgett and M. E. Russell, *Circulation*, 1998, **97**, 2059-2065.

16. L. Ruiz-Valdepeñas, J. A. Martínez-Orgado, C. Benito, Á. Millán, R. M. Tolón and J. Romero, *J. Neuroinflammation*, 2011, **8**:5.
17. J. Bultinck, P. Sips, L. Vakaet, P. Brouckaert and A. Cauwels, *FASEB J.*, 2006, **20**, 2363-2365.
18. M. J. A. Waer, P. A. M. M. Herdewijn, S. C. A. De Jonghe, A. D. M. Marchand, L. Yuan and S. El Hassane, *PCT Int. Appl.*, 2005, **WO 2005025574**.
19. A. Petros, D. Bennett and P. Vallance, *Lancet*, 1991, **338**, 1557-1558.
20. M. M. Kett, W. P. Anderson, J. F. Bertram and D. Alcorn, *Clin. Exp. Pharmacol. Physiol.*, 1996, **23**, 132-135.
21. M. Kelm, H. Preik-Steinhoff, M. Preik and B. E. Strauer, *Cardiovasc. Res.*, 1999, **41**, 765-772.
22. T. Munzel, T. Gori, R. M. Bruno and S. Taddei, *Eur. Heart J.*, 2010, **31**, 2741-2748.
23. P. Wenzel, A. Daiber, M. Oelze, M. Brandt, E. Closs, J. Xu, T. Thum, J. Bauersachs, G. Ertl, M.-H. Zou, U. Förstermann and T. Münzel, *Atherosclerosis*, 2008, **198**, 65-76.
24. M.-U. Manto and H. Fatemi, *Cerebellum*, 2004, **3**, 130-132.
25. L. Abbott and S.-S. Nahm, *Cerebellum*, 2004, **3**, 141-151.
26. A. V. Goryacheva, S. V. Kruglov, M. G. Pshennikova, B. V. Smirin, I. Y. Malyshev, I. V. Barskov, I. V. Viktorov, H. F. Downey and E. B. Manukhina, *Nitric Oxide*, 2010, **23**, 289-299.
27. C.-X. Luo and D.-Y. Zhu, *Neurosci. Bull.*, 2011, **27**, 23-35.
28. H.-L. Kim and Y. S. Park, *BMB Rep.*, 2010, **43**, 584-592.
29. T. Agapie, S. Suseno, J. J. Woodward, S. Stoll, R. D. Britt and M. A. Marletta, *PNAS*, 2009, **106**, 16221-16226.
30. J. Santolini, M. Roman, D. J. Stuehr and T. A. Mattioli, *Biochemistry*, 2006, **45**, 1480-1489.
31. F. J. M. Chartier and M. Couture, *Biophys. J.*, 2004, **87**, 1939-1950.
32. J. A. Kers, M. J. Wach, S. B. Krasnoff, J. Widom, K. D. Cameron, R. A. Bukhalid, D. M. Gibson, B. R. Crane and R. Loria, *Nature*, 2004, **429**, 79-82.

33. L. E. Bird, J. Ren, J. Zhang, N. Foxwell, A. R. Hawkins, I. G. Charles and D. K. Stammers, *Structure*, 2002, **10**, 1687-1696.
34. M. A. Tayeh and M. A. Marletta, *J. Biol. Chem.*, 1989, **264**, 19654-19658.
35. N. S. Kwon, C. F. Nathan and D. J. Stuehr, *J. Biol. Chem.*, 1989, **264**, 20496-20501.
36. C. Troy, D. Derossi, A. Prochiantz, L. Greene and M. Shelanski, *J. Neurosci.*, 1996, **16**, 253-261.
37. R. Touyz, *Curr. Hypertens. Rep.*, 2000, **2**, 98-105.
38. D. G. Musson, W. G. Kramer, E. D. Foehr, F. A. Bieberdorf, C. S. Hornfeldt, S. S. Kim and A. Dorenbaum, *Clin. Ther.*, 2010, **32**, 338-346.
39. T. S. Schmidt, E. McNeill, G. Douglas, M. J. Crabtree, A. B. Hale, J. Khoo, C. A. O'Neill, A. Cheng, K. M. Channon and N. J. Alp, *Clin. Sci.*, 2010, **119**, 131-142.
40. S. S. Al-Hassan, R. J. Cameron, A. W. C. Curran, W. J. S. Lyall, S. H. Nicholson, D. R. Robinson, A. Stuart, C. J. Suckling, I. Stirling and H. C. S. Wood, *J. Chem. Soc., Perkin Trans. 1*, 1985, 1645-1659.
41. H. C. S. Wood, *Chem. Br.*, 1966, **2**, 536-541
42. T. Rowan and H. C. S. Wood, *J. Chem. Soc. (C)*, 1968, 452-458
43. S. P. Kunuthur, P. H. Milliken, C. L. Gibson, C. J. Suckling and R. M. Wadsworth, *Eur. J. Pharmacol.*, 2011, **650**, 371-377.
44. R. Wadsworth, C. Suckling and C. Gibson, U.S. Pat. Appl. Publ., 2006. **20060194800**.
45. C. J. Suckling, C. L. Gibson, J. K. Huggan, R. R. Morthala, B. Clarke, S. Kununthur, R. M. Wadsworth, S. Daff and D. Papale, *Bioorg. Med. Chem. Lett.*, 2008, **18**, 1563-1566.
46. W. K. Alderton, C. E. Cooper and R. G. Knowles, *Biochem. J.*, 2001, **357**, 593-615.
47. S. Daff, *Nitric Oxide*, 2010, **23**, 1-11.
48. H. Li, C. S. Raman, C. B. Glaser, E. Blasko, T. A. Young, J. F. Parkinson, M. Whitlow and T. L. Poulos, *J. Biol. Chem.*, 1999, **274**, 21276-21284.
49. M. A. Marletta, A. R. Hurshman and K. M. Rusche, *Curr. Opin. Chem. Biol.* 1998, **2**, 656-663.



50. B. Mayer, M. John and E. Böhme, *FEBS Lett.*, 1990, **277**, 215-219.
51. C.-C. Wei, B. R. Crane and D. J. Stuehr, *Chem. Rev.*, 2003, **103**, 2365-2384.
52. A. Reif, L. G. Fröhlich, P. Kotsonis, A. Frey, H. M. Bömmel, D. A. Wink, W. Pfleiderer and H. H. H. W. Schmidt, *J. Biol. Chem.*, 1999, **274**, 24921-24929.
53. B. Mayer, C. Wu, A. C. F. Gorren, S. Pfeiffer, K. Schmidt, P. Clark, D. J. Stuehr and E. R. Werner, *Biochemistry*, 1997, **36**, 8422-8427.
54. S. Pfeiffer, A. C. F. Gorren, E. Pitters, K. Schmidt, E. R. Werner and B. Mayer, *Biochem. J.*, 1997, **328**, 349-352.
55. B. Fitzpatrick, M. Mehibel, R. L. Cowen and I. J. Stratford, *Nitric Oxide*, 2008, **19**, 217-224.
56. J. Santolini, *J. Inorg. Biochem.*, 2011, **105**, 127-141.
57. A. K. Kiemer and A. M. Vollmar, *Immunol. Cell. Biol.*, 2001, **79**, 11-17.
58. H. Xiao, H. Zhou, G. Chen, S. Liu and G. Li, *J. Proteome Res.*, 2007, **6**, 1426-1429.
59. R. Bogumil, M. Knipp, S. M. Fundel and M. Vašák, *Biochemistry*, 1998, **37**, 4791-4798.
60. J. P. Kiss, *Handbook of neurochemistry and molecular neurobiology*, ISBN: 978-0-387-30351-2, **Chapter 16**, 404-411.
61. B. R. Crane, A. S. Arvai, D. K. Ghosh, C. Wu, E. D. Getzoff, D. J. Stuehr and J. A. Tainer, *Science*, 1998, **279**, 2121-2126.
62. L. Mayahi, S. Heales, D. Owen, J. P. Casas, J. Harris, R. J. MacAllister and A. D. Hingorani, *Arte. Thromb. Vasc. Biol.*, 2007, **27**, 1334-1339.
63. M. Demosthenous, C. Antoniadis, D. Tousoulis, M. Margaritis, K. Marinou and C. Stefanadis, *Artery Res.*, 2011, **5**, 37-49
64. S. Sharma, X. Sun, S. Kumar, R. Rafikov, A. Aramburo, G. Kalkan, J. Tian, I. Rehmani, S. Kallarackal, J. R. Fineman and S. M. Black, *Free Radical Biol. Med.*, 2012, **53**, 216-229
65. C. Sumi-Ichinose, H. Ichinose, K. Ikemoto, J. Funami, T. Nomura and K. Kondo, *Pteridines*, 2009, **20** Spec. Iss, 99-101
66. <http://www.ncbi.nlm.nih.gov/sites/entrez?Db=gene&Cmd=ShowDetailView&TermToSearch=5092> (date visited 01/10/12).

- 67 N. Kostandyan, C. Britschgi, A. Matevosyan, A. Oganezova, A. Davtyan, N. Blau, B. Steinmann and B. Thöny, *Mol. Gen. Metab.*, 2011, **104**, S93-S96
- 68 D. M. Dudzinski and T. Michel, *Cardiovasc. Res.*, 2007, **75**, 247-260
- 69 L. Zehnder, M. Bennett, J. Meng, B. Huang, S. Ninkovic, F. Wang, J. Braganza, J. Tatlock, T. Jewell, J. Z. Zhou, B. Burke, J. Wang, K. Maegley, P. P. Mehta, M.-J. Yin, K. S. Gajiwala, M. J. Hickey, S. Yamazaki, E. Smith, P. Kang, A. Sistla, E. Dovalsantos, M. R. Gehring, R. Kania, M. Wythes and P.-P. Kung, *J. Med. Chem.*, 2011, **54**, 3368-3385.
- 70 D. J. Stuehr, N. S. Kwon, C. F. Nathan, O. W. Griffith, P. L. Feldman and J. Wiseman, *J. Biol. Chem.*, 1991, **266**, 6259-6263.
- 71 D. J. Stuehr, C.-C. Wei, Z. Wang and R. Hille, *Dalton Trans.*, 2005, 3427-3435.
- 72 I. G. Denisov, T. M. Makris, S. G. Sligar and I. Schlichting, *Chem. Rev.*, 2005, **105**, 2253-2278.
- 73 A. R. Hurshman, C. Krebs, D. E. Edmondson and M. A. Marletta, *Biochemistry*, 2003, **42**, 13287-13303.
- 74 C.-C. Wei, Z.-Q. Wang, A. S. Arvai, C. Hemann, R. Hille, E. D. Getzoff and D. J. Stuehr, *Biochemistry*, 2003, **42**, 1969-1977.
- 75 J. Vasquez-Vivar, P. Martasek, J. Whitsett, J. Joseph and B. Kalyanaraman, *Biochem. J.*, 2002, **362**, 733-739.
- 76 P. P. Schmidt, R. Lange, A. C. F. Gorren, E. R. Werner, B. Mayer and K. K. Andersson, *J. Biol. Inorg. Chem.*, 2001, **6**, 151-158.
- 77 E. R. Werner, H.-J. Habisch, A. C. F. Gorren, K. Schmidt, L. Canevari, G. Werner-Felmayer and B. Mayer, *Biochem. J.*, 2000, **348**, 579-583.
- 78 A. C. F. Gorren, N. Bec, A. Schrammel, E. R. Werner, R. Lange and B. Mayer, *Biochemistry*, 2000, **39**, 11763-11770.
- 79 C. Riethmuller, A. C. F. Gorren, E. Pitters, B. Hemmens, H.-J. Habisch, S. J. R. Heales, K. Schmidt, E. R. Werner and B. Mayer, *J. Biol. Chem.*, 1999, **274**, 16047-16051.
- 80 H. M. Abu-Soud, R. Gachhui, F. M. Raushel and D. J. Stuehr, *J. Biol. Chem.*, 1997, **272**, 17349-17353.
- 81 D. K. Menyhard, *J. Phys. Chem. B*, 2009, **113**, 3151-3159.

82. J. J. Robinet, K.-B. Cho and J. W. Gault, *J. Am. Chem. Soc.*, 2008, **130**, 3328-3334.
83. K.-B. Cho and J. W. Gault, *J. Am. Chem. Soc.*, 2004, **126**, 10267-10270.
84. K.-B. Cho and J. W. Gault, *J. Phys. Chem. B*, 2005, **109**, 23706-23714.
85. S. P. de Visser and L. S. Tan, *J. Am. Chem. Soc.*, 2008, **130**, 12961-12974.
86. D. Li, M. Kabir, D. J. Stuehr, D. L. Rousseau and S.-R. Yeh, *J. Am. Chem. Soc.*, 2007, **129**, 6943-6951.
87. S. Stoll, Y. NejatyJahromy, J. J. Woodward, A. Ozarowski, M. A. Marletta and R. D. Britt, *J. Am. Chem. Soc.*, 2010, **132**, 11812-11823.
88. J. J. Woodward, Y. NejatyJahromy, R. D. Britt and M. A. Marletta, *J. Am. Chem. Soc.*, 2010, **132**, 5105-5113.
89. H.-H. Chung, Z.-K. Dai, B.-N. Wu, J.-L. Yeh, C.-Y. Chai, K.-S. Chu, C.-P. Liu and I.-J. Chen, *Br. J. Pharmacol.*, 2010, **160**, 971-986.
90. A. Bahremand, S. E. Nasrabady, P. Ziai, R. Rahimian, T. Hedayat, B. Payandemehr and A. R. Dehpour, *Epilepsy Res.*, 2010, **89**, 295-302.
91. S. Gur, P. J. Kadowitz, L. Gurkan, S. Chandra, S. Y. DeWitt, A. Harbin, S. C. Sikka, K. C. Agrawal and W. J. G. Hellstrom, *BJU Int.*, 2010, **106**, 78-83.
92. F. Murad, *Circulation*, 1997, **95**, 1101-1103.
93. L. Ignarro, *FASEB J.*, 1989, **3**, 31-36.
94. X.-Q. Wei, I. G. Charles, A. Smith, J. Ure, G.-J. Feng, F.-P. Huang, D. Xu, W. Mullers, S. Moncada and F. Y. Liew, *Nature*, 1995, **375**, 408-411.
95. K. Van Crombruggen, L. Van Nassauw, P. Demetter, C. Cuvelier, J.-P. Timmermans and R. A. Lefebvre, *Eur. J. Pharmacol.*, 2008, **579**, 337-349.
96. G. Child, ed. E. dysfunction, wikicommons, Editon edn. [http://en.wikipedia.org/wiki/File:Endo\\_dysfunction\\_Athero.PNG](http://en.wikipedia.org/wiki/File:Endo_dysfunction_Athero.PNG) (Date visited 10/10/12).
97. E. R. Werner, N. Bau and B. Thöny, *Biochem. J.*, 2011, **438**, 397-414.
98. T. C. Bellamy and J. Garthwaite, *Mol. Cell. Biochem.*, 2002, **230**, 165-176.
99. F. Xue, H. Li, S. L. Delker, J. Fang, P. Martasek, L. J. Roman, T. L. Poulos and R. B. Silverman, *J. Am. Chem. Soc.*, 2010, **132**, 14229-14238.
100. P. K. Moore and R. L. C. Handy, *Trends Pharmacol. Sci.*, 1997, **18**, 204-211.

101. S. Habib and A. Ali, *Indian J. Clin. Biochem.*, 2011, **26**, 3-17.
102. B. R. Babu and O. W. Griffith, *Curr. Opin. Chem. Biol.*, 1998, **2**, 491-500.
103. S.-I. Muramatsu, *Ann. Neurosci.*, 2010, **17**, 92-95
104. J. C. Choy, Y. N. Wang, G. Tellides and J. S. Pober, *PNAS*, 2007, **104**, 1313-1318.
105. J. P. Cramer, F. P. Mockenhaupt, S. Ehrhardt, J. Burkhardt, R. N. Otchwemah, E. Dietz, S. Gellert and U. Bienzle, *Trop. Med. Int. Health*, 2004, **9**, 1074-1080.
106. P. J. Kuhlencordt, J. Chen, F. Han, J. Astern and P. L. Huang, *Circulation*, 2001, **103**, 3099-3104.
107. R. Kamijo, H. Harada, T. Matsuyama, M. Bosland, J. Gerecitano, D. Shapiro, J. Le, S. I. Koh, T. Kimura, S. J. Green T. W. Mak, T. Taniguchi and J Vilček, *Science*, 1994, **263**, 1612-1615.
108. K. Matsushita, W. Fujimaki, H. Kato, T. Uchiyama, H. Igarashi, H. Ohkuni, S. Nagaoka, M. Kawagoe, S. Kotani and H. Takada, *Infect. Immun.*, 1995, **63**, 785-793.
109. C. A. Nichol, C. L. Lee, M. P. Edelstein, J. Y. Chao and D. S. Duch, *PNAS*, 1983, **80**, 1546-1550.
110. G. Kapatos, S. Kaufman, J. L. Weller and D. C. Klein, *Brain Res.*, 1983, **258**, 351-355.
111. P. G. Jorens, J. Van Overveld, H. Bult, P. A. Vermeire and A. G. Herman, *Br. J. Pharmacol.*, 1992, **107**, 1088-1091.
112. E. R. Werner, M. Schmid, G. Werner-Felmayer, B. Mayer and H. Wachter, *Biochem. J.*, 1994, **304**, 189-193.
113. H. Shintaku, A. Niederwieser, W. Leimbacher and H. C. Curtius, *Eur. J. Pediatr.*, 1988, **147**, 15-19.
114. N. Blau, F. J. van Spronsen and H. L. Levy, *The Lancet*, 2010, **376**, 1417-1427.
115. A. J. Schneider and S. D. Garrard, *J. Pediatr.*, 1966, **68**, 704-712.
116. J. B. Laursen, M. Somers, S. Kurz, L. McCann, A. Warnholtz, B. A. Freeman, M. Tarpey, T. Fukai and D. G. Harrison, *Circulation*, 2001, **103**, 1282-1288.

117. P. F. Fitzpatrick, *Annu. Rev. Biochem.*, 1999, **68**, 355-381.
118. T. J. Kappock and J. P. Caradonna, *Chem. Rev.*, 1996, **96**, 2659-2756.
119. A. Bassan, M. R. A. Blomberg and P. E. M. Siegbahn, *Chemistry*, 2003, **9**, 106-115.
120. A. Ohashi, Y. Sugawara, K. Mamada, Y. Harada, T. Sumi, N. Anzai, S. Aizawa and H. Hasegawa, *Mol. Gen. Metab.*, 2011, **102**, 18-28.
121. A. Ponzzone, F. Porta, A. Mussa, A. Alluto, S. Ferraris and M. Spada, *Metabolism*, 2010, **59**, 645-652.
122. N. Blau, R. Koch, R. Matalon and R. C. Stevens, *Mol. Gen. Metab.*, 2005, **86**, S1-S1.
123. R. Koch, K. Moseley and F. Guttler, *Mol. Gen. Metab.*, 2005, **86**, S139-S141.
124. F. K. Trefz, D. Scheible, G. Frauendienst-Egger, H. Korall and N. Blau, *Mol. Gen. Metab.*, 2005, **86**, S75-S80.
125. C. Sumi-Ichinose, H. Ichinose, K. Ikemoto, T. Nomura and K. Kondo, *J. Pharmacol. Sci.*, 2010, **114**, 17-24.
126. J. M. Wood, B. Chavan, I. Hafeez and K. U. Schallreuter, *Biochem. Biophys. Res. Commun.*, 2004, **325**, 1412-1417.
127. F. Wöhler, *Liebigs Ann.*, 1857, **103**, 117-118.
128. H. Hlasiwetz, *Liebigs Ann.*, 1857, **103**, 200-218.
129. W. Pfeleiderer, *Chem. Ber.*, 1959, **92**, 2468-2477.
130. S. Gabriel and A. Sonn, *Chem. Ber.*, 1907, **40**, 4850-4860.
131. R. Kuhn and A. H. Cook, *Chem. Ber.*, 1937, **70**, 761-768.
132. C. Schöpf and E. Becker, *Liebigs Ann.*, 1933, **507**, 266-296.
133. H. Wieland, H. Metzger, C. Schöpf and M. Bulow, *Liebigs Ann.*, 1933, **507**, 226-265.
134. C. Schöpf, *Naturwissenschaften*, 1940, **28**, 478-479.
135. R. Purrmann, *Liebigs Ann.*, 1940, **544**, 182-190.
136. R. Purrmann, *Liebigs Ann.*, 1940, **546**, 98-102.
137. R. Purrmann, *Liebigs Ann.*, 1941, **548**, 284-292.

138. C. Schöpf, R. Reichert and K. Riefstahl, *Liebigs Ann.*, 1941, **548**, 82-94.
139. P. L. Day, W. C. Langston, W. J. Darby, J. G. Wahlin and V. Mims, *J. Exp. Med.*, 1940, **72**, 463-477.
140. B. H. Nicolet and L. A. Shinn, *J. Am. Chem. Soc.*, 1941, **63**, 2284-2285.
141. L. D. Wright and H. R. Skeggs, *Proc. Soc. Exp. Biol. Med.*, 1944, **55**, 92-95.
142. L. M. Meyer, F. R. Miller, M. J. Rowen, G. Bock and J. Rutzky, *Acta Haematol.*, 1950, **4**, 157-167.
143. D. J. Brown, *Chemistry of Heterocyclic compounds: Fused Pyrimidines Part III: Pteridines*, Volume 24. ISBN: 0-471-83041-0.
144. Anonymous, *Lancet*, 1970, **296**, 757-758.
145. S. M. Marques, É. A. Enyedy, C. T. Supuran, N. I. Krupenko, S. A. Krupenko and M. Amélia Santos, *Bioorg. Med. Chem.*, 2010, **18**, 5081-5089.
146. J. Adcock, C. L. Gibson, J. K. Huggan and C. J. Suckling, *Tetrahedron*, 2011, **67**, 3226-3237.
147. C. L. Gibson, J. K. Huggan, A. Kennedy, L. Kiefer, J. H. Lee, C. J. Suckling, C. Clements, A. L. Harvey, W. N. Hunter and L. B. Tulloch, *Org. Biomol. Chem.*, 2009, **7**, 1829-1842.
148. I. V. Kurinov, D. E. Myers, F. M. Uckun and J. D. Irvin, *Prot. Sci.*, 1999, **8**, 1765-1772.
149. P. A. M. M. Herdewijn, S. C. A. De Jonghe, W. J. Watkins and L. S. Chong, *PCT Int. Appl.*, 2008, **WO 2008009079 A2 20080124**.
150. S. Gabriel and J. Colman, *Ber. Deut. Chem. Ges.*, 1901, **34**, 1234-1257.
151. P. Waring and W. L. F. Armarego, *Aust. J. Chem.*, 1985, **38**, 629-631.
152. G. Heizmann and W. Pfeleiderer, *Helv. Chim. Acta*, 2007, **90**, 1856-1874
153. G. M. Timmins, *Nature*, 1949, **164**, 139.
154. O. Jungmann and W. Pfeleiderer, *Nucleosides Nucleotides Nucleic Acids*, 2009, **28**, 550-585.
155. W. R. Boon and W. G. M. Jones., *J. Chem. Soc.*, 1951, 591-596.
156. A. Rosowsky, R. A. Forsch, V. E. Reich, J. H. Freisheim and R. G. Moran, *J. Med. Chem.*, 1992, **35**, 1578-1588.

157. H. Bader and A. Rosowsky, *J. Org. Chem.*, 1991, **56**, 3386-3391.
158. A. Albert and H. Mizuno, *J. Chem. Soc., Perkin Trans. 1*, 1973, 1615-1619.
159. E. C. Taylor and C. K. Cain, *J. Am. Chem. Soc.*, 1952, **74**, 1644-1647.
160. E. C. Taylor and P. S. Ray, *J. Org. Chem.*, 1987, **52**, 3997-4000.
161. P. Kotsonis, L. G. Fröhlich, C. S. Raman, H. Li, M. Berg, R. Gerwig, V. Groehn, Y. Kang, N. Al-Masoudi, S. Taghavi-Moghadam, D. Mohr, U. Münch, J. Schnabel, P. Martasek, B. S. S. Masters, H. Strobel, T. Poulos, H. Matter, W. Pfeleiderer and H. H. H. W. Schmidt, *J. Biol. Chem.*, 2001, **276**, 49133-49141.
162. E. R. Werner, E. Pitters, K. Schmidt, H. Wachter, G. Werner-Felmayer and B. Mayer, *Biochem. J.*, 1996, **320**, 193-196.
163. L. V. D'Uscio, S. Milstien, D. Richardson, L. Smith and Z. S. Katusic, *Circ. Res.*, 2003, **92**, 88-95.
164. A. Huang, J. A. Vita, R. C. Venema and J. F. Keaney, *J. Biol. Chem.*, 2000, **275**, 17399-17406.
165. M. G. Nair, L. P. Mercer and C. M. Baugh, *J. Med. Chem.*, 1974, **17**, 1268-1272
166. D. MacMillan, *BSc (Hons) project dissertation, The University of Strathclyde*, 2008.
167. K. Hudson, *MSci project dissertation, The University of Strathclyde*, 2009.
168. R. D. Elliott, C. Temple and J. A. Montgomery, *J. Org. Chem.*, 1968, **33**, 2393-2397.
169. C. Temple, J. D. Rose, R. D. Elliott and J. A. Montgomery, *J. Med. Chem.*, 1968, **11**, 1216-1218.
170. C. Temple, J. D. Rose, R. D. Elliott and J. A. Montgomery, *J. Med. Chem.*, 1970, **13**, 853-857.
171. C. Temple, J. D. Rose and J. A. Montgomery, *J. Med. Chem.*, 1970, **13**, 1234-1235.
172. C. Temple, R. D. Elliott, J. L. Frye and J. A. Montgomery, *J. Org. Chem.*, 1971, **36**, 2818-2823.
173. C. Temple and G. A. Renner, *J. Med. Chem.*, 1992, **35**, 988-993.

174. C. Temple and G. A. Rener, *J. Med. Chem.*, 1992, **35**, 4809-4812.
175. C. Temple and G. A. Rener, *J. Med. Chem.*, 1990, **33**, 3044-3050.
176. C. Temple, G. A. Rener and R. N. Comber, *J. Med. Chem.*, 1989, **32**, 2363-2367.
177. C. Temple and G. A. Rener, *J. Med. Chem.*, 1989, **32**, 2089-2092.
178. G. P. Wheeler, B. J. Bowdon, C. Temple, D. J. Adamson and J. Webster, *Cancer Res.*, 1983, **43**, 3567-3575.
179. G. P. Wheeler, B. J. Bowdon, J. A. Werline, D. J. Adamson and C. G. Temple, *Cancer Res.*, 1982, **42**, 791-798.
180. C. Temple, G. P. Wheeler, R. D. Elliott, J. D. Rose, C. L. Kussner, R. N. Comber and J. A. Montgomery, *J. Med. Chem.*, 1982, **25**, 1045-1050.
181. K. Yoshiizumi, M. Yamamoto, T. Miyasaka, Y. Ito, H. Kumihara, M. Sawa, T. Kiyoi, T. Yamamoto, F. Nakajima, R. Hirayama, H. Kondo, E. Ishibushi, H. Ohmoto, Y. Inoue and K. Yoshino, *Bioorg. Med. Chem.*, 2003, **11**, 433-450.
182. S. Whittaker, D. Ménard, R. Kirk, L. Ogilvie, D. Hedley, A. Zambon, F. Lopes, N. Preece, H. Manne, S. Rana, M. Lambros, J. S. Reis-Filho, R. Marais and C. J. Springer, *Cancer Res.*, 2010, **70**, 8036-8044.
183. A. Zambon, D. Ménard, B. M. J. M. Suijkerbuijk, I. Niculescu-Duvaz, S. Whittaker, D. Niculescu-Duvaz, A. Nourry, L. Davies, H. A. Manne, F. Lopes, N. Preece, D. Hedley, L. M. Ogilvie, R. Kirk, R. Marais and C. J. Springer, *J. Med. Chem.*, 2010, **53**, 5639-5655.
184. D. Song, J. Major, J. Hutzler, T. W. Newton, M. Witschel, W. K. Moberg, L. Parra Rapado, T. Qu, F. Stelzer, A. A. Michrowska, T. Seitz, T. Ehrhardt, K. Kreuz, K. Grossmann, B. Sievernich, A. Simon and R. Niggeweg, *PCT Int. Appl.*, 2010, **WO 2010139658**.
185. P. J. Crowley, C. Lamberth, U. Müller, S. Wendeborn, O.-A. Sageot, J. Williams and A. Bartovic, *Tetrahedron Lett.*, 2010, **51**, 2652-2654.
186. K. J. Hodgetts, C. A. Blum, T. Caldwell, R. Bakthavatchalam, X. Zheng, S. Capitosti, J. E. Krause, D. Cortright, M. Crandall, B. A. Murphy, S. Boyce, A. B. Jones and B. L. Chenard, *Bioorg. Med. Chem. Lett.*, 2010, **20**, 4359-4363.
187. P. Koch, H. Jahns, V. Schattel, M. Goettert and S. Laufer, *J. Med. Chem.*, 2010, **53**, 1128-1137.



188. M. S. S. Palanki, E. Dneprovskaja, J. Doukas, R. M. Fine, J. Hood, X. Kang, D. Lohse, M. Martin, G. Noronha, R. M. Soll, W. Wrasidlo, S. Yee and H. Zhu, *J. Med. Chem.*, 2007, **50**, 4279-4294.
189. I. Seipelt, E. Claus, E. Guenther, T. Schuster, M. Czech and E. Polymeropoulos, *PCT Int. Appl.*, 2007, **US 20070123494**.
190. C. O. Kappe, *QSAR Comb. Sci.*, 2003, **22**, 630-645.
191. M. Sellstedt, G. K. Prasad, K. S. Krishnan and F. Almqvist, *Tetrahedron Lett.*, 2012, **53**, 6022-6024.
192. C. O. Kappe, *Eur. J. Med. Chem.*, 2000, **35**, 1043-1052.
193. K. S. Atwal, B. C. O'Reily, J. Z. Gougoutas and M. F. Malley, *Heterocycles*, 1987, **26**, 1189-1192.
194. L. Pouliquen, *MPhil Thesis, University of Strathclyde*, 2007.
195. R. R. Morthala, *PhD Thesis, The University of Strathclyde*, 2007.
196. P. Floersheim, W. Froestl, S. Guery, K. Kaupmann and M. Koller, *PCT Int. Appl.* 2006, **WO 2006136442**.
197. H. I. Ali, N. Ashida and T. Nagamatsu, *Bio. Med. Chem.*, 2007, **15**, 6336-6352
198. C. J. Suckling, *Unpublished data*
199. Q. Yao and W. Pfeleiderer, *Helv. Chim. Acta*, 2003, **86**, 1-12.
200. C.C.D.C [http://www.ccdc.cam.ac.uk/products/product\\_flyers/gold\\_2010.pdf](http://www.ccdc.cam.ac.uk/products/product_flyers/gold_2010.pdf), (date visited 10/10/12).
201. W. Pfeleiderer and H. Walter, *Liebigs Ann.*, 1964, **677**, 113-126.
202. M. G. Nair, B. R. Murthy, S. D. Patil, R. L. Kisliuk, J. Thorndike, Y. Gaumont, R. Ferone, D. S. Duch and M. P. Edelstein, *J. Med. Chem.*, 1989, **32**, 1277-1283.
203. W. Hübsch and W. Pfeleiderer, *Helv. Chim. Acta*, 1989, **72**, 738-743.
204. A. Komáromi, F. Szabó and Z. Novák, *Tetrahedron Lett.*, 2010, **51**, 5411-5414.
205. F. Marchetti, C. Cano, N. J. Curtin, B. T. Golding, R. J. Griffin, K. Haggerty, D. R. Newell, R. J. Parsons, S. L. Payne, L. Z. Wang and I. R. Hardcastle, *Org. Biomol. Chem.*, 2010, **8** (10) 2397-2407.

206. R. C. Reynolds, S. Srivastava, L. J. Ross, W. J. Suling and E. L. White, *Bioorg. Med. Chem. Lett.*, 2004, **14**, 3161-3164.
207. L. T. Burgdorf and T. Carell, *Chemistry*, 2002, **8**, 293-301.
208. A. A. Astrat'ev, D. V. Dashko, A. Y. Mershin, A. I. Stepanov and N. A. Urazgil'deev, *Russ. J. Org. Chem.*, 2001, **37**, 729-733.
209. W. Pfeleiderer, *Chem. Ber.*, 1974, **107**, 785-795.
210. T. Steinlin and A. Vasella, *Helv. Chim. Acta*, 2009, **92**, 588-606.
211. F. Yoneda and T. Nagamatsu, *J. Chem. Soc., Perkin Trans. 1*, 1976, 1547-1550.
212. I. Nakamura, Y. Sato and M. Terada, *J. Am. Chem. Soc.*, 2009, **131**, 4198-4199.
213. M. Wu and T. P. Begley, *Org. Lett.*, 2000, **2**, 1345-1348.
214. D. W. Kuykendall, C. A. Anderson and S. C. Zimmerman, *Org. Lett.*, 2009, **11**, 61-64.
215. C. J. Suckling, B. Clark and R. Wadsworth, *Unpublished data*
216. P. Benderitter, J. X. de Araújo Júnior, M. Schmitt and J.-J. Bourguignon, *Tetrahedron*, 2007, **63**, 12465-12470.
217. F. Reza, G. Bhaswati, K. Pei-Pei, B. L. Gaffney and R. A. Jones, *Tetrahedron Lett.*, 1990, **31**, 319-321.
218. G. Eberlein, T. C. Bruice, R. A. Lazarus, R. Henrie and S. J. Benkovic, *J. Am. Chem. Soc.*, 1984, **106**, 7916-7924.
219. C. Temple, L. L. Bennett, J. D. Rose, R. D. Elliott and J. H. Montgomery, *J. Med. Chem.*, 1982, **25**, 161-166.
220. E. C. Taylor and J. V. Berrier, *Heterocycles*, 1977, **6**, 499-457.
221. E. C. Bigham, G. K. Smith, J. F. Reinhard, W. R. Mallory, C. A. Nichol and R. W. Morrison, *J. Med. Chem.*, 1987, **30**, 40-45.
222. D. G. Markees and G. W. Kidder, *J. Am. Chem. Soc.*, 1956, **78**, 4130-4135.
223. M. Nettekoven and C. Jenny, *Org. Process Res. Dev.*, 2002, **7**, 38-43.
224. R. Shetty, D. Nguyen, D. Flubacher, F. Ruggle, A. Schumacher, M. Kelly and E. Michelotti, *Tetrahedron Lett.*, 2007, **48**, 113-117.

225. P. A. Petukhov and A. V. Tkachev, *Tetrahedron*, 1997, **53**, 2535-2550.
226. P. A. Petukhov and A. V. Tkachev, *Synlett*, 1993, 580.
227. M. C. Harris, O. Geis and S. L. Buchwald, *J. Org. Chem.*, 1999, **64**, 6019-6022.
228. J. P. Wolfe, S. Wagaw and S. L. Buchwald, *J. Am. Chem. Soc.*, 1996, **118**, 7215-7216.
229. J. F. Hartwig, *Synlett*, 1997, 329,340.
230. T. Lechel, J. Dash, P. Hommes, D. Lentz and H.-U. Reissig, *J. Org. Chem.*, 2010, **75**, 726-732.
231. A. Begouin, S. Hesse, M.-J. R. P. Queiroz and G. Kirsch, *Eur. J. Org. Chem.*, 2007, 1678-1682.
232. O. Navarro, N. Marion, J. Mei and S. P. Nolan, *Chemistry*, 2006, **12**, 5142-5148.
233. B. Schlummer and U. Scholz, *Adv. Synth. Catal.*, 2004, **346**, 1599-1626.
234. C. O. Kappe, *Angew. Chem. Int. Ed.*, 2004, **43**, 6250-6284.
235. J. T. Palmer, C. J. Lunnis, D. A. Offermann, L. C. Axford, M. Blair, D. Mitchell, N. Palmer, C. Steele, J. Atherall, D. Watson, D. Haydon, L. Czaplewski, D. Davies, I. Collins, E. M. Tyndall, L. Andrau and G. R. W. Pitt, *Int. Pat. App.*, **WO2012045124**.
236. I. Hamon, H. Gauthier-Moulinier, E. Grelet-Dessioux, L. Storme, J. Fresson and J. M. Hascoet, *Acta Paediatrica*, 2010, **99**, 1467-1473.
237. C. De Labra, C. Rivadulla, N. Espinosa, M. Dasilva, R. Cao and J. Cudeiro, *Front. Syst. Neurosci.*, 2009, **3**:9.
238. J. L. González-Mora, F. A. Martín, D. Rojas-Díaz, S. Hernández, I. Ramos-Pérez, V. D. Rodríguez and M. A. Castellano, *J. Neurosci. Methods*, 2002, **119**, 151-161.
239. W. W. Cleland, *Biochemistry*, 1964, **3**, 480-482.
240. H. M. Sauro, *Enzyme Kinetics for Systems Biology*, 2009, Ambrosius publishing, USA, ISBN 10: 0-9824773-3-3.
241. K. A. Johnson and R. S. Goody, *Biochemistry*, 2011, **50**, 8264-8269.
242. J.-M. Jault and W. S. Allison, *J. Biol. Chem.*, 1994, **269**, 319-325.

- 243 M. A. Khan, H. Miyoshi, S. Ray, T. Natsuaki, N. Suehiro and D. J. Goss, *J. Biol. Chem.*, 2006, **281**, 28002-28010.
- 244 W. C. Still, M. Kahn and A. Mitra, *J. Org. Chem.*, 1978, **43**, 2923-2925.
- 245 G. D'Atri, P. Gomasca, G. Resnati, G. Tronconi, C. Scolastico and C. R. Sirtori, *J. Med. Chem.*, 1984, **27**, 1621-1629.
- 246 H. C. Koppel, R. H. Springer, R. K. Robins and C. C. Cheng, *J. Org. Chem.*, 1961, **26**, 792-803.
- 247 W. R. Boon, *J. Chem. Soc.*, 1957, 2146-2158.
- 248 H. Takalo and J. Kankare, *Acta Chem. Scand.*, 1987, 219-221.